Structure-Property-Transfection Relationships in Polycation-mediated Non-viral DNA Delivery

John M. Layman

Dissertation submitted to the faculty of the
Virginia Polytechnic Institute and State University
in partial fulfillment of the requirements for the degree of

Doctor of Philosophy
in
Macromolecular Science and Engineering

Timothy E. Long, Chair
Garth L. Wilkes, co-Chair
Richey M. Davis
Yong Woo Lee
S. Richard Turner

November 3rd, 2008
Blacksburg, Virginia

Keywords: polyelectrolytes, plasmid DNA, gene delivery, non-viral agents, aqueous characterization, structure-property relationships

Structure-Property-Transfection Relationships in Polycation-mediated Non-viral DNA Delivery

John M. Layman

ABSTRACT

Non-viral gene delivery agents, such as cationic polyelectrolytes, are attractive replacements to viruses due to the absence of potential immunogenic risk and the ability to tune their macromolecular structure. Although non-viral vectors possess numerous design advantages, several investigators have shown that transfer efficiencies are considerably lower when compared to viral vectors. The work reported in this dissertation aims to fundamentally understand the underlying structure-transfection relationships involved in polycation-mediated gene delivery. Efforts focused on the influence of molecular weight, macromolecular topology, carbohydrate modifications, and charge density on the overall transfection activity *in vitro*. Several families of polycations were synthesized in order to correlate chemo-physical characterization with transfection results. Results revealed that seemingly small changes in the structure of cationic polyelectrolytes can have profound consequences on their transfection activity.

Acknowledgements

I would like to thank my advisor, Professor Tim Long, for his guidance, support, and friendship throughout graduate school. He always had tremendous confidence in me as we both learned the field of molecular biology together. Throughout my many failed experiments, he remained patient and always encouraged me to keep trying. I also thank my co-advisor, Prof. Garth Wilkes, for his help and input throughout the progression of my graduate work. I would also like to thank the rest of my advisory committee: Prof. Rick Davis, Prof. Yong Woo Lee, Prof. Craig Thatcher, and Prof. Richard Turner for their time and helpful suggestions.

I sincerely thank Dr. Dietmar Appelhans and Prof. Dr. Brigitte Voit for allowing me to work in their laboratories at the *IPF* in Dresden, Germany. I also thank Prof. Dr. Hirouki Nishide and his students at Waseda University for hosting me and teaching me the Japanese way of conducting experimental research. Both international experiences were once-in-a-lifetime opportunities that I am truly grateful for.

I would like to acknowledge the support of the Macromolecular Interfaces with Life Sciences (MILES) Integrative Graduate Education and Research Traineeship (IGERT) of the National Science Foundation. The MILES program gave me an opportunity to work in an interdisciplinary environment and supported me during an international internship. I would also like to acknowledge funding provided by the U.S. Army Research Laboratory and the U.S. Army Research Office under the Macromolecular Architecture for Performance Multidisciplinary University Research Initiative (MAP MURI).

I thank all of the students I had the privilege of working with while at Virginia Tech. I especially thank my immediate lab-mates who tolerated my personality and put up with my sloppy experimental habits. I thank Ann Fornof and Matt McKee for their leadership and support during my initial years in graduate school. They showed me how to have a good time and how to properly conduct myself in DAV 124A. I also thank Erika Borgerding and Rebecca Huyck for their guidance and help and keeping DAV 124A a fun place to work. I would also like to thank Matthew Cashion for his help in the lab and his friendship during our cohabitation for "financial reasons." I had many fun times with Matthew that I will never forget. I thank Bill Heath for his friendship and many discussions in the lab. His presence in the group helped elevate the quality of my research. I thank Sean Ramirez for his friendship and guidance during my last years of graduate school. His experience and suggestions saved me a tremendous amount of time during the preparation of this dissertation. I would like to thank Takeo Suga for his friendship and insightful discussions. He also provided invaluable recommendations before my trip to Japan. I also thank the rest of the Tim Long group members for their friendship and assistance during graduate school: Afia, Akshay, Andy, Brian, Emily, Eva, Gozde, Kalpana, Matt Hunley, Matt Green, Meghan, Mike, Philippe, Renlong, Serkan, Sharlene, Shijing, Steve, Taigyoo, Tianyu, and Tomonori. I also thank several students outside of the Long group: Josh, Patrick, Vijay, Yemin, and Yumin for their help and

friendship. I would also like to thank Tammy Jo Hiner, Mary Jane Smith, Laurie Good, and Mille Ryan for their help and support.

I would like to thank my family for their support and encouragement throughout my life. My brothers (Yung and David) and sisters (Tammy, Kim, Beth, Jennifer, Mary, Laura, and Debbie). I also thank the Swing family for their support and encouragement. I would like to especially thank Margaret; every molecule of whom I love.

Finally, I would like to express my greatest thanks to my parents (Dr. and Mrs. David A. Layman), who have always given me their unconditional love and support.

John Layman
November, 2008

ex scientia vera

Table of Contents

List of Tables

List of Schemes

List of Figures

Nomenclature

ATRP	Atom Transfer Radical Polymerization
BIEM	2-(2-bromoisobutyryloxy)ethyl methacrylate
CD	cyclodextrin
CTA	chain transfer agent
DP	degree of polymerization
DMAEA	2-(N,N-dimethylamino)ethyl acrylate
DMAEMA	2-(N,N-dimethylamino)ethyl methacrylate
DMAPMA	3-(N,N-dimethylamino)propyl methacrylamide
EGDMA	ethyleneglycol dimethacrylate
EMA	ethyl methacrylate
GTP	Group Transfer Polymerization
HEGMA	hexa(ethylene glycol)methacrylate
HPMA	N-(2-hydroxypropyl)methacrylamide
MAA	methacrylic acid
NIPA	N-isopropyl acrylamide
PAA	poly(acrylic acid)
PAMAM	poly(amidoamine)
PC	2-(methacroyloxyethyl phosphorylcholine)
PDEAEMA	poly[2-(N,N-diethylamino)ethyl methacrylate]
PDI	polydispersity index
PDMAEMA	poly[2-(N,N'-dimethylamino)ethyl methacrylate]
PEG	poly(ethylene glycol) *sometimes used synonymously with PEO
PEGMA	poly(ethylene glycol)methacrylate
PEI	poly(ethyleneimine)
PEO	poly(ethylene oxide) *sometimes used synonymously with PEG
PMAA	poly(methacrylic acid)
PPO	poly(propylene oxide)
PS	poly(styrene)
PTMAEMA	poly[2-(N,N,N-trimethylamino)ethyl methacrylate]
RAFT	Reversible Addition-Fragmentation chain Transfer
SCVCP	self-condensing vinyl copolymerization

Chapter 1. **Introduction**

1.1 Scientific Rationale and Perspective

Gene therapy has the potential to greatly enhance human medicine and ease the suffering of millions of people afflicted with acquired or inherited genetic diseases and disorders. Many common diseases, such as cystic fibrosis and hemophilia, result from the deficiency of a single protein. The principle of gene therapy is to produce a therapeutic amount of the deficient or defective protein and alleviate the phenotype(s) of the host's disease. Additionally, gene therapy has the potential to treat a wide-variety of cancers. This can be accomplished by delivering genes that encode regulatory proteins or by delivering small interfering RNA (siRNA) to down-regulate the expression of cancer-causing genes. Regardless of the type of nucleic acid being delivered (DNA or RNA), the biggest challenge associated with gene therapy is the efficient delivery and internalization of therapeutic gene(s) to the diseased cells. Historically, naturally abundant viruses have been modified to deliver these therapeutic genes. Viruses have evolved over millions of years to perform the single task of delivering their genetic payload to cells. When used as gene delivery vectors, viruses are typically rendered replication deficient, which is supposed to prevent potentially dangerous immunogenic response from the host. However, tragically, a few notable pre-clinical gene therapy trials have resulted in human fatalities and the development of cancer in some patients. It was later determined that the patient that died from the gene therapy trial had a severe immunogenic response to the viral delivery vector. Additionally, some viral vectors function to insert the therapeutic gene into the genome of the host. If this insertion occurs improperly, the genome of the host can be permanently damaged. Sadly, this

phenomenon has been observed in pre-clinical gene therapy trials. This resulted in several patients developing leukemia.

Non-viral vectors circumvent the problems associated with immogenicity, but currently lack high delivery efficiencies of their viral counterpart. Therefore, non-viral vectors will not find wide-spread clinical application until delivery efficiencies rival that of viruses. Non-viral delivery agents are generally divided into two classes; (1) cationic lipids and (2) cationic polyelectrolytes. Cationic lipids form a vesicular-like structure, termed a lipoplex, that encapsulates DNA in the core. Cationic polymers spontaneously form electrostatic complexes with anionic nucleic acids to form multi-macromolecular nanoparticles, termed polyplexes. Both lipoplexes and polyplexes function to screen the negative charges on nucleic acids to condense its hydrodynamic volume and prevent unfavorable interaction with the cellular membrane. Polyplexes are typically internalized by cells via non-specific endocytosis mechanisms. The polyplex is then released from endosomes through mechanisms that have yet to be established. The DNA is then translocated to the nucleus where it is transcribed and translated by the cell's existing protein synthesis machinery. The overall process, termed transfection, is shown schematically in Figure 1.1.

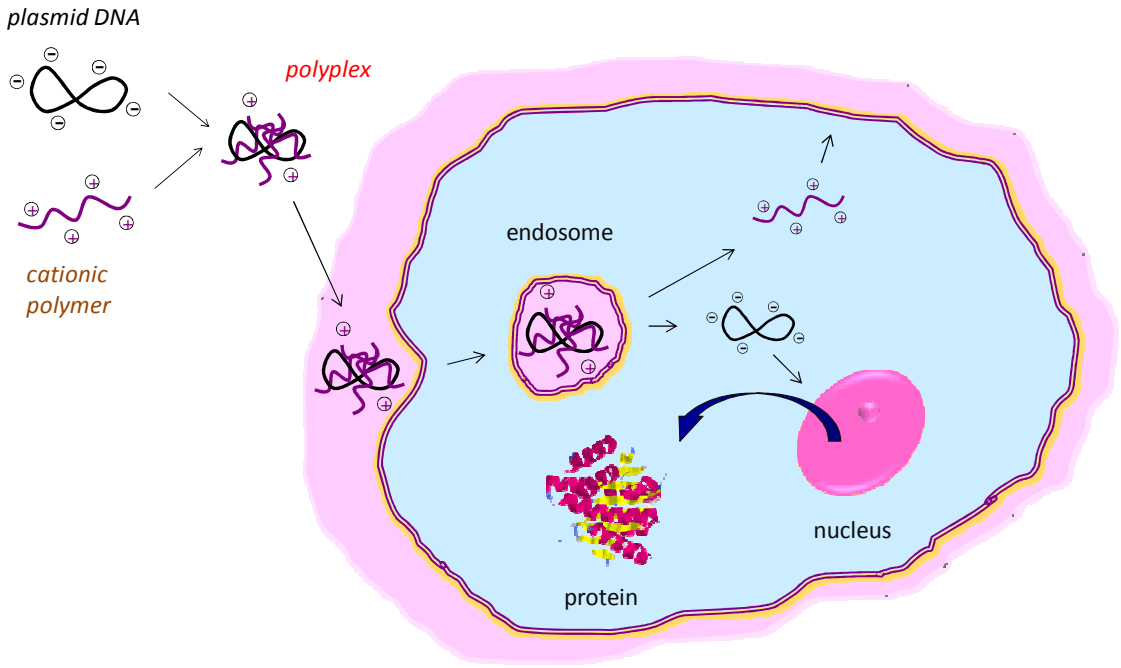

Figure 1.1. Schematic representation of polycation-mediated non-viral gene delivery.

One advantage of cationic polyelectrolytes is the ability to tune the macromolecular structure. Indeed, over the past decade, several investigators have been able to employ various elements in the design of cationic polymers to steadily improve transfection efficiencies. The field in general has attracted a significant amount of attention over the past two decades. Figure 1.2 shows a histogram of the number of scientific papers published dealing with gene delivery and polymer gene delivery. The number of scientific reports increased dramatically in the early to mid 1990's, likely coinciding with the mapping of the human genome beginning in the early 1990's. The number of papers dealing with polymer-mediated gene delivery lagged by a few years, but quickly grew in popularity and relevance over the past decade. However, despite years of prudent research, there are still many unanswered questions associated with the fundamental mechanisms that govern nonviral gene delivery. The work presented in this

dissertation aims to answer questions associated with the fundamental structure-property relationships in polymer-mediated gene transfection. In other words, determine how do seemingly small changes in the structure of polymer influence its ability to complex with and deliver DNA into cells.

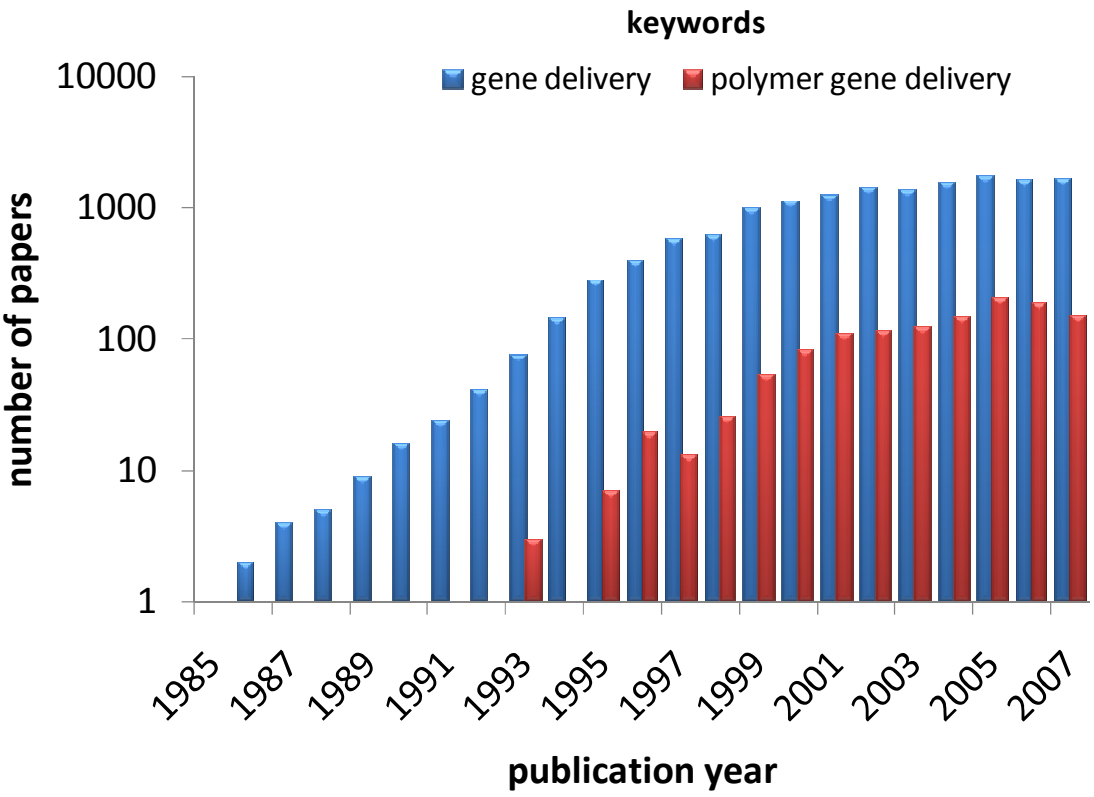

Figure 1.2. Number of scientific reports as function of publication year for the keyword terms "gene delivery" (blue bars) and "polymer gene delivery" (red bars). Source: SciFinder Scholar.

Chapter 2. **Review of the Literature**

2.1 Background and Scientific Rationale

Genes are the fundamental blueprints in all life forms. Located on chromosomes, genes function to store hereditary information in a molecular form of coded chemical sequences. This stored information directs the production of proteins as described by the central dogma of molecular biology. When genes are altered or missing, a disease phenotype usually exists. Some genetic diseases are harmless while others can cause immense suffering and death. Genetic mutation can be caused by a number of environmental factors encountered by the organism. However, these alterations or deviations from genetic normality are more frequently the result of heredity.

Recently, gene therapy has received considerable attention as a potential avenue to treat a number of acquired or inherited genetic disorders. In gene therapy, extra-chromosomal circular DNA segments, or plasmids, are transferred through the cellular membrane and expressed by the existing protein synthesis machinery in the cell. Even though the malfunction occurs in the gene, it is the alteration of the protein that results in the disease state. Single gene defects, such as cystic fibrosis, hemophilia, muscular dystrophy, and sickle cell anemia, are of particular consideration since treatment of these diseases will require the addition or supplementation of a single protein.

Progress towards gene therapy began with the advent of recombinant DNA technology. By the 1970's, advancements in molecular biology furnished the instrumentation and methodologies for the sequencing and cloning of human genes. Around that time, the efficient and reliable production of human insulin was a major concern. Diabetics lack sufficient levels of insulin, the hormone responsible for regulating blood sugar. Early

treatments of diabetes required the extraction of insulin from other organisms. This treatment modality was expensive and not sustainable. In 1972 Stanley Cohen and Herbert Boyer discovered a method to produce human insulin by inserting the protein-encoding gene into bacterial DNA. The modified bacteria produced human insulin, which can be harvested and therapeutically injected into diabetic patients. Gene therapy functions similar to recombinant DNA technology, however, genes are introduced directly into human cells rather than bacteria cells.

2.2 Plasmid DNA

In gene therapy, therapeutic DNA segments are typically fashioned into a closed, double-stranded circular loop called a plasmid. Plasmids are similar to viruses, however, they lack enzyme-protective proteins and therefore cannot move between cells. Plasmids are naturally found in most bacteria cells. DNA plasmids are usually extra-chromosomal and function autonomously in replication and expression. In some cases, the plasmid can be integrated into the host genome[1], however, this presents the danger of permanent genetic modification of the organism and its prodigy.

The main components of a DNA plasmid are commonly a promoter region, a region to express the desired protein, and a reporter gene region. The promoter region is the starting site of transcription which is ultimately the start of protein translation. The desired therapeutic exon follows the promoter region. For experimental purposes, a reporter gene typically follows or precedes the therapeutic gene sequence. Other necessary regions include “ori” (origin), antibiotic resistance, and restriction enzyme sites. The “ori” domain is the origin of replication in bacteria cells. Often, the plasmid is constructed to produce an enzyme-based antibiotic to confer drug resistance to

transformed cells. Antibiotic resistance is used to isolate trans/in-fected cells. The map of a functional *Renilla* luciferase plasmid is shown in Figure 2.1 as an example. This plasmid is frequently used to determine the efficiency of gene transfer vectors.

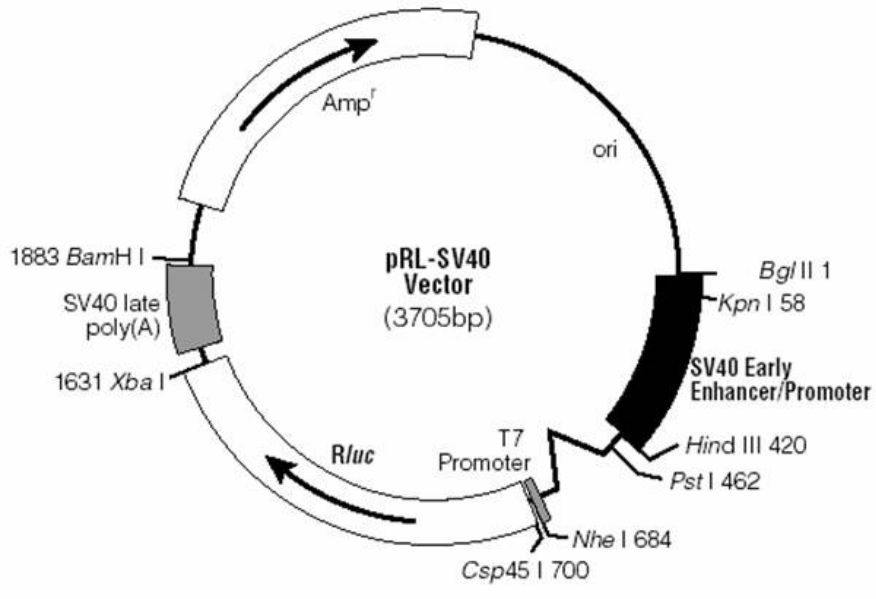

Figure 2.1. Gene map of the pRL-SV40 *Renilla* Luciferase expression plasmid.[2]

Therapeutic DNA segments can be inserted into a plasmid if both the circular plasmid and the source of DNA contain recognition sites for the same restriction endonuclease. The plasmid and the DNA are enzymatically cut by the restriction endonuclease producing fragments with complimentary ends. The complimentary ends recombine via hydrogen bonding. DNA ligases covalently link nucleotide strands into a new plasmid containing the inserted DNA segment(s). A schematic representation of this process is shown in Figure 2.2.

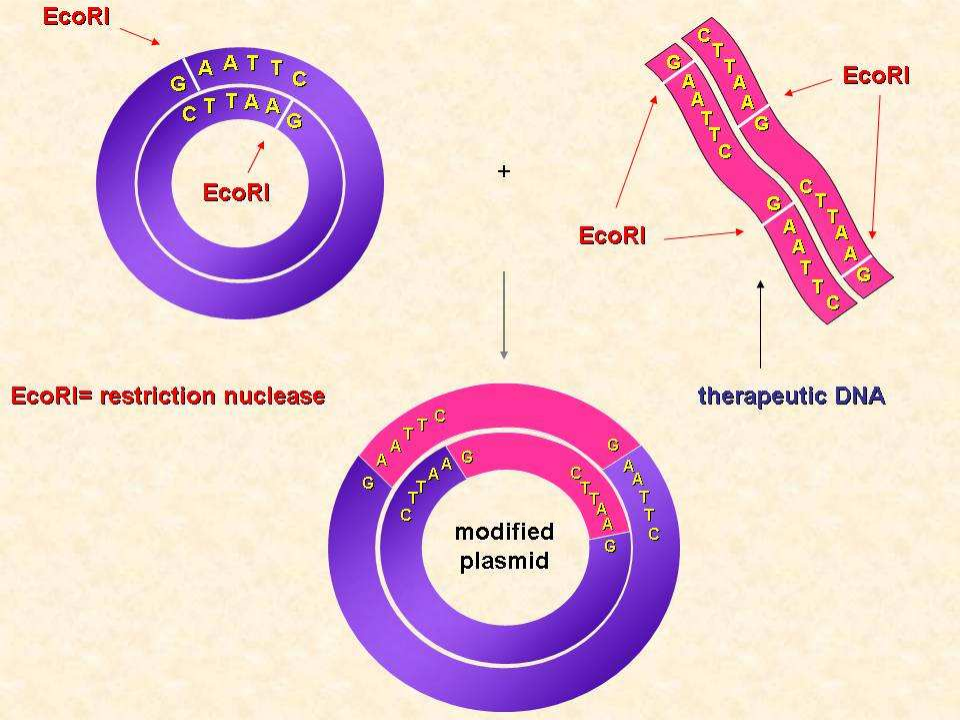

Figure 2.2. Recombinant construction of a DNA plasmid.

2.3 Gene Transfer Vectors and Agents

For efficacious gene therapy, transfer agents, also referred to as vectors, are needed to escort plasmids through the cell membrane since naked DNA is negatively charged and expanded in aqueous solution[3]. The negative charge from the phosphodiester bond in the DNA backbone interacts unfavorably with the lipid bilayer of the cell membrane. Furthermore, mutual charge repulsion along the polymeric nucleotide results in a chain-extended configuration of the macromolecule resulting in a large hydrodynamic volume. These two factors contribute to prevent internalization of therapeutic levels of DNA.[4]

Viruses have evolved over millions of years to accomplish this task. When a virus invades a cell, it infects the cell with its genetic material. The infected host cell will replicate the genes, which typically leads to an invasive viral infection. Viral gene

therapy exploits the infectious capability of viruses to insert therapeutic DNA plasmids. Viral vectors utilize a deactivated virus to infect diseased cells. Deactivating the virus renders it replication deficient. This prevents the virus from making copies of itself, while allowing it to insert its payload of DNA. Three types of viruses are currently being explored for gene therapy: retroviruses, adenoviruses, and adeno-associated viruses. Each virus type functions differently and possesses advantages and disadvantages over one another. Retroviruses store their genetic material in the form of RNA. Once the retrovirus infects a host cell, DNA is made from the RNA by a reverse transcription process. The retrovirus carries reverse transcriptase enzymes to carry out this process. In retrovirus-mediated gene therapy, the therapeutic DNA segment must be integrated into the genome of the host. Retroviruses also carry an enzyme called integrase to insert the DNA segment into the host. One of the major disadvantages of using retroviruses is the danger that the integrase enzyme will insert DNA in any arbitrary position in the host genome. The therapeutic gene could potentially be inserted into the genome at a site that codes for another vital protein, thus possibly causing another protein deficiency. If the DNA is inserted into the genome and disrupts the production of growth regulation proteins, unregulated cell division could result leading to the generation of cancerous cells. This threat alone has reduced the popularity of retroviruses for gene therapy. Adenoviruses carry their genetic material in the form of DNA. When adenoviruses infect cells, the DNA is inserted, however, not incorporated into the genome of the host. The inserted DNA is transcribed and translated similar to other genes in the cell. However, the inserted gene is not replicated during cell division. Cellular descendents will require the same treatment to produce the therapeutic protein. Adeno-associated viruses are

relatively small viruses that carry their genetic material in the form of single stranded DNA. Adeno-associated viruses function similar to adenoviruses in their infection and expression mechanisms. The main disadvantages of adeno-associated viruses are its limited DNA size and the difficulty involved in its production. Adeno-associated viruses are unique in that they are inherently non-pathogenic. In general, viral vectors are extremely efficient carrier molecules and even target cells by their natural tendency to infect certain cell types[5]. However, viral vectors are limited to small plasmids and although modified viruses are inactivated, host immune response is a frequent, and often severe, complication[3].

Non-viral agents are an attractive replacement to viruses due to reduced immunogenic risk and the ability to carry larger plasmids. Non-viral vectors are typically based on either cationic lipids or cationic polyelectrolytes. Cationic lipids function by forming a liposome around the DNA plasmid. One of the main disadvantages of cationic lipids is their high cytotoxicity.[6] Another major class of non-viral transfection agents is cationic polyelectrolytes. By definition, these compounds possess a positive charge on the polymer backbone. Several polymers are being evaluated with well known examples being poly(ethyleneimine), poly(L-lysine), diethylaminoethyl dextran, and poly(2-dimethylaminoethyl methacrylate) (PDMAEMA)[7,8,9].

Cationic polyelectrolytes function by electrostatically screening the anionic charges on the DNA plasmid to form a plasmid-polymer complex, also referred to as a polyplex.[10] This action neutralizes the net charge and alleviates mutual charge driven chain extension, thus condensing the hydrodynamic radius of the polyplex. The elimination of

net ionic charges and smaller size of the polyplex considerably increase the probability of gene transfection.[11] A schematic representation of this process is shown in Figure 2.3.

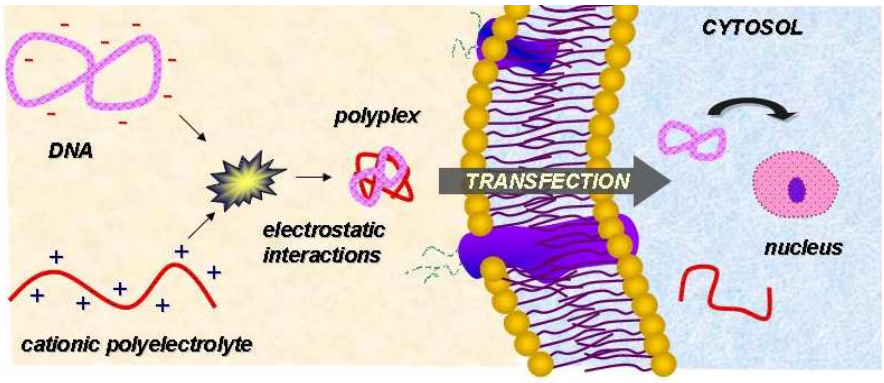

Figure 2.3. Complexation of plasmid DNA with a cationic polyelectrolyte, transfection, and disassociation of the plasmid from the polymer in the cytosol.

Cationic polyelectrolytes have also been shown to protect against enzymatic degradation from the host[12]. Although non-viral vectors possess numerous advantages, several investigators have shown that transfer efficiencies are considerably lower when compared to viral vectors. Improving the efficiency of non-viral gene transfer vectors is critical towards their application in gene therapy.

2.4 Poly(2-N,N'-dimethylaminoethyl methacrylate)

Poly(2-dimethylaminoethyl methacrylate) is synthetically produced by the free radical polymerization of 2-dimethylaminoethyl methacrylate (DMAEMA). Free radical synthesis can be conducted in either bulk or solution free radical processes. DMAEMA monomer can be converted into a quaternary salt if the synthesis is conducted in an aqueous solution with the pH adjusted below the pKa of the tertiary amine. In aqueous synthesis, the salt form of PDMAEMA is produced with the counter ion corresponding to

the acid used to adjust the pH of the polymerization solvent. An example of an aqueous synthetic scheme for PDMAEMA is shown in Figure 2.4.

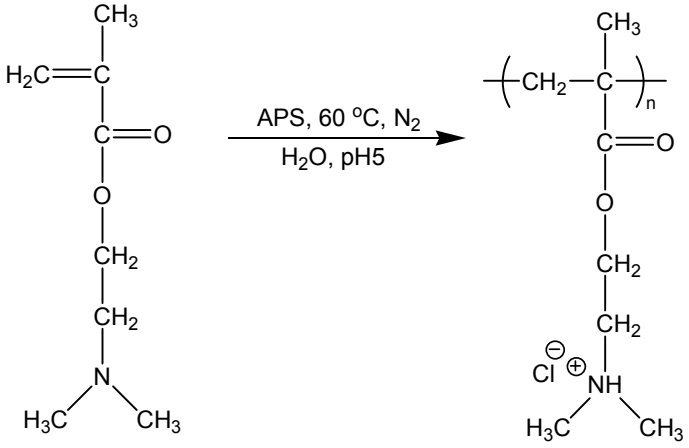

Figure 2.4. Aqueous synthesis of PDMAEMA.

DMAEMA can also be polymerized in an organic-based solvent. The synthesized PDMAMEA is neutral and must be converted into the water-soluble polyelectrolyte form. This conversion can be accomplished by simply dissolving the neutral polymer in acidic aqueous solutions. An example of an organic-based synthesis is shown in Figure 2.5.

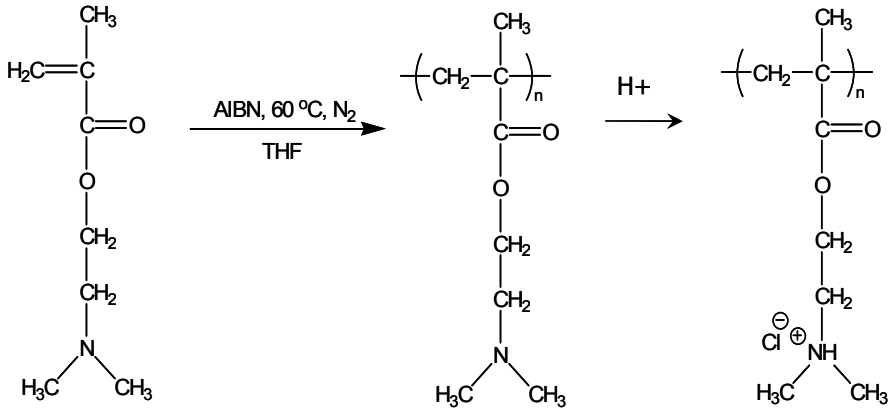

Figure 2.5. Organic solvent-based synthesis of PDMAEMA and conversion to the polyelectrolyte form.

PDMAEMA can also be synthesized by living radical polymerization methods. Living polymerization methods allow for controlled molecular weights and narrow molecular weight distributions. One such living polymerization method is atom transfer radical polymerization (ATRP). In ATRP, polymerization is controlled through a dynamic equilibrium between propagating and dormant species with a transition metal complexes acting as a reversible halogen atom transfer agent. PDMAEMA has been successfully synthesized using ATRP by several investigators.[13,14,15] The main disadvantage to using ATRP is the use of toxic catalysts, which impart a distant coloration on the polymer and can be difficult to remove. To help alleviate this problem, Pantoustier et al. developed a solvent-free synthesis and purification method using ATRP. In this study, synthesis was conducted under bulk conditions and purification was accomplished through selective water precipitation and filtration.[16] Additionally, some of these investigators used an ATRP macroinitiator containing poly(ethylene glycol) chains as an interesting method to produce copolymers of PDMAEMA.

PDMAEMA is a non-biodegradable, slightly cytotoxic polymer. These two attributes are the main disadvantages of PDMAEMA-based gene transfection agents. However, when complexed to DNA, the cytotoxicity is significantly reduced. As described in later sections of this review, many investigators have designed copolymers to reduce the toxic effects of this polymer.

2.5 Homopolymers of PDMAEMA as Transfection Agents

The first reported use of PDMAEMA as a gene transfection agent was published in 1996 by Cherng et al.[17] However, the use of other cationic polyelectrolytes was

published a decade earlier. In this study, linear homopolymers of DMAEMA (M_n=45,000 g/mol) were evaluated on their ability to complex a pCMV-lacZ plasmid coding for beta-galactosidase as a reporter gene. Dynamic light scattering (DLS) was used to measure the hydrodynamic diameters of PDMAEMA complexed to plasmid DNA. Electrophoretic mobility measurements were used to measure the charge of the polyplexes. Transfection experiments were conducted with COS-7 kidney cells *in vitro*. Optimum transfection efficiency was found at a polymer-plasmid ratio of 3 w/w. Polyplexes prepared at this ratio had diameters around 150 nm and possessed a slightly positive charge. Polyplexes prepared at lower polymer-plasmid ratios displayed lower transfection efficiencies. This study also found PDMAEMA to be slightly cytotoxic. Additionally, it was shown that the cytotoxicity of PDMAEMA is partially masked when complexed with plasmid DNA. Part of this study also evaluated the effect of serum proteins on transfection efficiency since these proteins have the potential to disrupt polyplexes and limit *in vivo* mobility. However, transfection efficiency was not affected the presence of serum proteins.

In previous study, only one molecular weight of PDMAEMA was evaluated. In a separate study by the same research group, van de Wetering et al. evaluated the effect of PDMAEMA molar mass on transfection efficiency.[30] The transfection efficiency was significantly influenced by molecular weight, with an increase in efficiency as molecular weight increased. This trend is shown graphically in Figure 2.6.

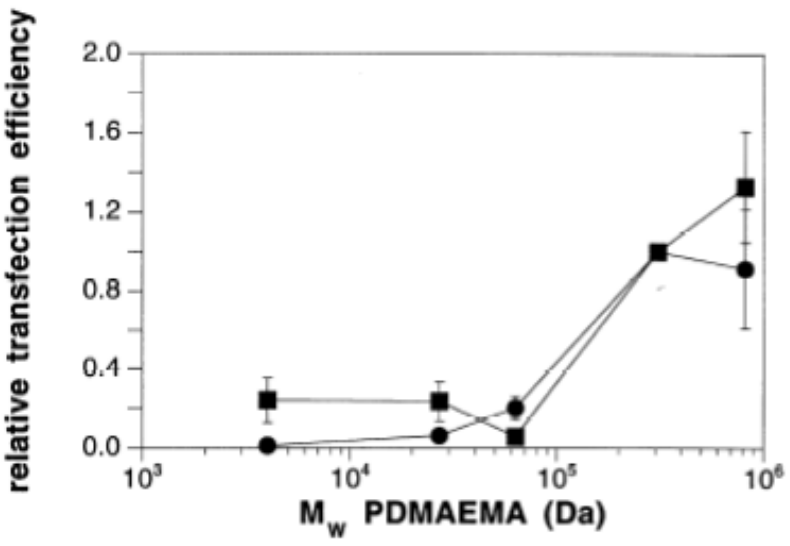

Figure 2.6. The effect of polymer molecular weight on maximum transfection efficiency of PDMAEMA/plasmid complexes in COS-7 (circles) and OVCAR-3 cells (boxes). Plasmid concentration was fixed at 1.7 mg/ml (in RSC). Values are normalized to the maximum number of transfected cells after incubation with plasmid complexed to PDMAEMA (*M* 309 kDa). X-Gal coloring time was 1 h. Each point represents the mean of three–six experiments.[30] Reprinted from Journal of Controlled Release, Vol. 53, P. van de Wetering, J. -Y. Cherng, H. Talsma, D. J. A. Crommelin and W. E. Hennink, "2-(dimethylamino)ethyl methacrylate based (co)polymers as gene transfer agents", Pages No. 9, Copyright 1998, with permission from Elsevier.

In another study by the same research group, the transfection ability of PDMAEMA was compared to other cationic polyelectrolytes. In Verbaan et al., the transfection of PDMAEMA was compared to poly(L-lysine) (PLL), branched poly(ethyleneimine) (BPEI), linear PEI (LPEI), and 1,2-dioleyl-3-trimethylammonium-

propane (DOTAP) *in vitro* and *in vivo* after intravenous administration into mice.[18] In both *in vivo* and *in vitro* experiments, the order of decreasing lung transfection efficiency was: DOTAP > LPEI > PDMAEMA > BPEI > PLL. Interestingly, the topology of PEI influences the transfection efficiency in this experiment, however, the degree of branching is not defined in this work. This group has also evaluated the effect of DNA topology on PDMAEMA-mediated transfection. In Cherng et al., transfection efficiencies with various DNA topologies occurred in the following decreasing order: supercoiled > open-circular ≅ heat-denatured > linear.[19]

One of the advantages of using cationic polyelectrolytes as gene transfection agents is the ability to tailor macromolecular architecture. Accordingly, star polymers have been synthesized and evaluated on their ability to transfect DNA into cells. In a recent article by Georgiou et al., star homopolymers of DMAEMA were synthesized by group transfer polymerization (a living polymerization method) and evaluated on their ability to transfect pRLSV40 enhanced green fluorescent protein (EGFP) plasmid into human cervical cancer cells.[20] The star polymers were produced using ethylene glycol dimethacrylate as a crosslinkable core. A schematic representation of the synthetic procedure is shown in Figure 2.7.

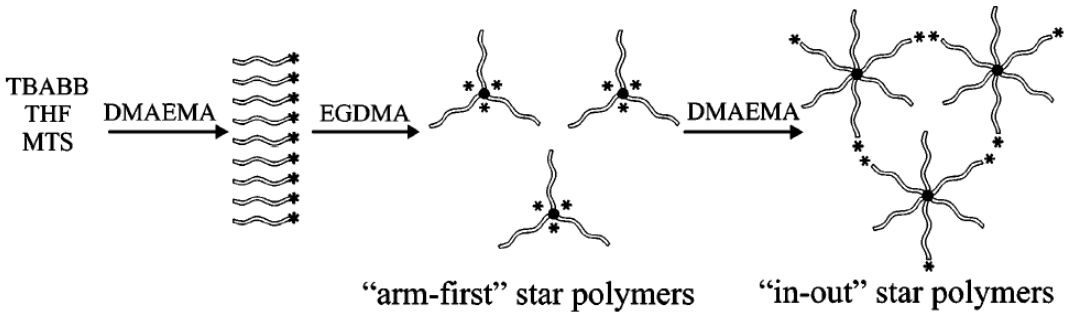

Figure 2.7. Schematic representation for the synthetic procedure used to produce "in-out" star polymers of DMAEMA.[20] Reprinted with permission from reference 20. Copyright 2004 American Chemical Society.

This study showed that increases in the degree of polymerization (DP) of the arm, varying from 10 to 100, resulted in increased transfection efficiency. However, the increase in arm length also resulted in increased cytotoxicity which caused the overall transfection efficiency to decrease. The results from this work are shown in Figure 2.8. Further experiments using arms of DP=10 length, found an optimum transfection efficiency of approximately 15%, which was slightly higher than the commercially available transfection reagent, Superfect®.

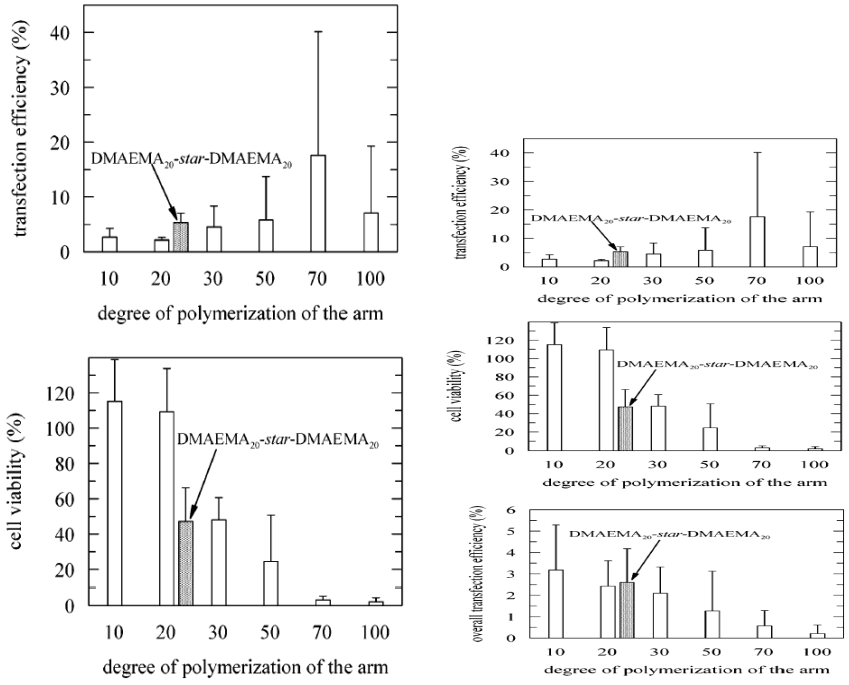

Figure 2.8. Transfection efficiency and cell viability studies using DMAEMA star polymers.[20] Adapted with permission from reference 20. Copyright 2004 American Chemical Society.

2.6 Polyplex Formation and Dissociation Events

Understanding how plasmid DNA interacts, binds, and disassociates with PDMAEMA is important towards its clinical development in gene therapy. Several investigators have examined the complexation process and defined the parameters involved in this event. In a study by van de Wetering et al., molecular modeling was used to evaluate the electrostatic and intermolecular interactions between PDMAEMA and DNA.[21] The authors utilized the Insight II 97.0 molecular modeling program to observe the binding of a DNA octamer to octa(DMAEMA), shown in Figure 2.9. This figure shows the cationic polymer docked in the major grove of the DNA. The electrostatic event occurs between the cationic amine moiety and the phosphodiester bond in DNA.

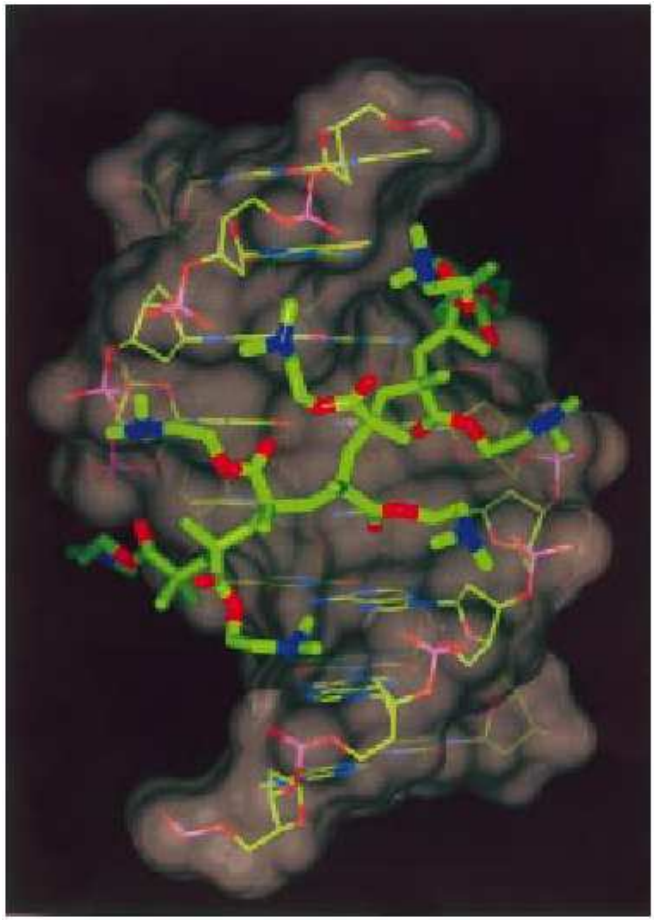

Figure 2.9. Octa(DMAEMA) docked to octa(DNA).[21] Reprinted with permission from reference 21. Copyright 1999 American Chemical Society.

In addition to the electrostatic interactions, intermolecular hydrogen bounding interactions were observed between the carbonyl of the methacrylate ester and the primary amine hydrogen in an adenine-thymine DNA hydrogen-bond. A schematic representation of this interaction is shown in Figure 2.10.

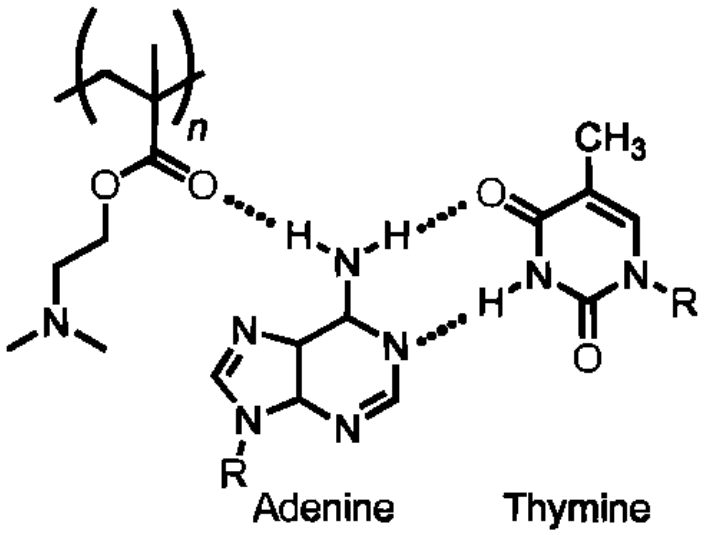

Figure 2.10. Interaction between adenine and PDMAEMA.[21] Reprinted with permission from reference 21. Copyright 1999 American Chemical Society.

Although the model shows the interaction between one DMEAMA molecule and one DNA molecule, it has been shown in a separate study by Van Rompaey et al. that, depending upon the relative amounts of polymer and DNA, that both mono-molecular and multi-molecular complexes are formed using PDMAEMA.[22] Also, PDMAEMA does not preferentially interact with DNA if other anionic species are present. In multi-polyanionic environments, such as physiological fluids, Leclercq et al. found a competition for binding polyanions to PDMAEMA.[23] Understanding how other polyanions compete for binding to PDMAEMA will be important for *in vivo* applications where blood proteins and other polynucleotides are present.

In a study by Arigita et al., the association/dissociation behavior of DNA to PDMAEMA and other cationic polyelectrolytes, such as poly(L-lysine) (PLL) and poly(2-(trimethylamino)ethyl methacrylate hydrochloride) (PTMAEMA), was

evaluated.[12] Complex formation and dissociation was studied using fluorescence spectroscopy and agarose gel electrophoresis. Dissociation of the complexes was performed by adding excess salt to solutions containing polyplexes. The binding ability of each cationic polymer was correlated with its respective transfection efficiency. It was found that PDMAEMA and PLL have similar DNA binding characteristics. Interestingly, this study also found that low molecular PDMAEMA has a lower affinity for DNA than higher molecular weight PDMAEMA. PTMAEMA bound tightly to DNA even in concentrated salt solutions. Transfection with this cationic reagent should low efficiency. The authors postulated this may be due to its inability to dissociate in the cytoplasm, which is necessary for protein synthesis. In a separate study by Zuidam et al., confocal laser fluorescence microscopy and electron microscopy techniques were used to study the cellular interaction of PDMAEMA and PTMAEMA polyplexes with human ovarian carcinoma cells.[24] It was found that both PDMAEMA and PTMAEMA polyplexes were internalized by endocytosis. However, PTMAEMA does not have the same endosomal escape properties as PDMAEMA. Polyplexes based on PDMAEMA are hypothesized to release from endosomes by the "proton-sponge" effect.[25] In this hypothesis, the unique buffering capacity of tertiary amines allows for partial protonation of these functional groups at physiological pH. In the endosomal environment, the pH is much lower, which results in an influx of protons, and subsequently halogen counter ions to maintain charge neutrality, into the endosome. The increased ion content would lead to an osmotic gradient between the endosome and the cytoplasm. It is proposed that water would then enter the endosome until it physically burst, which would release polyplexes into the cytoplasm.

Other investigators have found that PDMAEMA is internalized by endocytosis, however, the formed endosomes are not physically disrupted. Jones et al. examined the internalization and fate of umcomplexed PDMAEMA once internalized by transfected cells.[26] Additionally, this study determined the mode of cell death that PDMAEMA induces, its mechanism of entry, and its ability to release molecules into the cell cytosol. The results indicated that PDMAEMA is internalized by fluid-phase endocytosis and induces radpid, primarily necrotic cell death. Additionally, endsomes formed with PDMAEMA were not physically disrupted, as proposed by the proton sponge hypothesis. However, this experiment only evaluated one molecular weight of uncomplexed PDMAEMA, not polyplexes. Furthermore, only two cell lines were used in this study.

In a study by Lucas et al., Cy5-labled PDMAEMA and rhodamine green labeled oligonucleotides (RhGr-ON) were complexed and transfected into Vero cells.[27] Both the polymer and DNA were tracked by confocal laser scanning microscopy throughout the transfection process. The results showed dissociation of the complex in the cytosol. PDMAEMA polymer was only detected in the cytosol and the rhodamine-labeled oligonucleotide was found accumulated in the nucleus. Transmission and confocal microscopy images from this study are shown in Figure 2.11.

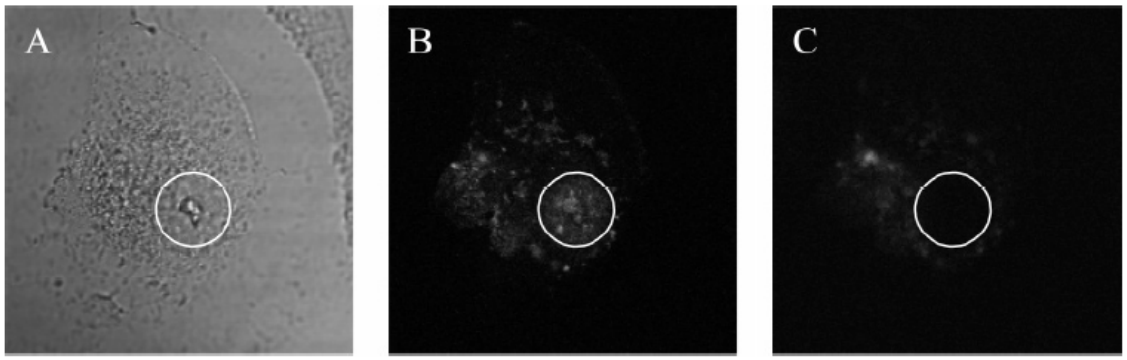

Figure 2.11. Transmission image (A) and confocal fluorescence images (B and C) of a Vero cell transfected for 3 h with Cy5-graft-pDMAEMA/ RhGr-ONs. A circle is drawn around the nucleus.[27] Reprinted with permission from reference 27. Copyright 2005 American Chemical Society.

It has also been shown that the ionization state of the cationic polyelectrolyte affects its polyplex characteristics. Rungsardthong et al. found that changing the pH environment of the polyplexes, and thus the ionization state of the polymer, greatly influences the morphology of PDMAEMA/DNA complexes.[28] Micrographs of the observed morphological changes are shown in Figure 2.12. This study also found that PDMAEMA has a greater affinity for DNA at low pH. This higher affinity would suggest spontaneous dissociation of PDMAEMA/DNA complexes is not probable in endosomes. However, this result does not discredit the proposed proton sponge theory, since excess PDMAEMA has a high buffering capacity.

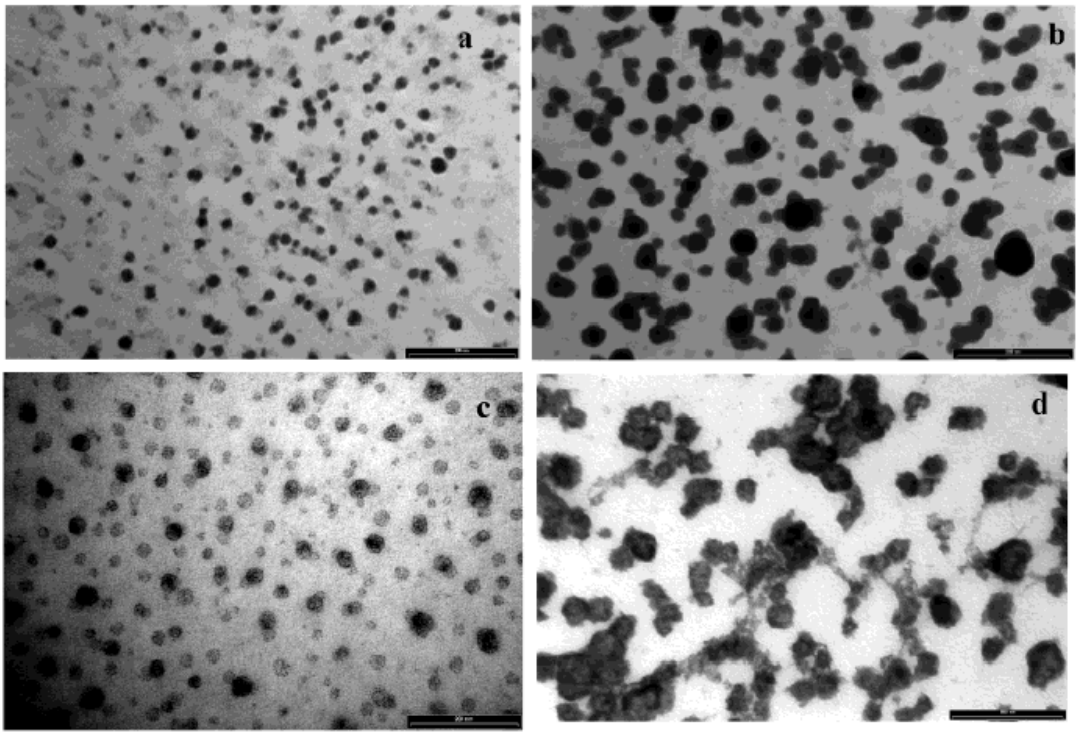

Figure 2.12. Morphology of the DMAEMA homopolymer and plasmid DNA complexes prepared at monomer:nucleotide molar ratio 1:1 in 1 mM phosphate buffer at pH 4.0 (a), 6.6 (b), 7.4 (c), and 8.0 (d) (bar = 200 nm, 200 000 magnification).[28] Reprinted with permission from reference 28. Copyright 2003 American Chemical Society.

However, it has been shown that the buffering capacity of the polymer it not the only critical element to successful gene delivery. In a study by Dubruel et al., confocal laser microscopy coupled with fluorophore labeling was used to track the internalization of various cationic polyelectrolytes, including PDMAEMA.[29] Interestingly, polyelectrolytes with similar buffering capacities displayed drastically different endosomal escape properties and transfection efficiencies.

2.7 Copolymers of PDMAEMA as Transfection Agents

In an effort to eliminate or suppress the disadvantages of PDMAEMA transfection systems, namely its cytotoxicity and relatively low overall transfection efficiency, several investigators have explored the use of PDMAEMA-based copolymers. Several creative copolymers have been explored with varying applications.

The first use of PDMAEMA copolymers as transfection agents was published by the same research group who were the first to use PDMAEMA homopolymers as transfection agents. van de Wetering et al. evaluated the complexation and transfection of DMAEMA copolymerized with N-vinyl-pyrrolidone (NVP), methyl methacrylate (MMA), and ethoxytriethylene glycol methacrylate (triEGMA).[30] Copolymers of PDMAEMA with 20 mol% MMA, as determined by ^{1}H NMR, showed reduced transfection efficiency and increased cytotoxicity when compared to PDMAEMA homopolymers of similar molar mass. Copolymers with 14 and 54 mol% NVP were found to have increased transfection efficiency and decreased cytotoxicity. NVP-Copolymer/DNA complexes produced lower particles sizes, as measured by dynamic light scattering. It was postulated that the decrease in complex size results from more polymer-DNA interactions with the addition of NVP, which is capable of hydrogen bonding with DNA. Copolymers with both 21 and 48 mol% triEGMA showed reduced cytotoxicity, however, this copolymer also showed reduced transfection efficiency. In a subsequent study by van de Wetering et al., copolymers of NVP and triEGMA with various molecular weights and comonomer compositions were evaluated as transfection reagents.[31] In this study, copolymers with molecular weights up to 170,000 g/mol showed similar transfection activity as homopolymers of comparable molar mass. Higher

molecular weight copolymers, M_n>170,000 g/mol, showed reduced transfection efficiencies when compared to PDMAEMA homopolymers.

Investigators have also evaluated other comonomer systems. Dubruel et al. evaluated PDMAEMA copolymerized with N-(2-hydroxyethyl)nicotinamide methacrylate (HENIMA), 4-(5-methylimidazoyl)methyl methacrylate) (HYMIMMA), methacrylic acid (MA), poly(ethylene oxide) methacrylate (PEOMA), and poly(ethylene oxide).[32] In this study, the particle size and charge was determined by DLS and zeta-potential measurements respectively. A significant effect of chemical structure on particle size and charge was found. In a later study by the same research group, the transfection activity of these PDMAEMA copolymers was evaluated.[33] A summary of these results are shown in Figure 2.13

β-Gal mass, amount of cell protein and cytotoxicity for the transfection of Cos-1 cells with different polymer–DNA complexes at a 2/1 and a 4/1 charge ratio, $n=3$

Code	Polymer	M_w (kDa)	2/1 charge ratio			4/1 charge ratio		
			β-Gal (ng/ml)	Cell protein (μg/ml)	Cell viability (%)	β-Gal (ng/ml)	Cell protein (μg/ml)	Cell viability (%)
P1	PDMAEMA	93	0.02 (±0.01)	36.39 (±4.47)	98 (±7)	0.36 (±0.03)	25.98 (±6.64)	101 (±6)
P4	PDMAEMA	201	5.78 (±0.63)	43.30 (±1.55)	108 (±3)	19.57 (±0.19)	40.04 (±2.38)	103 (±1)
P5	P(DMAEMA$_{0.82}$–co-MA$_{0.18}$)	108	0.04 (±0.03)	55.53 (±4.13)	103 (±5)	0.04 (±0.02)	52.36 (±7.18)	97 (±11)
P6	P(DMAEMA$_{0.65}$–co-MA$_{0.35}$)	316	0.02 (±0.02)	57.84 (±1.53)	106 (±2)	0.01 (±0.01)	48.70 (±3.80)	102 (±7)
P7	P(DMAEMA$_{0.9}$–co-HENIMA$_{0.1}$)	140	0.19 (±0.05)	50.53 (±3.94)	106 (±4)	5.20 (±0.90)	53.86 (±0.83)	103 (±2)
P9	P(DMAEMA$_{0.94}$–co-HYMIMMA$_{0.06}$)	99.5	0.23 (±0.10)	54.02 (±6.85)	109 (±3)	0.12 (±0.04)	46.71 (±3.04)	109 (±1)
P10	P(DMAEMA$_{0.88}$–co-HYMIMMA$_{0.12}$)	72	0.06 (±0.07)	63.80 (±3.62)	103 (±4)	0.01 (±0.01)	61.81 (±4.00)	100 (±4)
P11	P(DMAEMA$_{0.81}$–co-HYMIMMA$_{0.19}$)	54	0.03 (±0.02)	35.5 (±2.45)	108 (±2)	1.12 (±0.03)	30.36 (±3.87)	105 (±1)
PEI	Poly(ethyleneimine)	25	22.34 (±1.49)	22.24 (±4.89)	79 (±6)	9.25 (±0.83)	17.64 (±1.04)	65 (±9)

Control (DNA without polymer): β-gal mass 0.08 ng/ml (±0.05); amount of cell protein 51.77 μg/ml (±5.42). Lipofectamine: β-gal mass 60.10 ng/ml (±22.54); amount of cell protein 19.56 μg/ml (±1.83); cell viability 60% (±2).

Figure 2.13. Transfection and cell viability results obtained by Dubruel et al.[33] Reprinted from European Journal of Pharmaceutical Sciences, Vol 18, Peter Dubruel, Bart Christiaens, Berlinda Vanloo, Ken Bracke, Maryvonne Rosseneu, Joël Vandekerckhove and Etienne Schacht, "Physicochemical and biological evaluation of cationic polymethacrylates as vectors for gene delivery", Copyright 2003, with permission from Elsevier.

As shown in Figure 2.13, these investigators found that minor changes in chemical structure or molecular weight causes major effects on transfection activity. Furthermore, this study provides a method to tailor the DNA condensation activity of PDMAEMA by selecting the appropriate type and amount of comonomer(s).

In a study by Lam et al., diblock copolymers of DMAEMA and phosphorylcholine were synthesized by ATRP and tested as transfection agents.[34] Methacryloyloxyethyl phosphorylcholine (MPC) was used as the monomer to incorporate phosphorylcholine. The attraction to using MPC is its inherent biocompatibility and thus reduction in vector cytotoxicity. Additionally, MPC copolymers have also been shown to resist protein adsorption.[35,36] The structure of the DMAEMA-MPC copolymer is shown in Figure 2.14.

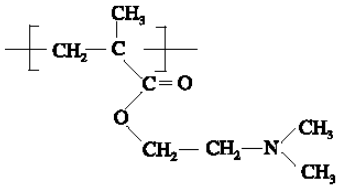

DMA

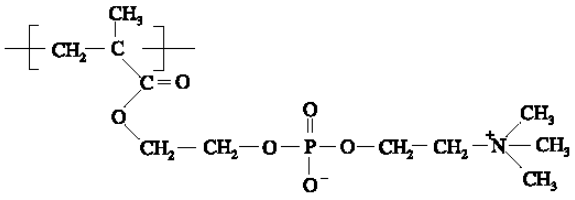

MPC

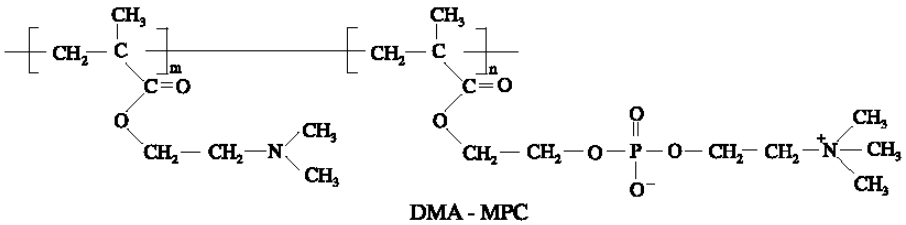

DMA - MPC

Figure 2.14. Chemical structures of DMAEMA homopolymer, MPC homopolymer and the DMAEMA–MPC diblock copolymers.[34] Reprinted from Journal of Controlled Release, Vol 100, J.K.W. Lam, Y. Ma, S.P. Armes, A.L. Lewis, T. Baldwin and S. Stolnik, "Phosphorylcholine–polycation diblock copolymers as synthetic vectors for gene delivery", Copyright 2004, with permission from Elsevier.

Transfection with various DMAEMA/MPC diblock compositions showed that transfection efficiency was greatly influenced by the chemical content of each monomer, with optimum transfection observed at DMAEMA DP=100 and MPC DP=30. Transmission electron microscopy was used to image polyplexes formed with the DMAEMA-MPC copolymer. The investigators observed rod and toroid morphologies, which are common structures for polyplexes.[37] The TEM images are shown in Figure 2.15.

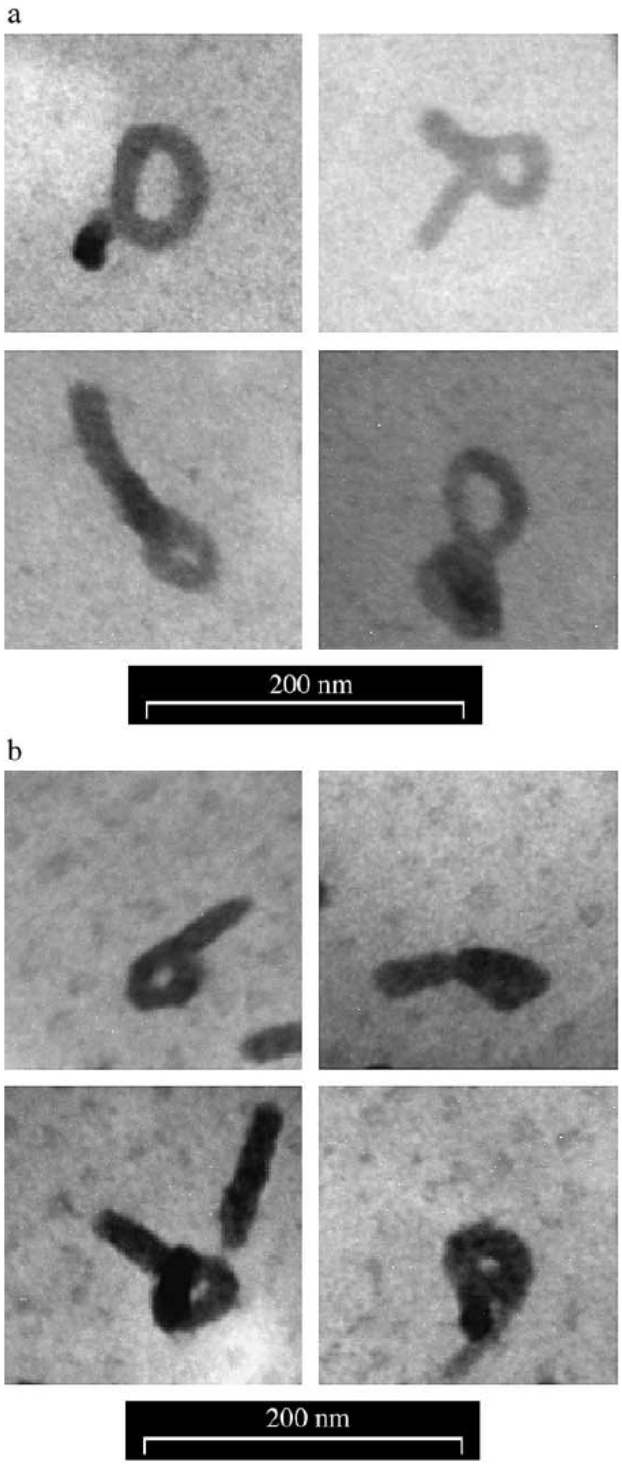

Figure 2.15. (a and b) TEM images of the DNA–copolymer complexes with $DMAEMA_{40}MPC_{30}$ and $DMAEMA_{40}MPC_{40}$ copolymers obtained at a 2:1 molar ratio, respectively (scale bar=200 nm in each case). These structures appear intermediate

between rod and toroid morphologies.[34] Reprinted from Journal of Controlled Release, Vol 100, J.K.W. Lam, Y. Ma, S.P. Armes, A.L. Lewis, T. Baldwin and S. Stolnik, "Phosphorylcholine–polycation diblock copolymers as synthetic vectors for gene delivery", Copyright 2004, with permission from Elsevier.

2.8 References

[1] Wang, Z.; Troilo1, P.J.; Wang, X.; Griffiths, T.G.; Pacchione, S.J.; Barnum, A.B; Harper, L.B.; Pauley, J.; Niu, Z.; Denisova, L.; Follmer, T.T.; Rizzuto, G.; Ciliberto, G.; Fattori, E.; Monica, N.; Manam, S.; and Ledwith, B.J. "Detection of integration of plasmid DNA into host genomic DNA following intramuscular injection and electroporation" *Gene Therapy* **2004**, 11, 711-721.

[2] Promega Corporation "pRL-SV40 Vector*" Promega Technical Bulletin No. 239* Revised July, **2001**

[3] Ma H.; and Diamond S. L. "Nonviral gene therapy and its delivery systems" *Current Pharmaceutical Biotechnology* **2001**, 2(1) 1-17.

[4] Morgan, R.A. and Anderson, W.F. "Human gene therapy" *Annu. Rev. Biochem*. **1993**, 62, 191-217.

[5] Grimm, D. and Kay, M.A. "From virus evolution to vector revolution" Use of naturally occurring serotypes of adeno-associated virus (AAV) as novel vectors for human gene therapy" *Current Gene Therapy*. **2003**, 3, 281-304.

[6] Miller, A.D. "The Problem with Cationic Liposome / Micelle-Based Non-Viral Vector Systems for Gene Therapy" *Current Medicinal Chemistry* **2003**, 10, 1195-1211.

[7] Boussif, O.; Lezoualc'h, F.; Zanta, M.A.; Mergny, M.D.; Scherman, D.; Demeneiz, B; and Behr, J.P. "A versatile vector for gene and oligonucleotide transfer into cells in culture and in vivo: polyethyleneimine" *Proc. Nat. Acd. Sci.* **1995**, 92, 7297-7301.

[8] Curiel, D.T.; Wagner, E.; Cotton, M.; Birnstiel, M.L.; Agarwal, S.; Li, c.M.; Loechel, S.; and Hu, P.C. "High-efficiency gene transfer mediated by adenovirus coupled to DNA-complexes" *Human Gene Therapy* **1992**, 3, 147-154.

[9] Kawai, S. and Nishizawa, M. "New procedure for DNA transfection with polycation and dimethyl sulfoxide" *Mol. Ce.. Biol*. **1984**, 4, 1171-1174.

[10] Felgner, P.L.; Barenholz, Y.; Behr, J.P.; Cheng, S.H.; Cullis, P.; Huang, L.; Jessee, J. A.; Symour, L.; Szoka, F.; Thierry, A.R.; Wagner, E.; and Wu, G. "Nomenclature for synthetic gene delivery systems" *Human Gene Therapy* **1997**, 8, 511-512

[11] Cherng, J.Y.; Talsma, H.; Verrijk, R.; Crommelin, D.J.; and Hennink, W.E. "The effect of formulation parameters on the size of poly-((2-dimethylamino)ethyl methacrylate)-plasmid complexes" *Eur. J. Pharm. Biopharm.* **1999**, 47, 215-224.

[12] Arigita, C.; Zuidam, N.J.; Crommelin, D.J.A.; and Hennink, W.E. "Association and dissociation characteristics of polymer/DNA complexes used for gene delivery" *Pharmaceutical Research* **1999**, 16(10), 1534-1541.

[13] Shen, Y.; Zhu, S.; Zeng, F.; and Pelton, R.H. "Versatile Initiators For Macromonomer Syntheses of Acrylates, Methacrylates and Styrene By Atom Transfer Radical Polymerization" *Macromolecules* **2000**, 33, 5399-5404.

[14]Zhang, X.; Xia, J.; Matyjaszewski, K. "Controlled/"living" Radical Polymerization of 2-(Dimethylamino)ethyl Methacrylate" *Macromolecules* **1998**, 31, 5167

[15]Liu, S.; Tang, Y.; Weaver, J.V.M.; Billingham, N.C.; Armes, S.P.; and Tribe, K. "Synthesis of shell cross-linked micelles with pH-responsive cores using ABC triblock copolymers" *Macromolecules* **2002**, *35*, 6121.

[16] Pantoustier, N.; Moins, S.; Wautier, M.; Degee, P.; and Dubois, P. "Solvent-free synthesis and purification of poly[2-(dimethylamino)ethyl methacrylate] by atom transfer radical polymerization" *Chem. Commun*. **2003**, 340-341.

[17] Cherng, J.Y.; van de Wetering, P.; Talsma, H.; Cromelin, D.J.A.; and Hennink, W.E. "Effect of size and serum proteins on transfection efficiency of poly((2-dimethylamino)ethyl methacrylate)-plasmid nanoparticles" *Pharm. Res*. **1996**, 13, 1038-1042.

[18] Verbaan, F.J.; Bos, G.W.; Oussoren, C.; Woodle, M.C.; Hennink, W.E.; and Storm, G. "A comparative study of different cationic transfection agents for in vivo gene delivery after intravenous administration" *Journal of Drug Delivery Science and Technology* **2004**, 14(2), 105-111.

[19] Cherng, J.Y.; Schuurmans-Nieuwenbroek, N.M.E.; Jiskoot, W.; Talsma, H.; Zuidam, N.J.; Hennink, W.E.; and Crommelin, D.J.A. "Effect of DNA topology on the transfection efficiency of poly((2-dimethylamino)ethyl methacrylate)–plasmid complexes" *Journal of Controlled Release* **1999**, 60, 343-353.

[20] Georgiou, T.K., Vamvakaki, M.; and Patrickios, C.S. "Nanoscopic Cationic Methacrylate Star Homopolymers: Syntheis by Group Transfer Polymerization, Characterization and Evaluation as Transfection Reagents" *Biomacromolecules* **2004**, 5, 2221-2229.

[21] van de Wetering, P; Moret, E.E; Schuurmans-Nieuwenbroek, N.M.E; van Steenbergen, M.J.; and Hennink, W.E. "Strcuture-Activity Relationships of Water-Soluble Cationic Methacrylate/Methacrylamide Polymers for Nonviral Gene Delivery" *Bioconjugate Chem*. **1999**, 10, 589-597.

[22] Van Rompaey, E.; Engelborghs, Y.; Sanders, N.; De Smedt, C. and Demeester, J. "Interactions Between Oligonucleotides and Cationic Polymers Investigated by Fluorescence Correlation Spectroscopy" *Pharmaceutical Research* **2001**, 18(7), 928-936.

[23] Leclercq, L.; boustta, M.; and Vert, M. "A Physico-chemical Approach of Polyanion-Polycation Interactions Aimed at Better Understanding the *In Vivo* Behaviour of Polyelectrolyte-based Drug Delivery and Gene Transfection" *Journal of Drug Targeting* **2003**, 11(3), 129-138.

[24] Zuidam, N.J.; Posthuma, G.; De Vries, E.T.J.; Crommelin, D.J.A.; Hennink, W.E.; and Storm, G. "Effects of physiochemical characteristics of poly(2-(dimethylamino)ethyl methacrylate)-based polyplexes on cellular association and internalization" *Journal of Drug Targeting* **2000**, 8(1), 51-66.

[25] Remy-Kristensen, A.; Clamme, J.P.; Vuilleumier, C.; Kuhry, J.G.; and Mely, Y. "Role of endocytosis in the transfection of L929 fibroblasts by polyethlenimine/DNA complexes" *Bio-Chem. Biophys. Acta* **2001**, 1514, 21-32.

[26] Jones, R.A.; Poniris, M.H.; and Wilson, M.R. "pDMAEMA is internalized by endocytosis but does not physically disrupt endosomes" *Journal of Controlled Release* **2004**, 96, 379-391

[27] Lucas, B.; Remaut, K.; Sander, N.N.; Braeckmans, K.; De Smedt, S.C.; and Demeester, J. "Studying the Intracellular Dissociation of Polymer-Oligonucleotide Complexes by Dual Color Fluorescence Fluctuation Spectroscopy and Confocal Imaging" *Biochemistry* **2005**, 44, 9905-9912.

[28] Rungsardthong, U.; Ehtezazi, T.; Bailey, L.; Armes, S.P.; Garnett, M.c.; and Stolnik, S. "Effect of Polymer Ionization on the Interation with DNA in Nonviral Gene Delivery Systems" *Biomacromolecules* **2003**, 4, 683-690.

[29] Dubruel, P.; Christiaens, B.; Rosseneu, M.; Vandekerckhove, J.; Grooten, J.; Goossens, V.; and Schacht, E. "Buffering Properties of Cationic Polymethacrylates Are Not the Only Key to Successful Gene Delivery" *Biomacromolecules* **2004**, 5, 379-388.

[30] van de Wetering, P.; Cherng, J.Y.; Talsma, H.; Crommelin, D.J.A.; and Hennink, W.E. "2-(dimethylamino)ethyl methacrylate based (co)polymers as gene transfer agents" *Journal of Controlled Release* **1998**, 53, 145-153.

[31] van de Wetering, P.; Schuurmans-Nieuwenbroek, N.M.E.; van Steenbergen, M.J.; Crommelin, D.J.A.; and Hennink, W.E. "Copolymers of 2-(dimethylamino)ethyl methacrylate with ethoxytriethylene glycol methacrylate or N-vinyl-pyrrolidone as gene transfer agents" *Journal of Controlled Release* **2000**, 64, 193-203

[32] Dubruel, P.; De Strycker, J.; Westbroek, P.; Bracke, K.; Temmerman, E.; Vandervoort, J.; Ludwig, A.; and Schacht, E. "Synthetic polyamines as vectors for gene delivery" *Polymer International* **2002**, 51, 948-957.

[33] Dubruel, P.; Christiaens, B.; Vanloo, B.; Bracke, K.; Rosseneu, M.; Vandekerckhove, J.; and Schacht, E. "Physiochemical and biological evaluation of cationic polymethacrylates as vectors for gene delivery" *European Journal of Pharmaceutical Sciences* **2003**, 18, 211-220

[34] Lam, J.K.W.; Ma, Y.; Armes, S.P.; Lewis, A.L.; Baldwin, T.; and Stolnik, S. "Phosphorylcholine-polycation diblock copolymers as synthetic vectors for gene delivery" *Journal of Controlled Release* **2004**, 100, 293-312

[35] Lewis, A.L. "Phosphorylcholine-based polymers and their use in the prevention of biofouling" *Colloids Surf., B Biointerfaces* **2000**, 18, 261-275

[36] Murphy, E.F.; Lu,J.R.; Lewis, A.L.; Brewer, J.; Russell, J.; and Stratford, P. "Characterization of protein adsorption at the phosphorylcholine incorporated polymer-water interface" *Macromolecules* **2000**, 33, 4545-4554

[37] Tang, M.X.; and Szoka, F.C. "The influence of polymer structure on the interaction of cationic polymers with DNA and morphology of the resulting complexes" *Gene Therapy* **1997**, 4, 828-832

Chapter 3. **Charged Polymers via Controlled Radical Polymerization and their Implications for Gene Delivery**

John M. Layman, William H. Heath, Askim F. Senyurt, and Timothy E. Long

3.1 Summary

Non-viral gene delivery agents are notorious for their poor nucleic acid transfection efficiency and relatively high cell cytotoxicity. Thus, many investigators are exploring the important parameters involved in charged polymer-mediated gene delivery, such as chemical composition, molecular weight, structural architecture, surface charge, etc. It is important to develop clear structure-property relationships in order to design successful nucleic acid delivery agents for gene therapy. To elucidate these relationships, well-defined materials are necessary. Controlled radical polymerization methods offer a facile route to systematically produce well-defined, structurally distinct gene delivery agents. The use of charged polymers prepared via controlled radical polymerizations to elucidate transfection mechanisms or develop new delivery vectors will be reviewed herein.

3.2 Introduction

The synthesis and characterization of charged polymers, also known as polyelectrolytes, is a rich and diverse field of study that dates back to the 1930's.[1] The presence of charged functionality produces interesting solid-state morphologies and

solution properties as a result of both, inter- and intramolecular Coulombic interactions. These properties have made charged polymers the focus of significant research as evidenced by the large number of papers, patents, and reviews on the subject.[1,2] Charged polymers have found use in a wide range of high performance applications including nanosensors, nanoactuators, artificial muscles, fuel cells, ion-exchange resins, semi-permeable membranes and floor coatings. Despite the often perceived maturity of this family of polymers, continued growth is evident through expanded polymerization techniques, creative new polymer compositions, and diverse applications. Due to their similarity to charged biopolymers, such as proteins, certain polysaccharides and nucleic acids, synthetic charged polymers have been intensively investigated for use in many biomedical applications.

Gene therapy, which involves the insertion of a target gene into cells to prevent or treat a disease associated with a mutant or defective gene, is a promising and rapidly developing therapeutic technique. It enables the correction of inherited or acquired genetic defects or the ablation of diseased cells such as tumors in cancer therapy. For efficacious gene therapy, a carrier vector is needed to escort the negatively charged nucleic acid through the cell membrane. There are two types of carriers used in gene therapy, viral and non-viral vectors. The safety and efficiency of the carriers are the primary issues of gene therapy. Although naked DNA can be delivered to cells, rapid enzymatic degradation of DNA and poor delivery efficiency are the major drawbacks of this method. Viral vectors (viruses), which are rendered replication deficient (deactivated), are effective delivery agents, however, there are numerous safety issues related with the use of viruses, such as immunogenicity and mutation of the host genome.

Charged lipids and polymers are safer alternatives and offer advantages such as facile synthesis, tunable properties (degradation, toxicity, charge density, and morphology), and efficient protection of DNA. However, they exhibit low transfection efficiency relative to viruses. There are several recent reviews discussing the advantages and disadvantages of viral and non-viral delivery vectors.[3-8]

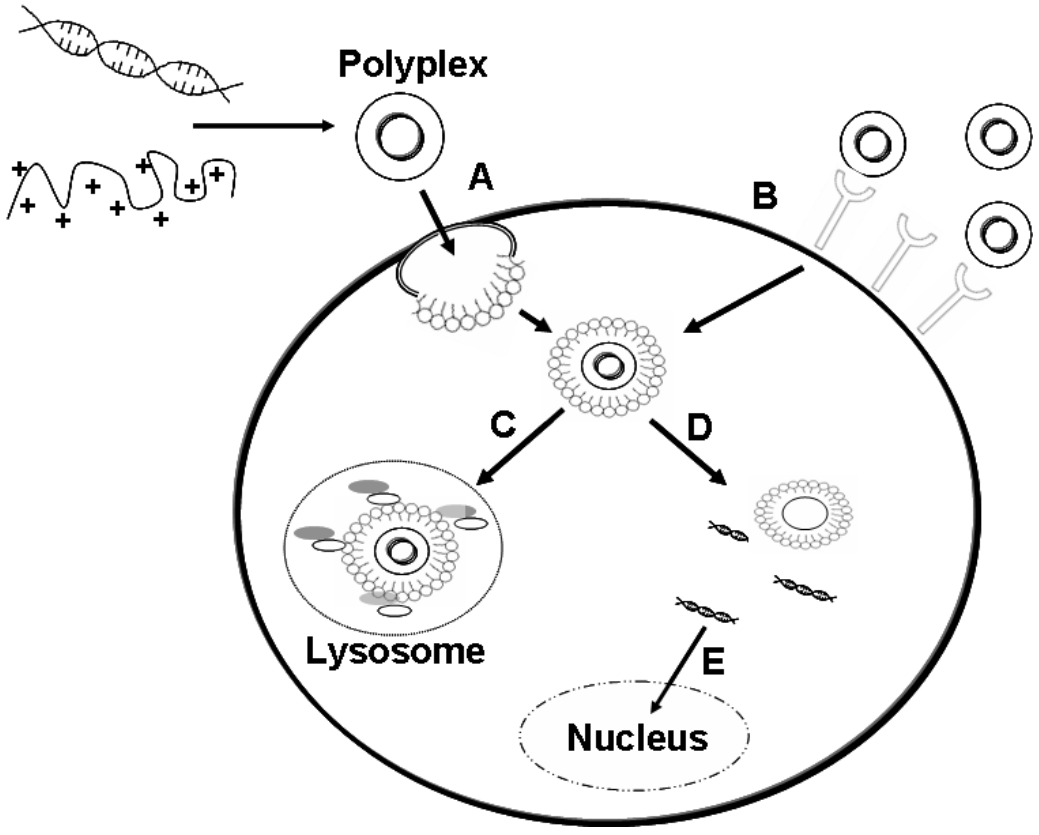

Figure 3.1. The intracellular pathways for the transfection of DNA-cationic polymer complex (polyplex) through the cell membrane, A) Non-specific endocytosis, B) receptor-mediated endocytosis, C) lysosome degradation, D) dissociation of polyplex and release of DNA, and E) translocation to nucleus.

Cationic polymers complex negatively charged DNA or RNA into neutral or positively charged polyplexes amenable to translocation across the negatively charged cell membrane. A schematic representation of possible gene delivery mechanisms is given in Figure 3.1. The cationic polymer condenses DNA into a small polyplex amenable to endocytosis. Polyplexes are transported into the cell by non-specific (pathway A), or receptor-mediated (pathway B) endocytosis. After cellular uptake, if the polyplex is not stable to nuclease degradation, it will be destroyed in the liposome (pathway C). Release of the genetic material from the polyplex (pathway D) allows the internalization of DNA into the nucleus (pathway D).

The majority of work done in polynucleotide delivery, has been done with natural polymers e.g. dextran, Chitosan, poly (L-lysine) or synthetic polymers such as PEI or PDMAEMA.[6] The different polymer architectures used in gene/drug delivery are given in Figure 3.2. Each of these systems has specific limitations.[3,8] An ideal non-viral vector should deliver the nucleic acid with high gene expression in the target cells without any inflammatory response. It should be biodegradable, non-toxic, stable against enzymatic degradation, and non-immunogenic. We are now learning that factors such as molecular weight, polydispersity, charge density, cationic or anionic functionality, polymer structure, charge ratio and size of the polymer-nucleic acid complex, as well as the pH of the medium play crucial roles in efficacy and toxicity for *in vitro* and *in vivo* applications.[5-8] The use of polymers as delivery vectors for non-viral gene therapy is well-established and has been extensively reviewed elsewhere.[3-8]

Researchers are developing more sophisticated gene and drug delivery vehicles and "living"/controlled polymerization techniques are vital synthetic tools for the

synthesis of well-defined, functionalized polymers that meet the long list of requirements for a potentially successful delivery system. This article will focus on recent advances in the synthesis of charged polymers via controlled radical polymerization for biomedical applications with an emphasis on gene delivery.

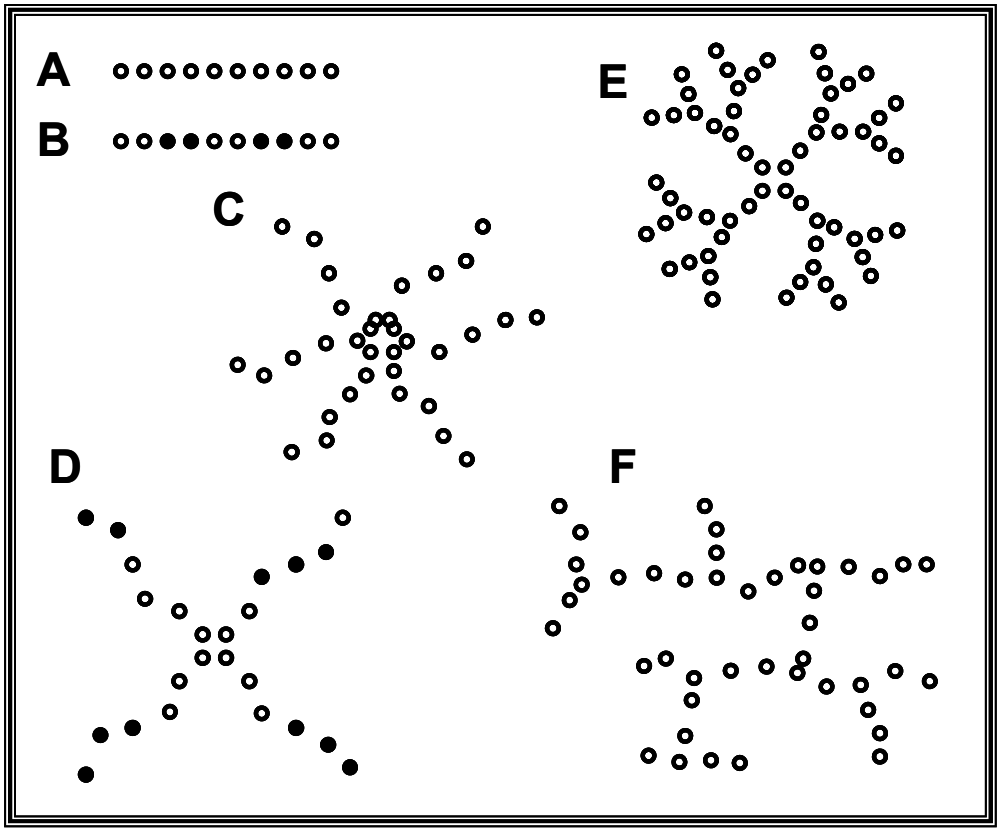

Figure 3.2 The polymer architectures used in gene/drug delivery, A) homopolymer, B) copolymer, C) star polymer, D) star copolymer, E) dendrimer, and F) branched polymer.

3.3 Synthesis of Linear Polymers by Controlled Radical Polymerization

It is important to differentiate the effects of polymer molecular weight, polydispersity, topology, and chemical structure on efficacy and toxicity of the polymeric delivery vectors.[4] Understanding structure-transfection relationships is critical in the development of clinically relevant non-viral gene delivery vectors. These relationships are difficult to assess with conventionally synthesized polymers. The complexity of the variables requires controlled polymerization techniques to identify key parameters for the development of efficient carriers.[9] ATRP is a process in which the propagating radicals are end-capped with a halide resulting in an equilibrium with transition metal species in the medium providing control over growing polymer chains. ATRP provides facile access to well-defined polymers, and several different polymers have been synthesized with this method for biomedical applications.[9,10] PDMAEMA is a cationic polymer at physiological pH which has been used extensively in gene transfection studies.[5] PDEAEMA is similar to PDMAEMA except the two methyl groups on the tertiary amine are switched for two ethyl groups; however it is not a viable polymer for transfection due to its toxicity.[11] The effect of this relatively small difference in the chemical structure of PDMAEMA-*b*-PEO and PDEAEMA-*b*-PEO was established by Too et al. after synthesizing block copolymers with ATRP.[11] PDEAEMA-*b*-PEO was found to form micellar structures at concentrations that coincided with maximum cytotoxicity indicating that membrane disruption may play a role in its cytotoxicity. Additionally, only small amounts of plasmid DNA were found in the cytosol indicating that membrane translocation, not polyplex dissociation, was the limiting factor in transfection for this polymer system.

It has been shown that the conjugation of PEG to polyelectrolytes increases aqueous solubility and reduces cytotoxicity by masking the polymer's positive charge.[7] The ability to initiate ATRP from a well defined macro-initiator has proven useful for the synthesis of controlled linear block copolymers.[10] Mallapragada et al. recently prepared a pentablock copolymer using ATRP, consisting of a PEO-*b*-PPO-*b*-PEO (also known as Pluronic^{TM}) triblock with terminal PDEAEMA blocks.[12] It was shown that biocompatibility was increased with the mole ratio of the Pluronic^{TM} block and the copolymers were less cytotoxic than the commercially available transfection agent ExGen 500^{TM}.[12] Stolnik and coworkers utilized ATRP to synthesize diblock copolymers of DMAEMA and PC in order to stabilize DNA complexes with the inclusion of a biomimetic zwitterionic functionality.[13]

Another approach to improve gene transfection and drug delivery is the use of cell targeting functionality. Again the use of functional initiators in ATRP provides a facile route to such conjugation. Stolnik et al. recently combined the biocompatibility of PC containing copolymers with the cell targeting ability of folic acid, a compound for which cancer cells over-express receptors on their cell membrane. An Fmoc-protected initiator was used to introduce a terminal folic acid unit for cell targeting through post-polymerization modification as shown in Figure 3.3.[14]

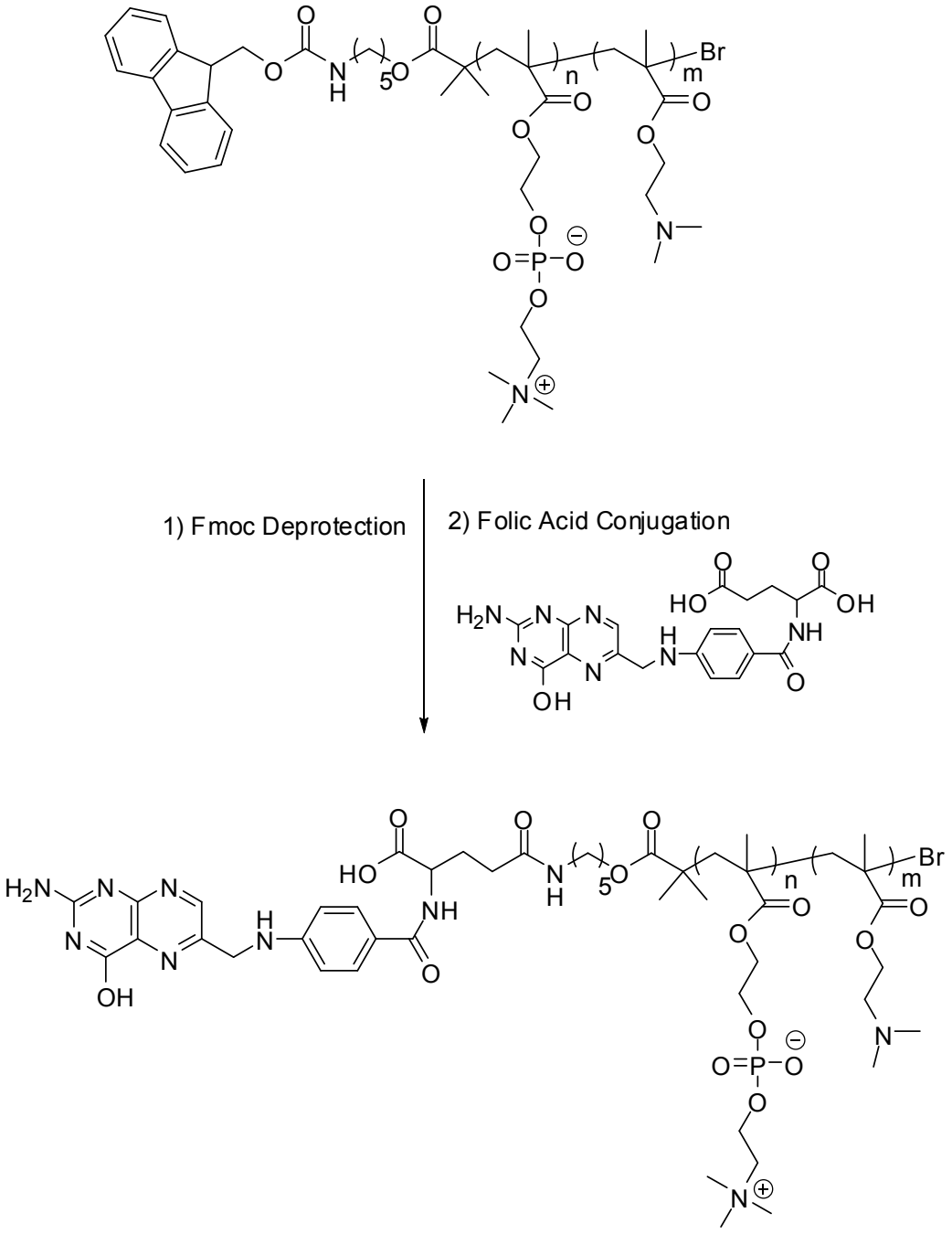

Figure 3.3. Synthesis of folic acid conjugated poly(PC-*b*-DMAEMA) by ATRP.

RAFT mediated polymerization is another controlled polymerization technique that is finding increased use in the preparation of charged polymers.[9,10,15-17] In addition to applicability to a wide range of monomers under non-stringent conditions, a possible

advantage of RAFT polymerizations over ATRP is that they do not require a transition metal catalyst which is highly toxic and must be removed prior to subsequent biomedical applications.[9,15]

McCormick and coworkers have greatly improved the synthetic utility of RAFT polymerizations by expanding the range of accessible monomers.[2,15,17,18] They recently reported the synthesis of poly(DMAPMA-*b*-HPMA) with well defined composition and low polydispersity (<1.11).[18] It was found that siRNA was efficiently complexed and protected from degradation under physiological conditions (Figure 3.4). Yanjarappa et al. employed RAFT mediated polymerization to synthesize the copolymer of HPMA with an active ester group which was subsequently bio-functionalized with a peptide sequence.[19] These well-defined polymer-peptide conjugates with low polydispersities (1.1-1.3) exhibited inhibitor potential for anthrax toxin. The authors speculated about the utility of activated poly(HPMA) for gene and drug delivery applications for future studies. RAFT mediated polymerizations have also been utilized in the synthesis of polybetaines.[2] Yusa et al. prepared poly(2-methacryloyloxyethylphosphorylcholine-*b*-n-butyl methacrylate) for use as a micellar solubilizer of the anticancer drug Paclitaxel.[20]

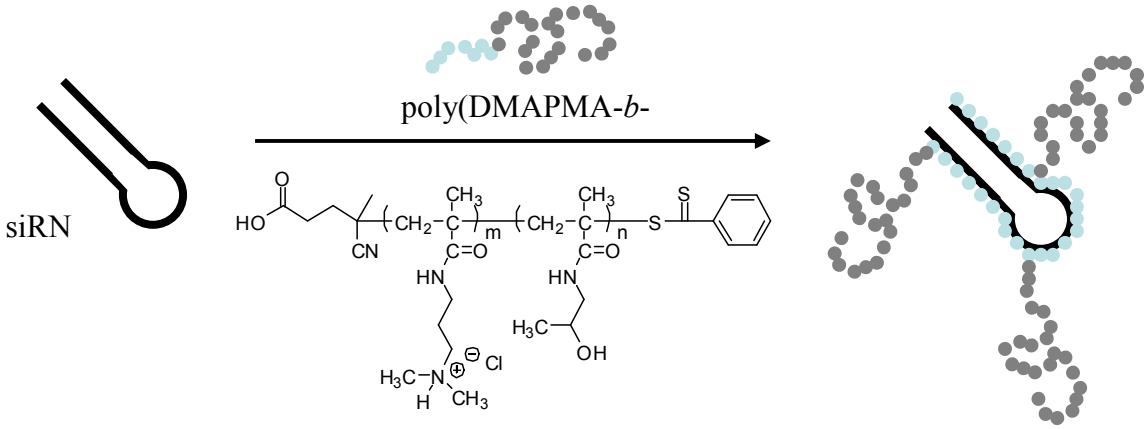

Figure 3.4. Synthesis of poly(DMAPMA-b-HPMA) by RAFT mediated polymerization for complexation of siRNA.

3.4 Synthesis of Star/Branched Polymers by Controlled Radical Polymerization

Dendrimers have received a great deal of attention as potential "nanocarriers" for the solubilization of hydrophobic drugs[21] and dendrimers such as PAMAM are now commercially available for research purposes as transfection aids either in intact (Polyfect®) or degraded (Superfect®) form.[5] The appeal of PAMAM dendrimers is their well defined unimolecular architecture and the ability to bind the nucleic acid with the peripheral amino groups while the inner amine groups provides buffer protection against endo-lysosomal degradation.[4] Studies have shown that the transfection ability of dendrimers is not simply dependent on their size and shape but also the flexibility of the polymer structure.[3-8] Thus, flexible star polymers form more compact DNA complexes and they are considerably easier to synthesize with less expensive methods. Recently

Georgiou et al. prepared a series of cationic PDMAEMA containing star copolymers by group transfer polymerization for DNA transfection.[22] In this first study, the star PDMAEMA homopolymers that had degrees of polymerization (DP) of the arms from 10 to 100, were synthesized and their ability to transfect human cervical cancer cells was studied. Their study showed that DMAEMA-star polymers with DP of 10 have slightly higher transfection efficiency with higher toxicities than linear DMAEMA and Superfect®. In an effort to reduce cell toxicity, star copolymers of DMAEMA with HEGMA were synthesized with different architectures. Incorporation of the HEGMA unit in the exterior reduced cytotoxicity and transfection efficiency, whereas, the opposite trend was observed when HEGMA was incorporated in the interior of the polymer structure.[23]

Leroux et al. recently used ATRP to prepare star-P(EMA-co-MAA)-b-P(PEGMA) from a tetrabis(2-bromoisobutyryl) pentaerythitolate initiator.[24] It was shown that the ionizable core aided in release of hydrophobic drugs when exposed to an alkaline environment. Xiao used a functional CD core for the direct aqueous polymerization of cationic [2-(methacryloyloxy)ethyl] trimethyl ammonium chloride by ATRP as shown in Figure 3.5. Although it was not tested, it was proposed as a potential DNA vector.[25]

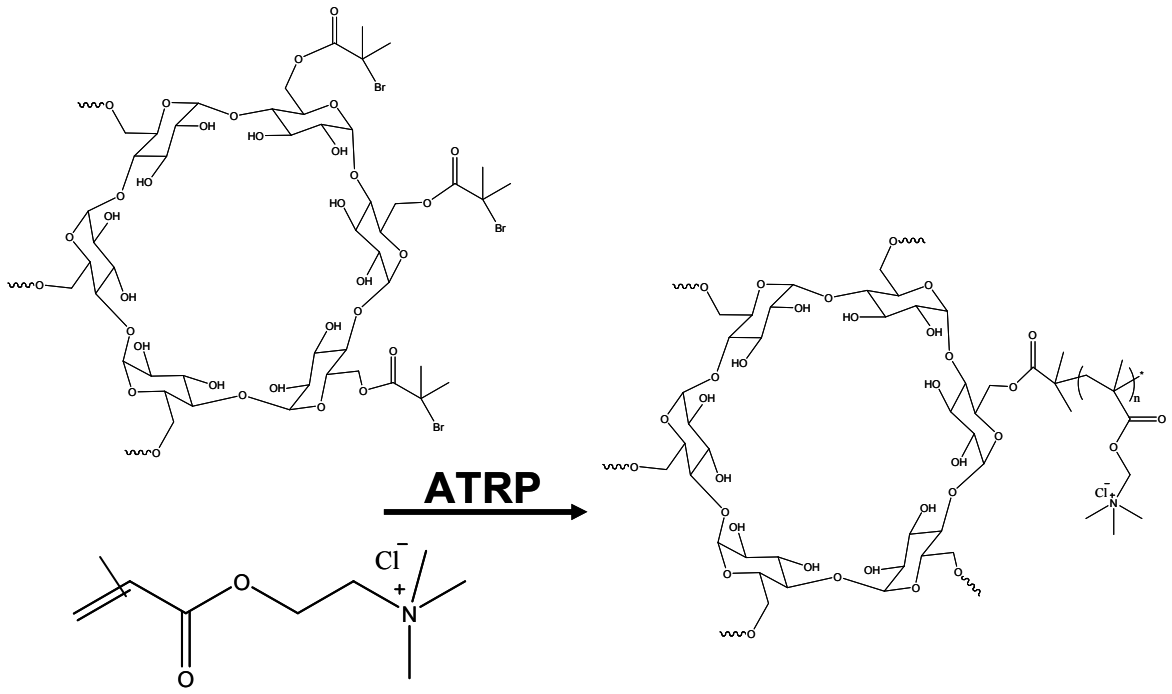

Figure 3.5. Synthesis of star-poly(TMAEMA) with 21 arms via ATRP polymerization by using a multifunctional cyclodextrin initiator.

There are significantly fewer examples of star polymers formed by RAFT mediated polymerizations due to the challenges encountered with this technique such as increased star-star coupling. Despite this, stars of modest polydispersity have been obtained when using the so-called Z-technique in which the RAFT agent is attached to the core through the Z group rather than the R group.[26,27] Wan et al. prepared poly(DMAEA-b-NIPA) stars from a dendritic polyglycerol macro-RAFT agent and subsequently crosslinked the PDMAEA core by quarternization with 1,8-diiodooctane (PDI <1.5).[28] An amphiphilic PS-*b*-PAA star polymer was prepared via the protected *t*-butyl acrylate with PDIs less than 1.5.[29] An alternative to the core-first route is the arm first route, which usually produces less well-defined products but eliminates star-star coupling. Stenzel was able to overcome this by self-assembling amphiphilic block co-

polymers prepared by RAFT before crosslinking the core and obtained PDIs below 1.25.[30] This appears to be an attractive route to "star-like" polymers via RAFT polymerizations in light of the fact that many of the polymers of interest are amphiphilic in nature. Although these polymers were not applied to biomedical applications, they illustrate the potential to prepare charged star polymers with diverse monomer compositions that are only available via RAFT polymerization.

It has been shown that partial degradation of dendrimers does not drastically decrease their ability to function as drug delivery aids. Therefore, it can be hypothesized that branched polymers, though less well-defined, should also be good candidates. An attractive method for the preparation of branched polymers is via the so-called "self-condensing vinyl copolymerization" (SCVCP) technique originally reported by Fréchet, and due to the living nature, provides branched polymers of lower polydispersity.[31] Müller recently reported the SCVCP of DEAEMA with the AB* inimer, BIEM, using ATRP to provide highly branched polymers with M_n ranging from 6.3-35 kg/mol and PDIs of 1.20-2.75.[32] Armes et al. also reported the controlled anionic copolymerization of DMAEMA with EGDMA using potassium benzyl alkoxide as an initiator. This is significant because oxyanionic polymerizations were previously thought to only occur in the presence of functional monomers that could coordinate to the K^+ counterion increasing the reactivity of the oxyanion.

Our laboratories are currently focused on synthesizing various topologies of PDMAEMA using EGDMA as the branching agent and 1-dodecanthiol as a CTA to control the level of branching. The main objective of this work is to evaluate the influence of the level of branching on transfection efficiency and cell cytotoxicity.[33,34]

We have found that an increase in branching in low M_W (*ca*. 100,000) PDMAEMA has an insignificant effect on efficiency, while high M_W (*ca*. 350,000) samples showed improved transfection activity with increased levels of branching. The molecular mechanisms responsible for the increased transfection efficiency observed are still unclear. Additionally, it is difficult to distinguish branching effects from polydisperisty effects associated with conventional polymerization methods. Controlled polymerization techniques are necessary to address this issue in future investigations.

3.5 Outlook

Recent advances in controlled polymerization techniques in conjunction with molecular biology provide insight into the controlling parameters of gene and drug delivery, which in turn aids in the development of more efficient carrier vectors. In this article, a brief discussion of the new strategies for the synthesis of charged polymers via controlled free radical polymerization and their biomedical applications is provided. Controlled polymerization techniques have proven to be useful for creating different polymer architectures with precise molecular weights, charge densities, and low molecular weight distributions. These are important parameters for the polymer/drug or polymer/nucleic acid complex formation, however high transfection efficiencies in target cells have not yet been realized. More sophisticated functionalized polymers may be required to gain entry into the cell without disrupting its integrity yet providing high gene expressions. Development of stimuli-responsive polymers for adjusting the pH changes in the cell environment or introducing bioreversible crosslinked units are proposed strategies for the delivery systems by utilizing controlled radical polymerization techniques.

In order to elucidate structure-transfection relationships, future research will benefit from materials produced via controlled living polymerization. Previous efforts by pioneers in the field of controlled polymerizations have made these techniques accessible to most synthetic polymer chemists. With these advances in synthetic polymer chemistry, there is great potential for continued success in the discovery of non-viral gene delivery agents.

3.6 References

[1]Eisenberg, A.; Kim, J.-S. *Introduction to Ionomers*, 1998.

[2]Lowe Andrew, B.; McCormick Charles, L. *Chemical reviews* **2002**, *102*, 4177-89.

[3]Kodama, K.; Katayama, Y.; Shoji, Y.; Nakashima, H. *Curr Med Chem FIELD Full Journal Title:Current medicinal chemistry* **2006**, *13*, 2155-61.

[4]Haag, R.; Kratz, F. Angewandte Chemie (International ed. in English) **2006**, 45, 1198-215.

[5]Eliyahu, H.; Barenholz, Y.; Domb, A. J. *Molecules* **2005**, *10*, 34-64.

[6]Tiera Marcio, J.; Winnik Fran Oise, M.; Fernandes Julio, C. *Curr Gene Ther FIELD Full Journal Title:Current gene therapy* **2006**, *6*, 59-71.

[7]Dubruel, P.; Schacht, E. *Macromolecular Bioscience* **2006**, *6*, 789-810.

[8]Lv, H.; Zhang, S.; Wang, B.; Cui, S.; Yan, J. *Journal of Controlled Release* **2006**, *114*, 100-109.

[9]Ali, M.; Brocchini, S. *Advanced Drug Delivery Reviews* **2006**, *58*, 1671-1687.

[10]Braunecker, W. A.; Matyjaszewski, K. *Progress in Polymer Science* **2007**, *32*, 93-146.

[11]Tan, J. F.; Hatton, T. A.; Tam, K. C.; Too, H. P. *Biomacromolecules* **2007**, *8*, 448-54.

[12]Agarwal, A.; Unfer, R.; Mallapragada, S. K. *Journal of Controlled Release* **2005**, *103*, 245-258.

[13]Lam, J. K. W.; Ma, Y.; Armes, S. P.; Lewis, A. L.; Baldwin, T.; Stolnik, S. *Journal of controlled release : official journal of the Controlled Release Society* **2004**, *100*, 293-312.

[14]Licciardi, M.; Tang, Y.; Billingham, N. C.; Armes, S. P.; Lewis, A. L. *Biomacromolecules* **2005**, *6*, 1085-1096.

[15]Lowe, A. B.; McCormick, C. L. *Progress in Polymer Science* **2007**, *32*, 283-351.

[16]Moad, G.; Rizzardo, E.; Thang, S. H. *Australian Journal of Chemistry* **2005**, *58*, 379-410.

[17]Lokitz, B. S.; Lowe, A. B.; McCormick, C. L. *ACS Symposium Series* **2006**, *937*, 95-115.

[18]Scales, C. W.; Huang, F.; Li, N.; Vasilieva, Y. A.; Ray, J.; Convertine, A. J.; McCormick, C. L. *Macromolecules* **2006**, *39*, 6871-6881.

[19]Yanjarappa, M. J.; Gujraty, K. V.; Joshi, A.; Saraph, A.; Kane, R. S. *Biomacromolecules* **2006**, *7*, 1665-1670.

[20]Yusa, S.-I.; Fukuda, K.; Yamamoto, T.; Ishihara, K.; Morishima, Y. *Biomacromolecules* **2005**, *6*, 663-670.

[21]Duncan, R.; Izzo, L. *Advanced drug delivery reviews* **2005**, *57*, 2215-37.

[22]Georgiou Theoni, K.; Vamvakaki, M.; Patrickios Costas, S.; Yamasaki Edna, N.; Phylactou Leonidas, A. *Biomacromolecules* **2004**, *5*, 2221-9.

[23]Georgiou Theoni, K.; Vamvakaki, M.; Phylactou Leonidas, A.; Patrickios Costas, S. *Biomacromolecules* **2005**, *6*, 2990-7.

[24]Jones, M.-C.; Ranger, M.; Leroux, J.-C. *Bioconjugate Chemistry* **2003**, *14*, 774-781.

[25]Li, J.; Xiao, H.; Kim, Y. S.; Lowe, T. L. *Journal of Polymer Science, Part A: Polymer Chemistry* **2005**, *43*, 6345-6354.

[26]Barner-Kowollik, C.; Davis, T. P.; Stenzel, M. H. *Australian Journal of Chemistry* **2006**, *59*, 719-727.

[27]Perrier, S.; Takolpuckdee, P. *Journal of Polymer Science, Part A: Polymer Chemistry* **2005**, *43*, 5347-5393.

[28]Wan, D.; Fu, Q.; Huang, J. Journal of Polymer Science, Part A: Polymer Chemistry **2005**, 43, 5652-5660.

[29]Whittaker, M. R.; Monteiro, M. J. *Langmuir* **2006**, *22*, 9746-9752.

[30]Zhang, L.; Katapodi, K.; Davis, T. P.; Barner-Kowollik, C.; Stenzel, M. H. *Journal of Polymer Science, Part A: Polymer Chemistry* **2006**, *44*, 2177-2194.

[31]Hawker, C. J.; Frechet, J. M. J.; Grubbs, R. B.; Dao, J. *Journal of the American Chemical Society* **1995**, *117*, 10763-4.

[32]Mori, H.; Walther, A.; Andre, X.; Lanzendoerfer, M. G.; Mueller, A. H. E. *Macromolecules* **2004**, *37*, 2054-2066.

[33]Layman, J. M.; Hirani, A. A.; Pickel, J. M.; Britf, P. F.; Lee, Y. W.; Long, T. E. *Polymer Preprints (American Chemical Society, Division of Polymer Chemistry)* **2006**, *47*, 70-71.

[34]Layman, J. M.; Hirani, A. A.; McKee, M. G.; Britt, P. F.; Pickel, J. M.; Lee, Y. W.; Long, T. E. *Polymer Preprints (American Chemical Society, Division of Polymer Chemistry)* **2006**, *47*, 39-40.

Chapter 4. **Synthesis and Aqueous Solution Characterization of Linear and Randomly Branched Poly(2-N,N'-dimethylaminoethyl methacrylate)**

John M. Layman,[†] Sean M. Ramirez,[†] Joseph M. Pickel,[‡] Phillip F. Britt,[‡]

and Timothy E. Long[†]

[†]Department of Chemistry, Macromolecules and Interfaces Institute, Virginia Tech, Blacksburg, Virginia 24061-0131

[‡]Center for Nanophase Materials Sciences (CNMS), Oak Ridge National Laboratory, Oak Ridge, Tennessee 37831-6197

4.1 Abstract

Conventional free radical polymerization was used to synthesize various molecular weights of linear and randomly branched cationic polyelectrolytes based on poly(2-N,N'-dimethylaminoethyl methacrylate) (PDMAEMA). Randomly long-chain branched (LCB) topologies were synthesized utilizing ethylene glycol dimethacrylate as a branching agent. Additionally, a chain transfer agent (1-dodecanthiol, DT) was added during polymerization to prevent gelation and tune topology. Aqueous size exclusion chromatography (SEC), coupled with multiangle laser light scattering (MALLS), differential refractive index (dRI), and capililary viscometer detectors, was employed to

characterize polymer molecular weight, radius of gyration, and intrinsic viscosity as a function of molecular weight distribution. The level of branching was quantified using the well-established, semi-quantitative, g' contraction factor, which is the ratio of intrinsic viscosities of branched and linear polymers at equivalent molar mass. Dynamic light scattering (DLS) was used to study the hydrodynamic behavior of polyelectrolyte chains in different aqueous salt (NaCl) and pH conditions. The results indicated that the level of branching in PDMAEMA was not sensitive to the incorporation of DT. However, the molecular weight of the resulting branched polyelectrolytes were significantly influenced by the addition of chain transfer agent. The hydrodynamic sizes of linear and randomly branched PDMAEMA were influenced by the addition of salt and pH. In addition, linear PDMAEMA displayed the characteristic polyelectrolyte effect in response to polymer concentration.

KEYWORDS polyelectrolytes, branched polyelectrolytes, g' contraction factor, aqueous SEC

4.2 Introduction

Cationic polyelectrolytes are currently being explored as non-viral alternatives in the delivery of therapeutic nucleic acids.[1-3] Macromolecular architecture is an important parameter in the design of polyelectrolytes for gene delivery.[4-12] Although these references described the importance of molecular topology, many describe linear versus branched polymers categorically, and it is necessary to fundamentally understand the role of branching in a more quantitative fashion. In an attempt to address this issue, we

describe the level of branching in our cationic polyelectrolytes using the well-established, semi-quantitative, g' contraction factor. This dimensionless value is calculated as the ratio of the intrinsic viscosities of branched and linear polymers at equivalent molecular weight. This viscometric method provides an easy and rapid approach to phenomenologically characterize the level of branching in polymers. This contraction factor has been employed in earlier efforts by Müller et al. to characterize branching in a similar polyelectrolyte, poly(2-diethylaminoethyl methacrylate).[13] In addition, other investigators have utilized solution parameters, such as the Mark-Houwink-Sakurada (MHS) alpha value, to evaluate incidental branching in other polycationic systems.[14-16]

Polyelectrolytes are unique in their ability to change conformation in response to solution environment.[17] Polyelectrolytes typically adopt rod-like conformations due to mutual charge repulsion along the polymer backbone.[17] However, the introduction of salt or a change in pH can drastically influence the conformation of polyelectrolytes. Previous work by Sherrington et al. has shown that the addition of branching in charged polymers suppressed the polyelectrolyte effect.[18] The authors proposed that branched polyelectrolytes are not able to undergo significant changes in conformation due to the compactness of branched structures. In addition to having a more "fixed" structure, Koper et al. has shown that it is more difficult to protonate branched polyelectrolytes due to neighboring mutual charge interactions that would be forced during the protonation of branched structures.[19]

In this study, linear and randomly branched cationic polyelectrolytes based on poly(2-N,N'-dimethylaminoethyl methacrylate) (PDMAEMA), a transfectant pioneered and widely studied by the group of Hennink et al.[20-30] were synthesized by conventional

free-radical polymerization methods. The level of random, long-chain branching was characterized utilizing dilute solution viscometry. This dilute solution characterization was accomplished using an online viscosity detector attached to an aqueous size exclusion chromatography (SEC) system. This system, which also employed a multiangle laser light scattering (MALLS) detector and a differential refractive index (dRI) detector, simultaneously provides molecular weight and viscosity measurements across a given molecular weight distribution. Additionally, dynamic light scattering (DLS) was used to study the hydrodynamic behavior of linear and randomly branched PDMAEMA in different aqueous environments. Specifically, we studied the hydrodynamic size of both linear and branched topologies as a function of polymer concentration, NaCl concentration, and pH.

4.3 Experimental Section

4.3.1 Materials.

2-(N,N'-dimethylamino)ethyl methacrylate (DMAEMA, 98%, Sigma-Aldrich) was passed through a neutral alumina column to remove free-radical inhibitor. 2,2'-azobisisobutyronitrile (AIBN, 99%, Sigma-Aldrich) and ammonium persulfate (APS, 98%, Sigma-Aldrich) were used as received. The branching agent ethylene glycol dimethacrylate (EGDMA, 98%, Sigma-Aldrich) was passed through a neutral alumina column to remove free-radical inhibitor. Deuterium oxide (D_2O, 99.9%, Cambridge Isotope Laboratories) was used as received for all NMR measurements. Sodium nitrate ($NaNO_3$, 99.0%, Alfa Aesar), trishydroxymethylaminomethane (TRIS, 99.8%, Alfa Aesar), glacial acetic acid (AcOH, 99.7%, Alfa Aesar), sodium azide (NaN_3, 99%, Alfa

Aesar), sodium chloride (NaCl, 99.0%, Sigma-Aldrich), 1-dodecanethiol (DT, 98%, Sigma-Aldrich) were all used as received. Ultrapure water having a resistivity of 18.2 MΩ·cm was obtained using a Millipore Direct-Q5 purification system. All other solvents and reagents were used as received from commercial sources unless specifically noted elsewhere.

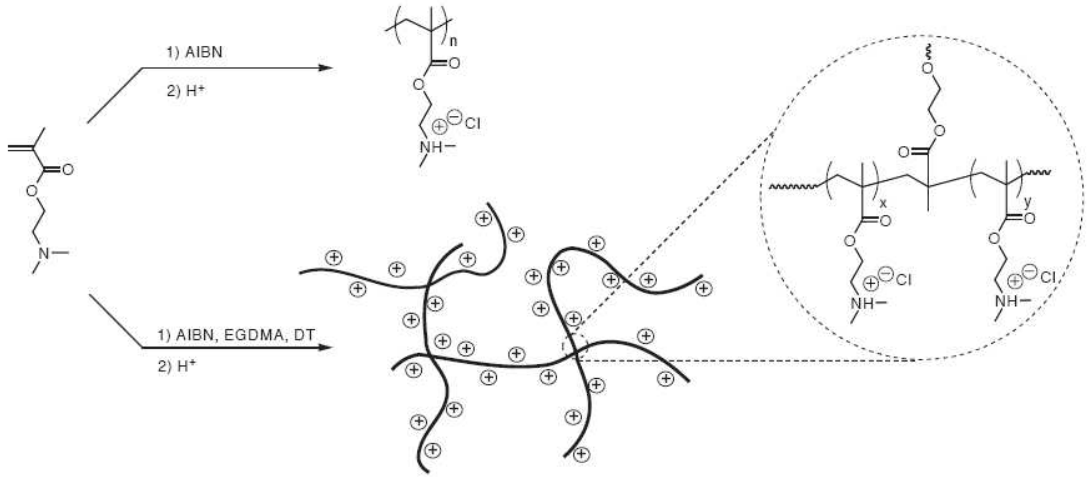

Scheme 4.1. Synthetic approach used to produce linear and randomly branched PDMAEMA polyelectrolytes.

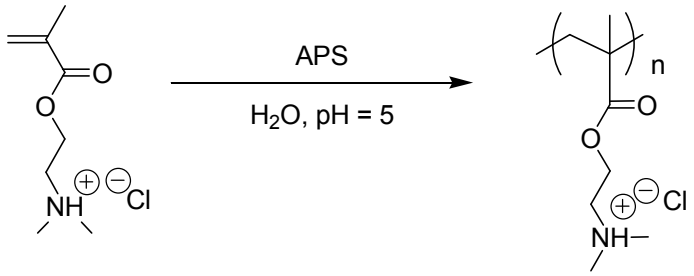

Scheme 4.2. Aqueous synthesis of linear PDMAEMA·HCl polyelectrolytes.

4.3.2 Synthesis of linear poly(2-N,N'-dimethylaminoethyl methacrylate).

In a typical synthesis, DMAEMA was charged with AIBN (0.10-0.30 wt% monomer) in THF at 20 wt% solids in a multi-necked, round-bottomed flask. A reflux condenser was affixed to the flask and the reaction mixture was purged with nitrogen for approximately 30 min. The flask was then submerged in an oil bath preheated to 60 ^{o}C. The polymerization was allowed to proceed for 24 h under magnetic stirring. The resulting polymer was precipitated in hexanes. After decantation of the hexanes, the polymer was dried under vacuum at 80 ^{o}C. Dissolution of the neutral PDMAEMA product in aqueous HCl (pH=5.0) under magnetic stirring was used to convert each polymer to a hydrochloride salt. The PDMAEMA·HCl polyelectrolyte was then precipitated in acetone. The acetone was decanted and the white powder product was dried under vacuum at 80 ^{o}C. To synthesize higher molecular weight PDMAEMA, DMAEMA was charged with APS (0.1-1.0 wt% monomer) in ultrapure water at 20 wt% solids in a multi-necked, round-bottomed flask. The pH of the reaction solution was adjusted to 5 using concentrated HCl prior to polymerization. A rubber septum was affixed to the flask and the reaction mixture was purged with nitrogen for approximately 30 min. The flask was then submerged in an oil bath preheated to 60 ^{o}C. The polymerization was allowed to proceed for 24 h under magnetic stirring. The resulting polymer was precipitated in acetone.

All samples were dialyzed against distilled water for at least 48 h using Spectra/Por dialysis tubing (MWCO=3,500 g/mol). Lyophilization was used to recover samples prior to characterization. ^{1}H NMR (400 MHz, D_2O): δ (ppm)= 4.40 (br, 2H),

3.59 (br, 2H), 3.01 (br, 6H), 2.05 (br, 2H), 1.02 (br, 3H). M_n and M_w are summarized in Table 4.1 and Table 4.2.

4.3.3 Synthesis of randomly branched poly(2-N,N'-dimethylaminoethyl methacrylate):

Randomly branched PDMAEMA was synthesized and isolated using the methods described above with the addition of EGDMA (0.10-2.0 wt% monomer). A chain transfer agent (1-dodecanethiol) was needed to prevent gelation in reactions where the EGDMA concentration was 1.0 wt% and higher. The molar ratio of dodecanethiol to EGDMA was adjusted between 0.5:1 to 1:1. ^{1}H NMR (400 MHz, D_2O): δ (ppm)= 4.40 (br, 2H), 3.59 (br, 2H), 3.01 (br, 6H), 2.05 (br, 2H), 1.02 (br, 3H). M_n and M_w are summarized in Table 4.3.

4.3.4 Aqueous size exclusion chromatography-multiangle laser light scattering (SEC-MALLS).

Aqueous SEC experiments were run in a buffered solution consisting of 0.7 M sodium nitrate and 0.1 M TRIS adjusted to pH 6.0 with glacial acetic acid. The pH of the resulting solution was measured using a Thermo Orion 3 Star portable pH meter equipped with a Thermo Orion Triode pH electrode. Sodium azide was added at 200 ppm to the solution as a precaution to prevent bacterial growth in the SEC system. Samples were analyzed at 0.8 mL/min through 2x Waters Ultrahydrogel Linear and 1x Water Ultrahydrogel 250 columns, with all columns measuring 7.8 x 300 mm and equilibrated to 30 ^{o}C. SEC-MALLS instrumentation consisted of a Waters 1515 isocratic HPLC pump, Waters 717plus Autosampler, Wyatt miniDAWN multiangle laser light

scattering (MALLS) detector operating a He-Ne laser at a wavelength of 690 nm, Viscotek 270 capillary viscosity detector, and a Waters 2414 differential refractive index detector operating at a wavelength of 880 nm and 35 ^{o}C. The only calibration constant, the Wyatt Astra V AUX1, was calculated using a series of aqueous sodium chloride solutions. The accuracy and reproducibility was confirmed with poly(ethylene oxide) (Sigma-Aldrich) standards ranging in molecular weight from 230 to 1,000,000 g/mol. Absolute molecular weights and intrinsic viscosities were determined using the Wyatt Astra V and Viscotek OmiSEC software packages, respectively. The specific refractive index increments (*dn/dc*) for linear and randomly branched PDMAEMA were determined offline. A Wyatt OptiRex differential/absolute refractive index detector operating at a wavelength of 690 nm and 30 ^{o}C was used for all specific refractive index increment measurements. Polymer samples (0.05 – 2.00 mg/mL) were allowed to dissolve in the SEC mobile phase overnight. Samples were metered at 0.8 mL/min into the RI detector at 30 ˚C using a syringe pump and a syringe affixed with a 0.45 μm PTFE syringe filter. The *dn/dc* values were determined using the Wyatt Astra V software package.

The level of branching in synthesized samples was measured using the g' contraction factor, which is the ratio of the intrinsic viscosities of a branched polymer to a linear polymer at equivalent molecular weight, see Equation 1.

$$g' = \frac{[\eta]_{branched}}{[\eta]_{linear}} \qquad (1)$$

Since branched macromolecules have smaller hydrodynamic sizes than a linear analog at identical molecular weight, their intrinsic viscosity is lower. Thus, g' values are always less than one. Therefore, as the level of branching increases at a given molecular weight, g' decreases.

4.3.5 Dynamic light scattering (DLS) of aqueous PDMAEMA solutions.

Dynamic light scattering measurements were performed on a Malvern Zeta Sizer Nano Series Nano-ZS instrument at a wavelength of 633 nm using a 4.0 mW, solid state He-Ne laser at a scattering angle of 173˚ using Dispersion Technology Software (DTS) version 4.20. All experiments were performed at a temperature of 25 ˚C. Data was reported as the intensity-average of the nominal peak corresponding to free polymer chains. All measurements were performed in triplicate and reported as the mean ± standard deviation (S.D.). The refractive index and viscosity for aqueous NaCl solutions were obtained from the literature.[31]

Aqueous salt solutions were prepared by dissolving anhydrous NaCl in ultrapure water at 5 mols/L, and then diluting the stock solution into lower molarity aliquots. Polymer samples were prepared at 0.2 mg/mL (below the overlap concentration for PDMAEMA) and allowed to dissolve in the salt solutions overnight. The pH of all PDMAEMA NaCl solutions was measured to be approximately 5 (measured using a Thermo Orion 3 Star portable pH meter) and little variability was observed between samples.

To produce polymer solutions with varying pH, 100 mL of 0.2 mg/mL PDMAEMA in 0.15 M NaCl was adjusted to a pH of 10.5 using 0.5 M NaOH. One mL

aliquots were then sampled as a function of pH as the solution was titrated with 0.5 M HCl. We assumed the NaCl produced during neutralization of NaOH with HCl to be insignificant in comparison to original NaCl solution molarity of 0.15 M. All samples were syringed through 0.45 μm PTFE syringe filters directly into a clean 50 μL cuvette.

4.3.6 Potentiometric titration of linear and randomly branched PDMAEMA.

pH measurements were performed using a Thermo Orion 3 Star portable pH meter equipped with a Thermo Orion Triode pH electrode. Both linear and branched PDMAEMA were dissolved at 1 mg/mL in ultrapure water having a resistivity of 18 MΩ·cm. Using 15 mL of polymer solution, the pH was then adjusted to ~10.5 using 100 μL aliquots of 0.5 M NaOH. The solutions were then titrated with 20-40 μL aliquots of 0.1 N HCl. The pH of the solution was measured after the addition of each aliquot.

4.4 Results and Discussion

Conventional free-radical polymerization methods were employed to prepare PDMAEMA polyelectrolytes with various topologies and molecular weights. ^{1}H NMR spectroscopy verified the chemical structure all polymers. However, in randomly branched polymers, protons from the ethylene linkage of the EGDMA crosslinker were undetectable by ^{1}H NMR since the concentration of the branching agent was less than 1 mol%. To obtain absolute molecular weights by SEC-MALLS, the specific refractive index increment (*dn/dc*) of the polymer in the mobile phase of the SEC system must be accurately known.[32] Due to counter-ion dissociation and sample adsorption, online 100% mass recovery methods cannot be used to obtain *dn/dc* values of polyelectrolytes.

Batch-mode *dn/dc* measurements revealed that linear samples had *dn/dc* values ranging from 0.145-0.149 ± 0.002 mL/g and randomly branched polymers had similar values, around 0.146-0.148 ± 0.002 mL/g.

The aqueous SEC-MALLS molecular weights of linear and randomly branched PDMAEMA synthesized in organic solvent are summarized in Tables 1-3. Results showed weight-average molecular weights of linear and randomly branched polymers between 43,000 and 1,210,000 g/mol with polydispersities ranging from 1.17-5.40. The molecular weights of samples synthesized in acidic aqueous solution are summarized in Table 4.2. The relatively narrow molecular weight distributions in some polymers were attributed to slight sample adsorption occurring during aqueous SEC measurements. This adsorption phenomenon is common when high-salt eluents are used for aqueous SEC since hydrophobic interactions become more prevalent.[32] However, adsorption does not interfere with the measurement of the weight-average molecular weight and only slightly overestimates the number-average molecular weight.[32]

Table 4.1. Summary of synthetic conditions used to synthesize low and intermediate molecular weight linear PDMAEMA and resulting molecular weights.

sample	AIBN (wt.%)	M_w (g/mol)	M_n (g/mol)	M_w/M_n
L1	0.10	215,000	158,000	1.36
L2	0.25	152,000	85,000	1.79
L3	0.75	119,000	55,000	2.16
L4	1.00	105,000	62,000	1.69
L5	3.00	80,000	52,000	1.54
L6	6.00	43,000	25,000	1.72

Table 4.2. Summary of synthetic conditions used to synthesize high molecular weight linear PDMAEMA and resulting molecular weights.

sample	APS (wt.%)	M_w (g/mol)	M_n (g/mol)	M_w/M_n
L7	0.25	1,210,000	470,000	2.58
L8	0.50	527,000	326,000	1.62
L9	0.50	324,000	109,000	2.97
L10	0.75	915,000	405,000	2.26
L11	1.50	563,000	244,000	2.31

The aqueous SEC chromatograms (LS traces) of linear PDMAEMA·HCl synthesized in THF are shown in Figure 4.1. As expected, the molecular weights of the PDMAEMA·HCl polyelectrolytes increased with decreasing concentrations of AIBN. The molecular weight distributions ranged from 1.36 to 2.16. The aqueous SEC chromatograms (LS traces) of linear PDMAEMA·HCl synthesized from acidic aqueous solution are shown in Figure 4.2. Aqueous polymerizations resulted in higher molecular weights due to the absence of chain transfer events.[33] Additionally, changing the initiator concentration (APS) in aqueous polymerizations did not provide the same degree of control when compared to organic solvent-based synthesis. The molecular weight distributions for the aqueous syntheses ranged from 1.62 to 2.97. The higher polydispersities (compared to the THF syntheses) likely resulted from the inability to completely degass reaction solutions.

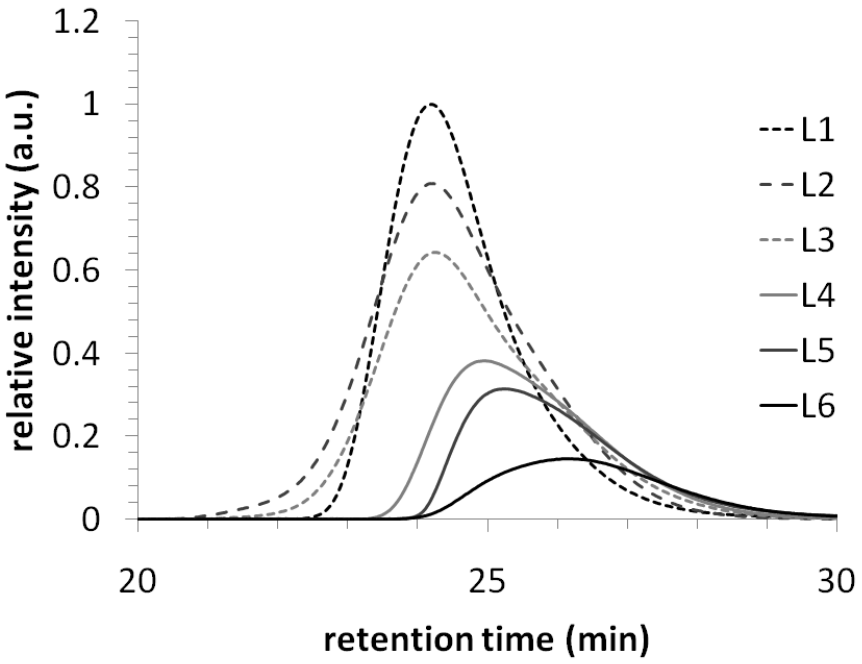

Figure 4.1. Aqueous SEC chromatograms (LStraces) of linear PDMAEMA synthesized from THF.

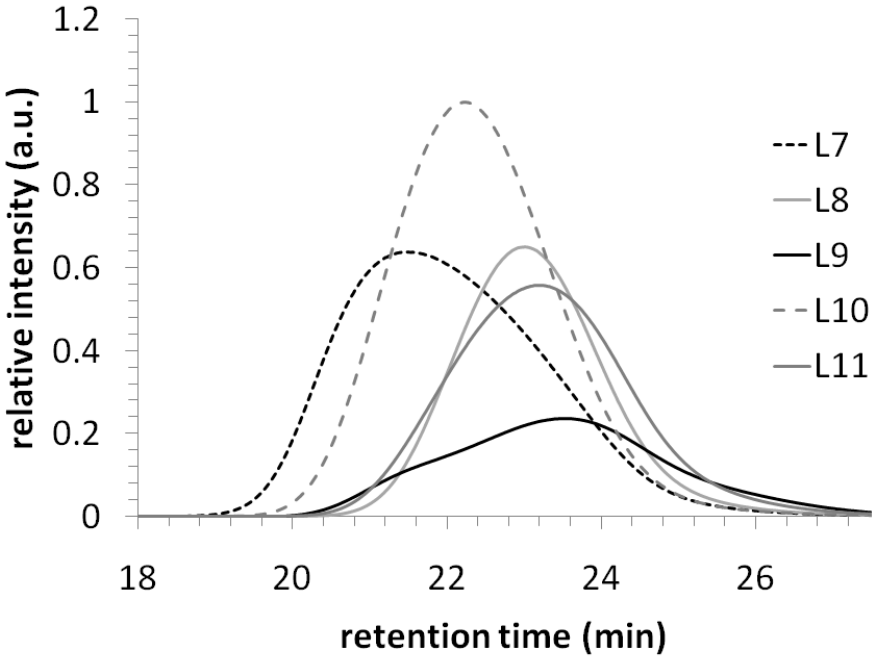

Figure 4.2. Aqueous SEC chromatograms (LS traces) of linear PDMAEMA synthesized from water.

SEC-MALLS can be used to determine a polymer's radius of gyration as a function of molecular weight distribution. Additionally, Mourey et al. has shown that this data can be used to estimate the persistence length (*lp*) of stiff and semi-flexible by the Kratky-Porod (KP) chain model.[34] The KP model is given as:

$$R_g^2 = \frac{l_p M}{3M_L} - l_p + \frac{2l_p^3 M_L}{M} - \frac{2l_p^4 M_L^2}{M^2}\left(1 - e^{-\frac{M}{l_p M_L}}\right) \qquad (2)$$

where *Rg* is the radius gyration, *lp* is the persistence length, *M* is molecular weight, and M_L is the molecular weight per unit counter length. We fit the KP model to the radius of gyration versus molecular weight for linear PDMAEMA.

We fit the KP model to radius of gyration versus molecular weight data using least squared analysis. Figure 4.3 shows the plot of radius of gyration versus molecular weight for linear PDMAEMA (sample **L8**) and the fit of the KP chain model. Fitting the KP model to the data revealed that linear PDMAEMA has an estimated persistence length of 6.2 nm in the SEC-MALLS mobile phase (see experimental for composition).

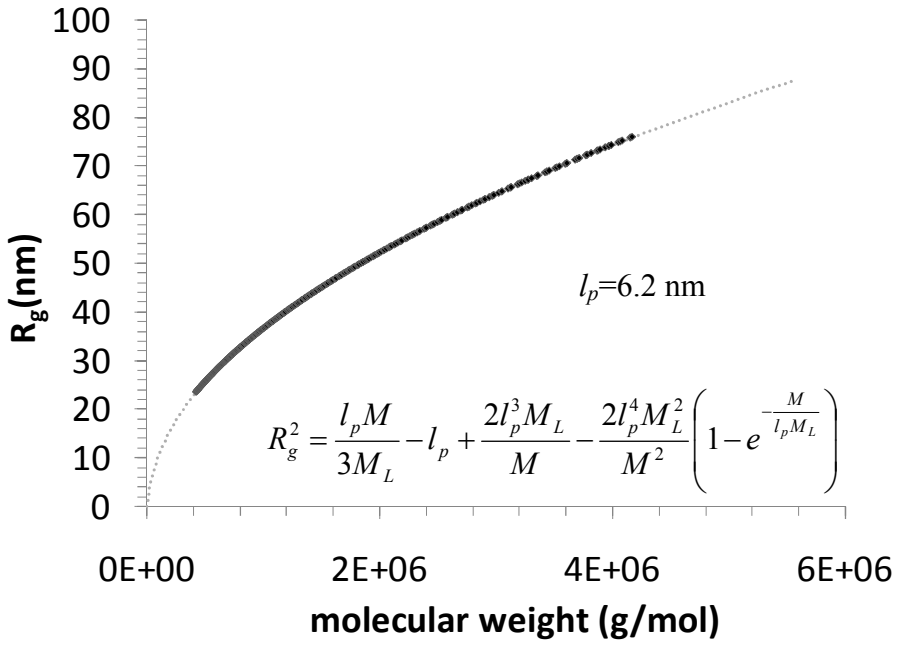

Figure 4.3. Radius of gyration (in 0.7 M $NaNO_3$, 0.1 M TRIS, pH=6) as a function of molecular weight for linear PDMAEMA (sample **L8**) measured using aqueous SEC-MALLS. Experimental data is shown as a dark-gray diamonds and the fit for the KP chain model is shown as a dotted gray line.

Randomly branched PDMAEMA polyelectrolytes were synthesized in THF using a procedure similar to the one used to synthesize linear polymers with addition of ethylene glycol dimethacrylate (EGDMA) as a tetrafunctional branching agent. In reactions with high concentrations of EGDMA branching agent (>0.75 wt% monomer), 1-dodecanethiol (DT) was added as a chain transfer agent to prevent gelation. In this study, in addition to preventing crosslinking, the chain transfer agent was also used to tune the topology of the resulting randomly branched PDMAEMA polyelectrolyte. This was accomplished by adjusting the relative concentration of chain transfer agent to EGDMA. Titterton et al. has shown this was an effective way to synthesize branched polymers from vinyl-based monomers. However, it is instructive to note that the ratio of

chain transfer agent to branching agent has no theoretical basis, it only serves as a convenient method to scale the amount of chain transfer agent with EGDMA. In reactions with high concentrations of both EGMDA and chain transfer agent, one would imagine a polymer with a greater number of shorter branches. In contrast, in reactions with low levels of EGDMA and no chain transfer agent, one would imagine a polymer with a fewer number of longer branches. The amounts of AIBN, EGDMA, and DT used to prepare randomly branched PDMAEMA and the resulting molecular weights are summarized in Table 4.3.

Table 4.3. Summary of synthetic conditions used to synthesize randomly branched PDMAEMA·HCl and resulting molecular weights and g' contraction factors.

sample	AIBN (wt.%)	EGDMA (wt.%)	DT:EGDMA	M_w (g/mol)	M_n (g/mol)	M_w/M_n	g'_w
B1	1.00	0.50	-	342,000	81,000	4.22	0.63
B2	0.50	0.75	-	636,000	153,000	4.16	0.71
B3	0.75	0.75	-	605,000	112,000	5.40	0.64
G1	1.00	1.00	-	gel	gel	-	-
B4	1.00	1.00	0.50:1.00	136,000	76,000	1.79	0.73
B5	1.00	0.75	1:00:1.00	87,000	62,000	1.40	0.63
B6	1.00	0.75	0.50:1.00	220,00	96,00	2.29	0.59

Figure 4.4 shows the aqueous SEC chromatograms of randomly branched PDMAEMA samples **B1** through **B3**. Samples **B1** through **B3** were synthesized using EGDMA without any added DT. SEC-MALLS analysis revealed weight-average molecular weights of 342,000 and 636,000 g/mol under these synthetic conditions. Furthermore, the molecular weight of the randomly branched PDMAEMA was lowest at the highest level of AIBN (**B1**, 1.00 wt% monomer). It is important to point out that

when the same initiator concentration was used to synthesis linear PDMAEMA (sample **L4**) the weight-average molecular weight was only 105,000 g/mol. The addition of 0.50 wt% monomer EGDMA resulted in a polymer with a weight-average molecular weight of 342,000 g/mol. This indicated that the addition of EGDMA produced a branched structure, which would explain the 3-fold increase in weight-average molecular weight. Samples **B2** and **B3** were synthesized with the same amount of EGDMA (0.75 wt% monomer), but with different amounts of AIBN initiator. SEC-MALLS analysis revealed that molecular weight decreased with increasing AIBN concentration, as expected. However, it seemed that the molecular weight of randomly branched PDMAEMA was more sensitive to EGDMA concentration than the amount of initiator. The molecular weight of sample **B2** was almost double that of sample **B1**. This was explained by the fact that sample B2 was synthesized with a greater concentration of EGDMA and a lower concentration of AIBN, both of which would result in higher molecular weight. However, the difference between samples **B2** and **B3**, where the EGDMA concentration was held constant and initiator concentration was changed by 0.25 wt%, was only about 5%. Samples **B1** through **B3** had polydispersities between 4.16 and 5.40. These relatively high molecular weight distributions are characteristic for branched polymers.

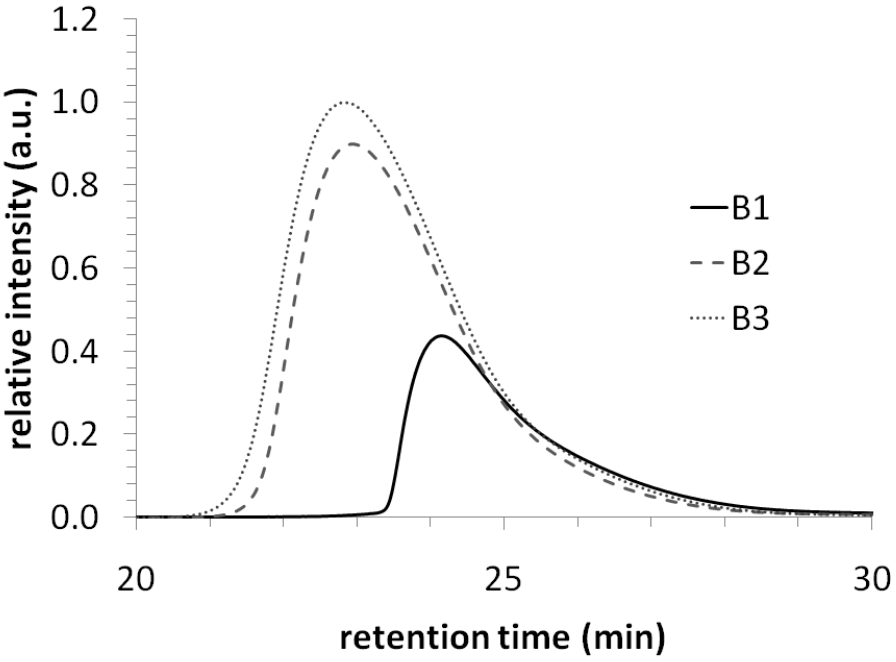

Figure 4.4. Aqueous SEC chromatograms (LS traces) of randomly branched PDMAEMA (samples **B1** – **B3**).

When the EGDMA concentration was increased to 1.00 wt% monomer, only insoluble gels were produced. However, when DT was added to reaction mixtures, soluble polymers were obtained with 1.00 wt% EGDMA. Figure 4.5 shows the aqueous SEC chromatograms (LS traces) of randomly branched PDMAEMA samples (**B4** through **B6**) polymerized with the addition of DT. As shown in the chromatograms, all samples remained soluble and had monomodal peaks. Sample **B4** was polymerized using 1.00 wt% AIBN and 1.00 wt% EGDMA with the addition of DT at a molar ratio of DT to EGDMA of 0.5. These conditions would result in gelation if DT was not used. Samples **B5** and **B6** were synthesized using EGDMA at 0.75 wt%. Even though this concentration of branching doesn't produce cross-linked gels, DT was added to determine its influence on the resulting polymers molecular weight. DT was found to have a significant

influence on the molecular weight. When the molar ratio of DT to EGDMA was changed from 1 (sample **B5**) to 0.5 (sample **B6**) the weight average molecular weight went from 87,000 to 220,000 g/mol. The concentration of initiator (1.00 wt%) and EGDMA (0.75 wt%) was the same for both samples. Samples **B4** through **B6** had polydispersities between 1.40 and 2.29. These polydispersity values were much lower than randomly branched sample polymerized in the absence of DT (**B1** through **B3**).

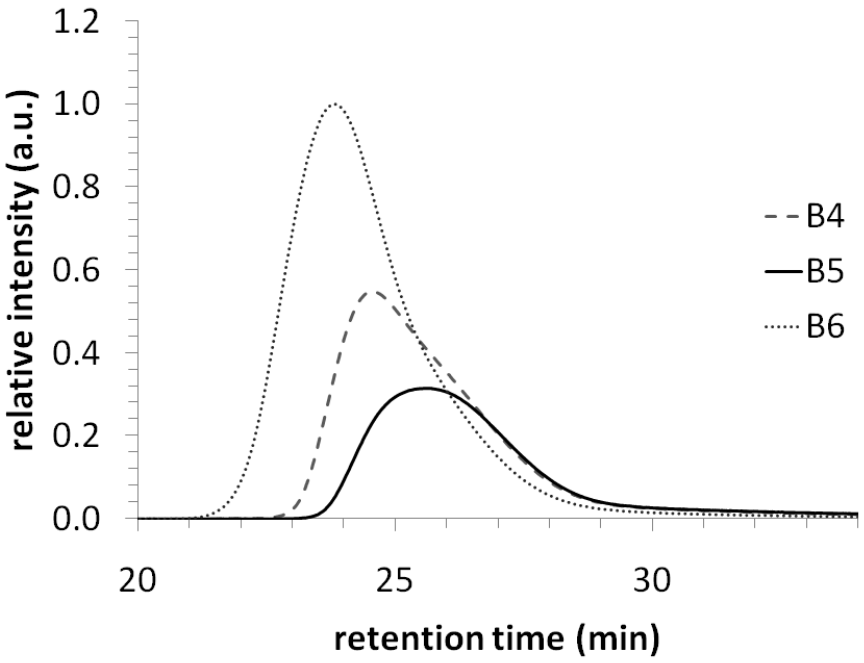

Figure 4.5. Aqueous SEC chromatograms (LS traces) of randomly branched PDMAEMA (samples **B4** – **B6**).

Linear and randomly branched PDMAEMA were further characterized using SEC-MALLS coupled with an on-line capillary viscometer. Figure 4.6 shows the MHS plot of log IV as a function of log MW for linear PDMAEMA samples **L1**, **L4**, and **L11** in the aqueous SEC mobile phase. The slope of the MHS plot gives the MHS alpha

parameter. The slope for the linear PDMAMEA samples decreased from 0.651 to 0.566 as the molecular weight of the polymer increased. This trend is commonly observed in MHS plots.

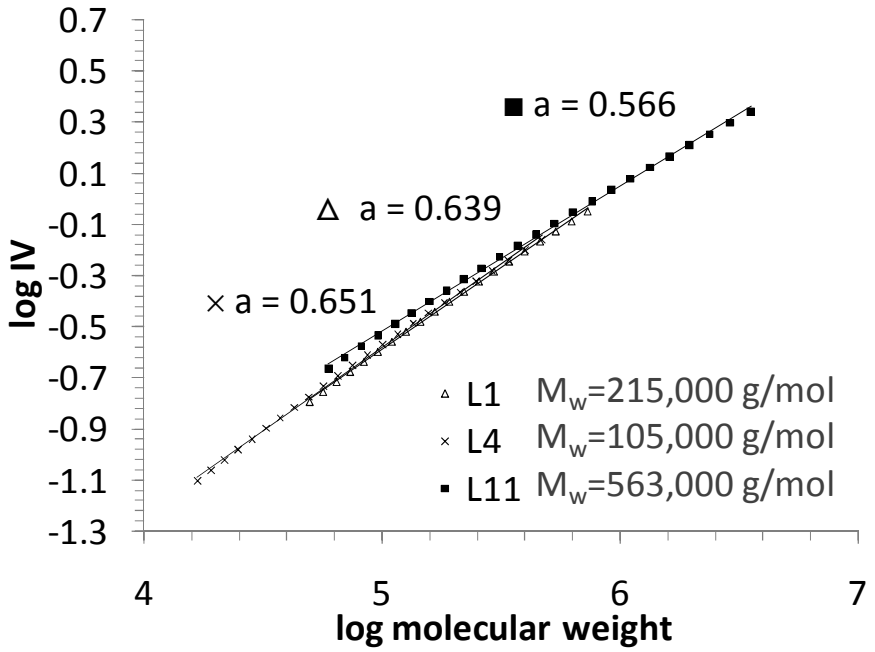

Figure 4.6. MHS-plot of various molecular weights of linear PDMAMEA (samples **L1**, **L4**, and **L11**) obtained using SEC-MALLS with an online viscometer.

The MHS alpha parameter for branched polymers is lower than that of a linear analog. Figure 4.7 shows the MHS plot for randomly branched PDMAMEA. The MHS data for a linear PDMAEMA sample is shown as a comparison. As expected, the alpha parameter for the randomly branched sample (**B6**) was lower (0.48) compared to the linear sample (**B1**, 0.64). These data was then used to calculate g' as a function of molecular weight. Recall that g' is the ratio of the IV a branched polymer to the IV of a linear polymer at equivalent molecular weight. Figure 4.8 shows the plot of g' as a

function of molecular weight for the randomly branched PDMAEMA sample **B6**. As shown in the plot, the g' contraction factor ranged from ~0.78 to ~0.40. Typically, g' is lower for higher moments of the molecular weight distribution. This result is consistent with the fact that higher molecular weight chains likely contain more branching sites.

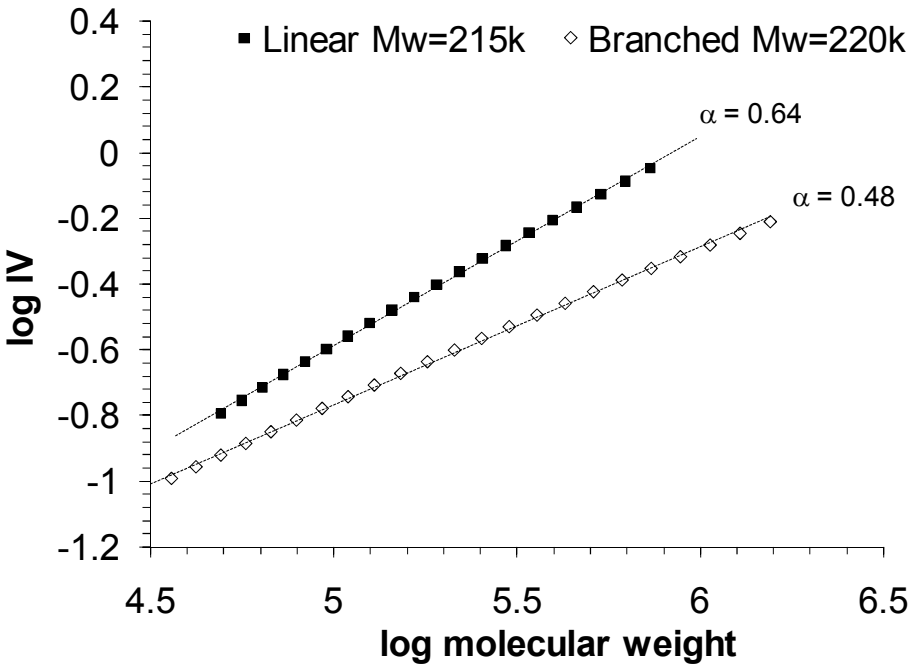

Figure 4.7. MHS-plot of linear (sample **L1**) and randomly branched (sample **B6**) PDMAEMA obtained using SEC-MALLS with an online viscometer.

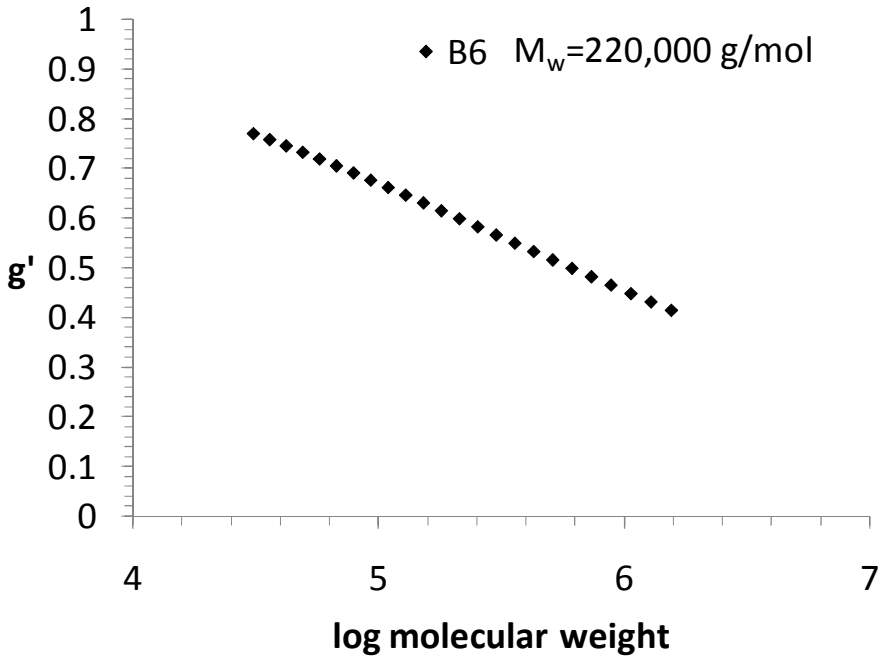

Figure 4.8. Calculated g' contraction factor as a function of molecular weight for randomly branched PDMAEMA (sample **B6**).

The g' calculation was then applied to all synthesized branched PDMAEMA samples. Figure 4.9 shows the MHS plots for randomly branched PDMAEMA samples **B1** through **B6**. A linear PDMAEMA sample (**L11**) was added to the plot for comparison purposes. By visual inspection of the plots, it is clear that all samples have a lower slope (lower MHS alpha parameter) than that of linear PDMAEMA sample. Figure 4.10 shows the calculated g' values as a function of molecular weight for samples **B1** through **B6**. For all samples, g' values ranged from ~0.92 to ~0.40. Additionally, g' decreased as a function of molecular weight for all randomly branched samples. The g' values also show that the synthesized PDMAEMA samples were only slightly branched. If these polymers were highly branched, the g' values would be much lower than 0.40.

However, the low level of branching was expected since the branching agent was incorporated at less than 1 wt% monomer. The g' values shown in Table 4.3 correspond to the calculated contraction factor (g'_w) at the weight average molecular weight. As shown in the table, g'_w values ranged from 0.73 to 0.59. A systematic trend in g' values as function of various synthetic conditions was not observed. In fact, most samples had relatively similar levels of branching (the g' values ranged only from 0.73 to 0.59). However, recall that the various synthetic conditions produced significantly different molecular weights.

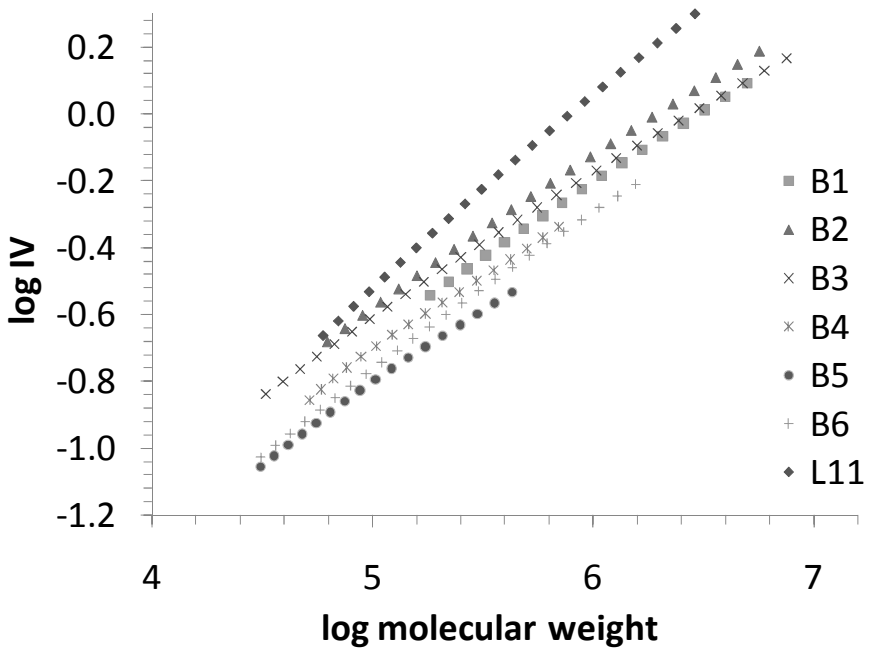

Figure 4.9. MHS-plot of randomly branched PDMAEMA samples **B1** through **B6** obtained using SEC-MALLS with an online viscometer. A linear PDMAEMA sample (**L11**) was added to the plot as a comparison.

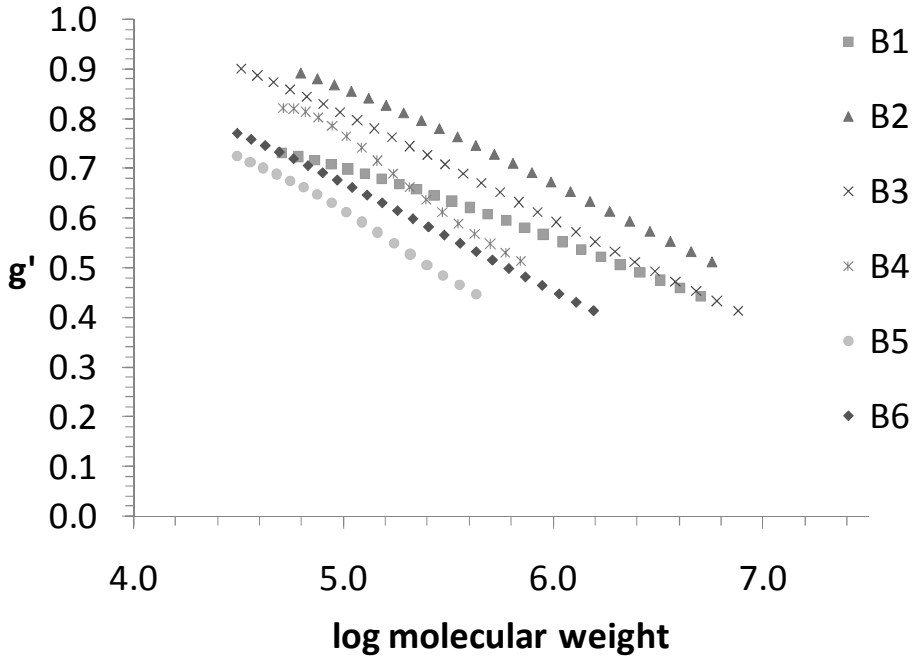

Figure 4.10. Calculated g' contraction factors as a function of molecular weight for randomly branched PDMAEMA samples **B1** through **B6**.

DLS was used to evaluate the influence of various aqueous environments on the hydrodynamic size of linear and randomly branched PDMAEMA. Figure 4.11 shows a plot of hydrodynamic radius as a function of polymer concentration (0.05 to 1.0 mg/mL in PBS) for linear PDMAEMA (M_w=915,000 g/mol). As shown in the figure, the hydrodynamic radius was greater at a lower concentration of polymer. This increase in hydrodynamic size as a function of decreasing concentration is a phenomenon known as the polyelectrolyte effect. Mutual charge repulsion drives causes the polymer to adopt a rod-like conformation. As the concentration of the polyelectrolyte increases, the charges on the backbone of the polymer screen inter- and intra-molecular charge repulsions. This charge screening causes the polymer to relax and adopt a more coil-like conformation.

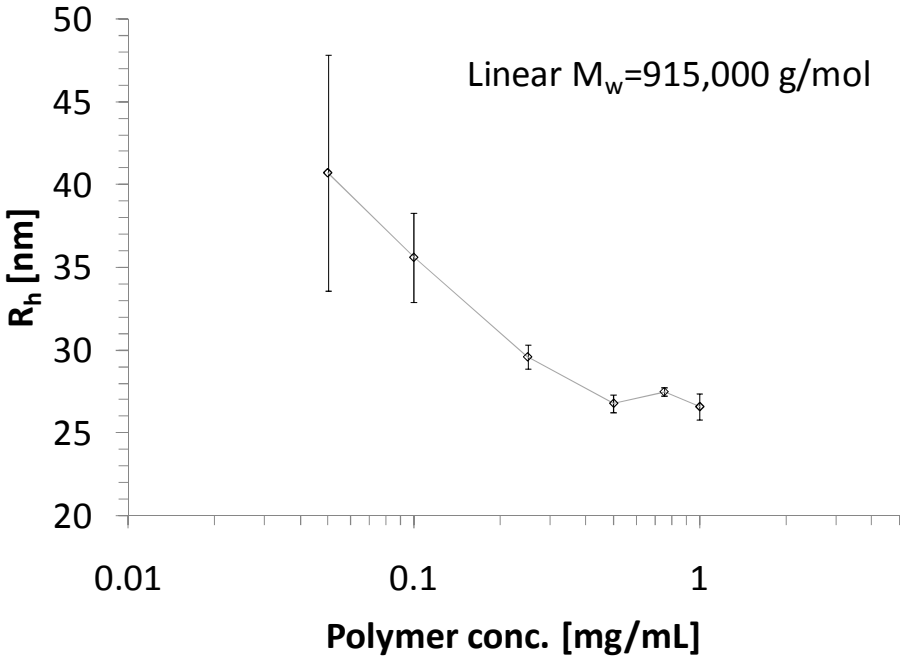

Figure 4.11. Hydrodynamic radius as a function of polymer concentration in PBS for linear PDMAEMA (M_w=915,000 g/mol).

In addition to polymer concentration, the introduction of salt can screen the charges that cause rod-like conformations. Figure 4.12 shows hydrodynamic radius as a function of NaCl concentration for two different molecular weights of linear PDMAEMA. The pH and polymer concentrations were held constant for these experiments. As shown in the figure, both molecular weights were found to have decreasing hydrodynamic sizes as a function of increasing concentration of NaCl. Similar to polymer concentration, the added salt screens electrostatic charges which allows the polymer to adopt a more coil-like conformation. Both molecular weights of

linear PDMAEMA show the same trend in hydrodynamic radius as a function of added salt, however, the magnitude of the line is higher for the higher molecular weight sample. Also, the change in hydrodynamic radius upon the introduction of salt is greater for the higher molecular PDMAEMA sample.

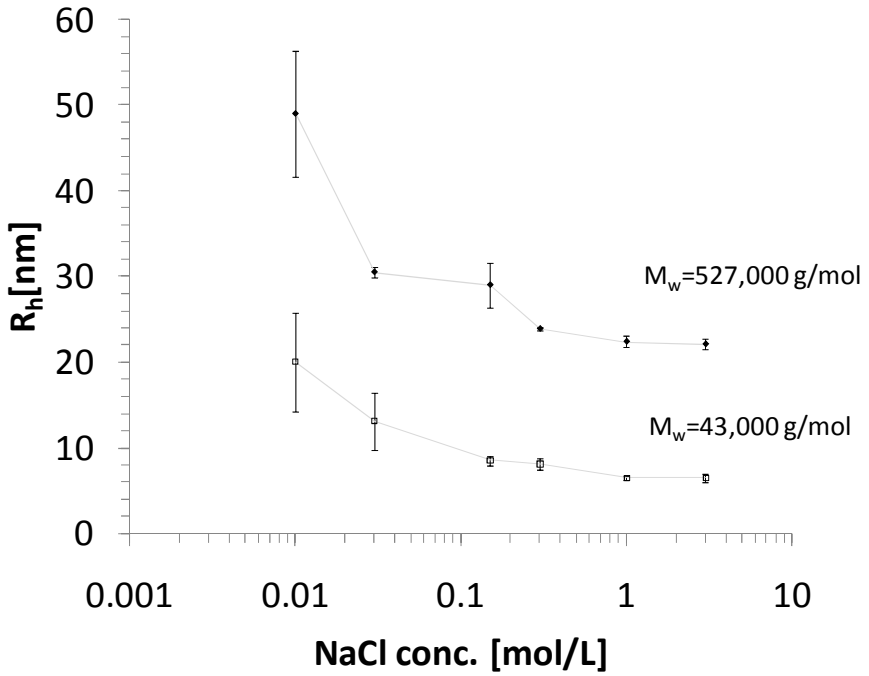

Figure 4.12. Hydrodynamic radius as a function of NaCl concentration for linear PDMAEMA (M_w=43,000 and 915,000 g/mol).

Figure 4.13 shows hydrodynamic radius as a function of NaCl concentration for linear and randomly branched PDMAEMA. As shown in the figure, the change in hydrodynamic size of the randomly branched PDMAEMA is much less than that of linear PDMAEMA. This behavior can be explained by the fact that branched polymers are more restricted in their ability to expand from mutual charge repulsion. A schematic of this behavior is shown in Figure 4.14.

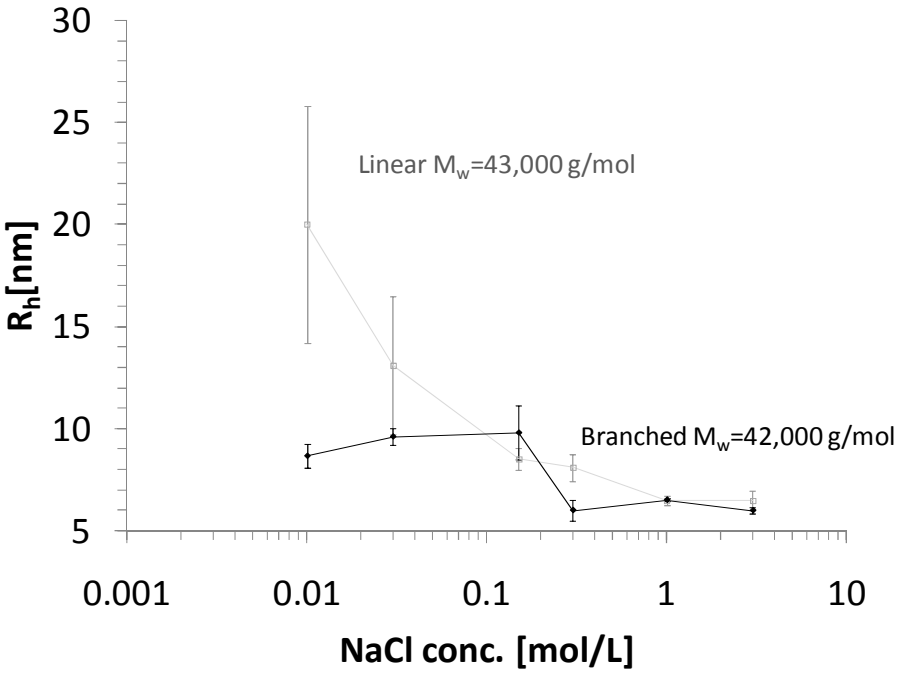

Figure 4.13. Hydrodynamic radius as a function of NaCl concentration for linear (M_w=43,000 g/mol) and randomly branched (M_w=42,000 g/mol) PDMAEMA.

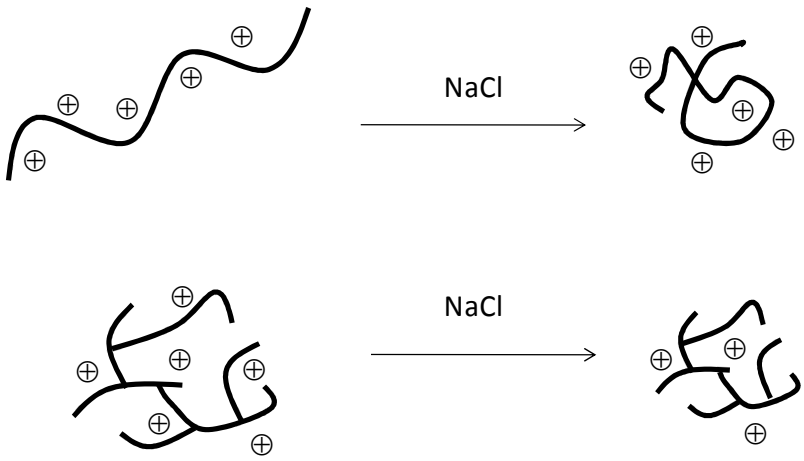

Figure 4.14. Schematic representation of the hydrodynamic size of linear and randomly branched PDMAEMA with and without NaCl.

Figure 4.15 shows hydrodynamic radius as a function of pH for linear (M_w=43,000 g/mol) and randomly branched (M_w=42,000 g/mol) PDMAEMA. Polymer concentration (1 mg/mL) and NaCl concentration (0.15 M) were held constant in these experiments. As shown in the plot, the hydrodynamic size of both linear and randomly branched PDMAEMA decreased as a function of increasing pH. This behavior can be explained by the fact that more acidic pHs protonate more tertiary amines on the polymer backbone, which creates more charge and leads to a greater polyelectrolyte effect.

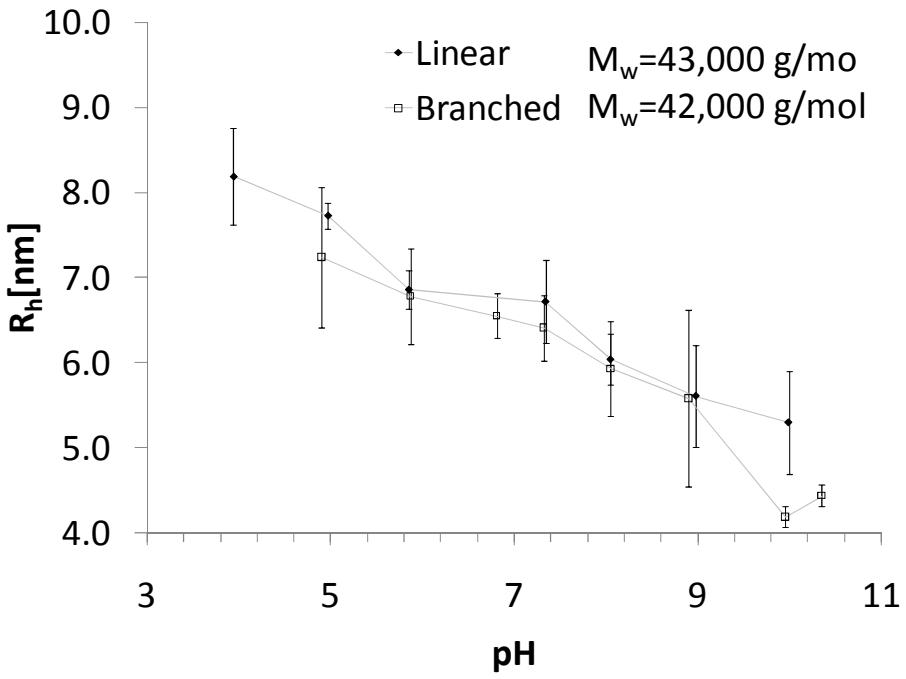

Figure 4.15. Hydrodynamic radius as a function of pH for linear (M_w=43,000 g/mol) and randomly branched (M_w=42,000 g/mol) PDMAEMA.

The relative ability to protonate linear versus randomly branched PDMAEMA topologies was explored using potentiometric titration. Figure 4.16 shows the titration behavior of linear and randomly branched PDMAEMA. Both linear and randomly branched PDMAEMA were able to buffer protons during the addition of acid. However, the titration experiments revealed that it was more difficult to protonate the randomly branched topology. In other words, it required more acid to completely protonate randomly branched PDMAMEA. Furthermore, the titration experiments showed that the pKa of amines on linear PDMAEMA was around 6.4 and slightly lower, around 6.2 on randomly branched PDMAEMA. These results are consistent with theoretical models proposed by Koper et al. that show it is more difficult to protonate randomly branched topologies due to the potential occurrence of double and triply coordinated charge sites.[19] Additionally, Müller et al. has proposed that the osmotic pressure created in the microenvironment of branched polyelectrolytes resists protonation.[35]

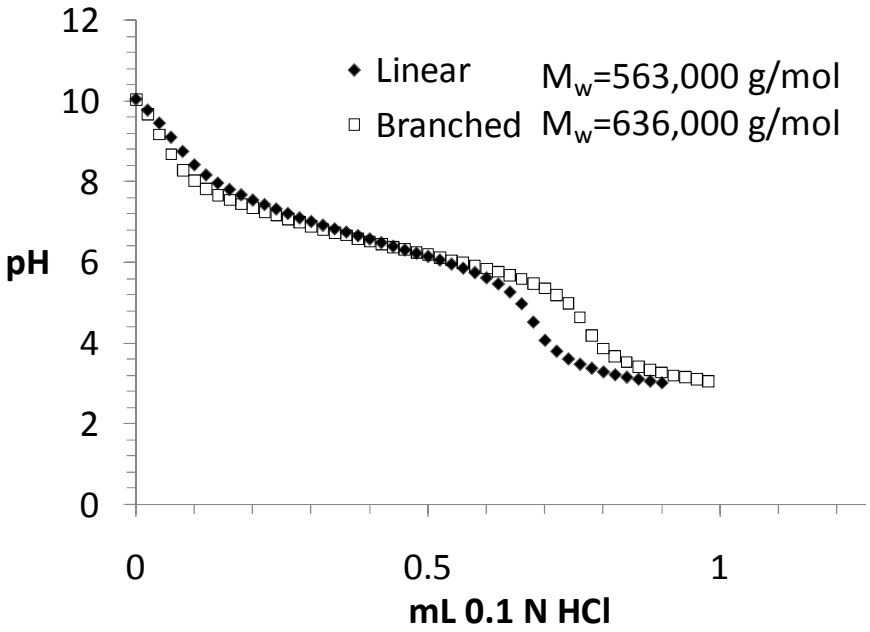

Figure 4.16. Potentiometric titration of linear and randomly branched PDMAEMA.

4.5 Conclusions

Conventional free radical polymerization was used to synthesize linear and randomly branched cationic polyelectrolytes based on PDMAEMA. The incorporation of EGDMA was found to produce branched topologies. However, higher concentrations of EGDMA resulted in gelation. To prevent network formation, a chain transfer agent (DT) was added during polymerization. The DT chain transfer agent prevented gelation and provided more molecular weight control for randomly branched PDMAEMA. An online viscometer used to create MHS plots and to determine the level of branching, calculated as the g' contraction factor. The level of branching was not overly sensitive to the use of chain transfer agent, with g' values for all samples being similar. However, the DT was

found to significantly influence the molecular weight of the resulting branched polyelectrolytes. DLS results showed that linear PDMAEMA behaved like a typical polyelectrolyte, with increasing hydrodynamic sizes as a function of decreasing polymer concentration. Furthermore, DLS showed that both linear and randomly branched topologies decreased in hydrodynamic size as a function of increased acid or salt. Titration experiments showed that both linear and randomly branched PDMAEMA buffered proton during the addition of acid, however, randomly branched topologies were slightly more difficult to protonate.

4.6 Acknowledgments

This material is based upon work supported in part by the Macromolecular Interfaces with Life Sciences (MILES) Integrative Graduate Education and Research Traineeship (IGERT) of the National Science Foundation under Agreement No. DGE-0333378. This material is based upon work supported in part by the U.S. Army Research Laboratory and the U.S. Army Research Office under grant number DAAD19-02-1-0275 Macromolecular Architecture for Performance (MAP) MURI.

4.7 References

[1]Wong, S. Y.; Pelet, J. M.; Putnam, D., Polymer systems for gene delivery--Past, present, and future. *Progress in Polymer Science* **2007,** 32, (8-9), 799-837.

[2]Schaffert, D.; Wagner, E., Gene therapy progress and prospects: synthetic polymer-based systems. *Gene Ther.* **2008,** 15, (16), 1131-1138.

[3]Jeong, J. H.; Kim, S. W.; Park, T. G., Molecular design of functional polymers for gene therapy. *Progress in Polymer Science* **2007,** 32, (11), 1239-1274.

[4]Heath, W. H.; Senyurt, A. F.; Layman, J.; Long, T. E., Charged Polymers via Controlled Radical Polymerization and their Implications for Gene Delivery. *Macromolecular Chemistry and Physics* **2007,** 208, (12), 1243-1249.

[5]Vlasov, G., Starlike branched and hyperbranched biodegradable polymer systems as DNA carriers. *Russian Journal of Bioorganic Chemistry* **2006,** 32, (3), 205-218.

[6]Oster, C. G.; Wittmar, M.; Bakowsky, U.; Kissel, T., DNA nano-carriers from biodegradable cationic branched polyesters are formed by a modified solvent displacement method. *Journal of Controlled Release* **2006,** 111, (3), 371-381.

[7]Verbaan, F. J.; Bos, G. W.; Oussoren, C.; Woodle, M. C.; Hennink, W. E.; Storm, G., A comparative study of different cationic transfection agents for in vivo gene delivery after intravenous administration. **2004,** 14, (2), 105-111.

[8]Banerjee, P.; Reichardt, W.; Weissleder, R.; Bogdanov, A., Novel Hyperbranched Dendron for Gene Transfer in Vitro and in Vivo. *Bioconjugate Chem.* **2004,** 15, (5), 960-968.

[9]Männistö, M.; Vanderkerken, S.; Toncheva, V.; Elomaa, M.; Ruponen, M.; Schacht, E.; Urtti, A., Structure-activity relationships of poly(-lysines): effects of pegylation and molecular shape on physicochemical and biological properties in gene delivery. *Journal of Controlled Release* **2002,** 83, (1), 169-182.

[10]Fischer, D.; von Harpe, A.; Kunath, K.; Petersen, H.; Li, Y.; Kissel, T., Copolymers of Ethylene Imine and N-(2-Hydroxyethyl)-ethylene Imine as Tools To Study Effects of Polymer Structure on Physicochemical and Biological Properties of DNA Complexes. *Bioconjugate Chem.* **2002,** 13, (5), 1124-1133.

[11]Fischer, D.; Bieber, T.; Li, Y.; Elsässer, H.-P.; Kissel, T., A Novel Non-Viral Vector for DNA Delivery Based on Low Molecular Weight, Branched Polyethylenimine: Effect of Molecular Weight on Transfection Efficiency and Cytotoxicity. *Pharmaceutical Research* **1999,** 16, (8), 1273-1279.

[12]Storkle, D.; Duschner, S.; Heimann, N.; Maskos, M.; Schmidt, M., Complex Formation of DNA with Oppositely Charged Polyelectrolytes of Different Chain Topology: Cylindrical Brushes and Dendrimers. *Macromolecules* **2007,** 40, (22), 7998-8006.

[13]Mori, H.; Walther, A.; Andre, X.; Lanzendorfer, M. G.; Muller, A. H. E., Synthesis of Highly Branched Cationic Polyelectrolytes via Self-Condensing Atom Transfer Radical Copolymerization with 2-(Diethylamino)ethyl Methacrylate. *Macromolecules* **2004,** 37, (6), 2054-2066.

[14]Liu, Y.; Wenning, L.; Lynch, M.; Reineke, T. M., New Poly(D-glucaramidoamine)s Induce DNA Nanoparticle Formation and Efficient Gene Delivery into Mammalian Cells. *J. Am. Chem. Soc.* **2004,** 126, (24), 7422-7423.

[15]Srinivasachari, S.; Liu, Y.; Zhang, G.; Prevette, L.; Reineke, T. M., Trehalose Click Polymers Inhibit Nanoparticle Aggregation and Promote pDNA Delivery in Serum. *J. Am. Chem. Soc.* **2006,** 128, (25), 8176-8184.

[16]Liu, Y.; Reineke, T. M., Poly(glycoamidoamine)s for Gene Delivery: Stability of Polyplexes and Efficacy with Cardiomyoblast Cells. *Bioconjugate Chem.* **2006,** 17, (1), 101-108.

[17]Dobrynin, A. V., Electrostatic Persistence Length of Semiflexible and Flexible Polyelectrolytes. *Macromolecules* **2005,** 38, (22), 9304-9314.

[18]Graham, S.; Cormack, P. A. G.; Sherrington, D. C., One-Pot Synthesis of Branched Poly(methacrylic acid)s and Suppression of the Rheological "Polyelectrolyte Effect". *Macromolecules* **2005,** 38, (1), 86-90.

[19]Borkovec, M.; Koper, G. J. M., Proton Binding Characteristics of Branched Polyelectrolytes. *Macromolecules* **1997,** 30, (7), 2151-2158.

[20]van der Aa, M.; Huth, U.; Häfele, S.; Schubert, R.; Oosting, R.; Mastrobattista, E.; Hennink, W.; Peschka-Süss, R.; Koning, G.; Crommelin, D., Cellular Uptake of Cationic Polymer-DNA Complexes Via Caveolae Plays a Pivotal Role in Gene Transfection in COS-7 Cells. *Pharmaceutical Research* **2007,** 24, (8), 1590-1598.

[21]Verbaan, F. J.; Klouwenberg, P. K.; Steenis, J. H. v.; Snel, C. J.; Boerman, O.; Hennink, W. E.; Storm, G., Application of poly(2-(dimethylamino)ethyl methacrylate)-based polyplexes for gene transfer into human ovarian carcinoma cells. *International Journal of Pharmaceutics* **2005,** 304, (1-2), 185-192.

[22]Funhoff, A. M.; van Nostrum, C. F.; Lok, M. C.; Kruijtzer, J. A. W.; Crommelin, D. J. A.; Hennink, W. E., Cationic polymethacrylates with covalently linked membrane

destabilizing peptides as gene delivery vectors. *Journal of Controlled Release* **2005,** 101, (1-3), 233-246.

[23]Verbaan, F.; van Dam, I.; Takakura, Y.; Hashida, M.; Hennink, W.; Storm, G.; Oussoren, C., Intravenous fate of poly(2-(dimethylamino)ethyl methacrylate)-based polyplexes. *European Journal of Pharmaceutical Sciences* **2003,** 20, (4-5), 419-427.

[24]Verbaan, F. J.; Oussoren, C.; van Dam, I. M.; Takakura, Y.; Hashida, M.; Crommelin, D. J. A.; Hennink, W. E.; Storm, G., The fate of poly(2-dimethyl amino ethyl)methacrylate-based polyplexes after intravenous administration. *International Journal of Pharmaceutics* **2001,** 214, (1-2), 99-101.

[25]van de Wetering, P.; Schuurmans-Nieuwenbroek, N. M. E.; van Steenbergen, M. J.; Crommelin, D. J. A.; Hennink, W. E., Copolymers of 2-(dimethylamino)ethyl methacrylate with ethoxytriethylene glycol methacrylate or N-vinyl-pyrrolidone as gene transfer agents. *Journal of Controlled Release* **2000,** 64, (1-3), 193-203.

[26]Bos, G. W.; Trullas-Jimeno, A.; Jiskoot, W.; Crommelin, D. J. A.; Hennink, W. E., Sterilization of poly(dimethylamino) ethyl methacrylate-based gene transfer complexes. *International Journal of Pharmaceutics* **2000,** 211, (1-2), 79-88.

[27]van de Wetering, P.; Moret, E. E.; Schuurmans-Nieuwenbroek, N. M. E.; van Steenbergen, M. J.; Hennink, W. E., Structure-Activity Relationships of Water-Soluble Cationic Methacrylate/Methacrylamide Polymers for Nonviral Gene Delivery. *Bioconjugate Chem.* **1999,** 10, (4), 589-597.

[28]Cherng, J. Y.; Wetering, P. v. d.; Talsma, H.; Crommelin, D. J. A.; Hennink, W. E., Stabilization of polymer-based gene delivery systems. *International Journal of Pharmaceutics* **1999,** 183, (1), 25-28.

[29]van de Wetering, P.; Cherng, J. Y.; Talsma, H.; Crommelin, D. J. A.; Hennink, W. E., 2-(dimethylamino)ethyl methacrylate based (co)polymers as gene transfer agents. *Journal of Controlled Release* **1998,** 53, (1-3), 145-153.

[30]Cherng, J.-Y.; van de Wetering, P.; Talsma, H.; Crommelin, D. J. A.; Hennink, W. E., Effect of Size and Serum Proteins on Transfection Efficiency of Poly ((2-dimethylamino)ethyl Methacrylate)-Plasmid Nanoparticles. *Pharmaceutical Research* **1996,** 13, (7), 1038-1042.

[31]Lide, D. R., CRC Handbook of Chemistry and Physics, 83rd Edition. 2002; p 2664 pp.

[32]Layman, J. M.; Borgerding, E. M.; Williams, S. R.; Heath, W. H.; Long, T. E., Synthesis and Characterization of Aliphatic Ammonium Ionenes: Aqueous Size Exclusion Chromatography for Absolute Molecular Weight Characterization. *Macromolecules* **2008,** 41, (13), 4635-4641.

[33]Qiu, J.; Charleux, B.; Matyjaszewski, K., Controlled/living radical polymerization in aqueous media: homogeneous and heterogeneous systems. *Progress in Polymer Science* **2001,** 26, (10), 2083-2134.

[34]Mourey, T.; Le, K.; Bryan, T.; Zheng, S.; Bennett, G., Determining persistence length by size-exclusion chromatography. *Polymer* **2005,** 46, (21), 9033-9042.

[35]Plamper, F. A.; Ruppel, M.; Schmalz, A.; Borisov, O.; Ballauff, M.; Muller, A. H. E., Tuning the Thermoresponsive Properties of Weak Polyelectrolytes: Aqueous Solutions of Star-Shaped and Linear Poly(N,N-dimethylaminoethyl Methacrylate). *Macromolecules* **2007,** 40, (23), 8361-8366.

Chapter 5. **Influence of Random Branching on Poly(2-dimethylaminoethyl methacrylate)-Mediated DNA Delivery *In Vitro***

John M. Layman[†], Sean M. Ramirez[†], Anjali A. Hirani[‡], Yong Woo Lee[‡],

*and Timothy E. Long[†]**

Departments of [†]Chemistry and [‡]Biomedical Engineering,

Macromolecules and Interfaces Institute,

Virginia Tech

5.1 Abstract

Non-viral gene transfection agents, such as cationic polyelectrolytes, are attractive alternatives to viral vectors due to the absence of potential immunogenic risk and the ability to tune macromolecular architecture. In this paper, conventional free radical polymerization was used to synthesize various molecular weights of linear and randomly branched cationic polyelectrolytes based on poly(2-N,N'-dimethylaminoethyl methacrylate) (PDMAEMA). Randomly long-chain branched (LCB) topologies were synthesized utilizing an ethylene glycol based dimethacrylate as a branching agent. We evaluated the influence of the level of branching on transfection efficiency and toxicity in human brain microvascular endothelial cells (HBMEC) and Cos-7 cells. The level of

branching in the polyelectrolytes was quantified using the well established, semi-quantitative, g' contraction factor, which is the ratio of intrinsic viscosities of branched and linear polymers at equivalent molar mass. A series of linear and randomly branched polyelectrolytes were synthesized and grouped according to similar molecular weight. The presence of long chain branching in PDMAEMA did not significantly influence gene transfection in HBMEC or Cos-7 cells.

KEYWORDS polyelectrolytes, branched polyelectrolytes, g' contraction factor, gene therapy, gene delivery, DNA transfection, nucleic acid transfection

5.2 Introduction

In gene therapy, extra-chromosomal nucleic acids, typically circular DNA segments, or plasmids, are transferred through the cellular membrane and express a therapeutic level of a defective or deficient protein. Although this technology holds great promise, wide-spread clinical application of gene therapy is limited, predominantly due to the absence of safe and effective nucleic acid delivery agents.[1, 2] These agents are needed to escort plasmids through the cell membrane since naked DNA is negatively charged and adopts a rod-like confirmation in dilute aqueous solution. Also, the negative charge from the phosphodiester bond in the DNA backbone interacts unfavorably with negatively charged glycoproteins on the surface of the cell membrane.[3] Viral vectors, which utilize an inactivated virus, are extremely efficient carrier molecules and infect a wide variety of cell types. However, viral vectors are limited to small plasmids and although modified viruses are rendered replication deficient, host immune response is

still a frequent complication.[4] Non-viral agents, such as cationic polyelectrolytes, are an attractive synthetic replacement to viruses due to absence of immunogenic risk and the ability to tailor their macromolecular architecture. Non-viral vectors electrostatically screen the anionic charges on the nucleic acid to form a plasmid-polymer complex, termed a polyplex. This action neutralizes the net charge and alleviates mutual charge driven chain extension, thus condensing the hydrodynamic radius of the polyplex.[5-8] The elimination of net negative charge and smaller size of the polyplex considerably increases the likelihood of gene transfection. Most strategies employ a molar excess of the polycation to give the polyplex a net positive charge, which facilitates attraction of the polyplex to the surface of the cell membrane.[9, 10] After juxtaposition with the cell membrane, the polyplex is internalized via conventional, non-specific endocytosis mechanisms.[11] Although non-viral vectors possess numerous design advantages, several investigators have shown that transfer efficiencies are considerably lower compared to viral vectors.[12-14] Therefore, clinical use of cationic polyelectrolytes will be limited until transfection efficiencies rival that of viral vectors.

In the development of non-viral transfection agents, it is important to note the minimum requirements necessary for successful protein production from the delivered therapeutic gene.

An efficacious gene transfer agent should enable the following operations:

1) condense the hydrodynamic size of the nucleic acid,
2) protect the nucleic acid from enzymatic degradation,
3) release the nucleic acid into the cytoplasm.

In most cases, endosomal release is presumed to be the limiting step in nucleic acid availability after transfection.[15] Thus, there is a delicate balance of mediocrity between sufficient binding of the nucleic acid for successful transfection, however, sufficiently weak to release the nucleic acid during endosomal escape. Indeed, many previously tested agents are extremely effective transfection agents, but without efficient release and translocation to the nucleus, the transfected nucleic acid is ineffective for treatment of the diseased cell.

In this study, linear and randomly branched cationic polyelectrolytes based on poly(2-N,N'-dimethylaminoethyl methacrylate) (PDMAEMA), a transfection agent pioneered and comprehensively studied by Hennink et al.,[10, 16-21] were synthesized and comparatively analyzed for transfection activity and cytotoxicity. Cationic dendrimers that contain cores such as polyamidoamine (PAMAM),[22] polypropyleneamine (PPI),[23] polyethyleneimine (PEI),[24] and L-lysine[25] as well as other branched polycations[26, 27] were studied earlier and showed high transfection efficiencies. However, it is not fundamentally clear why these branched structures increase the transfection capabilities of cationic polymers. In order to gain more fundamental understanding of structure-transfection relationships, several investigators examined the transfection activity of branched versus linear cationic polyelectrolytes[28-33] including star,[34-37] hyperbranched,[38, 39] and dendritic[40, 41] topologies. Although these references described the importance of molecular topology, studies were rarely performed with similar chemical compositions or equivalent molecular weight. The molecular weight of the polymer, both in linear and branched forms, has a significant effect on transfection activity.[21] Therefore, it is important to evaluate contributions from molecular weight when evaluating the influence

of branching. Also, many sources describe linear versus branched polymers categorically, and it is necessary to fundamentally understand the role of branching in a more quantitative fashion. In an attempt to address this issue, we describe the level of branching using the well-established, semi-quantitative, g' contraction factor, which is the ratio of intrinsic viscosities of branched and linear polymers at equivalent molecular weight. This viscometric method provides an easy and rapid approach to phenomenologically characterize the level of branching. This contraction factor was employed earlier to characterize branching in a similar polyelectrolyte, poly(2-diethylaminoethyl methacrylate), although these studies did not involve gene delivery evaluation.[42] In addition, other investigators have utilized solution parameters, such as the Mark-Houwink alpha value, to evaluate incidental branching in other polycationic gene transfection agents.[43-45] Herein, we correlate transfection and cytotoxicity results with viscometric levels of branching in at two different weight-average molecular weights of linear and branched PDMAEMA.

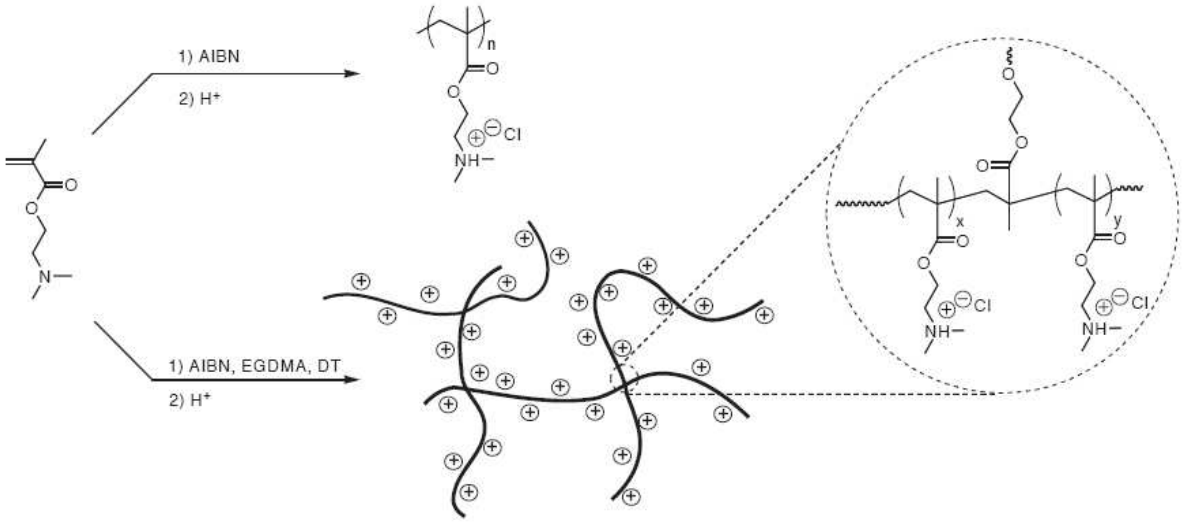

Scheme 5.1. Synthetic approach employed to produce linear and randomly branched PDMAEMA polyelectrolytes.

5.3 Experimental Section

5.3.1 General Methods and Materials.

2-(N,N'-dimethylamino)ethyl methacrylate (DMAEMA, 98%, Sigma-Aldrich) was passed through a neutral alumina column to remove free-radical inhibitor. 2,2'-azobisisobutyronitrile (AIBN, 99%, Sigma-Aldrich) were used as received. The branching agent ethylene glycol dimethacrylate (EGDMA, 98%, Sigma-Aldrich) was passed through a neutral alumina column to remove free-radical inhibitor. Deuterium oxide (D_2O, 99.9%, Cambridge Isotope Laboratories) was used as received for all NMR measurements. Sodium nitrate ($NaNO_3$, 99.0%, Alfa Aesar), trishydroxymethylaminomethane (TRIS, 99.8%, Alfa Aesar), glacial acetic acid (AcOH, 99.7%, Alfa Aesar), sodium azide (NaN_3, 99%, Alfa Aesar), sodium chloride (NaCl, 99.0%, Sigma-Aldrich), 1-dodecanethiol (DT, 98%, Sigma-Aldrich) were all used as received. Ultrapure water having a resistivity of 18.2 MΩ·cm was obtained using a Millipore Direct-Q5 purification system. All other solvents and reagents were used as received from commercial sources without further purification unless specifically noted elsewhere.

^1H NMR spectra were recorded on a Varian Inova 400 MHz spectrometer. Chemical shifts are reported in ppm downfield from TMS using the residual protonated solvent as an internal standard (D_2O, 1H 4.79 ppm). Circular dichroism (CD) spectra were obtained using a JASCO Corp. J-820 spectrometer at 25^oC.

5.3.2 Synthesis of linear PDMAEMA.

In a typical synthesis, DMAEMA was charged with AIBN (0.10-0.30 wt% monomer) in THF at 20 wt% solids in a multi-necked, round-bottomed flask. A reflux condenser was affixed to the flask and the reaction mixture was purged with nitrogen for approximately 30 min. The flask was then submerged in an oil bath preheated to 60 ^{o}C. The polymerization was allowed to proceed for 24 h under magnetic stirring. The resulting polymer was precipitated in hexanes. After decantation of the hexanes, the polymer was dried under vacuum at 80 ^{o}C. Dissolution of the neutral PDMAEMA product in aqueous HCl (pH=5.0) under magnetic stirring was used to convert each polymer to a hydrochloride salt. The PDMAEMA·HCl polyelectrolyte was then precipitated in acetone. The acetone was decanted and the white powder product was dried under vacuum at 80 ^{o}C.

All samples were dialyzed against distilled water for at least 48 h using Spectra/Por dialysis tubing (MWCO=3,500 g/mol). Lyophilization was used to recover samples prior to characterization. ^{1}H NMR (400 MHz, D_2O): δ (ppm)= 4.40 (br, 2H), 3.59 (br, 2H), 3.01 (br, 6H), 2.05 (br, 2H), 1.02 (br, 3H). M_n and M_w are summarized in Table 5.1.

5.3.3 Synthesis of randomly branched PDMAEMA.

Randomly branched PDMAEMA was synthesized and isolated using the methods described above with the addition of EGDMA (0.10-2.0 wt% monomer). A chain transfer agent (1-dodecanethiol) was needed to prevent gelation in reactions where the EGDMA concentration was 1.0 wt% and higher. The molar ratio of dodecanethiol to EGDMA was adjusted between 0.5:1 to 1:1. ^{1}H NMR (400 MHz, D_2O): δ (ppm)= 4.40

(br, 2H), 3.59 (br, 2H), 3.01 (br, 6H), 2.05 (br, 2H), 1.02 (br, 3H). M_n and M_w are summarized in Table 5.1.

5.3.4 Aqueous size exclusion chromatography-multiangle laser light scattering (SEC-MALLS).

Aqueous SEC experiments were run in a buffered solution consisting of 0.7 M sodium nitrate and 0.1 M TRIS adjusted to pH 6.0 with glacial acetic acid. The pH of the resulting solution was measured using a Thermo Orion 3 Star portable pH meter with a Thermo Orion Triode pH electrode. Sodium azide was added at 200 ppm to the solution as a precaution to prevent bacterial growth in the SEC system. Samples were analyzed at 0.8 mL/min through 2x Waters Ultrahydrogel Linear and 1x Water Ultrahydrogel 250 columns, with all columns measuring 7.8 x 300 mm and equilibrated to 30 ^{o}C. SEC-MALLS instrumentation consisted of a Waters 1515 isocratic HPLC pump, Waters 717plus Autosampler, Wyatt miniDAWN multiangle laser light scattering (MALLS) detector operating a He-Ne laser at a wavelength of 690 nm, Viscotek 270 capillary viscosity detector, and a Waters 2414 differential refractive index detector operating at a wavelength of 880 nm and 35 ^{o}C. The only calibration constant, the Wyatt Astra V AUX1, was calculated using a series of aqueous sodium chloride solutions. The accuracy and reproducibility was confirmed with poly(ethylene oxide) and poly(methacrylic acid) sodium salt standards (both obtained from Sigma-Aldrich) ranging in molecular weight from 1,000 to 1,000,000 g/mol. Absolute molecular weights and intrinsic viscosities were determined using the Wyatt Astra V and Viscotek OmiSEC software packages, respectively. The specific refractive index increments (*dn/dc*) for linear and randomly

branched PDMAEMA were determined offline. A Wyatt OptiRex differential/absolute refractive index detector operating at a wavelength of 690 nm and 30 ^{o}C was used for all specific refractive index increment measurements. Polymer samples (0.05 – 2.00 mg/mL) were allowed to dissolve in the appropriate solvent overnight. Samples were metered at 0.8 mL/min into the RI detector at 30 ˚C using a syringe pump and a syringe affixed with a 0.45 μm PTFE syringe filter. The *dn/dc* values were determined using the Wyatt Astra V software package.

The level of branching in synthesized samples was measured using the g' contraction factor, which is the ratio of the intrinsic viscosities of a branched polymer to a linear polymer at equivalent molecular weight, see Equation 1.

$$g' = \frac{[\eta]_{branched}}{[\eta]_{linear}} \qquad (1)$$

Since branched macromolecules have a smaller hydrodynamic sizes than a linear analog at identical molecular weight, their intrinsic viscosity is lower. Thus, g' values are always less than one. Therefore, as the level of branching increases at a given molecular weight, g' decreases.

5.3.5 Titration of linear and randomly branched PDMAEMA.

pH measurements were performed using a Thermo Orion 3 Star portable pH meter equipped with a Thermo Orion Triode pH electrode. Both linear and branched PDMAEMA were dissolved at 1 mg/mL in ultrapure water having a resistivity of 18 MΩ·cm. Using 15 mL of polymer solution, the pH was then adjusted to ~10.5 using

100 μL aliquots of 0.5 M NaOH. The solutions were then titrated with 20-40 μL aliquots of 0.1 N HCl. The pH of the solution was measured after the addition of each aliquot.

5.3.6 Gel electrophoresis.

Agarose powder (BioRad Laboratories) was dissolved in 1X TAE buffer (Sigma-Aldrich) to produce 0.9 wt% agarose gel slabs. Polyplexes were prepared in 1 mL microcentrifuge tubes. The pRL-SV40 plasmid (0.5 μL of 0.2 μg/μL DNA stock solution) was mixed with the appropriate amount of polymer solution (0.2 or 0.8 μL of 1 μg/μL polymer stock solution) corresponding to DNA/polymer N/P ratio of 4. The polyplex solutions and a DNA only solution (0.5 μL of 0.2 μg/μL DNA stock solution) were diluted to a total volume of ~35 μL with 28 μL of 1X TAE buffer and 7 μL of 40 wt% sucrose 1X TAE solution. The polyplex and DNA only solutions were incubated at room temperature for 30 min prior to loading into a submerged agarose gel. The gel was electropheresed at 75 V for 90 min in 1X TAE running buffer. Gels were stained with ethidium bromide (Sigma-Aldrich) and imaged using a UV transilluminator table and a digital camera.

5.3.7 Cell culture.

Human brain microvascular endothelial cells (HBMEC) were isolated, cultivated, and purified as previously described.[46] HBMEC cells were grown in RPMI 1640-based medium with 10% fetal bovine serum (Mediatech), 10% NuSerum (Becton Dickinson), 30 μg/ml of endothelial cell growth supplement (ECGS; Becton Dickinson), 15 U/ml of heparin (Sigma-Aldrich), 2 mM L-glutamine, 2 mM sodium pyruvate, nonessential amino acids, vitamins, 100 U/ml of penicillin, and 100 μg/ml of streptomycin (all

reagents from Mediatech). African green monkey kidney cells (Cos-7) (ATCC) were cultured in DMEM-based medium with 10% fetal bovine serum, 100 U/mL penicillin, and 100 μg/ml of streptomycin. Cultures were incubated at 37 °C in a humid atmosphere of 5% CO_2.

5.3.8 Renilla Luciferase Protein Expression Assay.

To prepare polyplexes for transfection experiments, pRL-SV40 (1 μg/μL in H_2O) was diluted in basal RPMI or DMEM media to a concentration of 0.8 μg/mL and incubated at room temperature for 10 min. At the same time, the appropriate type and amount of polymer was diluted in basal RPMI or DMEM to the final concentrations corresponding to the various nitrogen/phosphorus (N/P) ratios and allowed to incubate for 10 min at room temperature. Equal volumes of the plasmid and corresponding polymer solutions were combined (final pDNA concentration of 0.4 μg/mL) and incubated for 20-30 min at room temperature to complex the plasmid DNA with PDMAEMA. HBMEC or Cos-7 cells were plated at a concentration of $2.0x10^5$ cells/well on 12-well plates 24 h prior to transfection. Each well was treated with 1 mL of transfection solution and then incubated for 12 h at 37 ^oC, 5% CO_2. After 12 h, the transfection solution was replaced with complete RPMI or DMEM growth media. The cells were then incubated for 24 h at 37^oC, 5% CO_2 to allow for protein expression. After incubation, the cells were rinsed with approximately 1 mL of PBS and 100 μL of lysis buffer was added. Immediately after adding lysis buffer, each well was scraped and incubated for 30 min at room temperature with gentle mixing. The lysate mixture was then subjected to two -80 ^oC/37 ^oC freeze/thaw cycles. Luciferase activity was measured

using a luciferase assay kit (Promega) and a Molecular Devices Corp. SPECTRAmax L luminometer according to the assay kit manufacturer's instructions.

5.4 Results and Discussion

Free radical methods were employed to prepare PDMAEMA polyelectrolytes with various topologies and molecular weights, as shown in Scheme 5.1. ^{1}H NMR spectroscopy verified the chemical structure of each sample. ^{1}H NMR confirmed identical chemical composition of linear and branched samples, except for the EGDMA branch point. Batch-mode specific refractive index increment (dn/dc) measurements revealed that linear samples had *dn/dc* values ranging from 0.145-0.149 and branched products containing the highest amounts of EGDMA had similar values, around 0.146-0.148. Aqueous SEC results showed weight average molecular weights of linear and branched polymers between 110,000 and 220,000 g/mol with polydispersities ranging from 1.29-2.29. PDMAEMA samples were grouped according to similar weight-average molecular weight. In other words, sample **L1** has a similar weight-average molecular weight to sample **B1**. The synthetic conditions, aqueous SEC-MALLS molecular weights, and calculated g' contraction factors (explained in later text) are summarized in Table 5.1. The relatively narrow molecular weight distributions were attributed to either precipitation of the polymer after polymerization or imperfect SEC separation, which can cause underestimated polydispersities.[47]

Table 5.1. Aqueous SEC molecular weights, g' contraction factor, and hydrodynamic radii of linear and branched PDMAEMA polyelectrolytes.

sample	AIBN (wt.%)	EGDMA (wt.%)	DT: EGDMA	M_w (g/mol)	M_n (g/mol)	M_w/M_n	g'_w
L1	1.00	-	-	112,000	87,000	1.29	-
B1	1.00	0.50	0.50	111,000	84,000	1.32	0.75
L2	0.10	-	-	215,000	158,000	1.36	-
B2	1.00	0.75	0.50	220,000	96,000	2.29	0.60

Figure 5.1 shows the MHS plots for linear and randomly branched PDMAEMA samples **L1** and **B1**, respectively. The plot shows log IV versus log MW for linear and randomly branched PDMAEMA, determined using aqueous SEC equipped with an online viscometer. The SEC column separates the sample, allowing for viscosity measurements across a sample's molecular weight distribution. As shown in the figure, the randomly branched PDMAEMA (**B1**) displayed lower intrinsic viscosities compared to the linear PDMAEMA (**L1**) of equivalent molecular weight. The slope of log IV versus log MW gives the MHS alpha value. The greater the level of branching in a sample, the lower the MHS alpha value. The viscometry results revealed that the randomly branched PDMAEMA (**B1**) had a MHS value of 0.57 whereas the linear PDMAEMA (**L1**) had a MHS value of 0.67, which confirmed branching in **B1**. The ratio of the intrinsic viscosity of the randomly branched PDMAEMA over the intrinsic viscosity of the linear PDMAEMA gives the g' contraction factor. Figure 5.2 shows the calculated g' as a function of molecular weight for the randomly branched PDMAEMA

sample **B1**. This sample had g' values ranging from ~0.65 to 0.80. Additionally, the level of branching (decreasing g' value) increased as function of molecular weight.

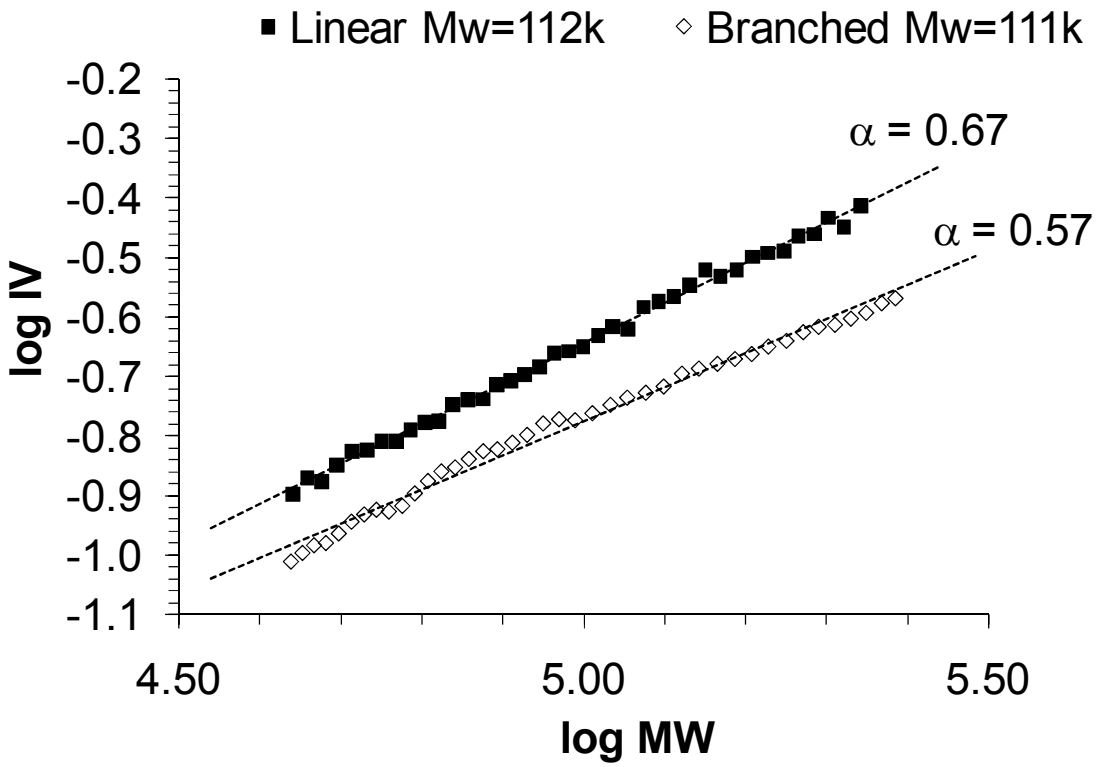

Figure 5.1. Log IV as function of log MW for linear (**L1**) and randomly branched (**B1**) PDMAEMA in 0.7 M $NaNO_3$, 0.1 M Tris Buffer, pH=6.0.

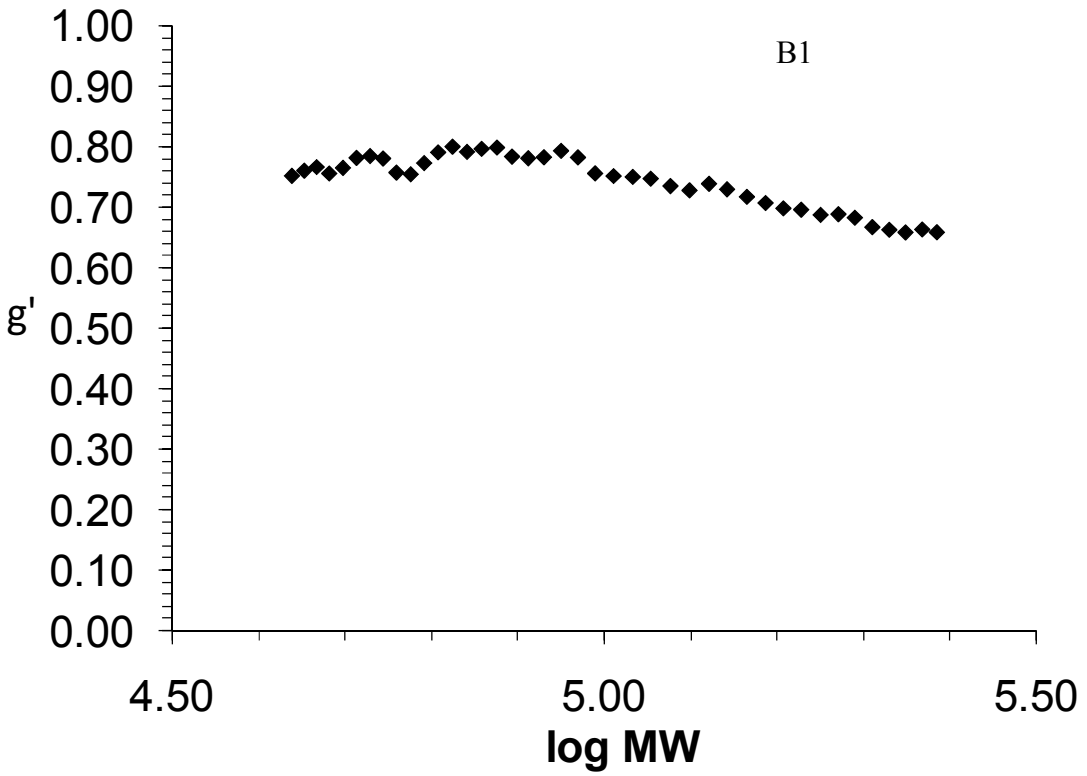

Figure 5.2. Contraction factor g' as a function of log MW for randomly branched PDMAEMA sample **B1**.

Figure 5.3 shows the MHS plots for linear and randomly branched PDMAEMA samples **L2** and **B2**, respectively. Similar to sample **B1**, the randomly branched PDMAEMA (**B2**) displayed lower intrinsic viscosities compared to the linear PDMAEMA (**L2**) of equivalent molecular weight. The viscometry results revealed that the randomly branched PDMAEMA (**B2**) had a MHS value of 0.48 whereas the linear PDMAEMA (**L2**) had a MHS value of 0.64. Since the randomly branched PDMAEMA sample **B2** had a slightly lower MHS value (0.48) than sample **B1** (0.57), it had a slightly higher level of branching. This was also evident in the calculated g'. Figure 5.4 shows the calculated g' as a function of molecular weight for the randomly branched

PDMAEMA sample **B2**. This sample had g' values ranging from ~0.40 to 0.76. The lower g' values of **B2** versus **B1** also indicated higher levels of branching in this sample.

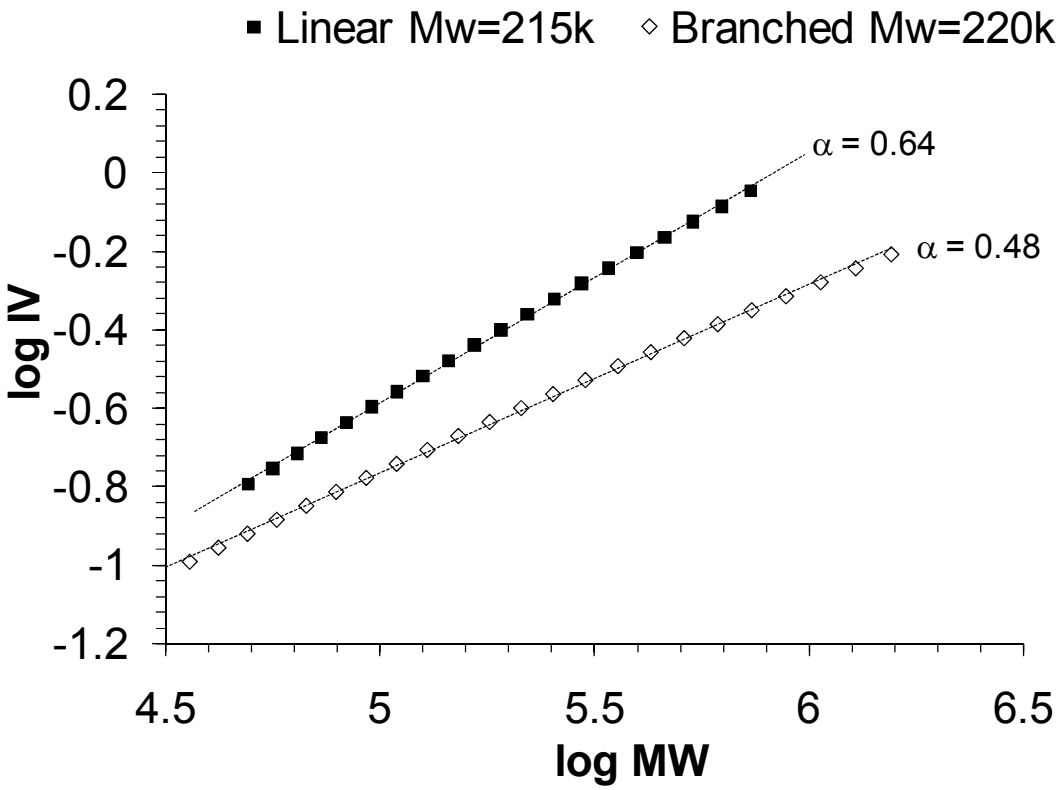

Figure 5.3. Log IV as function of log MW for linear (**L2**) and randomly branched (**B2**) PDMAEMA in 0.7 M $NaNO_3$, 0.1 M Tris Buffer, pH=6.0.

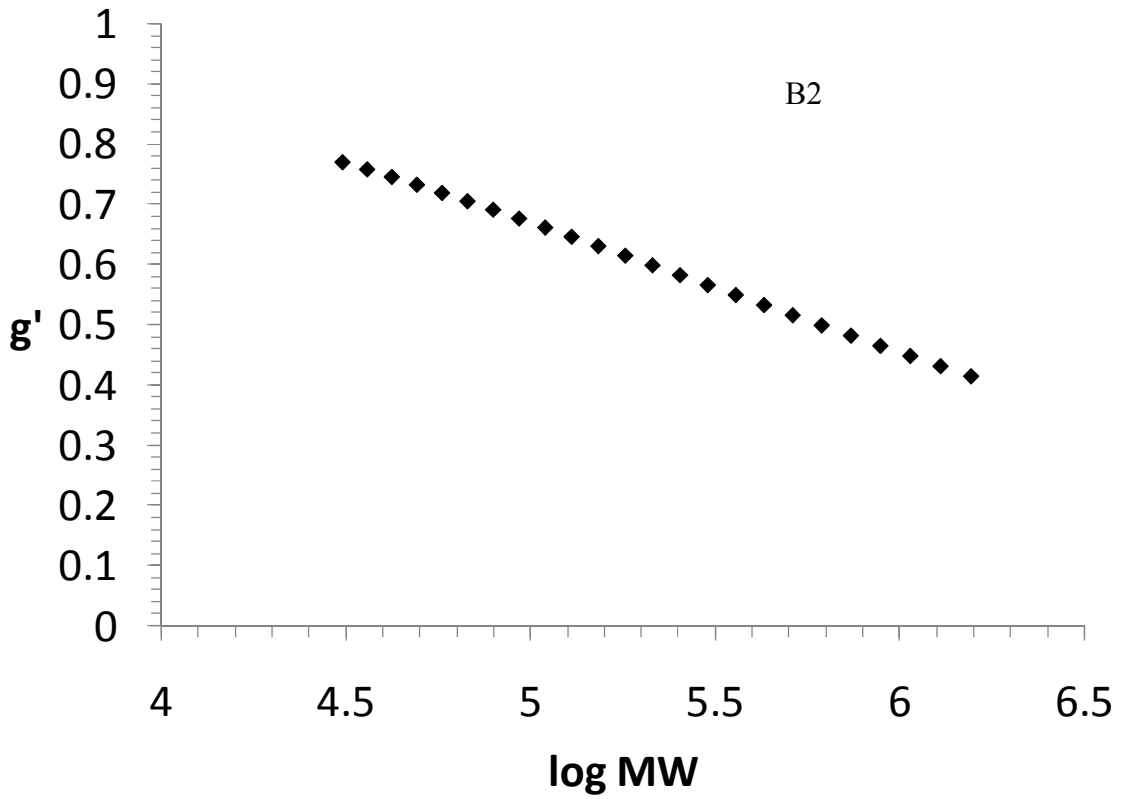

Figure 5.4. Contraction factor g' as a function of log MW for randomly branched PDMAEMA sample **B2**.

The most widely accepted mechanism for polyplex release and dissociation during transfection involves the so-called "proton-sponge hypothesis." This mechanism is based on the principle that, during endocytosis, the pH of the biological environment drops from 7.4 to ~5.0. During this pH drop, protonation of any free amines occurs resulting in an influx of chloride counter-ions. As chloride counter-ions accumulate in the endosome, the osmotic pressure increases and eventually causing the endosomal vesicle to burst and release polyplexes. Exactly how the plasmid DNA dissociated from the cationic polymer is uncertain. Since this mechanism relies on protonation of free amines during the endocytosis pH drop, we studied the titration behavior of linear and

randomly branched PDMAEMA. These experiments demonstrate how sensitive a polycation's ionization level is pH, especially in the range experienced during endocytosis. Figure 5.5 shows the pH of linear (**L2**) and randomly branched (**B2**) PDMAEMA aqueous solutions as a function of titrated HCl. The titration curves show that the linear PDMAEMA had a pKa of ~6.8 and the randomly branched PDMAEMA had a slightly lower pKa of ~6.4. These data revealed that it is slightly more difficult (requires a lower pH or more acid) to protonate randomly branched PDMAEMA than the linear polyelectrolyte. This is consistent with models proposed by Borkovec et al., which demonstrated that the topology of a weak polyelectrolyte significantly influenced its protonation behavior.[48]

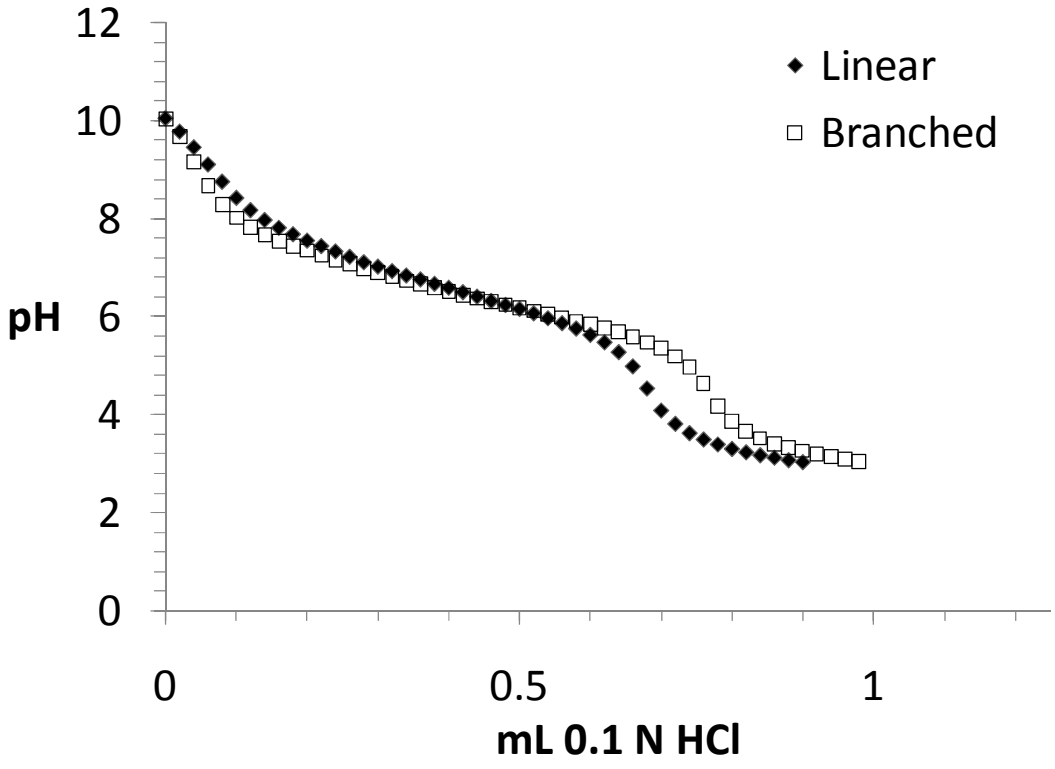

Figure 5.5. Titration of linear (**L2**) and randomly branched (**B2**) PDMAEMA .

An electrophoretic gel shift assay revealed that all PDMAEMA samples (linear and randomly branched) completely complexed (N/P ratio=4) with plasmid DNA. Figure 5.6 shows the electrophoresis results of all samples with only the free plasmid DNA (far left in the figure) showing electrophoretic mobility. All other lanes did not show any free plasmid DNA. CD spectroscopy was used to evaluate the influence of polycation topology on the secondary structure of plasmid DNA in polyplexes. As shown in Figure 5.7, the CD spectrum of plasmid DNA only demonstrates the absorption behavior of the DNA double helix with positive CD at ~225 and 275 nm and negative CD at ~240 nm. Once complexed with linear or randomly branched PDMAEMA, the CD at ~225 remained, however, the negative peak at ~240 nm shifted to ~250 nm and the positive peak at ~275 nm shifted to ~290 nm. These results demonstrated that the secondary structure of DNA was altered once complexed with PDMAEMA. However, the CD spectra showed that the topology of the PDMAEMA did not significantly influence its interaction with plasmid DNA. In other words, the CD spectra of linear PDMAEMA complexed with plasmid DNA looked almost identical to the CD spectra of randomly branched PDMAEMA complexed with plasmid DNA. However, it was clear that the binding event between both polyelectrolytes influenced the helical structure of plasmid DNA.

Figure 5.6. Agarose gel electrophoresis of pRL-SV40 plasmid complexed to linear and branched PDMAEMA samples **L1**, **B1**, **L2**, and **B2**. Electrophoresis conditions: 1% gel, 500ng pRL-SV40 per well, N/P=4, TAE running buffer, ethidium bromide staining.

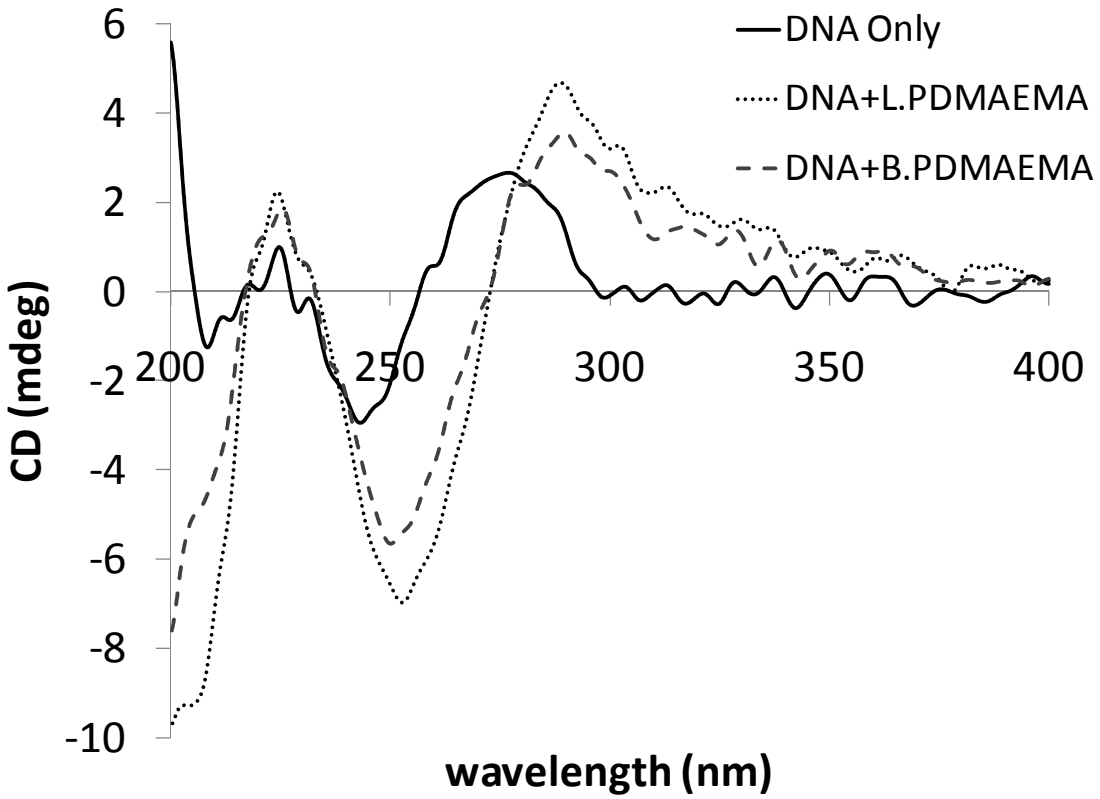

Figure 5.7. CD spectra of plasmid DNA (solid dark line), plasmid DNA complexed with linear PDMAEMA (doted gray line), and plasmid DNA complexed with randomly branched PDMAEMA (dashed gray line). All samples had a plasmid DNA concentration of 50 μg/mL in PBS. Polyplex samples had an N/P ratio of 4.

All PDMAEMA samples (linear and randomly branched) were evaluated for their ability to transfect pRL-SV40 and express catalytically active *Renilla* luciferase in HBMEC and Cos-7 cells. We first evaluated the influence of linear PDMAEMA molecular weight on luciferase expression. Figure 5.8 shows luciferase expression in HBMEC cells as a function of N/P ratio for two different linear PDMAEMA molecular weights (M_w=112,000 (**L1**) and 215,000 (**L2**) g/mol). As shown in the figure, the molecular weight of linear PDMAEMA had an influence on luciferase expression, with

the higher molecular weight sample (**L2**, 215k) showed greater transfection efficiency. Additionally, the difference in transfection activity was more pronounced at lower N/P ratios. This trend was also observed in Cos-7 cells, as shown in Figure 5.9. However, the influence of linear PDMAEMA molecular weight was less significant in Cos-7 cells. In fact, at N/P ratios of 12, 16, and 20, there was no significant difference between the lower molecular weight PDMAEMA (**L1**, 112k) and the higher molecular weight (**L2**, 215k). In is clear from these data that the influence from molecular weight must be distinguished from the influence of topology. Thus, it is important to compare linear versus branched topologies at equivalent molecular weight.

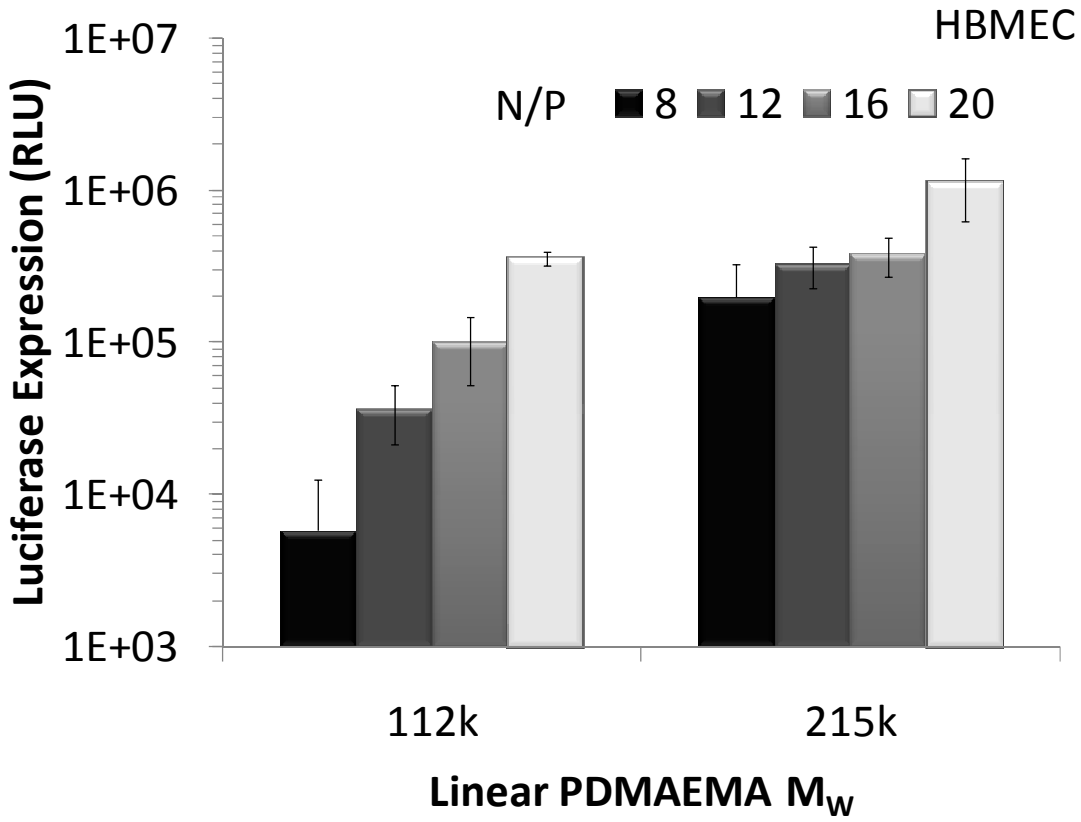

Figure 5.8. Luciferase expression in HBMEC cells transfected using two different weight-average molecular weights of linear PDMAEMA as a function of N/P ratio. Values represent the mean ± S.D.

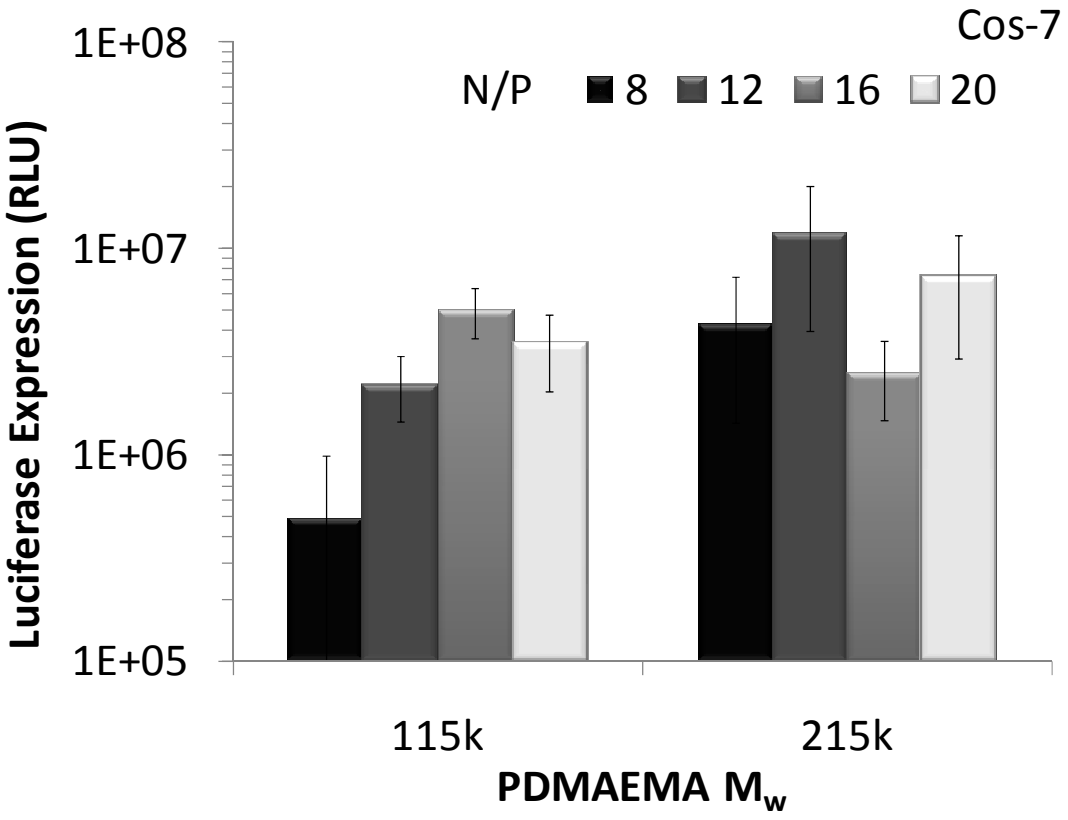

Figure 5.9. Luciferase expression in Cos-7 cells transfected using two different weight-average molecular weights of linear PDMAEMA as a function of N/P ratio. Values represent the mean ± S.D.

After demonstrating the influence of molecular weight on transfection, we next compared the transfection efficiency of linear versus randomly branched PDMAEMA at equivalent molecular weight. Figure 5.10 shows luciferase expression in HBMEC cells

as a function of N/P ratio for linear (**L1**) and randomly branched (**B1**) PDMAEMA with weight-average molecular weights of approximately M_w=110,000 g/mol. The data revealed that there was not a significant difference in transfection efficiency between the linear and randomly branched (**B1**, g'=0.75) PDMAEMA. Figure 5.11 shows luciferase expression in Cos-7 cells as a function of N/P ratio for the same two samples (**L1** and **B1**). Transfection in Cos-7 cells revealed the same trend, with linear and randomly branched PDMAEMA showing the same plasmid DNA delivery efficiency. However, the Cos-7 cells did show slight differences in transfection efficiency for N/P ratio of 8 and 20. However, no discernable trend was seen since the intermediate N/P of 12 and 16 showed similar transfection efficiencies.

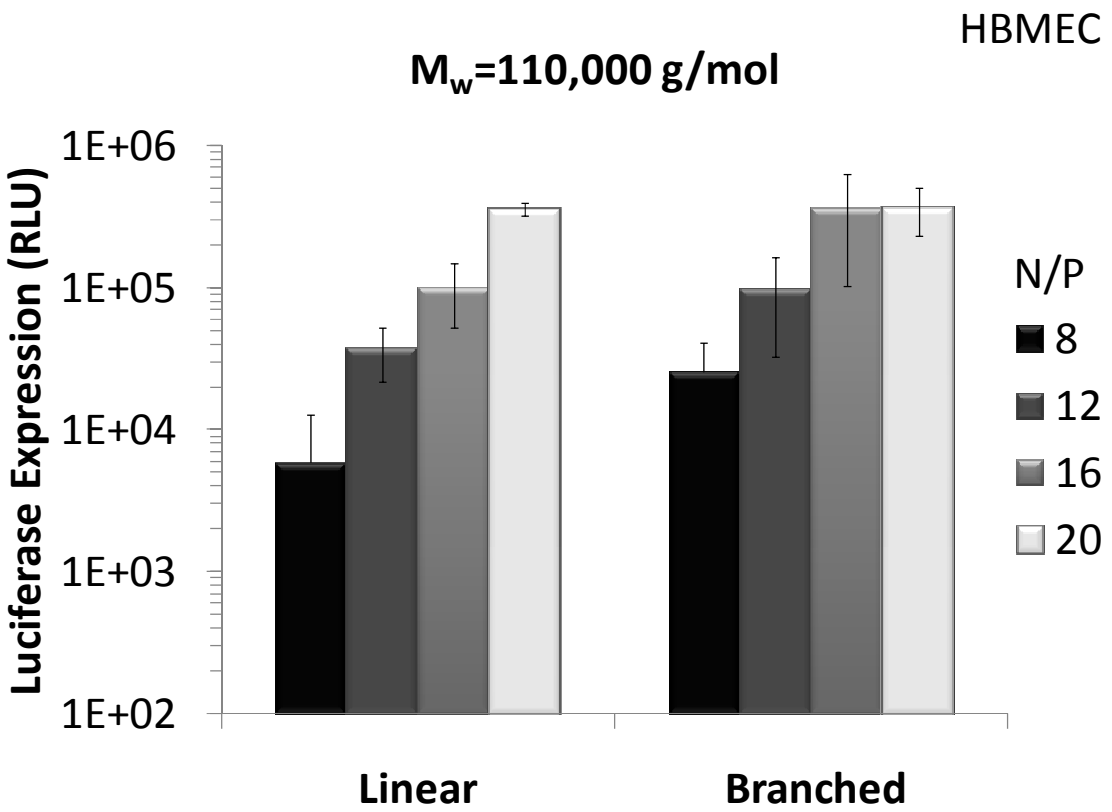

Figure 5.10. Luciferase expression in HBMEC cells transfected using linear and branched PDMAEMA with similar weight-average molecular weights (~110,000 g/mol) as a function of N/P ratio. Values represent the mean ± S.D.

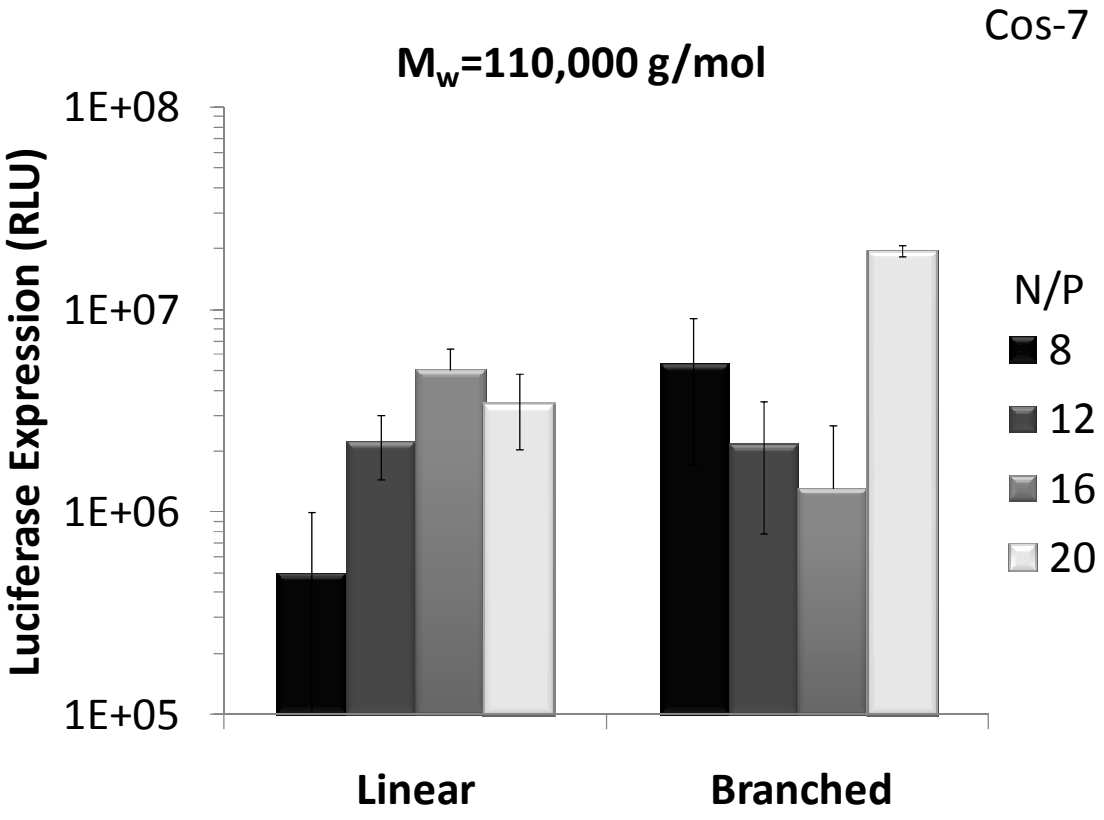

Figure 5.11. Luciferase expression in Cos-7 cells transfected using linear and branched PDMAEMA with similar weight-average molecular weights (~110,000 g/mol) as a function of N/P ratio. Values represent the mean ± S.D.

Figure 5.12 shows luciferase expression in HBMEC cells as a function of N/P ratio for linear (**L2**) and randomly branched (**B2**) PDMAEMA with weight-average molecular weights of approximately M_w=220,000 g/mol. In HBMEC cells, there was a

subtle difference in transfection efficiency between the linear and randomly branched PDMAEMA, with the branched sample (**B2**, g'=0.60) showing slightly reduced luciferase expression. The differences in transfection efficiencies were statistically significant for all N/P ratios, however, the separation in error bars between the linear and randomly branched samples was not drastic. Furthermore, in Cos-7 cells (shown in Figure 5.13), the same two samples (L2 and B2) did not show any statistical difference in transfection activity for all N/P ratios.

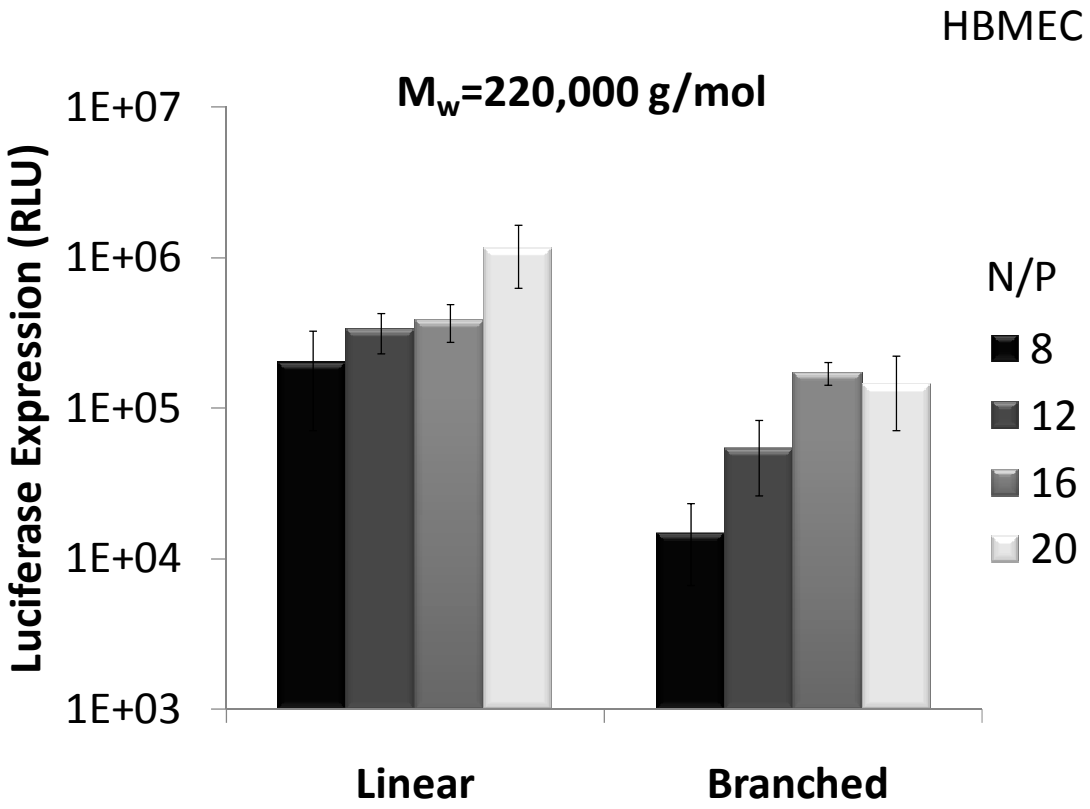

Figure 5.12. Luciferase expression in HBMEC cells transfected using linear and branched PDMAEMA with similar weight-average molecular weights (~220,000 g/mol) as a function of N/P ratio. Values represent the mean ± S.D.

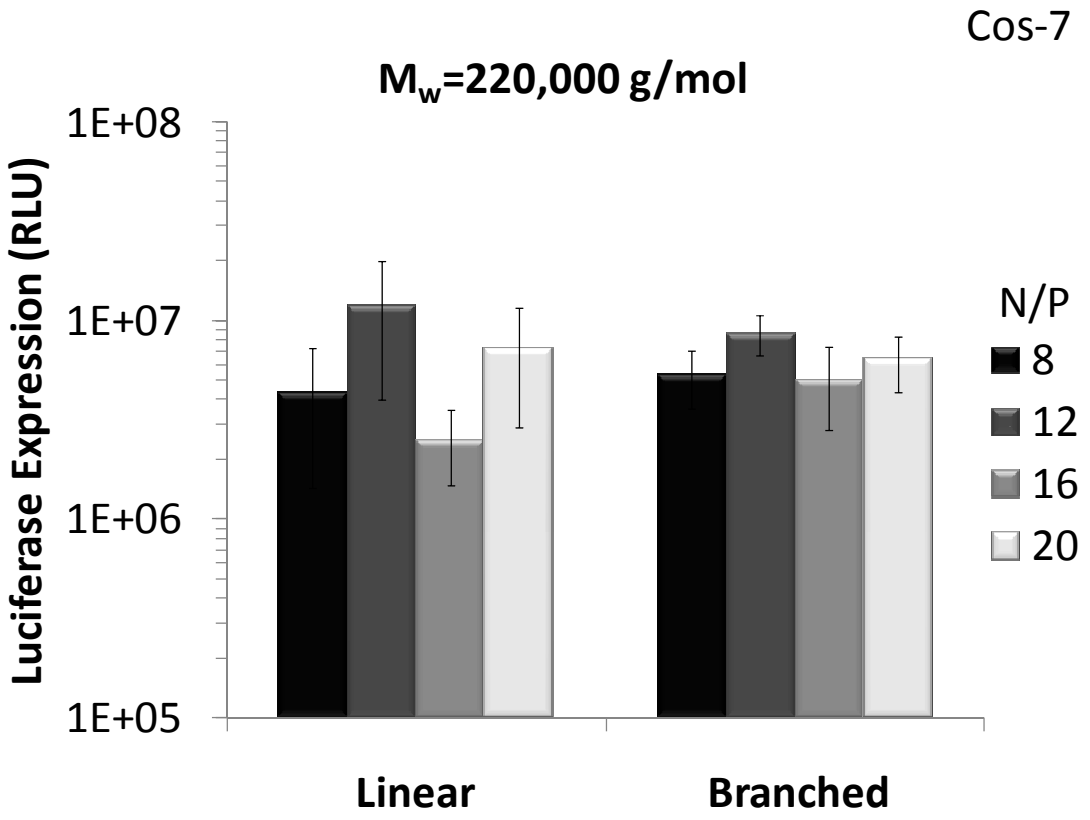

Figure 5.13. Luciferase expression in Cos-7 cells transfected using linear and branched PDMAEMA with similar weight-average molecular weights (~220,000 g/mol) as a function of N/P ratio. Values represent the mean ± S.D.

Collectively, the transfection data revealed that sparse random branching in PDMAMEA did not significantly influence plasmid DNA delivery. Only subtle differences were observed under certain conditions (cell type, specific N/P ratio). We originally hypothesized that branching would influence DNA delivery in some way since previous studies by von Gersforff et al. reported that linear and branched PEI's are internalized by different endosomal routes with size of the polyplex being the main factor.[49] However, we did not observe in influence from polycation topology, either

increasing or decreasing transfection activity. One reason we did not observe any difference in transfection activity could arise from the low levels of branching introduced into the synthesized branched samples. The g' values (**B1** g'=0.75, **B2** g'=0.60) indicated that these samples were only sparsely branched. Perhaps if randomly branched PDMAEMA samples were synthesized with greater amounts of EGDMA, lower g' values could be achieved and show significantly different transfection behavior compared to a linear analog at equivalent molecular weight.

5.5 Conclusions

Conventional free radical polymerization was used to synthesize linear and randomly branched cationic polyelectrolytes based on PDMAEMA. Rheological methods were used to determine the level of branching, calculated as the g' contraction factor. Four samples, grouped according to similar weight-average molecular weights (M_w=110,000 and 215,000 g/mol), were comparatively analyzed for their ability to form complexes with and transfect plasmid DNA *in vitro*. Gel electrophoresis and CD spectroscopy demonstrated that the topology of PDMAEMA did not influence its binding with plasmid DNA. For both HBMEC and Cos-7 cells *in vitro*, the topology of the PDMAEMA did not have a significant influence on gene transfection efficiency.

5.6 Acknowledgments

The authors would like to thank the laboratory Dr. Carla V. Finkielstein for assistance with experiments to amplify plasmid DNA and helpful discussions. This

material is based upon work supported in part by the Macromolecular Interfaces with Life Sciences (MILES) Integrative Graduate Education and Research Traineeship (IGERT) of the National Science Foundation under Agreement No. DGE-0333378.

5.7 References

[1]Emery, D. W., Gene therapy for genetic diseases: On the horizon. *Clinical and Applied Immunology Reviews* **2004,** 4, (6), 411-422.

[2]Palmer, D. H.; Young, L. S.; Mautner, V., Cancer gene-therapy: clinical trials. *Trends in Biotechnology* **2006,** 24, (2), 76-82.

[3]Ma, H.; Diamond, S. L., Nonviral Gene Therapy and its Delivery Systems. *Current Pharmaceutical Biotechnology* **2001,** 2, 1-17.

[4]Kaiser, J., CLINICAL RESEARCH: Death Prompts a Review of Gene Therapy Vector. *Science* **2007,** 317, (5838), 580-.

[5]Rungsardthong, U.; Ehtezazi, T.; Bailey, L.; Armes, S. P.; Garnett, M. C.; Stolnik, S., Effect of Polymer Ionization on the Interaction with DNA in Nonviral Gene Delivery Systems. *Biomacromolecules* **2003,** 4, (3), 683-690.

[6]Dubruel, P.; De Strycker, J.; Westbroek, P.; Bracke, K.; Temmerman, E.; Vandervoort, J.; Ludwig, A.; Schacht, E., Synthetic polyamines as vectors for gene delivery. *Polymer International* **2002,** 51, (10), 948-957.

[7]De Smedt, S. C.; Demeester, J.; Hennink, W. E., Cationic Polymer Based Gene Delivery Systems. *Pharmaceutical Research* **2000,** 17, (2), 113-126.

[8]Leclercq, L.; Boustta, M.; Vert, M., A Physico-chemical Approach of Polyanion-Polycation Interactions Aimed at Better Understanding the In Vivo Behaviour of Polyelectrolyte-based Drug Delivery and Gene Transfection. *Journal of Drug Targeting* **2003,** 11, 129-138.

[9]Eliyahu, H.; Barenholz, Y.; Domb, A. J., Polymers for DNA delivery. *Molecules* **2005,** 10, (1), 34-64.

[10]van de Wetering, P.; Moret, E. E.; Schuurmans-Nieuwenbroek, N. M. E.; van Steenbergen, M. J.; Hennink, W. E., Structure-Activity Relationships of Water-Soluble Cationic Methacrylate/Methacrylamide Polymers for Nonviral Gene Delivery. *Bioconjugate Chem.* **1999,** 10, (4), 589-597.

[11]Jones, R. A.; Poniris, M. H.; Wilson, M. R., pDMAEMA is internalised by endocytosis but does not physically disrupt endosomes. *Journal of Controlled Release* **2004,** 96, (3), 379-391.

[12]Tiera, M. J.; Winnik, F. M.; Fernandes, J. C., Synthetic and Natural Polycations for Gene Therapy: State of the Art and New Perspectives. *Current Gene Therapy* **2006,** 6, 59-71.

[13]Kodama, K.; Katayama, Y.; Shoji, Y.; Nakashima, H., The Features and Shortcomings for Gene Delivery of Current Non-Viral Carriers. *Current Medicinal Chemistry* **2006,** 13, 2155-2161.

[14]Miller, A. D., The Problem with Cationic Liposome / Micelle-Based Non-Viral Vector Systems for Gene Therapy. *Current Medicinal Chemistry* **2003,** 10, 1195-1211.

[15]Dubruel, P.; Christiaens, B.; Rosseneu, M.; Vandekerckhove, J.; Grooten, J.; Goossens, V.; Schacht, E., Buffering Properties of Cationic Polymethacrylates Are Not the Only Key to Successful Gene Delivery. *Biomacromolecules* **2004,** 5, (2), 379-388.

[16]Cherng, J.-Y.; van de Wetering, P.; Talsma, H.; Crommelin, D. J. A.; Hennink, W. E., Effect of Size and Serum Proteins on Transfection Efficiency of Poly ((2-dimethylamino)ethyl Methacrylate)-Plasmid Nanoparticles. *Pharmaceutical Research* **1996,** 13, (7), 1038-1042.

[17]Verbaan, F. J.; Klouwenberg, P. K.; Steenis, J. H. v.; Snel, C. J.; Boerman, O.; Hennink, W. E.; Storm, G., Application of poly(2-(dimethylamino)ethyl methacrylate)-based polyplexes for gene transfer into human ovarian carcinoma cells. *International Journal of Pharmaceutics* **2005,** 304, (1-2), 185-192.

[18]van der Aa, M.; Huth, U.; Häfele, S.; Schubert, R.; Oosting, R.; Mastrobattista, E.; Hennink, W.; Peschka-Süss, R.; Koning, G.; Crommelin, D., Cellular Uptake of Cationic

Polymer-DNA Complexes Via Caveolae Plays a Pivotal Role in Gene Transfection in COS-7 Cells. *Pharmaceutical Research* **2007,** 24, (8), 1590-1598.

[19]Verbaan, F.; van Dam, I.; Takakura, Y.; Hashida, M.; Hennink, W.; Storm, G.; Oussoren, C., Intravenous fate of poly(2-(dimethylamino)ethyl methacrylate)-based polyplexes. *European Journal of Pharmaceutical Sciences* **2003,** 20, (4-5), 419-427.

[20]Verbaan, F. J.; Oussoren, C.; van Dam, I. M.; Takakura, Y.; Hashida, M.; Crommelin, D. J. A.; Hennink, W. E.; Storm, G., The fate of poly(2-dimethyl amino ethyl)methacrylate-based polyplexes after intravenous administration. *International Journal of Pharmaceutics* **2001,** 214, (1-2), 99-101.

[21]van de Wetering, P.; Cherng, J. Y.; Talsma, H.; Crommelin, D. J. A.; Hennink, W. E., 2-(dimethylamino)ethyl methacrylate based (co)polymers as gene transfer agents. *Journal of Controlled Release* **1998,** 53, (1-3), 145-153.

[22]Taira, K.; Kataoka, K.; Niidome, T.; Editors, *Non-viral Gene Therapy: Gene Design and Delivery*. 2005; p 487 pp.

[23]Santhakumaran, L. M.; Thomas, T.; Thomas, T. J., Enhanced cellular uptake of a triplex-forming oligonucleotide by nanoparticle formation in the presence of polypropylenimine dendrimers. *Nucl. Acids Res.* **2004,** 32, (7), 2102-2112.

[24]Banerjee, P.; Reichardt, W.; Weissleder, R.; Bogdanov, A., Novel Hyperbranched Dendron for Gene Transfer in Vitro and in Vivo. *Bioconjugate Chem.* **2004,** 15, (5), 960-968.

[25]Vlasov, G., Starlike branched and hyperbranched biodegradable polymer systems as DNA carriers. *Russian Journal of Bioorganic Chemistry* **2006,** 32, (3), 205-218.

[26]Fischer, D.; Bieber, T.; Li, Y.; Elsässer, H.-P.; Kissel, T., A Novel Non-Viral Vector for DNA Delivery Based on Low Molecular Weight, Branched Polyethylenimine: Effect of Molecular Weight on Transfection Efficiency and Cytotoxicity. *Pharmaceutical Research* **1999,** 16, (8), 1273-1279.

[27]Oster, C. G.; Wittmar, M.; Bakowsky, U.; Kissel, T., DNA nano-carriers from biodegradable cationic branched polyesters are formed by a modified solvent displacement method. *Journal of Controlled Release* **2006,** 111, (3), 371-381.

[28]Wiseman, J. W.; Goddard, C. A.; McLelland, D.; Colledge, W. H., A comparison of linear and branched polyethylenimine (PEI) with DCChol//DOPE liposomes for gene delivery to epithelial cells in vitro and in vivo. *Gene Ther* **2003,** 10, (19), 1654-1662.

[29]Verbaan, F. J.; Bos, G. W.; Oussoren, C.; Woodle, M. C.; Hennink, W. E.; Storm, G., A comparative study of different cationic transfection agents for in vivo gene delivery after intravenous administration. **2004,** 14, (2), 105-111.

[30]Boletta, A.; Benigni, A.; Lutz, J.; Remuzzi, G.; Soria, M. R.; Monaco, L., Nonviral gene delivery to the rat kidney with polyethylenimine. *Hum Gene Ther* **1997,** 8, (10), 1243-51.

[31]Kawakami, S.; Ito, Y.; Charoensit, P.; Yamashita, F.; Hashida, M., Evaluation of Proinflammatory Cytokine Production Induced by Linear and Branched Polyethylenimine/Plasmid DNA Complexes in Mice. *J Pharmacol Exp Ther* **2006,** 317, (3), 1382-1390.

[32]Fischer, D.; von Harpe, A.; Kunath, K.; Petersen, H.; Li, Y.; Kissel, T., Copolymers of Ethylene Imine and N-(2-Hydroxyethyl)-ethylene Imine as Tools To Study Effects of Polymer Structure on Physicochemical and Biological Properties of DNA Complexes. *Bioconjugate Chem.* **2002,** 13, (5), 1124-1133.

[33]Zhang, C.; Yadava, P.; Hughes, J., Polyethylenimine strategies for plasmid delivery to brain-derived cells. *Methods* **2004,** 33, (2), 144-150.

[34]Georgiou, T. K.; Vamvakaki, M.; Phylactou, L. A.; Patrickios, C. S., Synthesis, Characterization, and Evaluation as Transfection Reagents of Double-Hydrophilic Star Copolymers: Effect of Star Architecture. *Biomacromolecules* **2005,** 6, (6), 2990-2997.

[35]Georgiou, T. K.; Vamvakaki, M.; Patrickios, C. S.; Yamasaki, E. N.; Phylactou, L. A., Nanoscopic Cationic Methacrylate Star Homopolymers: Synthesis by Group Transfer Polymerization, Characterization and Evaluation as Transfection Reagents. *Biomacromolecules* **2004,** 5, (6), 2221-2229.

[36]Yasuhide, N.; Takeshi, M.; Makoto, N.; Michiko, H.; Moto, O.; Mariko, H.-S., High Performance Gene Delivery Polymeric Vector: Nano-Structured Cationic Star Polymers (Star Vectors). *Current Drug Delivery* **2005,** 2, 53-57.

[37]Petersen, H.; Kunath, K.; Martin, A. L.; Stolnik, S.; Roberts, C. J.; Davies, M. C.; Kissel, T., Star-Shaped Poly(ethylene glycol)-block-polyethylenimine Copolymers

Enhance DNA Condensation of Low Molecular Weight Polyethylenimines. *Biomacromolecules* **2002,** 3, (5), 926-936.

[38]Wu, D.-C.; Liu, Y.; Jiang, X.; Chen, L.; He, C.-B.; Goh, S. H.; Leong, K. W., Evaluation of Hyperbranched Poly(amino ester)s of Amine Constitutions Similar to Polyethylenimine for DNA Delivery. *Biomacromolecules* **2005,** 6, (6), 3166-3173.

[39]Zhong, Z.; Song, Y.; Engbersen, J. F. J.; Lok, M. C.; Hennink, W. E.; Feijen, J., A versatile family of degradable non-viral gene carriers based on hyperbranched poly(ester amine)s. *Journal of Controlled Release* **2005,** 109, (1-3), 317-329.

[40]Hollins, A.; Benboubetra, M.; Omidi, Y.; Zinselmeyer, B.; Schatzlein, A.; Uchegbu, I.; Akhtar, S., Evaluation of Generation 2 and 3 Poly(Propylenimine) Dendrimers for the Potential Cellular Delivery of Antisense Oligonucleotides Targeting the Epidermal Growth Factor Receptor. *Pharmaceutical Research* **2004,** 21, (3), 458-466.

[41]Krämer, M.; Stumbé, J.-F.; Grimm, G.; Kaufmann, B.; Krüger, U.; Weber, M.; Haag, R., Dendritic Polyamines: Simple Access to New Materials with Defined Treelike Structures for Application in Nonviral Gene Delivery. *ChemBioChem* **2004,** 5, (8), 1081-1087.

[42]Mori, H.; Walther, A.; Andre, X.; Lanzendorfer, M. G.; Muller, A. H. E., Synthesis of Highly Branched Cationic Polyelectrolytes via Self-Condensing Atom Transfer Radical Copolymerization with 2-(Diethylamino)ethyl Methacrylate. *Macromolecules* **2004,** 37, (6), 2054-2066.

[43]Liu, Y.; Wenning, L.; Lynch, M.; Reineke, T. M., New Poly(D-glucaramidoamine)s Induce DNA Nanoparticle Formation and Efficient Gene Delivery into Mammalian Cells. *J. Am. Chem. Soc.* **2004,** 126, (24), 7422-7423.

[44]Liu, Y.; Reineke, T. M., Poly(glycoamidoamine)s for Gene Delivery: Stability of Polyplexes and Efficacy with Cardiomyoblast Cells. *Bioconjugate Chem.* **2006,** 17, (1), 101-108.

[45]Srinivasachari, S.; Liu, Y.; Zhang, G.; Prevette, L.; Reineke, T. M., Trehalose Click Polymers Inhibit Nanoparticle Aggregation and Promote pDNA Delivery in Serum. *J. Am. Chem. Soc.* **2006,** 128, (25), 8176-8184.

[46]Stins, M. F.; Gilles, F.; Kim, K. S., Selective expression of adhesion molecules on human brain microvascular endothelial cells. *Journal of Neuroimmunology* **1997,** 76, (1-2), 81-90.

[47]Layman, J. M.; Borgerding, E. M.; Williams, S. R.; Heath, W. H.; Long, T. E., Synthesis and Characterization of Aliphatic Ammonium Ionenes: Aqueous Size Exclusion Chromatography for Absolute Molecular Weight Characterization. *Macromolecules* **2008,** 41, (13), 4635-4641.

[48]Borkovec, M.; Koper, G. J. M., Proton Binding Characteristics of Branched Polyelectrolytes. *Macromolecules* **1997,** 30, (7), 2151-2158.

[49]von Gersdorff, K.; Sanders, N. N.; Vandenbroucke, R.; De Smedt, S. C.; Wagner, E.; Ogris, M., The Internalization Route Resulting in Successful Gene Expression Depends on both Cell Line and Polyethylenimine Polyplex Type. *Mol Ther* **2006,** 14, (5), 745-753.

Chapter 6. **Influence of Polycation Molecular Weight on Poly(2-dimethylaminoethyl methacrylate)-Mediated DNA Delivery In Vitro**

John M. Layman, Sean M. Ramirez, Matthew D. Green, and Timothy E. Long

6.1 Abstract

Establishing clear structure-property-transfection relationships is a critical step in the development of clinically relevant polymers for non-viral gene therapy. In this study, we determined the influence of poly(2-dimethylaminoethyl methacrylate) (PDMAEMA) molecular weight on cytotoxicity, DNA binding, and *in vitro* plasmid DNA delivery efficiency in human brain microvascular endothelial cells (HBMEC). Conventional free-radical polymerization was used to synthesize PDMAEMA with weight-average molecular weights ranging from 43,000 to 915,000 g/mol. MTT and LDH assays revealed that lower molecular weight PDMAEMA (M_w=43,000 g/mol) was slightly less toxic than higher molecular weights (M_w >112,000 g/mol) and that the primary mode of toxicity was cellular membrane destabilization. An electrophoretic gel shift assay revealed that all PDMAEMA molecular weights completely bound with plasmid DNA. However, heparin competitive binding experiments revealed that higher molecular weight PDMAEMA (M_w=915,000 g/mol) had a greater binding affinity towards plasmid DNA than lower molecular weight PDMAEMA (M_w=43,000 g/mol). The molecular weight of

PDMAEMA was found to have a dramatic influence on transfection efficiency, and gene expression increased as a function of increasing molecular weight. However, cellular uptake of polyplexes was determined to be insensitive to PDMAEMA molecular weight. In addition, our data did not correlate polyplex size with transfection efficiency. Collectively, our data suggested that the intracellular fate of the polyplexes, which involves endosomal release and DNase resistance, is more important to overall transfection efficiency than barriers to entry, such as polyplex size.

KEYWORDS: gene delivery, plasmid DNA, non-viral agents, polycation, PDMAEMA, molecular weight

6.2 Introduction

Non-viral gene therapy is an area of intense study due to the potential to greatly enhance human medicine. In gene therapy, extra-chromosomal nucleic acids are transferred through the cellular membrane and express a therapeutic level of a defective or deficient protein.[1] Delivery agents, or vectors, are needed due to the polyanionic nature of nucleic acids, which interacts unfavorably with the slightly negatively charged cellular membrane. The goal is to transfer a sufficient amount of DNA to produce a therapeutic level of protein and subsequently alleviate the phenotype(s) of the disease. Historically, many deactivated viruses have been used since these carriers provide the highest delivery efficiencies.[2, 3] However, despite being rendered replication deficient, viral vectors often provoke severe immune response in the host, tragically leading to fatalities in some pre-clinical gene therapy trials.[4] Non-viral agents, such as cationic

polyelectrolytes, offer a synthetic alternative to viral vectors due to reduction of immunogenic risk and the ability to tailor their macromolecular structure.[5-14] However, despite the advantages of non-viral agents, several investigators have shown that transfection efficiencies are considerably lower compared to viral vectors.[15, 16] Therefore, non-viral vectors may not find wide-spread clinical application until transfection efficiencies rival viral-based vectors.

Cationic polymers spontaneously form nanoscale, electrostatic complexes with anionic nucleic acids, termed polyplexes.[17] Over the past decade, several investigators have employed various elements in the design of cationic polymers to steadily improve transfection efficiencies; this topic was recently and comprehensively reviewed by Park et al.[7] and Putnam et al.[6] However, despite the improvements to date, there are many unanswered questions associated with the fundamental mechanisms that govern non-viral gene delivery. Our work aimed to elucidate structure-transfection relationships in polycation-mediated plasmid DNA delivery.

In this paper, we investigated the influence of polycation molecular weight on transfection efficiency. Pioneering work by Hennink et al. determined that the molecular weight of poly(2-dimethylaminoethyl methacrylate) (PDMAEMA) significantly influenced transfection efficiency, and higher molecular weights (M_w >300,000 g/mol) showed higher transfection efficiencies.[18] The authors associated the molecular weight dependence with polyplex size.[18] Reineke et al. have shown that the molecular weight (M_w=26,000-70,000 g/mol) of trehalose oligoethylenamine click polymers[19, 20] influenced luciferase expression but not cellular uptake.[21] Mikos et al. also found that higher molecular weight poly(ethylene imine) (PEI) (M_p=70,000 g/mol) transfected better than

lower molecular weight PEI (M_p=1,800 g/mol).[22] However, a narrow molecular weight range and relatively low molecular weights were investigated. In addition, Hashida et al. showed an opposite trend and found that lower molecular weight PEI (M_p=1,800 g/mol) gave higher transfection efficiencies than higher molecular weight PEI (M_p=70,000 g/mol).[23] It should be noted that PEI used by Mikos et al. and Hashida et al. were obtained from the same commercial source (Polysciences), however each group independently obtained contrasting results. Each group transfected different cell lines, which may partially explain the reported differences. Similar to Hashida et al., Kissel et al. found that lower molecular weight PEI (M_w=11,900 g/mol) enabled higher transfection efficiencies than higher molecular weight PEI (M_w=1,616,000 g/mol).[24] It is clear from the contrasting results obtained from the aforementioned investigators[21-24] that a fundamental understanding of the influence of polycation molecular weight on DNA delivery remains elusive. In addition to influencing *in vitro* transfection efficiency, Seymour et al. have shown that the molecular weight of poly(L-lysine) influences *in vivo* systemic circulation time of polyplexes,[25] which will be important if cationic polymers find utility in the clinical setting.

In order to fundamentally understand macromolecular structure-transfection relationships, our laboratories evaluated the influence of polycation molecular weight on DNA binding, cytotoxicity, and *in vitro* DNA delivery. In this work, we synthesized a broad range of molecular weights of PDMAEMA (M_w=43,000 - 915,000 g/mol) using conventional free-radical polymerization. It addition, it is important to note that all molecular weights distributions were between 1.29 and 2.26. Although PDMAEMA does not show exceptionally high transfection efficiency compared to other cationic

polymers, strategies for synthesis and characterization using conventional techniques are well-established, and PDMAEMA serves as an excellent model for structure-transfection studies. Furthermore, several investigators have studied the transfection behavior of PDMAEMA, including pioneering efforts by Hennink et al.[18, 26-35] We analyzed the transfection efficiency of five PDMAEMA samples with weight-average molecular weights 43,000, 112,000, 215,000, 527,000, and 915,000 g/mol. Polymer characterization, plasmid DNA binding, cytotoxicity, cellular uptake, and transfection performance are reported.

6.3 Experimental

6.3.1 General Methods and Materials.

2-(N,N'-dimethylamino)ethyl methacrylate (DMAEMA, 98%, Sigma-Aldrich) was passed through a neutral alumina column to remove free-radical inhibitor. 2,2'-azobisisobutyronitrile (AIBN, 99%, Sigma-Aldrich) and ammonium persulfate (APS, 98%, Sigma-Aldrich) were used as received. Deuterium oxide (D_2O, 99.9%, Cambridge Isotope Laboratories) was used as received for all NMR measurements. Sodium nitrate ($NaNO_3$, 99.0%, Alfa Aesar), trishydroxymethylaminomethane (TRIS, 99.8%, Alfa Aesar), glacial acetic acid (AcOH, 99.7%, Alfa Aesar), sodium azide (NaN_3, 99%, Alfa Aesar), sodium chloride (NaCl, 99.0%, Sigma-Aldrich), 1-dodecanethiol (DT, 98%, Sigma-Aldrich) were all used as received. Ultrapure water having a resistivity of 18.2 MΩ·cm was obtained using a Millipore Direct-Q5 purification system. All other solvents and reagents were used as received from commercial sources without further purification unless specifically noted elsewhere.

^{1}H NMR spectra were recorded on a Varian Inova 400 MHz spectrometer. Chemical shifts are reported in ppm downfield from TMS using the residual protonated solvent as an internal standard (D_2O, 1H 4.79 ppm).

6.3.2 Synthesis of PDMAEMA.

In a typical synthesis, DMAEMA was charged with AIBN (0.10-0.30 wt% monomer) in THF at 20 wt% solids in a multi-necked, round-bottomed flask. A reflux condenser was affixed to the flask and the reaction mixture was purged with nitrogen for approximately 30 min. The flask was then submerged in an oil bath preheated to 60 ^oC. The polymerization was allowed to proceed for 24 h under magnetic stirring. The resulting polymer was precipitated in hexanes. After decantation of the hexanes, the polymer was dried under vacuum at 80 ^oC. Dissolution of the neutral PDMAEMA product in aqueous HCl (pH=5.0) under magnetic stirring was used to convert each polymer to a hydrochloride salt. The PDMAEMA·HCl polyelectrolyte was then precipitated in acetone. The acetone was decanted and a white powder was dried under vacuum at 80 ^oC. High molecular weight PDMAEMA (M_w > 250,000 g/mol) was synthesized according to methods previously described.[36] DMAEMA was charged with APS (0.1-1.0 wt% monomer) in ultrapure water at 20 wt% solids in a multi-necked, round-bottomed flask. The pH of the reaction solution was adjusted to 5 using concentrated HCl prior to polymerization. A rubber septum was affixed to the flask and the reaction mixture was purged with nitrogen for approximately 30 min. The flask was then submerged in an oil bath preheated to 60 ^oC. The polymerization was allowed to proceed for 24 h under magnetic stirring. The resulting polymer was precipitated in acetone.

All samples were dialyzed against distilled water for at least 48 h using Spectra/Por dialysis tubing (MWCO=3,500 g/mol). Lyophilization was used to recover samples prior to characterization. ^{1}H NMR (400 MHz, D_2O): δ (ppm)= 4.40 (br, 2H), 3.59 (br, 2H), 3.01 (br, 6H), 2.05 (br, 2H), 1.02 (br, 3H). M_n and M_w are summarized in Table 6.1.

6.3.3 Aqueous size exclusion chromatography-multiangle laser light scattering (SEC-MALLS).

Aqueous SEC experiments were performed in a buffered solution consisting of 0.7 M sodium nitrate and 0.1 M TRIS adjusted to pH 6.0 with glacial acetic acid. The pH of the resulting solution was measured using a Thermo Orion 3 Star portable pH meter with a Thermo Orion Triode pH electrode. Sodium azide was added at 200 ppm to the solution as a precaution to prevent bacterial growth in the SEC system. Samples were analyzed at 0.8 mL/min through 2x Waters Ultrahydrogel Linear and 1x Water Ultrahydrogel 250 columns, with all columns measuring 7.8 x 300 mm and equilibrated to 30 ^{o}C. SEC-MALLS instrumentation consisted of a Waters 1515 isocratic HPLC pump, Waters 717plus Autosampler, Wyatt miniDAWN multiangle laser light scattering (MALLS) detector operating a He-Ne laser at a wavelength of 690 nm, Viscotek 270 capillary viscosity detector, and a Waters 2414 differential refractive index detector operating at a wavelength of 880 nm and 35 ^{o}C. The only calibration constant, the Wyatt Astra V AUX1, was calculated using a series of aqueous sodium chloride solutions. The accuracy and reproducibility was confirmed with poly(ethylene oxide) (Sigma-Aldrich) ranging in molecular weight from 230 to 1,000,000 g/mol. Absolute molecular weights were determined using the Wyatt Astra V software package. The specific refractive

index increment (*dn/dc*) for linear PDMAEMA was determined offline. A Wyatt OptiRex differential/absolute refractive index detector operating at a wavelength of 690 nm and 30 ^{o}C was used for all specific refractive index increment measurements. Polymer samples (0.05 – 2.00 mg/mL) were allowed to dissolve in the appropriate solvent overnight. Samples were metered at 0.8 mL/min into the RI detector at 30 ˚C using a syringe pump and a syringe affixed with a 0.45 μm PTFE syringe filter. The *dn/dc* values were determined using the Wyatt Astra V software package. The *dn/dc* for all linear PDMAEMA samples was determined to be 0.149 ± 0.002 mL/g.

6.3.4 Dynamic Light Scattering.

To prepare polyplexes for DLS experiments, gWiz-Luc plasmid (1 μg/μL in H_2O, Aldevron) was diluted in phosphate buffered saline to a concentration of 0.8 μg/mL and incubated at room temperature for 10 min. At the same time, the appropriate type and amount of polymer was diluted in basal RPMI to final concentrations corresponding to the various nitrogen/phosphorus (N/P) ratios and allowed to incubate for 10 min at room temperature. N/P ratios were calculated according to equation 1,

$$\frac{N}{P} = \frac{m_p \overline{M}_{o,D}}{2 m_D M_{o,p}} \qquad (1)$$

where N/P is the ratio of nitrogen atoms in the polymer to phosphorous atoms in DNA, m_p is the mass of polymer, m_D is the mass of DNA, $\overline{M}_{o,D}$ is the average repeat unit molecular weight of DNA, and $M_{o,p}$ is the repeat unit molecular weight of the polymer. Equation 1 assumes there is only one ionizable nitrogen group per repeat unit of the polymer. Then, 100 μL of plasmid and 100 μL of the corresponding polymer solutions

were combined (final DNA concentration of 0.4 μg/mL) and incubated for 20-30 min at room temperature to complex the plasmid DNA with PDMAEMA. Dynamic light scattering measurements were performed on a Malvern Zeta Sizer Nano Series Nano-ZS instrument using Dispersion Technology Software (DTS) version 4.20 at a wavelength of 633 nm using a 4.0 mW, solid state He-Ne laser at a scattering angle of 173˚. The experiments were performed at a temperature of 25 ˚C. All experiments were performed in triplicate.

6.3.5 DNA Gel Shift Assay.

To prepare polyplexes for DNA gel shift experiments, 0.20 μL of gWiz-Luc plasmid (1 μg/μL in H_2O) was diluted in ~28 μL tris-acetate-EDTA buffer (TAE, Sigma) in 0.65mL microcentrifuge tubes. Then, 0.93 μL of each PDMAEMA sample (1 μg/μL in PBS) was added to each tube corresponding to a nitrogen/phosphorous ratio of 8. The polyplex and DNA only solutions were incubated for 30 min at room temperature. Prior to loading in submerged agarose gel slabs, 7 μL of a 40 wt% sucrose, 0.3 w/v% bromphenol blue in 1X TAE loading buffer solution was added to each tube. Agarose powder (BioRad Laboratories) was dissolved in hot 1X TAE buffer containing 1X SYBR Green I (Sigma) to produce 0.9 wt% agarose gel slabs. The gel was electropheresed at 75 V for 35 min in 1X TAE buffer. Gels were imaged using a UV transilluminator table and a digital camera equipped with a hood and green filter.

6.3.6 Heparin Competitive Binding Assay.

To prepare polyplexes for competitive binding experiments, 0.20 μL of gWiz-Luc plasmid (1 μg/μL in H_2O) was diluted in ~25 μL of TAE buffer in 0.65mL

microcentrifuge tubes. Then, 0.23-1.16 μL of either M_w=43,000 g/mol or M_w=915,000 g/mol PDMAEMA (1 μg/μL in PBS) was added to 12 tubes for each N/P ratio of 2, 6, and 10. The polyplexes were then incubated for 30 min at room temperature. After incubation, 0.01 to 0.40 units (U) of heparin (2 U/uL in 1X TAE, 100 U/mg, Sigma) was added to the 12 tubes for each N/P ratio. The amount of heparin added corresponded to 0-2.0 units per microgram of plasmid DNA. The heparin-challenged polyplexes were then incubated for 30 min at room temperature. Prior to loading in submerged agarose gel slabs, 7 μL of a 40 wt% sucrose, 0.3 w/v% bromphenol blue in 1X TAE loading buffer solution was added to each tube. Agarose powder was dissolved in hot 1X TAE buffer containing 1X SYBR Green I to produce 0.9 wt% agarose gel slabs. The gel was electropheresed at 75 V for 35 min in 1X TAE buffer. Gels were imaged using a UV transilluminator table and a digital camera equipped with a hood and green filter.

6.3.7 Cell culture.

Human brain microvascular endothelial cells (HBMEC) were isolated, cultivated, and purified as previously described.[37] HBMEC were grown in RPMI 1640-based medium with 10% fetal bovine serum (Mediatech), 10% NuSerum (Becton Dickinson), 30 μg/ml of endothelial cell growth supplement (ECGS; Becton Dickinson), 15 U/ml of heparin (Sigma, 2 mM L-glutamine, 2 mM sodium pyruvate, nonessential amino acids, vitamins, 100 U/ml of penicillin, and 100 μg/ml of streptomycin (all reagents from Mediatech). Cultures were incubated at 37 °C in a humid atmosphere of 5% CO_2.

6.3.8 Cell Viability Assay.

Each polymer sample was dissolved at 1 mg/mL in phosphate buffered saline. Then, 25-250 μL of 1 mg/mL polymer solution was diluted in 5 mL of basal RPMI 1640 to produce 5-50 μg/mL treatment solutions. Cell viability was determined using the 3-[4,5-dimethylthiazol-2-yl]2,5-diphenyltetrazolium bromide (MTT, Sigma-Aldrich) conversion assay. HBMEC cells were plated at a concentration of approximately 5,000 cells/well on 96-well plates 24 h prior to each experiment. Prior to each assay, HBMEC cells were washed with approximately 100 μL of basal RPMI. After washing, 100 μL of polymer treatment solution was placed in each well. The plates were then incubated for 12 h at 37^{o}C, 5% CO_2. After 12 h, the cells were rinsed with approximately 100 μL of HBSS, followed by the addition of 100 μL of RPMI 1640 medium containing 0.5 mg/ml of MTT. After incubation for 4 h at 37 ^{o}C, the medium was aspirated and the formazan product was solubilized with DMSO. Absorbance at 570 nm was measured for each well using a Molecular Devices Corp. SPECTRAmax M2 microplate reader.

6.3.9 Lactate Dehydrogenase (LDH) Membrane Integrity Assay.

PDMAEMA solutions (1 mg/mL in PBS) were diluted in basal RPMI 1640 to produce 2-50 μg/mL treatment solutions. HBMEC cells were plated at a concentration of 15,000 cells/well on 96-well plates 24 h prior to each experiment. Prior to each assay, HBMEC cells were washed with approximately 100 μL of basal RPMI. After washing, 100 μL of polymer treatment solution was placed in each well. The plates were then incubated for 12 h at 37^{o}C, 5% CO_2. LDH release was determined using a CytoTox-ONE™ Homogeneous Membrane Integrity Assay (Promega) and a Molecular Devices Corp. SPECTRAmax M2 microplate fluorometer.

6.3.10 Luciferase Expression Assay.

To prepare polyplexes for transfection experiments, gWiz-Luc plasmid (1 μg/μL in H_2O) was diluted in basal RPMI media to a concentration of 0.8 μg/mL and incubated at room temperature for 10 min. At the same time, the appropriate type and amount of polymer was diluted in basal RPMI to the final concentrations corresponding to the various nitrogen/phosphorus (N/P) ratios and allowed to incubate for 10 min at room temperature. Equal volumes of the plasmid and corresponding polymer solutions were combined (final pDNA concentration of 0.4 μg/mL) and incubated for 20-30 min at room temperature to complex the plasmid DNA with PDMAEMA. HBMEC cells were plated at a concentration of $2.0x10^5$ cells/well on 12-well plates 24 h prior to transfection. Each well was treated with 1 mL of transfection solution and then incubated for 12 h at 37 ^oC, 5% CO_2.. After 12 h, the transfection solution was replaced with complete RPMI growth media. The cells were then incubated for 24 h at 37^oC, 5% CO_2 to allow for protein expression. After incubation, the cells were rinsed with approximately 1 mL PBS and 100 μL of lysis buffer was added. Immediately after adding lysis buffer, each well was scraped and incubated for 30 min at room temperature with gentle mixing. The lysate mixture was then subjected to two -80 ^oC/37 ^oC freeze/thaw cycles. Luciferase activity was measured using a luciferase assay kit (Promega) and a Molecular Devices Corp. SPECTRAmax L luminometer according to the assay kit manufacturer's instructions.

6.3.11 Flow Cytometry.

gWiz-luc DNA was labeled with a Label-IT Cy5 DNA labeling kit (Mirus), using labeling reagent at $1/10^{th}$ the manufacturers recommendation. To prepare polyplexes for cellular up-take experiments, Cy5-labled gWiz-Luc plasmid (0.1 μg/μL in H_2O) was

diluted in basal RPMI media to a concentration of 0.8 μg/mL and incubated at room temperature for 10 min. At the same time, the appropriate type and amount of polymer was diluted in basal RPMI to the final concentration corresponding to a N/P ratio of 12, and allowed to incubate for 10 min at room temperature. Equal volumes of the plasmid and corresponding polymer solutions were combined (final pDNA concentration of 0.4 μg/mL) and incubated for 20-30 min at room temperature to complex the plasmid DNA with PDMAEMA. HBMEC cells were plated at a concentration of $2.0x10^5$ cells/well on 12-well plates 24 h prior to transfection. Each well was treated with 1 mL of transfection solution and then incubated for 2 h at 37 ^oC, 5% CO_2. After 2 h, the cells were washed with PBS to remove any untransfected polyplexes. The cells were then trypsinized, pelleted, and resuspeneded in PBS supplemented with 2 vol% FBS. Fluorescence activated cell sorting (FACS) analysis was performing using a BD Biosciences FACS Canto II. Propidium Iodide (PI, Molecular Probes) was used to label dead cells and was detected using a solid-state air cooled laser (excitation, 488 nm) and a 670 longpass filter. Cy5-positive cells were detected using a He-Ne air-cooled laser (excitation, 635 nm) and a 661/20 bandpass filter. Appropriate gating procedures were used to ensure only PI-negative cells were analyzed for Cy5 fluorescence.

6.3.12 Wide-field Fluorescence Optical Microscopy.

To prepare polyplexes for cellular up-take experiments, Cy5-labled gWiz-Luc plasmid (0.1 μg/μL in H_2O) was diluted in basal RPMI media to a concentration of 2.0 μg/mL and incubated at room temperature for 10 min. At the same time, PDMAEMA (sample M_w=915,000 g/mol) was diluted in basal RPMI to a final concentration corresponding to a N/P ratio of 8, and allowed to incubate for 10 min at room

temperature. Equal volumes of the plasmid and corresponding polymer solutions were combined (final pDNA concentration of 1.0 μg/mL) and incubated for 20-30 min at room temperature to complex the plasmid DNA with PDMAEMA. HBMEC cells were plated at a concentration of $1.0x10^5$ cells/well on glass bottom culture dishes (MaTek Corp.) 24 h prior to transfection. Each well was treated with 1 mL of transfection solution and then incubated at 37 ^oC, 5% CO_2. After 30 min of incubation, 1 μL of 4',6-diamidino-2-phenylindole (DAPI, 1 μg/μL in PBS) was added to the transfection media. Optical microscopy instrumentation consisted of a Nikon Eclipse TE2000-U inverted microscope equipped a Nikon C-HGFI Intensilight epifluorescence system and Nikon DS-Qi,Mc BW CCD digital camera. Nikon UV-2E/C, Cy5 HQ, and F/EGFP emission filters were used to acquire multichannel fluorescence images. After DAPI was added to the transfection media, images of live cells were obtained using Cy5 and UV-2EC fluorescence filters and a conventional white light source. The cells were then incubated for another 30 min at 37 ^oC, 5% CO_2. After incubation, the cells were washed twice with PBS, fixed with paraformaldehyde (2 wt% in PBS, Sigma), and permabilized with TritonX-100 (0.1 vol% in PBS, Sigma). After washing with PBS, cellular F-actin was stained with Alexa Fluor® 488 phalloidin (5 Units/mL in PBS, Invitrogen). The cells were then washed and stored in PBS. Images of fixed cells were acquired using Cy5, UV-2EC, and F/EGFP fluorescence filters.

6.4 Results and Discussion

Conventional free-radical polymerization was used to prepare PDMAEMA·HCl polyelectrolytes with various molecular weights, as shown in Scheme 6.1. DMAEMA

was polymerized in THF with AIBN and then converted into the hydrochloride salt with HCl to prepare PDMAEMA·HCl with weight-average molecular weights of 43,000 to 215,000 g/mol. To prepare PDMAEMA with higher molecular weights (M_w=215,000 to 915,000 g/mol), DMAEMA·HCl was polymerized in aqueous HCl (pH=5) using APS as a free radical initiator.

Scheme 6.1. Synthesis of poly[2-(N,N'-dimethylamino)ethyl methacrylate] hydrochloride.

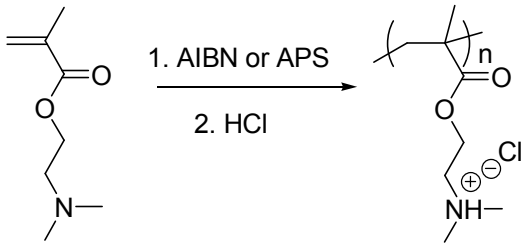

^{1}H NMR spectroscopy (in D_2O) verified the chemical structure of all polymers (see experimental for chemical shifts). To obtain absolute molecular weights by SEC-MALLS, the specific refractive index increment (*dn/dc*) of PDMAEMA in the aqueous SEC mobile phase (0.7M $NaNO_3$, 0.1M Tris, pH=6) must be accurately known.[38] Due to counter-ion dissociation and sample adsorption, online 100% mass recovery methods cannot be used to obtain *dn/dc* values of polyelectrolytes.[38] Batch-mode *dn/dc* measurements revealed that PDMAEMA samples had *dn/dc* values of 0.149 ± 0.002

mL/g. The aqueous SEC-MALLS molecular weights of all PDMAEMA products are summarized in Table 6.1. SEC-MALLS analysis showed weight-average molecular weights of PDMAEMA between 43,000 and 915,000 g/mol with polydispersities ranging from 1.29-2.26. Overlaid aqueous SEC chromatograms (dRI traces) for all PDMAEMA·HCl samples are shown in Figure 6.1. As expected, the molecular weight of PDMAEMA·HCl polyelectrolytes increased with decreasing concentrations of initiator. Aqueous polymerizations resulted in higher molecular weights due to the absence of chain transfer events.[39]

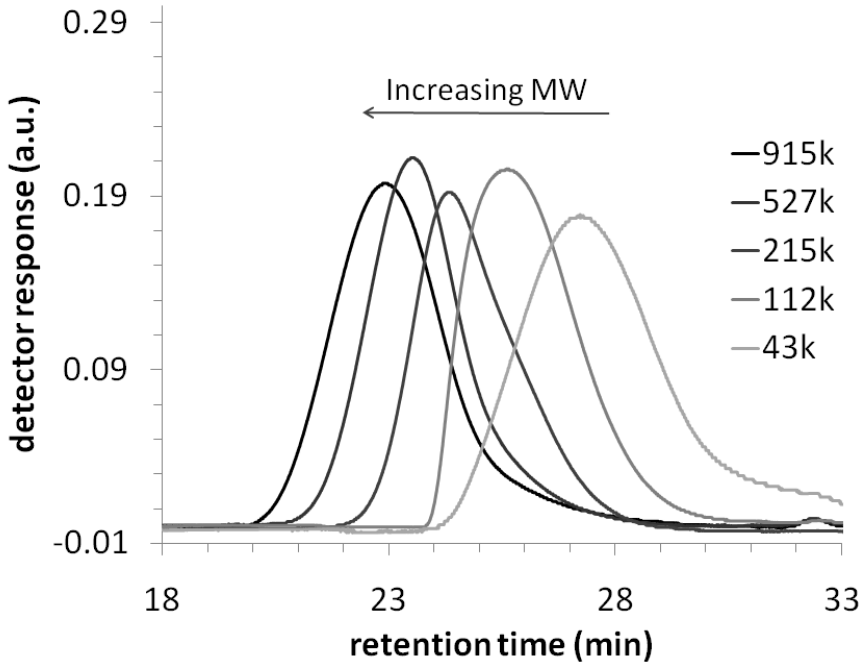

Figure 6.1. Overlaid aqueous SEC chromatograms (dRI traces) of PDMAMEA demonstrating the range of molecular weights used in this study.

Table 6.1. Molecular weights of PDMAEMA.

sample	Initiator (wt.% monomer)	M_w (g/mol)[c]	M_n (g/mol)[c]	M_w/M_n
43k	6.00[a]	43,000	25,000	1.72
112k	0.75[a]	112,000	87,000	1.29
215k	0.10[a]	215,000	158,000	1.36
527k	0.50[b]	527,000	326,000	1.62
915k	0.75[b]	915,000	405,000	2.26

[a]Initiator used in synthesis was AIBN
[b]Initiator used in synthesis was APS
[c]Determined with aqueous SEC-MALLS in 0.7M NaNO3, 0.1M Tris, pH=6

An electrophoretic gel shift assay was used to determine if the molecular weight of PDMAEMA influenced its ability to bind with plasmid DNA. As shown in Figure 6.2, all molecular weights (M_w=915,000 to 43,000 g/mol, lanes 1-5) were able to completely bind DNA. These results were expected since the group of Rädler et al. showed, using small-angle X-ray scattering, that the molecular weight (M_w=30,000 – 70,000 g/mol) of poly(L-lysine) did not significantly influence polyplex packing or structure.[40]

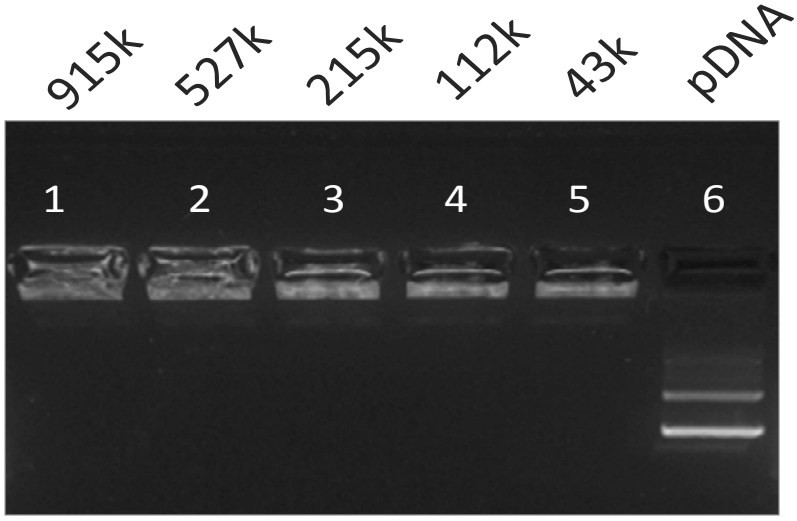

Figure 6.2. Electrophoretic gel shift assay of PDMAEMA of various MWs (N/P=8) binding with pDNA.

Cytotoxicity experiments were conducted using the MTT conversion assay. Figure 6.3 shows the influence of PDMAEMA M_w and polymer concentration (5-50 μg/mL in media) on HBMEC cell viability. In general, cell viabilities were more sensitive to polymer concentration than molecular weight. However, PDMAEMA with M_w=43,000 g/mol maintained higher cell viabilities as a function polymer concentration when compared to the higher PDMAEMA molecular weight samples. At a polymer concentration of 5 μg/mL, PDMAEMA weight-average molecular weights of 43,000-215,000 g/mol showed no toxicity. Samples with weight-average molecular weights of 527,000 and 915,000 g/mol showed slightly reduced cell viabilities (~90%). At a polymer concentration of 10 μg/mL, cells treated with the PDMAEMA M_w=43,000 g/mol sample had viabilities of ~90%, but all higher M_w samples had significantly lower viabilities ranging from ~40-70%. At 20 μg/mL the disparity between the M_w=43,000 g/mol sample and all other molecular weights became even greater with this sample maintaining viabilities of ~60% while all other samples reduced viabilities to ~20%. At concentrations of 50 μg/mL, all molecular weights reduced cell viability to slightly less than 20%.

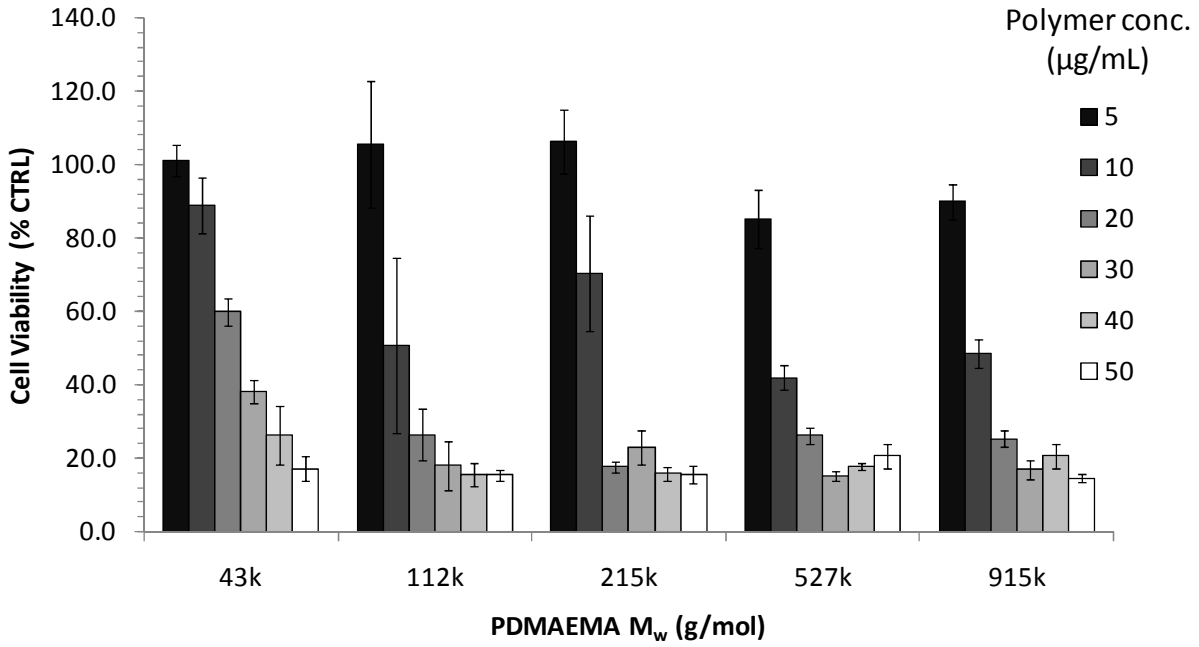

Figure 6.3. HBMEC Cell viability as a function of PDMAEMA M_w and polymer concentration. Values represent mean ± S.D. (n=4).

An LDH release assay was used to evaluate the cellular membrane integrity of HBMEC cells treated with 2-50 μg/mL of all PDMAEMA molecular weights. As shown in Figure 6.4, the results were similar to the MTT assay with LDH release being more sensitive to polymer concentration than molecular weight. PDMAEMA with M_w=43,000 g/mol showed reduced LDH release as a function polymer concentration when compared to the higher PDMAEMA molecular weight samples, reflecting the same trend observed in the MTT assay. PDMAEMA concentrations of 2 μg/mL showed minimal LDH release versus an untreated control group (RFU of ~6,500, shown as a dashed line in Figure 6.4). At concentrations of 5 μg/mL, the M_w=43,000 g/mol sample was observed to have minimal LDH release values compared to all of the higher molecular weight

polymers, which all showed LDH release values at or above the untreated control. At 10 μg/mL, the M_w=43,000 g/mol sample showed slightly elevated LDH release versus the untreated control group, however, all higher molecular weights were found to have significantly higher levels of LDH at the same concentration. At PDMAEMA concentrations of >20 μg/mL, all molecular weights showed elevated LDH values approaching that of a cell only control group treated with lysis buffer (RFU ~18,000, shown as a dotted line in Figure 6.4). The LDH membrane integrity assay coupled with the MTT assay revealed that PDMAEMA's primary mode of toxicity to HBMEC cells is membrane destabilization. Furthermore, lower molecular weights of PDMAEMA are slightly less toxic than higher molecular weights at similar concentrations. It is worth noting that earlier work by Wilson et al. suggested that the toxicity of PDMAEMA to U937 human myelomonocytic cells could have resulted from the combination of membrane destabilization and lysosomal bursting.[41]

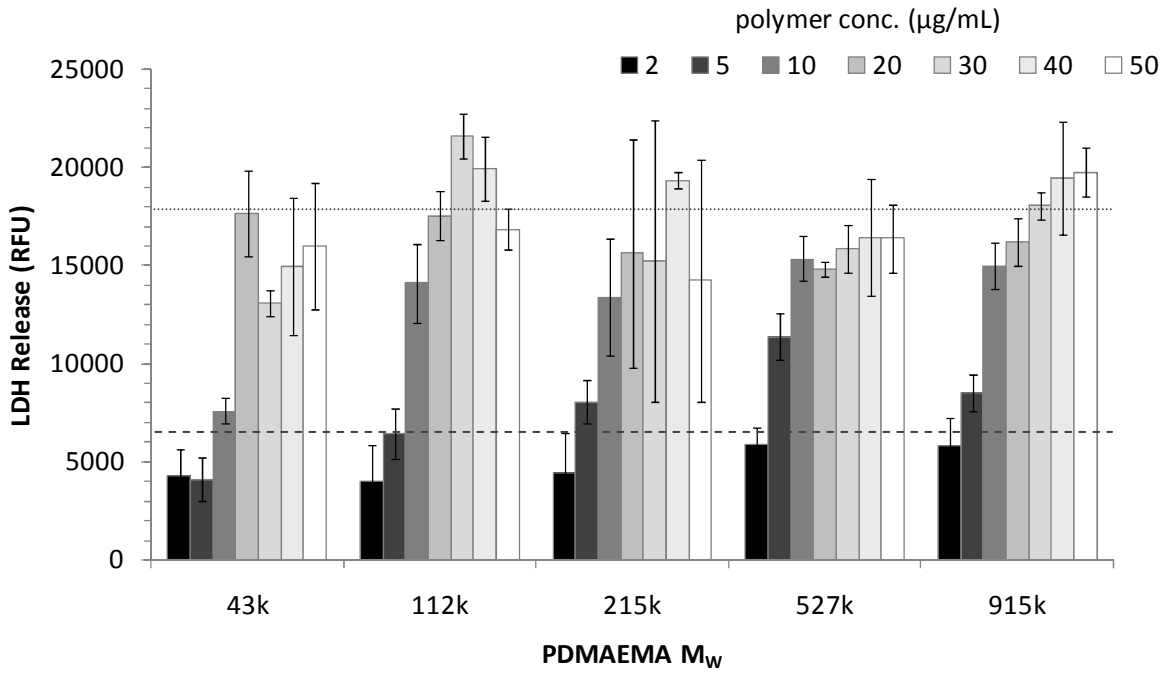

Figure 6.4. LDH release from HBMEC cells as function of PDMAEMA M_w and polymer concentration. Lower dashed line represents the mean LDH release from an untreated cell only control group and the upper dotted line represent the mean LDH release from a cell only control group treated with lysis buffer. Values represent mean ± S.D. (n=4).

Reporter gene transfection was conducted to evaluate the influence PDMAEMA molecular weight on *in vitro* plasmid DNA delivery. Figure 6.5 shows luciferase expression, in relative luminescence units (RLU), as a function of PDMAEMA weight-average molecular weight and N/P ratio. A dramatic increase in luciferase expression was observed as the weight-average molecular increased from 43,000 to 915,000 g/mol. In fact, the M_w=43,000 g/mol sample showed luciferase values only slightly higher than cells treated with DNA only (RLU ~500, not shown in Figure 6.5). For all samples,

luciferase expression generally increased as a function of N/P ratio. However, in all samples except M_w=527,000 g/mol, there was trend towards relatively lower luciferase expression at N/P values of 20. This was likely due to increased toxicity associated with higher N/P ratios. Our findings are in agreement with previously published work by Hennink et al.[18] In their work, they showed that relative transfection efficiency in both COS-7 and OVCAR-3 cells increased dramatically at PDMAEMA weight-average molecular weights >300,000 g/mol.[18] The authors attributed the increased transfection efficiency of higher molecular weight PDMAEMA to its ability to condense plasmid DNA into smaller polyplexes.[18] However, in our work, we were unable to establish this correlation. Figure 6.6 shows polyplex hydrodynamic diameter as function of N/P (1 to 20) for the highest (M_w=915,000 g/mol) and lowest (M_w=43,000 g/mol) PDMAEMA molecular weights used in our study. At lower N/Ps (1-12), the higher molecular weight PDMAEMA produced smaller polyplexes (D_h ~110-160 nm) compared to the lower molecular PDMAEMA, which produced relatively larger polyplexes (D_h ~200-340 nm). At an N/P of 16, both the M_w=43,000 and 915,000 g/mol PDMAEMA produced polyplexes with the same size (D_h ~170 nm). At N/Ps >16, the lower molecular weight PDMAEMA actually produced smaller polyplexes (D_h ~140 nm) and the higher molecular weight PDMAEMA produced much larger polyplexes (D_h ~360 nm). To further show the absence of a direct correlation of polyplex size to transfection, at an N/P of 16, the M_w=43,000 and 915,000 g/mol had virtually the same hydrodynamic size, however, from Figure 6.5, it is clear that these two samples displayed drastically different transfection efficiencies.

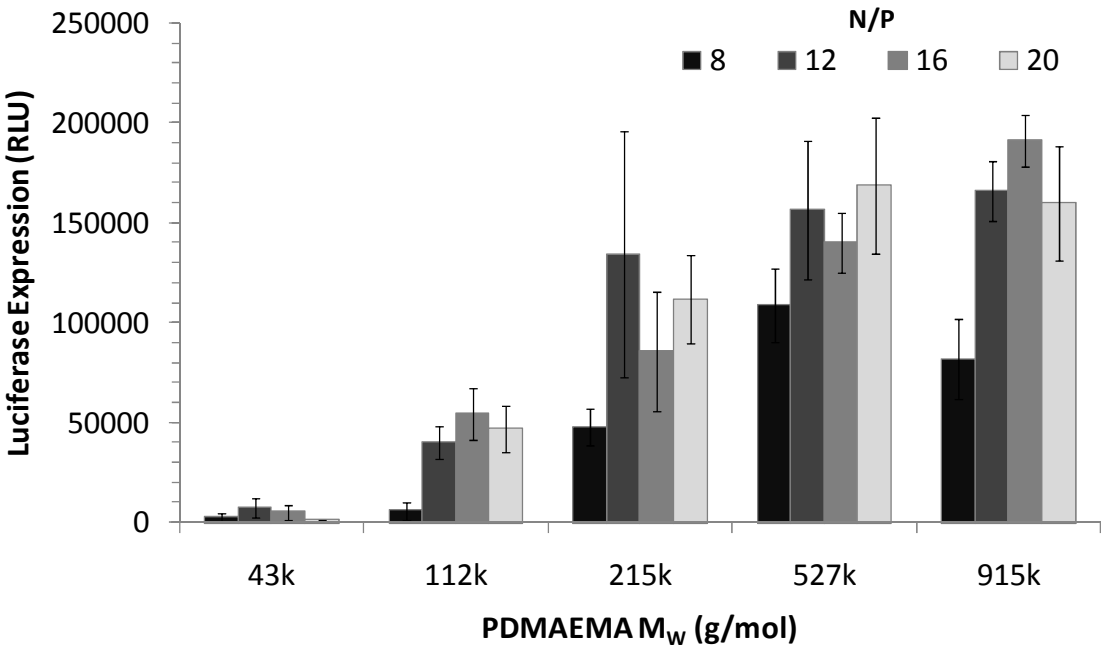

Figure 6.5. Luciferase expression as a function of PDMAEMA M_w and N/P ratio in HBMEC cells. Values represent mean ± S.D. (n=4).

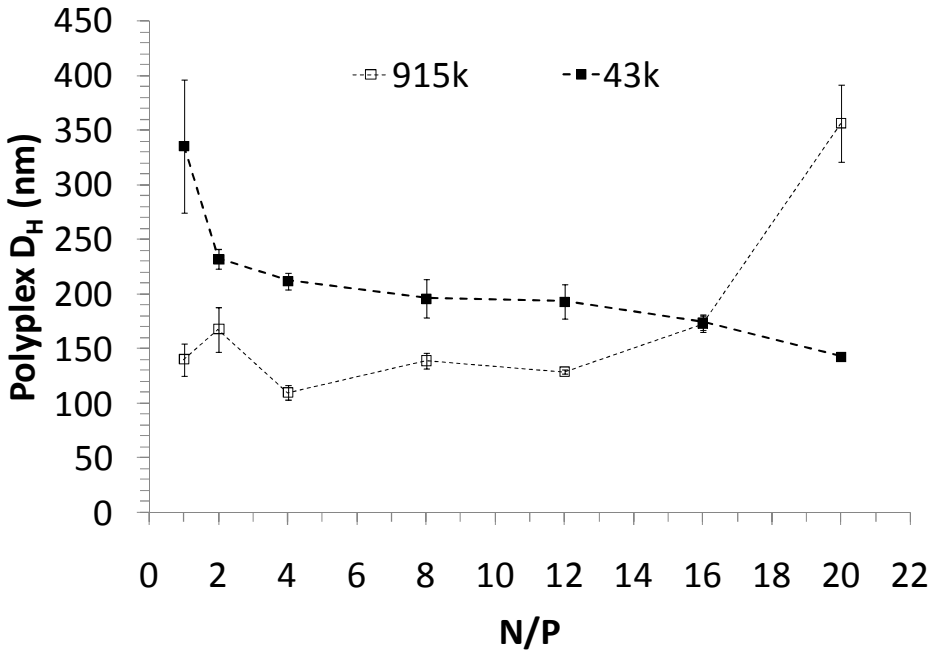

Figure 6.6. Polyplex hydrodynamic diameter in PBS as a function of N/P ratio for PDMAEMA M_w=43,000 g/mol and M_w=915,000 g/mol. Values represent mean ± S.D. (n=4).

Figure 6.7a shows a wide-field optical micrograph of live HBMEC cells undergoing transfection with Cy5-labeled polyplexes (PDMAEMA M_w=915,000 g/mol, N/P=8). The image was acquired 30 min after treatment with polyplexes. The polyplexes appear purple due to DAPI co-stain, which labels all DNA (HBMEC genomic DNA and polyplex pDNA). As shown in the figure, small vesicles containing Cy5-labled pDNA were observed internalizing into the HBMEC cells. An image was also acquired 1 h after treatment with polyplexes. Figure 6.8 (a-b) shows transfected HBMEC cells fixed and co-stained with DAPI (Figure 6.8c) and Alexa Fluor® 488 phalloidin (Figure 6.8d). Figure 6.8b shows Cy5-labeled polyplexes. The white arrows in the figure indicate areas of concentrated polyplexes, which also corresponded to the location of cellular nuclei (shown in Figure 6.8c). The multichannel image, shown in Figure 6.8a, shows polyplexes co-localized with nuclei and within the Alexa Fluor® 488 phalloidin-stained cytoskeleton.

The amount of Cy5-labled plasmid internalization was quantified using fluorescence activated cell sorting (FACS) analysis to evaluate the influence of PDMAEMA molecular weight on the cellular uptake of polyplexes. Figure 6.7b shows the mean Cy5 fluorescence intensity and percentage Cy5 positive cells (2 h after treatment with polyplexes) as a function of PDMAEMA weight-average molecular weight. In remarkable contrast to the luciferase expression data (Figure 6.5,

aforementioned), PDMAEMA molecular weight did not influence cellular uptake of polyplexes. All PDMAEMA molecular weights were found to have statistically similar Cy5 fluorescence intensity values, which were approximately an order of magnitude higher than untransfected cells only control. Furthermore, FACS analysis revealed that approximately 90% of live cells took up Cy5-labeled polyplexes for all PDMAEMA molecular weights. Our cellular uptake experiments are in agreement with work published by Reineke et al., who showed that the molecular weight (M_w=26,000-70,000 g/mol) of trehalose oligoethylenamine click polymers influenced luciferase expression but not cellular uptake.[21]

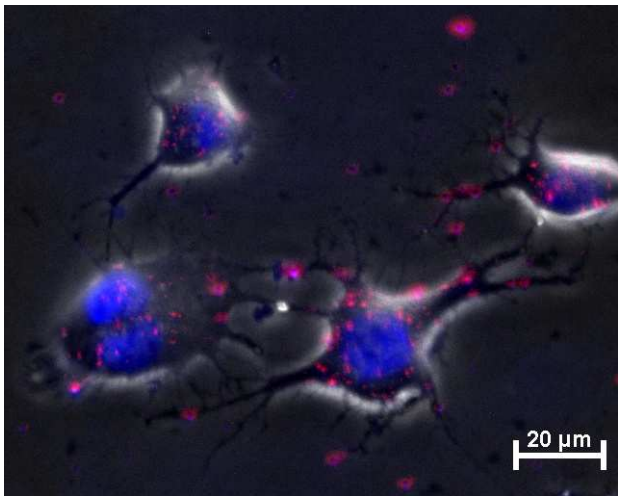

(a)

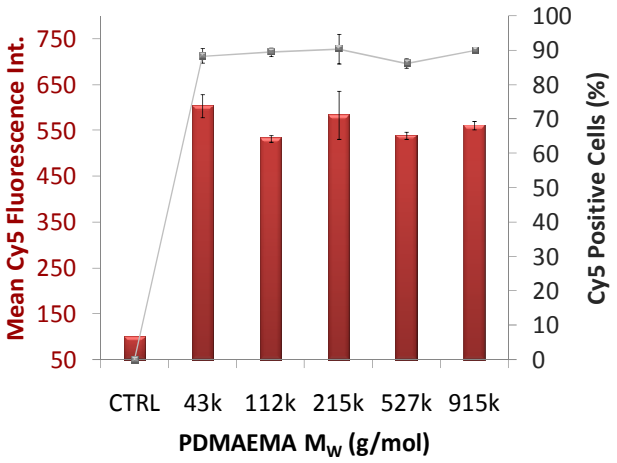

(b)

Figure 6.7. (a) Multichannel wide-field optical micrograph of live HBMEC cells taking up Cy5-labled PDMAEMA/pDNA polyplexes. PDMAEMA M_w=915,000 g/mol, 1 μg DNA per 100,000 cells, N/P=8, image was acquired 30 min after treatment with polyplexes. Cellular nuclei (blue) are stained with DAPI. Polyplexes appear purple due to the co-staining of Cy5-pDNA (red) with DAPI. (b) Cellular uptake of Cy5-labeled polyplexes in HBMEC cells using various MWs of PDMAEMA (N/P=12). Values represent mean ± S.D. (n=4).

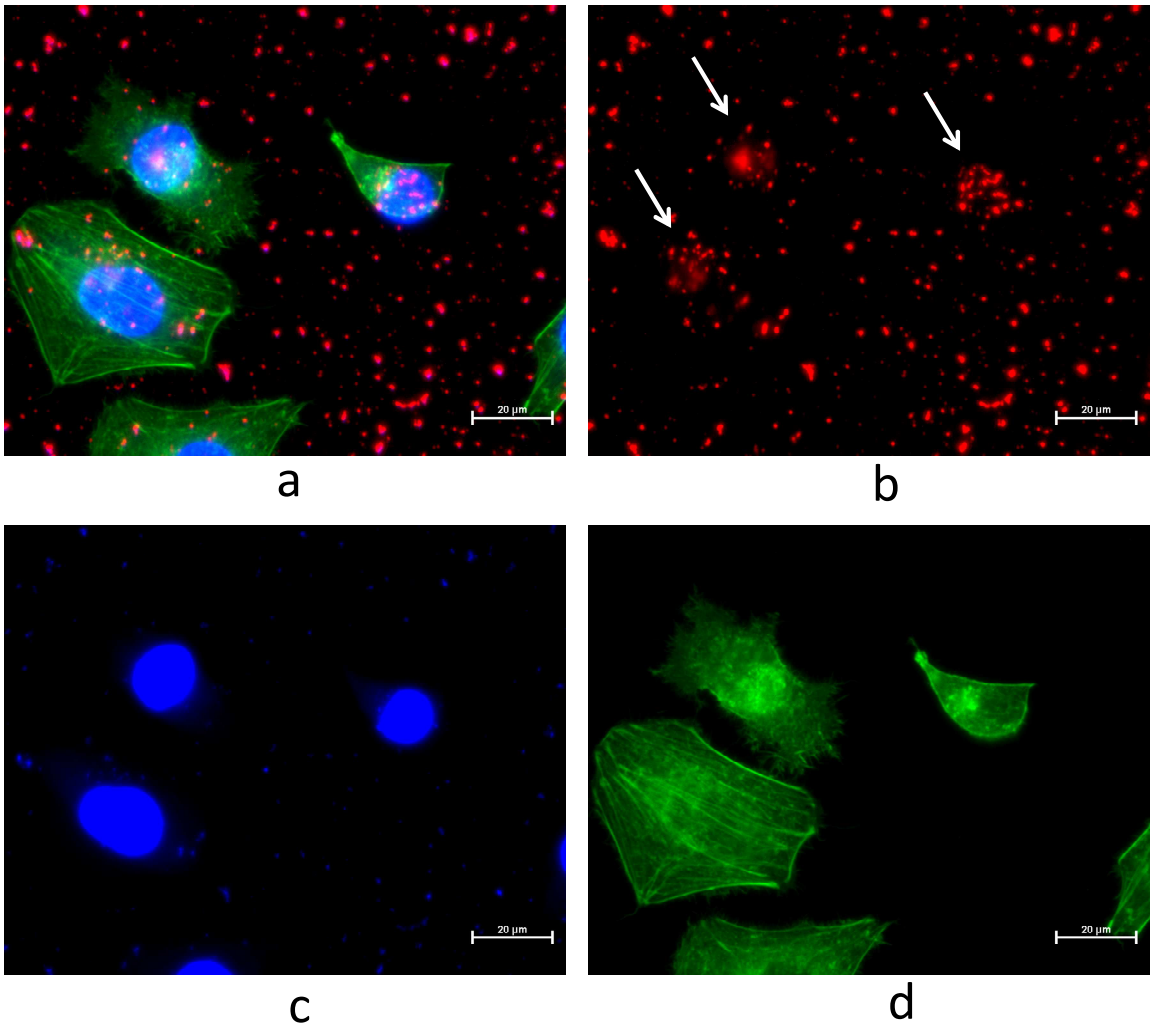

Figure 6.8. Fluorescence optical micrographs of HBMEC cells transfected with Cy5-labled PDMAEMA/pDNA polyplexes. PDMAEMA M_w=915,000 g/mol, 1 µg DNA per 100,000 cells, N/P=8, cells were fixed and stained 1 h after treatment with polyplexes. (a) Multichannel composite image, (b) Cy5 channel showing polyplexes (white arrows indicate areas of concentrated polyplexes), (c) DAPI channel showing cellular nuclei and polyplexes, (d) AlexaFluor 488-Phollodin channel showing F-actin.

The luciferase expression and cellular uptake experiments collectively demonstrated that the molecular weight of the polycation did not influence initial cellular

entry, but rather plays role at some point during intracellular trafficking. The binding affinity of a polycation towards plasmid DNA is an important parameter that influences endosomal release and the polymer's ability to protect DNA from DNase degradation.[14] Figure 6.9 shows electrophoretic gel shift assays of polyplexes prepared with PDMAEMA M_w=43,000 and 915,000 g/mol and then treated with increasing concentrations of heparin (units of heparin/μg plasmid DNA) for three N/P ratios (2, 6, and 10). The greater the amount of heparin needed to dissociate the polymer from the plasmid DNA, the greater the binding affinity. For the lower molecular weight PDMAEMA (43k in Figure 6.9), initial polyplex dissociation occurred at 0.20 Heparin U/μg DNA for an N/P of 2, 0.30 Heparin U/μg DNA for an N/P of 6, and 0.50 Heparin U/μg DNA for an N/P of 10. The increase in heparin concentration as a function of N/P ratio was expected since the polycation concentration is higher in these polyplex compositions. For the PDMAEMA M_w=43,000 g/mol, full dissociation of the polyplexes was observed as the concentration of heparin increased. However, when the higher molecular weight PDMAEMA (915k in Figure 6.9) polyplexes were treated with the same concentrations of heparin, we observed considerably less DNA release. Even though we observed free DNA bands in the 915k gel, the band intensities were much weaker than the intensity of the free DNA bands in the 43k gel, where full DNA release was observed. For the PDMAEMA M_w=915,000 g/mol, most of the plasmid DNA remained associated into a polyplex, even when challenged with relatively high concentrations of heparin (200 U/μg DNA, not shown in Figure 6.9). From these data it was clear that higher molecular weight PDMAEMA (M_w=915,000 g/mol) had a greater binding affinity for plasmid DNA than lower molecular weight PDMAEMA (M_w=43,000

g/mol). This greater binding affinity was likely responsible for the increased transfection efficiency observed with higher molecular weight PDMAEMA. It is uncertain exactly how polycation binding affinity influences the intracellular fate of polyplexes. Most likely, the greater binding affinity helps protect the plasmid DNA from DNase degradation, which allows for greater protein expression.

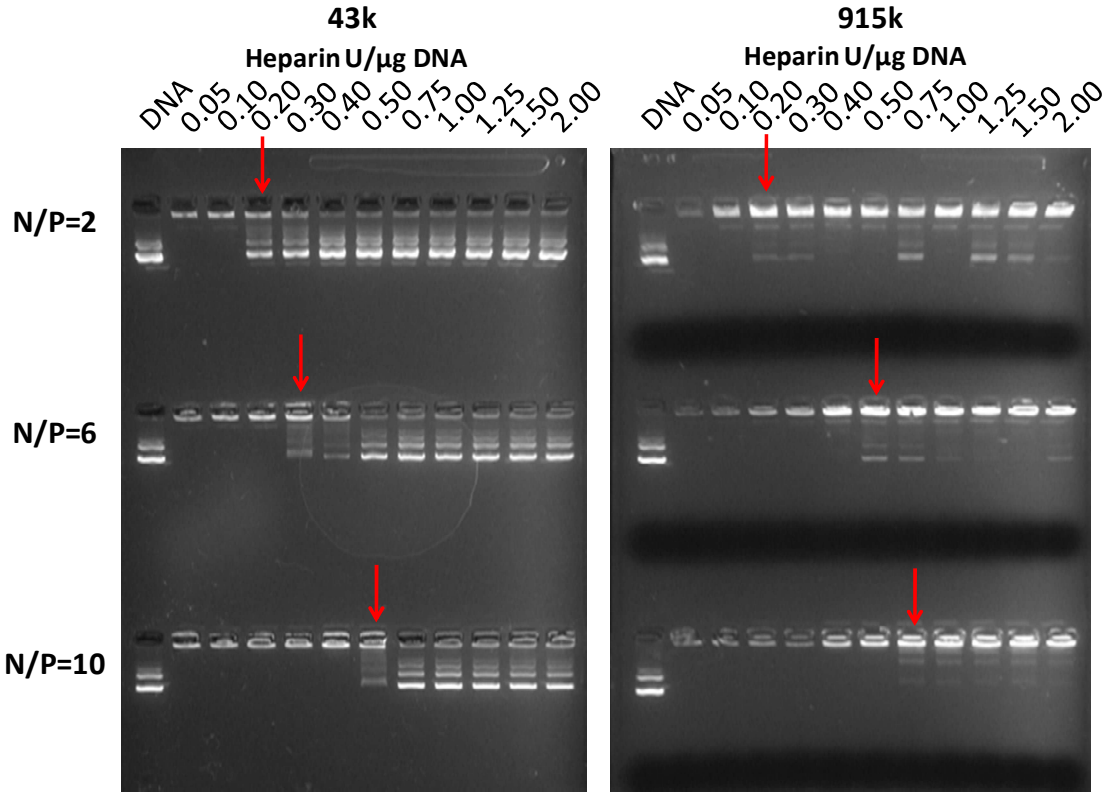

Figure 6.9. Heparin competitive binding assay for PDMAEMA M_w=43,000 g/mol and DNA) required to dissociate polyplexes.

6.5 Conclusions

Conventional free-radical polymerization was used to synthesize various molecular weights of PDMAEMA. Aqueous SEC-MALLS determined that the synthesized polymers had weight-average molecular weights between 43,000 and

915,000 g/mol. An MTT assay revealed that lower molecular weight PDMAEMA (M_w=43,000 g/mol) was slightly less toxic to HBMEC cells, however, cell viabilities were found to be more sensitive to polymer concentration. An LDH release assay determined that the primary mode of PDMAEMA toxicity to HBMEC cells was membrane destabilization. Furthermore, LDH release results showed the same molecular weight/toxicity trend as the MTT assay. An electrophoretic gel shift assay showed that all PDMAEMA molecular weights completely bound with plasmid DNA. However, heparin competitive binding assays revealed that higher molecular weight PDMAEMA (M_w=915,000 g/mol) had a greater binding affinity towards plasmid DNA compared to lower molecular weight (M_w=43,000 g/mol). The molecular weight of PDMAEMA was found to have a dramatic influence on transfection efficiency, with gene expression increasing as a function of increasing molecular weight. However, the molecular weight of PDMAEMA did not have any influence on the cellular uptake of polyplexes. DLS experiments indicated the absence of a direct correlation of polyplex size to transfection efficiency. Collectively, our data suggested that the intracellular fate of the polyplexes was more important to overall transfection efficiency than barriers to entry (such as polyplex size). Moreover, polymer binding affinity was likely a significant parameter associated with the polyplex's intracellular journey.

6.6 Acknowledgements

This material is based upon work supported in part by the Macromolecular Interfaces with Life Sciences (MILES) Integrative Graduate Education and Research

Traineeship (IGERT) of the National Science Foundation under Agreement No. DGE-0333378.

The authors sincerely thank Patrick McLendon of Prof. Theresa Reineke's research group at Virginia Tech for his assistance with plasmid labeling, flow cytometry, and several helpful discussions. We thank Joseph M. Pickel and Phillip F. Britt at the Center for Nanophase Materials Sciences (CNMS) at the Oak Ridge National Laboratory (ORNL) for their invaluable assistance with aqueous SEC. Research at the CNMS at ORNL was sponsored by the Division of Materials Sciences and Engineering, U.S. Department of Energy, under contract DE-AC05-00OR22725 with UT-Battelle, LLC. We also thank Lulit Affin for her assistance with gel electrophoresis.

6.7 References

[1]Emery, D. W., Gene therapy for genetic diseases: On the horizon. *Clinical and Applied Immunology Reviews* **2004,** 4, (6), 411-422.

[2]Kay, M. A.; Glorioso, J. C.; Naldini, L., Viral vectors for gene therapy: the art of turning infectious agents into vehicles of therapeutics. *Nat. Med.* **2001,** 7, (1), 33-40.

[3]Palmer, D. H.; Young, L. S.; Mautner, V., Cancer gene-therapy: clinical trials. *Trends in Biotechnology* **2006,** 24, (2), 76-82.

[4]Kaiser, J., CLINICAL RESEARCH: Death Prompts a Review of Gene Therapy Vector. *Science* **2007,** 317, (5838), 580-.

[5]Heath, W. H.; Senyurt, A. F.; Layman, J.; Long, T. E., Charged Polymers via Controlled Radical Polymerization and their Implications for Gene Delivery. *Macromolecular Chemistry and Physics* **2007,** 208, (12), 1243-1249.

[6]Wong, S. Y.; Pelet, J. M.; Putnam, D., Polymer systems for gene delivery--Past, present, and future. *Progress in Polymer Science* **2007,** 32, (8-9), 799-837.

[7]Jeong, J. H.; Kim, S. W.; Park, T. G., Molecular design of functional polymers for gene therapy. *Progress in Polymer Science* **2007,** 32, (11), 1239-1274.

[8]Morille, M.; Passirani, C.; Vonarbourg, A.; Clavreul, A.; Benoit, J.-P., Progress in developing cationic vectors for non-viral systemic gene therapy against cancer. *Biomaterials* **2008,** 29, (24-25), 3477-3496.

[9]Green, J. J.; Langer, R.; Anderson, D. G., A Combinatorial Polymer Library Approach Yields Insight into Nonviral Gene Delivery. *Acc. Chem. Res.* **2008,** 41, (6), 749-759.

[10]Tiera, M. J.; Winnik, F. M.; Fernandes, J. C., Synthetic and Natural Polycations for Gene Therapy: State of the Art and New Perspectives. *Current Gene Therapy* **2006,** 6, 59-71.

[11]Eliyahu, H.; Barenholz, Y.; Domb, A. J., Polymers for DNA delivery. *Molecules* **2005,** 10, (1), 34-64.

[12]Breitenkamp, R. B.; Emrick, T., Pentalysine-Grafted ROMP Polymers for DNA Complexation and Delivery. *Biomacromolecules* **2008,** 9, (9), 2495-2500.

[13]Liu, Y.; Reineke, T. M., Poly(glycoamidoamine)s for Gene Delivery. Structural Effects on Cellular Internalization, Buffering Capacity, and Gene Expression. *Bioconjugate Chem.* **2007,** 18, (1), 19-30.

[14]Liu, Y.; Reineke, T. M., Poly(glycoamidoamine)s for Gene Delivery: Stability of Polyplexes and Efficacy with Cardiomyoblast Cells. *Bioconjugate Chem.* **2006,** 17, (1), 101-108.

[15]Schaffert, D.; Wagner, E., Gene therapy progress and prospects: synthetic polymer-based systems. *Gene Ther.* **2008,** 15, (16), 1131-1138.

[16]Read, M. L.; Logan, A.; Seymour, L. W.; Leaf Huang, M.-C. H.; Ernst, W., Barriers to Gene Delivery Using Synthetic Vectors. In *Advances in Genetics*, Academic Press: 2005; Vol. Volume 53, pp 19-46.

[17]Prevette, L. E.; Kodger, T. E.; Reineke, T. M.; Lynch, M. L., Deciphering the Role of Hydrogen Bonding in Enhancing pDNA-Polycation Interactions. *Langmuir* **2007,** 23, (19), 9773-9784.

[18]van de Wetering, P.; Cherng, J. Y.; Talsma, H.; Crommelin, D. J. A.; Hennink, W. E., 2-(dimethylamino)ethyl methacrylate based (co)polymers as gene transfer agents. *Journal of Controlled Release* **1998,** 53, (1-3), 145-153.

[19]Srinivasachari, S.; Liu, Y.; Zhang, G.; Prevette, L.; Reineke, T. M., Trehalose Click Polymers Inhibit Nanoparticle Aggregation and Promote pDNA Delivery in Serum. *J. Am. Chem. Soc.* **2006,** 128, (25), 8176-8184.

[20]Prevette, L. E.; Lynch, M. L.; Kizjakina, K.; Reineke, T. M., Correlation of Amine Number and pDNA Binding Mechanism for Trehalose-Based Polycations. *Langmuir* **2008,** 24, (15), 8090-8101.

[21]Srinivasachari, S.; Liu, Y.; Prevette, L. E.; Reineke, T. M., Effects of trehalose click polymer length on pDNA complex stability and delivery efficacy. *Biomaterials* **2007,** 28, (18), 2885-2898.

[22]Godbey, W. T.; Wu, K. K.; Mikos, A. G., Size matters: Molecular weight affects the efficiency of poly(ethylenimine) as a gene delivery vehicle. *Journal of Biomedical Materials Research* **1999,** 45, (3), 268-275.

[23]Morimoto, K.; Nishikawa, M.; Kawakami, S.; Nakano, T.; Hattori, Y.; Fumoto, S.; Yamashita, F.; Hashida, M., Molecular Weight-Dependent Gene Transfection Activity of Unmodified and Galactosylated Polyethyleneimine on Hepatoma Cells and Mouse Liver. *Mol Ther* **2003,** 7, (2), 254-261.

[24]Fischer, D.; Bieber, T.; Li, Y.; Elsässer, H.-P.; Kissel, T., A Novel Non-Viral Vector for DNA Delivery Based on Low Molecular Weight, Branched Polyethylenimine: Effect of Molecular Weight on Transfection Efficiency and Cytotoxicity. *Pharmaceutical Research* **1999,** 16, (8), 1273-1279.

[25]Ward, C. M.; Read, M. L.; Seymour, L. W., Systemic circulation of poly(L-lysine)/DNA vectors is influenced by polycation molecular weight and type of DNA: differential circulation in mice and rats and the implications for human gene therapy. *Blood* **2001,** 97, (8), 2221-2229.

[26]Cherng, J.-Y.; van de Wetering, P.; Talsma, H.; Crommelin, D. J. A.; Hennink, W. E., Effect of Size and Serum Proteins on Transfection Efficiency of Poly ((2-dimethylamino)ethyl Methacrylate)-Plasmid Nanoparticles. *Pharmaceutical Research* **1996,** 13, (7), 1038-1042.

[27]Cherng, J. Y.; Schuurmans-Nieuwenbroek, N. M. E.; Jiskoot, W.; Talsma, H.; Zuidam, N. J.; Hennink, W. E.; Crommelin, D. J. A., Effect of DNA topology on the transfection efficiency of poly((2-dimethylamino)ethyl methacrylate)-plasmid complexes. *Journal of Controlled Release* **1999,** 60, (2-3), 343-353.

[28]Cherng, J. Y.; Wetering, P. v. d.; Talsma, H.; Crommelin, D. J. A.; Hennink, W. E., Stabilization of polymer-based gene delivery systems. *International Journal of Pharmaceutics* **1999,** 183, (1), 25-28.

[29]Hinrichs, W. L. J.; Schuurmans-Nieuwenbroek, N. M. E.; van de Wetering, P.; Hennink, W. E., Thermosensitive polymers as carriers for DNA delivery. *Journal of Controlled Release* **1999,** 60, (2-3), 249-259.

[30]van de Wetering, P.; Moret, E. E.; Schuurmans-Nieuwenbroek, N. M. E.; van Steenbergen, M. J.; Hennink, W. E., Structure-Activity Relationships of Water-Soluble Cationic Methacrylate/Methacrylamide Polymers for Nonviral Gene Delivery. *Bioconjugate Chem.* **1999,** 10, (4), 589-597.

[31]van de Wetering, P.; Schuurmans-Nieuwenbroek, N. M. E.; van Steenbergen, M. J.; Crommelin, D. J. A.; Hennink, W. E., Copolymers of 2-(dimethylamino)ethyl methacrylate with ethoxytriethylene glycol methacrylate or N-vinyl-pyrrolidone as gene transfer agents. *Journal of Controlled Release* **2000,** 64, (1-3), 193-203.

[32]Verbaan, F.; van Dam, I.; Takakura, Y.; Hashida, M.; Hennink, W.; Storm, G.; Oussoren, C., Intravenous fate of poly(2-(dimethylamino)ethyl methacrylate)-based polyplexes. *European Journal of Pharmaceutical Sciences* **2003,** 20, (4-5), 419-427.

[33]Funhoff, A. M.; van Nostrum, C. F.; Lok, M. C.; Kruijtzer, J. A. W.; Crommelin, D. J. A.; Hennink, W. E., Cationic polymethacrylates with covalently linked membrane destabilizing peptides as gene delivery vectors. *Journal of Controlled Release* **2005,** 101, (1-3), 233-246.

[34]Verbaan, F. J.; Klouwenberg, P. K.; Steenis, J. H. v.; Snel, C. J.; Boerman, O.; Hennink, W. E.; Storm, G., Application of poly(2-(dimethylamino)ethyl methacrylate)-based polyplexes for gene transfer into human ovarian carcinoma cells. *International Journal of Pharmaceutics* **2005,** 304, (1-2), 185-192.

[35]van der Aa, M.; Huth, U.; Häfele, S.; Schubert, R.; Oosting, R.; Mastrobattista, E.; Hennink, W.; Peschka-Süss, R.; Koning, G.; Crommelin, D., Cellular Uptake of Cationic Polymer-DNA Complexes Via Caveolae Plays a Pivotal Role in Gene Transfection in COS-7 Cells. *Pharmaceutical Research* **2007,** 24, (8), 1590-1598.

[36]McKee, M. G.; Hunley, M. T.; Layman, J. M.; Long, T. E., Solution Rheological Behavior and Electrospinning of Cationic Polyelectrolytes. *Macromolecules* **2006,** 39, (2), 575-583.

[37]Stins, M. F.; Gilles, F.; Kim, K. S., Selective expression of adhesion molecules on human brain microvascular endothelial cells. *Journal of Neuroimmunology* **1997,** 76, (1-2), 81-90.

[38]Layman, J. M.; Borgerding, E. M.; Williams, S. R.; Heath, W. H.; Long, T. E., Synthesis and Characterization of Aliphatic Ammonium Ionenes: Aqueous Size Exclusion Chromatography for Absolute Molecular Weight Characterization. *Macromolecules* **2008,** 41, (13), 4635-4641.

[39]Qiu, J.; Charleux, B.; Matyjaszewski, K., Controlled/living radical polymerization in aqueous media: homogeneous and heterogeneous systems. *Progress in Polymer Science* **2001,** 26, (10), 2083-2134.

[40]DeRouchey, J.; Netz, R. R.; Rädler, J. O., Structural investigations of DNA-polycation complexes. *The European Physical Journal E - Soft Matter* **2005,** 16, (1), 17-28.

[41]Jones, R. A.; Poniris, M. H.; Wilson, M. R., pDMAEMA is internalised by endocytosis but does not physically disrupt endosomes. *Journal of Controlled Release* **2004,** 96, (3), 379-391.

Chapter 7. **Influence of Glucosylation and Maltosylation on the Cytotoxicity and *in vitro* DNA Delivery of Low Molecular Weight Hyperbranched Poly(ethylene imine)**

John M. Layman,[†] Dietmar Appelhans,[‡] Sean M. Ramirez, [†] Brigitte Voit,[‡] and Timothy E. Long[†]

[†]Macromolecular Science and Engineering, Department of Chemistry, Virginia Tech, Blacksburg, VA 24061

[‡]Leibniz Institute of Polymer Research Dresden, Dresden, Germany 01069

7.1 Abstract

Fundamental understanding of structure-property relationships in polycation-mediated gene delivery is an important step in the development of efficient non-viral gene therapy agents. Thus, we report the influence of glucose and maltose modifications on the cytotoxicity and *in vitro* plasmid DNA delivery performance of hyperbranched poly(ethylene imine) (PEI) in human brain microvascular endothelial cells (HBMEC). Reductive amination was used to synthesize >99% carbohydrate-substituted hyperbranched PEI, and MTT assays revealed that both glucose and maltose modifications reduced the toxicity of hyperbranched PEI in HBMEC cells. However, these carbohydrate modifications on the periphery of the branched molecule drastically reduced transfection performance. These results were correlated with zeta-potential measurements, gel electrophoresis, and potentiometric titration experiments, which

collectively revealed that carbohydrate modifications eliminated the cationic charge on PEI at physiological pH. The elimination of cationic charge prevented the carbohydrate-substituted PEIs from electrostatically binding and ultimately delivering anionic plasmid DNA.

KEYWORDS: gene delivery, non-viral agents, hyperbranched PEI, carbohydrate, glucose, maltose

7.2 Introduction

In gene therapy, extra-chromosomal nucleic acids are transferred through the cellular membrane and express a therapeutic level of a defective or deficient protein.[1] Although this technology holds great promise, wide-spread clinical application of gene therapy is limited, predominantly due to the absence of safe and effective nucleic acid delivery agents.[2] Viral vectors, which utilize an inactivated virus, are extremely efficient carrier molecules and infect a wide variety of cell types.[3] However, viral vectors are limited to small plasmids, and although modified viruses are rendered replication deficient, host immune response is still a frequent and often severe complication.[4] Non-viral agents, such as cationic polyelectrolytes, are an attractive synthetic replacement to viral vectors due to reduction of immunogenic risk and the ability to tailor their macromolecular architecture.[5,6] Non-viral vectors electrostatically screen the anionic charges on the nucleic acid to form a plasmid-polymer complex, termed a polyplex. Although non-viral vectors possess numerous design advantages, several investigators have shown that transfection efficiencies are considerably lower compared to viral vectors.[7,8]

One of the main disadvantages of using cationic polymers as gene delivery agents is their inherent cytotoxicity. The cationic charges that are utilized to bind nucleic acids also disrupt and destabilize phospholipid membranes leading to lysis and ultimately cell death.[9] Several investigators have shown that the toxicity of cationic polymers can be attenuated with bio-derived or chemical elements.[9,10] Klibanov and co-workers synthesized branched poly(ethylene imine) (PEI) with various chemical modifications and observed enhanced transfection activity and decreased cytotoxicity using alanyl and dodecyl substitutions.[11] Klibanov also showed that other chemical modifications, such as methyl and ethyl, decreased the transfection efficiency of branched PEI.

Carbohydrate-modified cationic polyelectrolytes are intriguing candidates for gene delivery since they mimic many naturally occurring glycosylated biomacromolecules.[12] Additionally, carbohydrate-conjugated cationic polyelectrolytes are capable of binding cell-specific receptors which is desirable in targeted gene delivery.[13-18] The most common glycopolymer conjugates in the literature are based on β-cyclodextrin (β–CD),[19] pioneered by the group of Davis et al.[20-24] β–CD polycations were shown to be non-toxic, highly efficient transfection vectors, and when formed into CD inclusion complexes, cell specific targeting was achieved.[21] The same group showed that grafting linear or branched PEI with β–CD (up to 16% functional group substitution) was able to reduce polymer toxicity and improve plasmid uptake.[25] However, the authors showed that gene expression was sensitive to the grafting density. The group of Reineke et al. has extensively studied trehalose-containing polycations as well as poly(glycoamidoamine)s and found that small structural changes in carbohydrate groups dramatically influences DNA delivery.[26-30]

Glycopolymers can be synthesized directly from monomers such as acryloyl glucosamine[31], but more commonly, post-polymerization functionalization reactions are employed. The most common post-polymerization technique to react saccharides with amine-functional polymers involves the reductive amination of primary or secondary nitrogen atoms in the presence of a reducing agent.[13,32,33] Pioneering efforts by Remy et al. explored the influence of maltose and dextran modifications on toxicity and gene transfection of PEI (M_W=25,000 g/mol).[34] In their study, PEI was modified with end group degrees of substitution of 25% maltose and 9.5% dextran. In both cases, the authors showed that toxicity and transfection efficiency decreased with increasing carbohydrate substitution. Kissel and co-workers modified branched PEI (M_w=25,000 g/mol) with galactose (up to 31% degree of substitution) and found that the carbohydrate modifications reduced toxicity, but also reduced transfection efficiency.[35] The authors determined that transfection efficiency was directly dependent on the degree of substitution. Cho and co-workers modified branched PEI (M_W=25,000 g/mol) with glucose (up to 36% degree of substitution) via reductive amination of free amines with cellobiose.[13] The authors found that the glucose substitution reduced cell toxicity, but reduced transfection efficiency. However, the same group determined that galactosylated chitosan (degrees of substitution up to 9.3%) had low toxicity and increased transfection efficiencies compared to non-galactosylated chitosan.[36] Similar studies by Nagasaki and co-workers found that conjugation of galactose (degrees of substitution ranged from 3-50%) with a cationic chitosan derivative both reduced toxicity and increased transfection activity.[37]

In order to fundamentally understand macromolecular structure-transfection relationships, our laboratories evaluated the influence of two sugar modifications on the cytotoxicity and transfection activity of hyperbranched PEI (M_W=5,000 g/mol). PEI, one of the most extensively studied cationic polymers for DNA transfection, serves as an excellent basis for structure-transfection studies.[6,8,11,38-40] In addition, the reactive primary and secondary amines on hyperbranched PEI are suitable to provide a library of peripherally functionalized transfection agents. In this study > 90% glucosylated and > 90% maltosylated hyperbranched cationic polyelectrolytes, shown in Figure 1, were used for plasmid DNA binding, cytotoxicity, and transfection performance.

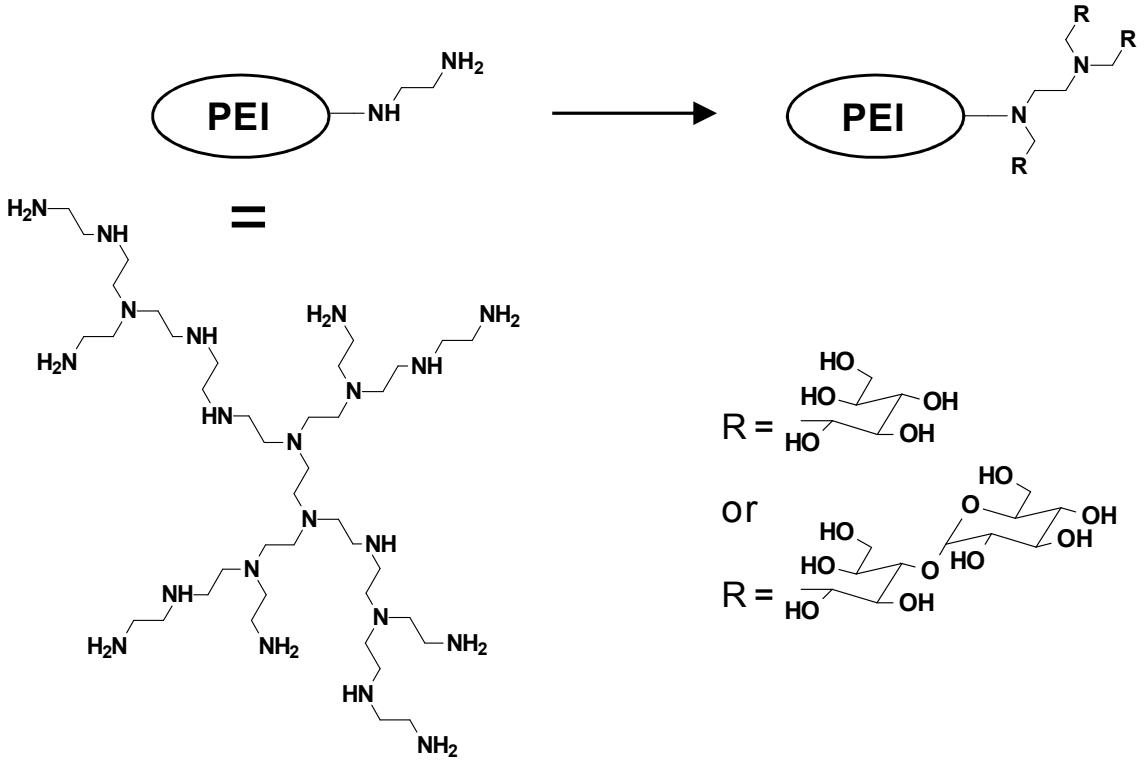

Figure 7.1. Synthesis of structure A by reductive amination of hyperbranched PEI with excess glucose or maltose.(41)

7.3 Experimental Procedures

7.3.1 Synthesis of glucose- and maltose-modified hyperbranched poly(ethylene imine).

Hyperbranched PEI (M_w = 5,000 g/mol; BASF – The chemical company / Ludwigshafen, Germany) was used without further purification. The glucose and maltose modified hyperbranched poly(ethylene imine) with structure A were synthesized by a reductive amination, using borane pyridine complex as strong reduction agent, of the hyperbranched PEI with glucose and maltose in sodium borate solution under similar conditions already described in references 41-43. A detailed characterization (NMR, elemental analysis, DLS, SLS, polyelectrolyte titration) of the glucose and maltose modified PEIs and other PEI structures are presented in a larger context at which the variation of the reductive amination of various hyperbranched PEI with excess and low-stoichiometric mono- and oligosaccharide units are described.[44]

7.3.2 Aqueous size exclusion chromatography-multiangle laser light scattering (SEC-MALLS).

Aqueous SEC experiments were performed in a buffered solution consisting of 0.7 M sodium nitrate and 0.1 M TRIS adjusted to pH 6.0 with glacial acetic acid. The pH of the resulting solution was measured using a Thermo Orion 3 Star portable pH meter with a Thermo Orion Triode pH electrode. Sodium azide was added at 200 ppm to the solution as a precaution to prevent bacterial growth in the SEC system. Samples were analyzed at 0.8 mL/min through 2x Waters Ultrahydrogel Linear and 1x Water Ultrahydrogel 250 columns, with all columns measuring 7.8 x 300 mm and equilibrated

to 30 ^{o}C. SEC instrumentation consisted of a Waters 1515 isocratic HPLC pump, Waters 717plus Autosampler, Wyatt miniDAWN multiangle laser light scattering (MALLS) detector operating a He-Ne laser at a wavelength of 690 nm, Viscotek 270 capillary viscosity detector, and a Waters 2414 differential refractive index detector operating at a wavelength of 880 nm and 35 ^{o}C. The only calibration constant, the Wyatt Astra V AUX1, was calculated using a series of aqueous sodium chloride solutions. The accuracy and reproducibility was confirmed with poly(ethylene oxide) and poly(methacrylic acid) sodium salt standards (Polymer Laboratories/Varian Inc.) ranging in molecular weight from 230 to 1,000,000 g/mol. Samples were processed using the Wyatt Astra V software package. Interdetector volume was determined through the superposition of a narrow polydispersity poly(ethylene oxide) standard. The specific refractive index increments (*dn/dc*) of the glucose- and maltose-modified hyperbranched were determined using 100% mass recovery methods.

7.3.3Zeta-potential measurements.

Zeta-potential measurements were performed on a Malvern Zeta Sizer Nano Series Nano-ZS instrument at a wavelength of 633 nm using a 4.0 mW, solid state He-Ne laser at a scattering angle of 173˚ using Dispersion Technology Software (DTS) version 4.20. All experiments were performed at 25 ˚C. Measurements were performed in triplicate and reported as the mean ± standard deviation. Polymer samples were dissolved at 1 mg/mL in phosphate buffered saline for all zeta-potential measurements.

7.3.4 Potentiometric titration.

pH measurements were performed using a Thermo Orion 3 Star portable pH meter equipped with a Thermo Orion Triode pH electrode. Both carbohydrate-modified

and unmodified hyperbranched PEI were dissolved at 1 mg/mL in ultrapure water having a resistivity of 18 MΩ·cm. Using 15 mL of polymer solution, the pH was then adjusted to ~10.5 using 100 μL aliquots of 0.5 M NaOH. The solutions were then titrated with 20-40 μL aliquots of 0.1 N HCl. The pH of the solution was measured after the addition of each aliquot.

7.3.5 Preparation of polyplexes.

The pRL-SV40 *Renilla* luciferase expression plasmid (Promega) was diluted in 2.5 mL basal RPMI media to a final concentration of 0.4 μg/mL and incubated at room temperature for 10 min. At the same time, the appropriate type and amount of polymer was diluted in 2.5 mL basal RPMI to the final concentrations corresponding to the various nitrogen/phosphorus (N/P) ratios and incubated for 10 min at room temperature. The plasmid and corresponding polymer solutions were combined and incubated for 20-30 min at room temperature to complex the DNA with various PEI compositions.

7.3.6 Gel electrophoresis.

Agarose powder (BioRad Laboratories) was dissolved in 1X TAE buffer (Sigma-Aldrich) to produce 0.9 wt% agarose gel slabs. Polyplexes were prepared in 1 mL microcentrifuge tubes. The pRL-SV40 plasmid (0.5 μL of 0.2 μg/μL DNA stock solution) was mixed with the appropriate amount of polymer solution (0.2 or 0.8 μL of 1 μg/μL polymer stock solution) corresponding to DNA/polymer mass ratios of 2 and 8. The polyplex solutions and a DNA only solution (0.5 μL of 0.2 μg/μL DNA stock solution) were diluted to a total volume of ~35 μL with 28 μL of 1X TAE buffer and 7 μL of 40 wt% sucrose 1X TAE solution. 20 μL of a plasmid DNA ladder (Bayou

Biolabs) was diluted with 15 μL of 1X TAE buffer. The polyplex, DNA only, and ladder solutions were incubated at room temperature for 30 min prior to loading into a submerged agarose gel. The gel was electropheresed at 75 V for 90 min in 1X TAE running buffer. Gels were stained with SYBR Green I (Sigma) and imaged using a UV transilluminator table and a digital camera equipped with a hood and green filter.

7.3.7 Cell culture.

Human brain microvascular endothelial cells (HBMEC) were isolated, cultivated, and purified as previously described.(*45*) HBMEC were grown in RPMI 1640-based medium with 10% fetal bovine serum (Mediatech), 10% NuSerum (Becton Dickinson), 30 μg/ml of endothelial cell growth supplement (ECGS; Becton Dickinson), 15 U/ml of heparin (Sigma-Aldrich), 2 mM L-glutamine, 2 mM sodium pyruvate, nonessential amino acids, vitamins, 100 U/ml of penicillin, and 100 μg/ml of streptomycin (all reagents from Mediatech). Cultures were incubated at 37 °C in a humid atmosphere of 5% CO_2.

7.3.8 Cell Viability Assay.

Each polymer sample was dissolved at 1 mg/mL in phosphate buffered saline. Then, 50-500 μL of 1 mg/mL polymer solution was diluted in 5 mL of basal RPMI 1640 to produce 10-100 μg/mL treatment solutions. Cell viability was determined using the 3-[4,5-dimethylthiazol-2-yl]2,5-diphenyltetrazolium bromide (MTT, Sigma-Aldrich) conversion assay. HBMEC cells were plated at a concentration of approximately $5.0x10^4$ cells/well on 24-well plates 24 h prior to each experiment. Prior to each assay, HBMEC cells were washed with approximately 1 mL of basal RPMI. After washing, 1 mL of

polymer treatment solution was placed in each well. The plates were then incubated for 12 h at 37°C, 5% CO_2. After 12 h, the cells were rinsed with approximately 1mL of HBSS, followed by the addition of 1 mL of RPMI 1640 medium containing 0.5 mg/ml of MTT. After incubation for 4 h at 37°C, the medium was aspirated and the formazan product was solubilized with DMSO. Absorbance at 570 nm was measured for each well using a Molecular Devices Corp. SPECTRAmax M2 microplate reader.

7.3.9 Lactate Dehydrogenase (LDH) Membrane Integrity Assay.

Polymer solutions (1 mg/mL in PBS) were diluted in basal RPMI 1640 to produce 10-200 μg/mL treatment solutions. HBMEC cells were plated at a concentration of $1.5x10^4$ cells/well on 96-well plates 24 h prior to each experiment. Prior to each assay, HBMEC cells were washed with approximately 100 μL of basal RPMI. After washing, 100 μL of polymer treatment solution was placed in each well. The plates were then incubated for 12 h at 37°C, 5% CO_2. LDH release was determined using a CytoTox-ONE™ Homogeneous Membrane Integrity Assay (Promega) and a Molecular Devices Corp. SPECTRAmax M2 microplate fluorometer.

7.3.10 Renilla Luciferase Expression Vector Assay.

HBMEC cells were plated at a concentration of $2.0x10^5$ cells/well on 12-well plates 24 h prior to transfection. DNA/polymer solutions were prepared as described above. All solutions were allowed to transfect for 12 h at 37 °C, 5% CO_2. After 12 h, the transfection solution was replaced with complete RPMI growth media. The cells were then incubated for 24 h at 37°C, 5% CO_2 to allow for protein expression. After incubation, the cells were rinsed with approximately 1 mL PBS and 100 μL of lysis buffer was added. Immediately after adding lysis buffer, each well was scraped and

incubated for 30 min at room temperature with gentle mixing. The lysate mixture was then subjected to two -80^{o}C/37^{o}C freeze/thaw cycles. HBMEC cells were treated with polyplexes carrying the pRL-SV40 plasmid, which expresses catalytically active *Renilla* luciferase. Upon treatment with the appropriate substrate, bioluminescence is quantified using a photon counter. The photon count thus correlates with plasmid transfection performance. The photon count was normalized to the total amount of protein harvested from the cell culture plates, which was determined using a commercially available spectrophotometric assay. Luciferase activity was measured using a *Renilla* luciferase assay kit (Promega) and a Molecular Devices Corp. SPECTRAmax L luminometer according to the assay kit manufacturer's instructions.

7.4 Results and Discussion

Elemental analysis and ^{1}H NMR spectroscopy was used to confirm the presence of both the glucose and maltose modifications as described in previous work by Appelhans et al.(*44*) In this study, both glucose- and maltose-modified PEI structures were found to have degrees of substitution >90%. In order to understand the complete structure-activity relationship of carbohydrate decorated hyperbranched PEI for DNA transfection performance, we answer the last open question about the influence of densely packed sugar shells on the periphery of hyperbranched PEI. The reductive amination method allowed us to realize the desired PEI structures with densely packed glucose and maltose shells (Figure 7.1). This study builds on the earlier efforts of Kissel et al.[35] and Remy et al.[34] who both reported the cell toxicity and transfection activity of partially carbohydrate-modified PEIs (up to 25% degrees of substitution in the work by

Remy et al. and 36% degrees of substitution in the work by Kissel et al.). In this work, we evaluated the cell toxicity and transfection activity of completely glucose- and maltose-modified hyperbranched PEI versus the unmodified precursor.

As shown in Figure 7.2, aqueous SEC was used to evaluate the relative molecular weights of the modified and unmodified hyperbranched PEIs. In the sodium nitrate buffer mobile phase, the unmodified hyperbranched PEI showed poor SEC separation. As shown in the chromatogram, the sample appeared to prematurely elute from the aqueous SEC column, indicating that the unmodified polymer was likely aggregating in solution. This was explained by the fact that larger aggregates do not sample the pores in the hydrogel columns. Additionally, the unmodified PEI chromatogram showed significant tailing which indicated that the sample was likely adsorbing to the column under these aqueous SEC conditions.[46] In the case of the glucose and maltose-modified hyperbranched PEI's, normal mono-modal SEC chromatograms were observed under the same aqueous SEC conditions. This observation indicated that the modified PEI's likely do not aggregate in solution and, since tailing was not observed in these chromatograms, these samples did not adsorb to the hydrogel columns. The maltose-modified hyperbranched PEI polymer was found to have a lower retention time than the glucose-modified polymer. Furthermore, SEC-MALLS calculations revealed that the maltose-modified PEI had a M_w=30,000 g/mol and the glucose-modified PEI had a M_w=23,000 g/mol. This result indicated that the maltose-modified polymer had a slightly higher molecular weight than the glucose-modified polymer, which was expected since maltose (342 g/mol) has a greater molar mass than glucose (180 g/mol). It is instructive to note that both the glucose and maltose-modified polymers were synthesized from the same

hyperbranched PEI precursor. Since aggregation and adsorption were observed in the chromatogram of unmodified PEI, SEC-MALLS molecular weights were not calculated for this sample. Aqueous SEC-MALLS values are summarized in Table 7.1. Aqueous SEC results indicated that the unmodified PEI had more cationic charge in the aqueous SEC mobile phase compared to the carbohydrate-modified polymers.

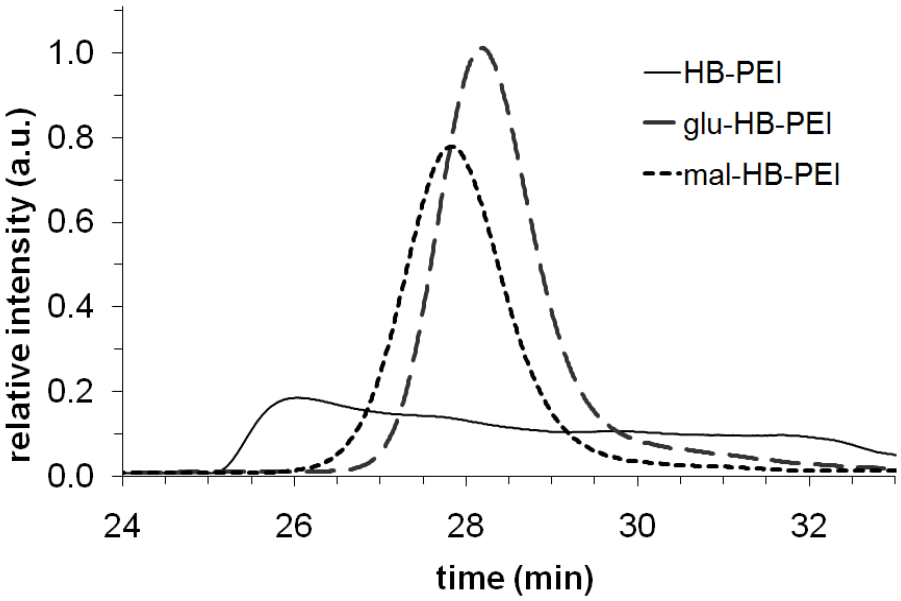

Figure 7.2. Aqueous SEC chromatograms (RI traces) of unmodified- and carbohydrate-modified hyperbranched PEI.

Table 7.1. Molecular weight characterization of glucose- and maltose-modified hyperbranched PEI.

Sample	type of substitution	degree of substitution (DS)[c]	[a]Mn (g/mol)	[a]Mw (g/mol)	[a]Mw/Mn
HB-PEI	-	-	-	~5,000[b]	-
glu-HB-PEI	glucose	>99%	12,000	23,000	1.92
mal-HB-PEI	maltose	>99%	15,000	30,000	2.00

[a]Aqueous SEC-MALLS calculated molecular weights in 0.7M $NaNO_3$, 0.1M Tris, pH=6.0.
[b]Molecular weight provided by the manufacturer.
[c]Determined with ^1H NMR spectroscopy.

Cytotoxicity experiments were conducted using the standard MTT conversion assay. The viability of treated cell groups was quantified relative to an untreated group. HBMEC cells were treated with 10 μg/mL and 100 μg/mL dosing levels to observe the influence of glucose and maltose modifications on the toxicity of hyperbranched PEI. As shown in Figure 7.3, 100% cell viability was maintained for both the unmodified and sugar-modified PEIs when the cells were treated with 10 μg/mL of polymer. However, when the cells were treated with the higher 100 μg/mL dose, a difference was observed between the modified and unmodified hyperbranched PEI. At the higher dose, a 30% reduction in HBMEC cell viability was observed for the unmodified PEI. Both the glucose and maltose-modified PEI maintained 100% HBMEC cell viability at the higher 100 μg/mL dose. These results showed that carbohydrate modifications significantly reduced to the cytotoxicity of hyperbranched PEI.

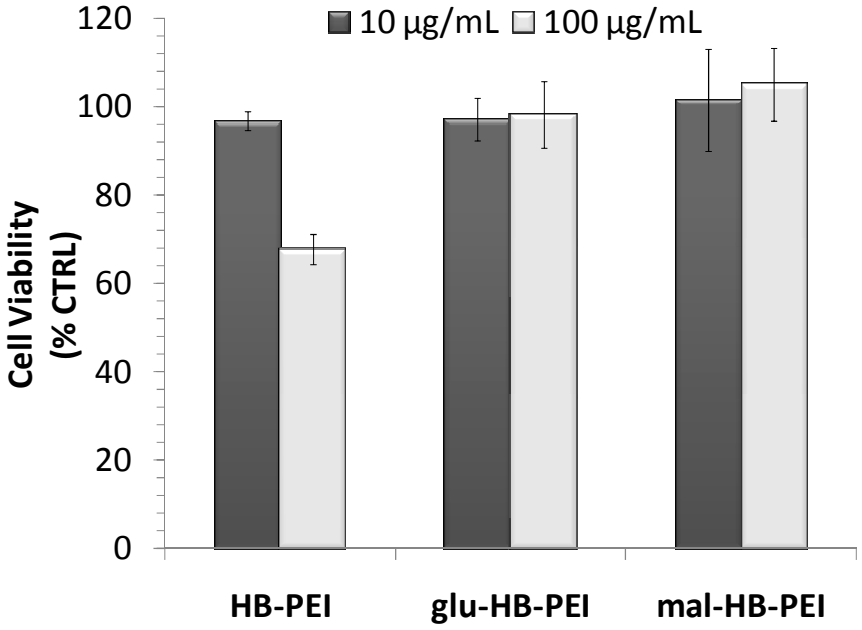

Figure 7.3. Dose-dependent relative cell viabilities of unmodified and sugar-modified hyperbranched PEI. Values represent mean ± σ (n=4).

An LDH release assay was used to evaluate the membrane integrity of HBMEC cells treated with various concentrations unmodified and carbohydrate-modified hyperbranched PEI. HBMEC cells were treated with 10, 100, and 200 µg/mL of unmodified-, glucose-, and maltose-modified hyperbranched PEI. As shown in Figure 7.4, increased LDH release (versus an untreated control group) was observed for unmodified hyperbranched PEI at all concentrations. However, both the glucose- and maltose-modified polymers did not show any increased LDH release versus the untreated control group. These data indicated that the unmodified hyperbranched PEI's cationic charge was disrupting cellular membranes causing the HBMEC cells to leak LDH. Conversely, since no increased LDH was observed with the carbohydrate-modified PEIs, these polymers did not disrupt cell membranes and thus were likely uncharged.

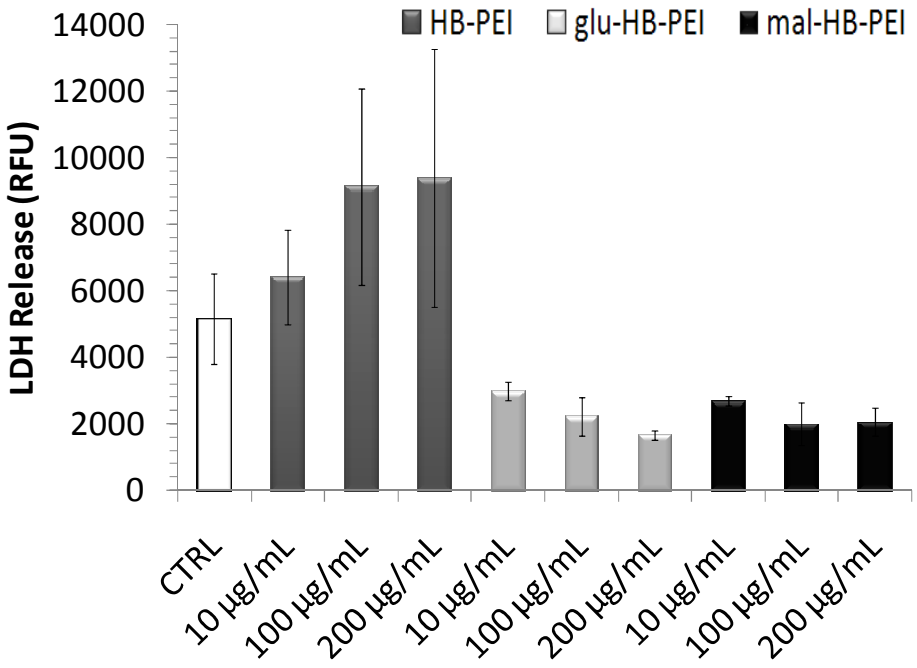

Figure 7.4. Lactate dehydrogenase (LDH) release from HBMEC cells treated with unmodified and carbohydrate-modified hyperbranched PEI. Values represent mean ± σ (n=4).

Reporter gene transfection was conducted to evaluate the influence of glucose and maltose modifications on *in vitro* plasmid DNA delivery. Figure 7.5 shows the transfection activity, in relative luminescence units (RLU) per mg of total protein, for the unmodified, glucose-modified, and maltose-modified hyperbranched PEIs. Transfection experiments revealed that the unmodified polymer (HB-PEI) delivered plasmid DNA more efficiently than both the glucose-modified (glu-HB-PEI) and maltose-modified (mal-HB-PEI) polymers. In fact, the glucose- and maltose-modified hyperbranched PEI samples were found to have RLU/mg total protein values similar to untreated, cells-only control groups (~8.5 RLU/mg total protein, shown as a dashed line in Figure 7.5). For

the unmodified PEI polymer, it was observed that luciferase activity increased as the DNA to polymer mass ratio increased from 2 to 8. However, influence of the DNA to polymer mass ratio was not observed for either the glucose- or maltose-modified hyperbranched PEI. The results in Figure 7.5 clearly show that the conjugation of hyperbranched PEI with either glucose or maltose renders the polymer ineffective as a DNA delivery agent.

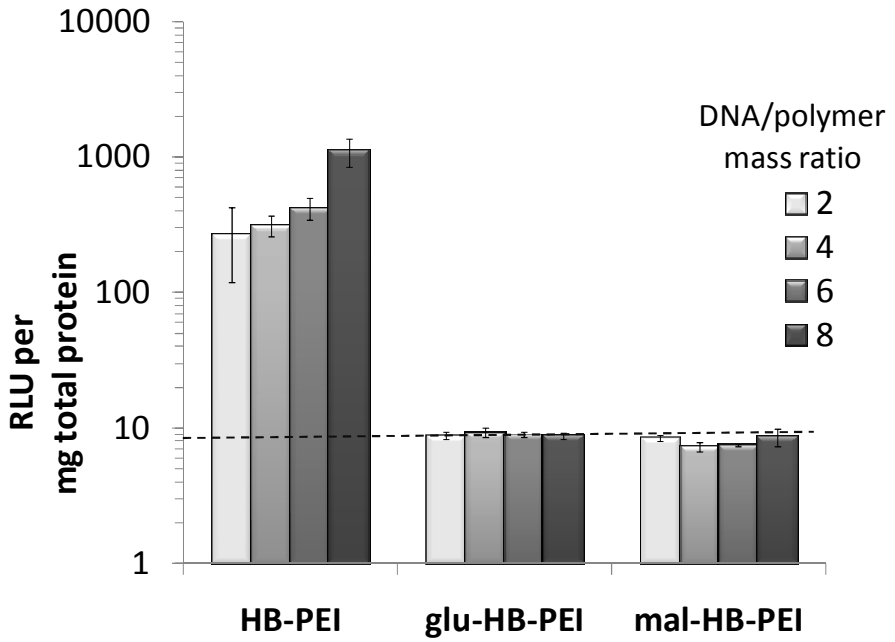

Figure 7.5. Transfection performance of unmodified and sugar-modified hyperbranched PEI at various polymer to DNA mass ratios. The dashed line represents the RLU/mg total protein of an untreated control group. Values represent mean ± σ (n=4).

We attributed the decrease in DNA delivery of the carbohydrate-modified polymers to reduced cationic charge. It is widely known that surface charge directly influences cellular internalization.[47] Although the primary and secondary amines were quantitatively converted into tertiary amines during the amination reaction, we originally

postulated that the peripheral and internal tertiary amines remain amenable to protonation at physiological pH. However, zeta-potential measurements, summarized in Table 7.2, revealed that the sugar-modified hyperbranched polymers did not possess cationic charge. The unmodified hyperbranched PEI had zeta-potentials of approximately +25 mV. This evidence suggested that the uncharged glucose- and maltose-modified PEIs is not able to electrostatically bind and deliver anionic plasmid DNA. Gel retardation experiments provided further evidence that the carbohydrate modifications eliminated the potential binding between hyperbranched PEI and plasmid DNA. Figure 7.6 shows the electrophoresed agarose gel of polyplexes prepared with unmodified- and carbohydrate-modified hyperbranched PEI. Polyplexes were prepared at DNA to polymer mass ratios of 2 and 8 for each polymer. As shown in lanes 3 and 4 of the gel, unmodified hyperbranched PEI sufficiently bound and retarded the movement of plasmid DNA. However, both the glucose- and maltose-modified hyperbranched PEIs (lanes 5-8) did not bind to plasmid DNA leading to free DNA movement in the gel.

Table 7.2. Zeta-potential of unmodified and sugar-modified hyperbranched PEI at pH=7.4.

sample	zeta-potential (mV)
HB-PEI	+25 ± 1
glu-HB-PEI	0 ± 0.5
mal-HB-PEI	0 ± 0.5

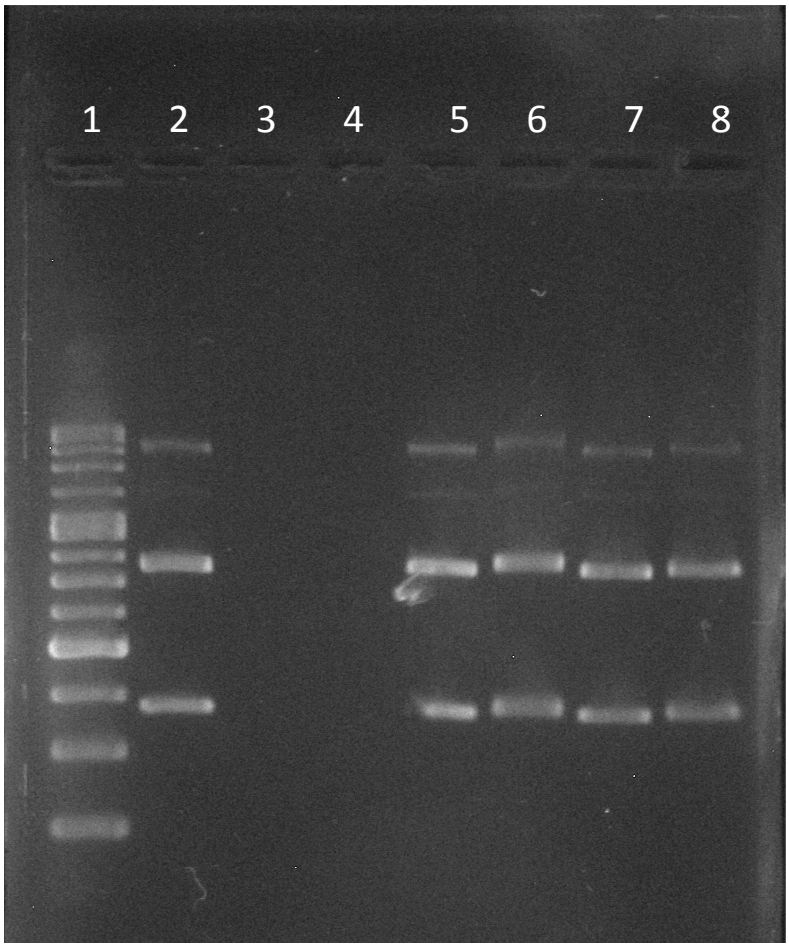

Figure 7.6. Agarose gel of polyplexes prepared with unmodified- and carbohydrate-modified hyperbranched PEI. Lane 1 is a 10-1 kbp ladder, lane 2 is pRL-SV40 DNA in the absence of polymer, lanes 3 and 4 are polyplexes prepared with unmodified HB-PEI at DNA/polymer mass ratios of 2 and 8 respectively, lanes 5 and 6 are polyplexes prepared with glucose-modified HB-PEI at DNA/polymer mass ratios of 2 and 8 respectively, lanes 7 and 8 are polyplexes prepared with maltose-modified HB-PEI at DNA/polymer mass ratios of 2 and 8 respectively.

Although the carbohydrate-modified hyperbranched PEIs were not cationically charged at physiological pH, we further explored their protonatability in an effort to

better understand the chemo/physical implications of conjugating PEI with glucose or maltose. Figure 7.7 shows the potentiometric titration curves for unmodified- and glucose-modified hyperbranched PEI. The titration experiments revealed that the unmodified, hyperbranched PEI was able to effectively buffer protons during the addition of aliquots of 0.1 N HCl. The buffering ability of the unmodified PEI was consistent with similar work published by Kissel et al.[48] However, the glucose-modified hyperbranched PEI was unable to buffer protons resulting in a sharp decrease in pH during the addition of strong acid (HCl). The maltose-modified hyperbranched PEI exhibited the same behavior (the data was removed from the figure for clarity). These results demonstrated that the conjugation of either glucose or maltose with hyperbranched PEI produced an unprotonatable polymer, even at low pH.

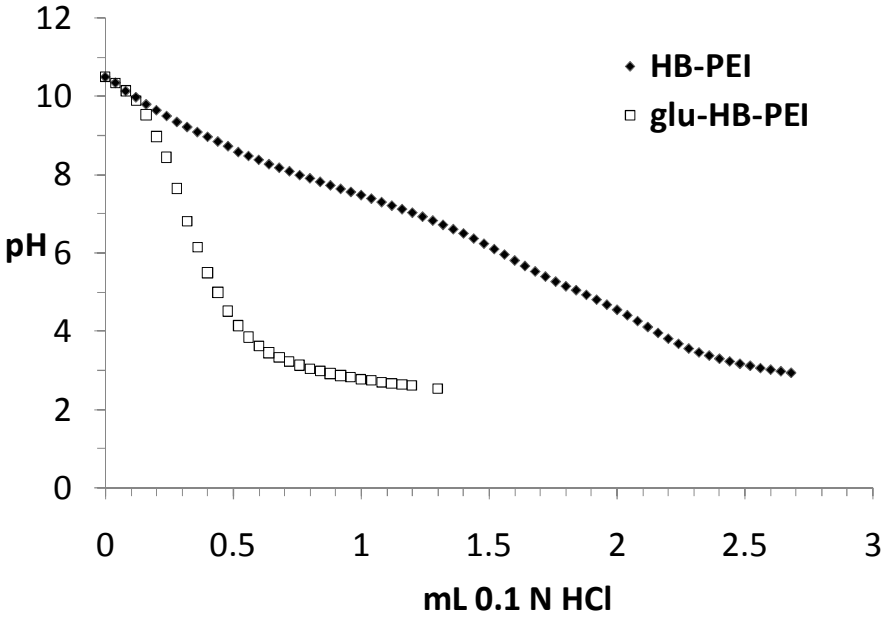

Figure 7.7. Potentiometric titration of unmodified and glucose-modified hyperbranched PEI.

7.5 Conclusions

In this study, we evaluated the influence of glucose and maltose modifications (degrees of substitution >90%) on the cytotoxicity and gene transfection performance of hyperbranched PEI in HBMEC cells. Aqueous SEC and zeta-potential characterization of the synthesized polymers determined that the carbohydrate substitutions eliminated the cationic charge of hyperbranched PEI. Titration experiments showed that the internal amines of peripherally substituted hyperbranched PEI were not accessible to protonation. Gel electrophoresis revealed that glucose and maltose substitutions prevented electrostatic binding with plasmid DNA. We determined that peripherally decorating PEI with either glucose or maltose significantly reduced toxicity, but these modifications also reduced transfection efficiency.

7.6 Acknowledgments

This material is based upon work supported in part by the Macromolecular Interfaces with Life Sciences (MILES) Integrative Graduate Education and Research Traineeship (IGERT) of the National Science Foundation under Agreement No. DGE-0333378.

7.7 References

[1]Emery, D. W. (2004) Gene therapy for genetic diseases: On the horizon. *Clinical and Applied Immunology Reviews 4*, 411-422.

[2]Palmer, D. H., Young, L. S., and Mautner, V. (2006) Cancer gene-therapy: clinical trials. *Trends in Biotechnology 24*, 76-82.

[3]Kay, M. A., Glorioso, J. C., and Naldini, L. (2001) Viral vectors for gene therapy: the art of turning infectious agents into vehicles of therapeutics. *Nat. Med. 7*, 33-40.

[4]Kaiser, J. (2007) CLINICAL RESEARCH: Death Prompts a Review of Gene Therapy Vector. *Science 317*, 580-.

[5]Heath, W. H., Senyurt, A. F., Layman, J., and Long, T. E. (2007) Charged Polymers via Controlled Radical Polymerization and their Implications for Gene Delivery. *Macromolecular Chemistry and Physics 208*, 1243-1249.

[6]Jeong, J. H., Kim, S. W., and Park, T. G. (2007) Molecular design of functional polymers for gene therapy. *Progress in Polymer Science 32*, 1239-1274.

[7]Schaffert, D., and Wagner, E. (2008) Gene therapy progress and prospects: synthetic polymer-based systems. *Gene Ther. 15*, 1131-1138.

[8]Wong, S. Y., Pelet, J. M., and Putnam, D. (2007) Polymer systems for gene delivery--Past, present, and future. *Progress in Polymer Science 32*, 799-837.

[9]Stasko, N. A., Johnson, C. B., Schoenfisch, M. H., Johnson, T. A., and Holmuhamedov, E. L. (2007) Cytotoxicity of Polypropylenimine Dendrimer Conjugates on Cultured Endothelial Cells. *Biomacromolecules 8*, 3853-3859.

[10]Zintchenko, A., Philipp, A., Dehshahri, A., and Wagner, E. (2008) Simple Modifications of Branched PEI Lead to Highly Efficient siRNA Carriers with Low Toxicity. *Bioconjugate Chem. 19*, 1448-1455.

[11]Thomas, M., and Klibanov, A. M. (2002) Enhancing polyethylenimine's delivery of plasmid DNA into mammalian cells. *Proc. Natl. Acad. Sci. U S A 99*, 14640-5.

[12]Rabuka, D., Forstner, M. B., Groves, J. T., and Bertozzi, C. R. (2008) Noncovalent Cell Surface Engineering: Incorporation of Bioactive Synthetic Glycopolymers into Cellular Membranes. *J. Am. Chem. Soc. 130*, 5947-5953.

[13]Park, I. K., Cook, S. E., Kim, Y. K., Kim, H. W., Cho, M. H., Jeong, H. J., Kim, E. M., Nah, J. W., Bom, H. S., and Cho, C. S. (2005) Glucosylated polyethylenimine as a tumor-targeting gene carrier. *Arch. Pharm. Res. 28*, 1302-10.

[14]Fajac, I., Thevenot, G., Bedouet, L., Danel, C., Riquet, M., Merten, M., Figarella, C., Dall'Ava-Santucci, J., Monsigny, M., and Briand, P. (2003) Uptake of plasmid/glycosylated polymer complexes and gene transfer efficiency in differentiated airway epithelial cells. *J. Gene Med. 5*, 38-48.

[15]Fajac, I., Briand, P., and Monsigny, M. (2001) Gene therapy of cystic fibrosis: The glycofection approach. *Glycoconjugate Journal 18*, 723-729.

[16]Popielarski, S. R., Pun, S. H., and Davis, M. E. (2005) A Nanoparticle-Based Model Delivery System To Guide the Rational Design of Gene Delivery to the Liver. 1. Synthesis and Characterization. *Bioconjugate Chem. 16*, 1063-1070.

[17]Popielarski, S. R., Hu-Lieskovan, S., French, S. W., Triche, T. J., and Davis, M. E. (2005) A Nanoparticle-Based Model Delivery System To Guide the Rational Design of Gene Delivery to the Liver. 2. In Vitro and In Vivo Uptake Results. *Bioconjugate Chem. 16*, 1071-1080.

[18]Lim, D. W., Yeom, Y. I., and Park, T. G. (2000) Poly(DMAEMA-NVP)-b-PEG-galactose as Gene Delivery Vector for Hepatocytes. *Bioconjugate Chem. 11*, 688-695.

[19]Narumi, A., and Kakuchi, T. (2008) Synthesis of Glycoconjugated Branched Macromolecular Architectures. *Polymer Journal 40*, 383-397.

[20]Davis, M. E., and Brewster, M. E. (2004) in *Nature Reviews Drug Discovery* pp 1023-1035, Nature Publishing Group.

[21]Bartlett, D. W., and Davis, M. E. (2007) Physicochemical and Biological Characterization of Targeted, Nucleic Acid-Containing Nanoparticles. *Bioconjugate Chem. 18*, 456-468.

[22]Mishra, S., Heidel, J. D., Webster, P., and Davis, M. E. (2006) Imidazole groups on a linear, cyclodextrin-containing polycation produce enhanced gene delivery via multiple processes. *J. of Controlled Release 116*, 179-191.

[23]Reineke, T. M., and Davis, M. E. (2003) Structural Effects of Carbohydrate-Containing Polycations on Gene Delivery. 1. Carbohydrate Size and Its Distance from Charge Centers. *Bioconjugate Chem. 14*, 247-254.

[24]Reineke, T. M., and Davis, M. E. (2003) Structural Effects of Carbohydrate-Containing Polycations on Gene Delivery. 2. Charge Center Type. *Bioconjugate Chem. 14*, 255-261.

[25]Pun, S. H., Bellocq, N. C., Liu, A., Jensen, G., Machemer, T., Quijano, E., Schluep, T., Wen, S., Engler, H., Heidel, J., and Davis, M. E. (2004) Cyclodextrin-Modified Polyethylenimine Polymers for Gene Delivery. *Bioconjugate Chem. 15*, 831-840.

[26]Srinivasachari, S., Liu, Y., Zhang, G., Prevette, L., and Reineke, T. M. (2006) Trehalose Click Polymers Inhibit Nanoparticle Aggregation and Promote pDNA Delivery in Serum. *J. Am. Chem. Soc. 128*, 8176-8184.

[27]Liu, Y., and Reineke, T. M. (2006) Poly(glycoamidoamine)s for Gene Delivery: Stability of Polyplexes and Efficacy with Cardiomyoblast Cells. *Bioconjugate Chem. 17*, 101-108.

[28]Liu, Y., and Reineke, T. M. (2007) Poly(glycoamidoamine)s for Gene Delivery. Structural Effects on Cellular Internalization, Buffering Capacity, and Gene Expression. *Bioconjugate Chem. 18*, 19-30.

[29]Prevette, L. E., Kodger, T. E., Reineke, T. M., and Lynch, M. L. (2007) Deciphering the Role of Hydrogen Bonding in Enhancing pDNA-Polycation Interactions. *Langmuir 23*, 9773-9784.

[30]Prevette, L. E., Lynch, M. L., Kizjakina, K., and Reineke, T. M. (2008) Correlation of Amine Number and pDNA Binding Mechanism for Trehalose-Based Polycations. *Langmuir 24*, 8090-8101.

[31]Spain, S. G., Gibson, M. I., and Cameron, N. R. (2007) Recent advances in the synthesis of well-defined glycopolymers. *Journal of Polymer Science Part A: Polymer Chemistry 45*, 2059-2072.

[32]Baigude, H., Katsuraya, K., Okuyama, K., Tokunaga, S., and Uryu, T. (2003) Synthesis of Sphere-Type Monodispersed Oligosaccharide-Polypeptide Dendrimers. *Macromolecules 36*, 7100-7106.

[33]Appelhans, D., Zhong, Y., Komber, H., Friedel, P., Oertel, U., Scheler, U., Morgner, N., Kuckling, D., Richter, S., Seidel, J., Brutschy, B., and Voit, B. (2007) Oligosaccharide-modified poly(propyleneimine) dendrimers: synthesis, structure determination, and Cu(II) complexation. *Macromol. Biosci. 7*, 373-83.

[34]Erbacher, P., Bettinger, T., Belguise-Valladier, P., Zou, S., Coll, J. L., Behr, J. P., and Remy, J. S. (1999) Transfection and physical properties of various saccharide, poly(ethylene glycol), and antibody-derivatized polyethylenimines (PEI). *J. Gene Med. 1*, 210-22.

[35]Kunath, K., von Harpe, A., Fischer, D., and Kissel, T. (2003) Galactose-PEI-DNA complexes for targeted gene delivery: degree of substitution affects complex size and transfection efficiency. *J. of Controlled Release 88*, 159-172.

[36]Kim, T. H., Park, I. K., Nah, J. W., Choi, Y. J., and Cho, C. S. (2004) Galactosylated chitosan/DNA nanoparticles prepared using water-soluble chitosan as a gene carrier. *Biomaterials 25*, 3783-92.

[37]Satoh, T., Kakimoto, S., Kano, H., Nakatani, M., Shinkai, S., and Nagasaki, T. (2007) In vitro gene delivery to HepG2 cells using galactosylated 6-amino-6-deoxychitosan as a DNA carrier. *Carbohydrate Research 342*, 1427-1433.

[38]Eliyahu, H., Barenholz, Y., and Domb, A. J. (2005) Polymers for DNA delivery. *Molecules 10*, 34-64.

[39]Breunig, M., Lungwitz, U., Liebl, R., Klar, J., Obermayer, B., Blunk, T., and Goepferich, A. (2007) Mechanistic insights into linear polyethylenimine-mediated gene transfer. *Biochimica et Biophysica Acta (BBA) - General Subjects 1770*, 196-205.

[40]Fischer, D., Bieber, T., Li, Y., Elsässer, H.-P., and Kissel, T. (1999) A Novel Non-Viral Vector for DNA Delivery Based on Low Molecular Weight, Branched Polyethylenimine: Effect of Molecular Weight on Transfection Efficiency and Cytotoxicity. *Pharmaceutical Research 16*, 1273-1279.

[41]Köth, A., Koetz, J., Appelhans, D., and Voit, B. (2008) "Sweet" gold nanoparticles with oligosaccharide-modified poly(ethyleneimine). *Colloid & Polymer Science 286*, 1317-1327.

[42]Appelhans, D., Komber, H., Morgner, N., Richter, S., Bienert, R., Thuenemann, A., Brutschy, B., and Voit, B. (2008) One pot approach for the establishment of dendritic polymers with various oligosaccharide architectures. *Polymer Preprints 49*, 590-591.

[43]Klajnert, B., Appelhans, D., Komber, H., Morgner, N., Schwarz, S., Richter, S., Brutschy, B., Ionov, M., Tonkikh, A. K., Bryszewska, M., and Voit, B. (2008) The Influence of Densely Organized Maltose Shells on the Biological Properties of Poly(propylene imine) Dendrimers: New Effects Dependent on Hydrogen Bonding. *Chemistry - A European Journal 14*, 7030-7041.

[44]Appelhans, D., Komber, H., Abdul Quadir, M., Richter, S., Schwarz, S., Aigner, A., Loos, K., Müller, M., Seidel, J., Arndt, K.-F., Haag, R., and Voit, B. (2008) Hyperbranched PEI with various oligosaccharide architectures: Synthesis, Characterization, ATP complexation and cellular uptake properties. *Biomacromolecules, submitted for publication*.

[45]Stins, M. F.; Gilles, F.; Kim, K. S., Selective expression of adhesion molecules on human brain microvascular endothelial cells. *Journal of Neuroimmunology* **1997,** 76, (1-2), 81-90.

[46]Layman, J. M., Borgerding, E. M., Williams, S. R., Heath, W. H., and Long, T. E. (2008) Synthesis and Characterization of Aliphatic Ammonium Ionenes: Aqueous Size Exclusion Chromatography for Absolute Molecular Weight Characterization. *Macromolecules 41*, 4635-4641.

[47]Gratton, S. E., Ropp, P. A., Pohlhaus, P. D., Luft, J. C., Madden, V. J., Napier, M. E., and DeSimone, J. M. (2008) The effect of particle design on cellular internalization pathways. *Proc. Natl. Acad. Sci. U S A 105*, 11613-8.

[48]von Harpe, A., Petersen, H., Li, Y., and Kissel, T. (2000) Characterization of commercially available and synthesized polyethylenimines for gene delivery. *J. of Controlled Release 69*, 309-322.

Chapter 8. **Synthesis and Characterization of Aliphatic Ammonium Ionenes: Aqueous Size Exclusion Chromatography for Absolute Molecular Weight Characterization**

John M. Layman, Erika M. Borgerding, Sharlene R. Williams, William H. Heath, and Timothy E. Long

8.1 Abstract

Cationic aliphatic ammonium polyionenes, specifically 12,12- and 6,12-ionenes, were synthesized using step-growth polymerization and aqueous-based size exclusion chromatography (SEC) coupled with multi-angle laser light scattering (MALLS) revealed absolute molecular weight information. The chromatographic separation of cationic polyelectrolytes presents many additional challenges compared to SEC of non-associating, neutral polymers. Therefore, an aqueous-based SEC-MALLS mobile phase composition was identified to separate these notoriously challenging polyelectrolytes in an effort to achieve absolute molecular weight analysis. Various solvent compositions were evaluated for their ability to solvate and reproducibly separate both 6,12- and 12,-12-ionenes. Dynamic light scattering (DLS) verified the absence of aggregation of polyionenes in preferred mobile phase compositions. The optimum solvent composition comprised a ternary mixture of 54/23/23 water/methanol/glacial acetic acid, 0.54 *M*

NaOAc, at a pH of 4.0. Weight average molecular weights for the synthesized ammonium 12,12-ionenes ranged from 11,000 – 40,000 g/mol and ammonium 6,12-ionenes had weight average molecular weights ranging from 19,000 – 49,900 g/mol. Mark-Houwink parameters were also determined for both the 12,12- and 6,12-ionenes in the optimum mobile phase using an online capillary viscometer.

KEYWORDS: ammonium ionenes, cationic polyelectrolytes, aqueous SEC-MALLS, light scattering

8.2 Introduction

Ammonium ionenes are ion-containing macromolecules containing quaternary nitrogens in the main chain.[1] The typical nomenclature for aliphatic ammonium ionenes is x,y-ionene, where x represents the number of methylene spacer units derived from the di-tertiary amine monomer, and y represents the methylene spacer units in the dihaloalkane monomer (Figure 1). Early efforts for the synthesis of ammonium ionenes involved the homopolymerization of ω-halo-alkyl dialkylamines; [1,2,3,4] however, more conventional synthetic methodologies for ammonium ionenes involved the copolymerization of dihaloalkanes and di-tertiary amines, which Rembaum et al, first reported.[5,6] The ability to easily control charge density and counter anion through monomer selection makes ammonium ionenes an ideal model in the study of well-defined cationic polyelectrolytes. Due to their unique coulombic interactions, ammonium ionenes were recently explored for several biomedical technologies including

antimicrobials,[7,8] gene transfection agents,[9] and polymeric cancer drugs.[10] Osada and co-workers performed cell binding and viability studies and found that ammonium ionenes with lower charge density disrupted cell membranes to a greater extent than structures with higher charge density despite less cell binding.[11] Furthermore, Rembaum reported ionenes as anti-tumor agents that exhibited selective inhibition of malignant cell growth without affecting normal cells.[10] These examples demonstrate the potential applications of ammonium ionenes, as well as the importance of determining their chemo-physical characteristics for conclusive structure-property relationships.

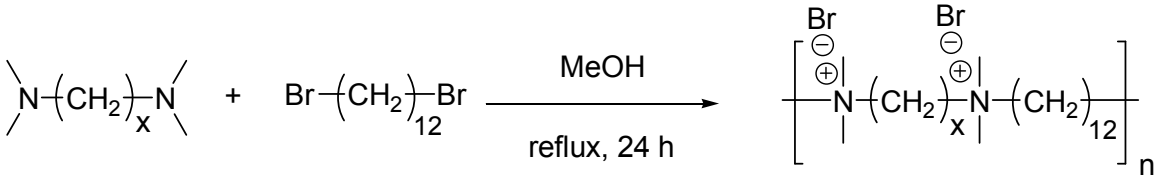

Figure 8.1. Synthesis of aliphatic ammonium x,12-ionenes.

Determination of molecular weight and molecular weight distribution is critical when establishing structure-property-performance relationships. In earlier investigations, a comparison of the amount of non-ionic bromine in an ionene solution to the amount of total bromide in the same solution yielded an "average apparent molecular weight."[12] In Rembaum's earlier work, extensive viscosity and light scattering studies were performed on ammonium 3,4- and 6,6-ionenes to determine molecular weights via the Mark-Houwink and Debye relationships, respectively.[13] Absolute molecular weights were determined; however, tedious sample preparation and lengthy experiments were required to complete these calculations. Size exclusion chromatography (SEC), also referred to as

gel permeation chromatography (GPC), coupled with multiangle laser light scattering (MALLS) is a well-established method for determining molecular weights of polymers. When MALLS detection is coupled with a concentration detector such as a differential refractometer (dRI), SEC provides a rapid method for determining absolute molecular weights with facile sample preparation. In addition, MALLS provides structural information, such as radii of gyration. Several texts and comprehensive reviews that describe SEC in detail are available.[14,15,16] Despite the appreciated value of SEC-MALLS and concurrent synthetic investigations of ionenes, SEC analysis for the determination of absolute molecular weights of ammonium ionenes has not been reported earlier. This is partly attributed to the challenges associated with SEC of polyelectrolytes. Difficulties arise from ionic aggregation[17] and non-size exclusion events,[14] such as ion interaction, ion exclusion, and hydrophobic interactions in the stationary phase of the chromatographic column. SEC of cationic polyelectrolytes is especially problematic due to the negative charge that is common on most stationary-phase packing materials and encourages unwanted electrostatic interactions.[18] To the best of our knowledge, earlier SEC analyses of ammonium ionenes were limited to calibrative methods, which provide only standard-equivalent molecular weights. Furthermore, SEC-MALLS determination of absolute molecular weights of ammonium 12,12-ionene compositions was not reported earlier. Kopecká et al. performed SEC on ammonium 5,2- and 10,2-ionenes and determined relative molecular weights based on polyacrylamide standards.[19] Similarly, Reisinger et al. performed SEC on ammonium ionenes using quaternized poly(vinylpyridinium) standards.[20] Although these earlier experiments provided molecular weight trends, absolute molecular weight data is critical

for the understanding of fundamental structure-property relationships. Moreover, meaningful molecular weight characterization of branched topologies is difficult using relative calculation methods. Furthermore, our aqueous SEC-MALLS data of ammonium ionenes using two mobile phase compositions that Kopecká and Reisinger reported earlier did not reveal any signals in the chromatograms.

Herein, we report aqueous-based SEC-MALLS of 6,12- and 12,12-ammonium ionenes. This manuscript reports the most suitable aqueous SEC mobile-phase composition for obtaining reliable separations of aliphatic ammonium ionenes through elimination of polymer-column interactions and reduction of polymer-polymer aggregation. In addition to absolute molecular weight determination, we also report dilute solution rheology of ammonium ionenes using an online, capillary-based viscometric detector. This complementary detector functions with dRI and MALLS detectors to determine the intrinsic viscosity of the sample across the molecular weight distribution.

8.3 Experimental

8.3.1 General Methods and Materials

HPLC-grade methanol was obtained from Fischer Scientific and distilled from calcium hydride (reagent grade, 95%), which was obtained from Sigma-Aldrich and used as received. 1,12-dibromododecane (98%) was obtained from Sigma-Aldrich, recrystallized from ethanol (AAPER Alcohol and Chemical Co.) and dried under reduced pressure. N,N,N',N'-tetramethyl-1,6-hexanediamine (99%) was obtained from Sigma-Aldrich and distilled from calcium hydride. Dimethylamine (60% in water, ~11.0 *M*) was obtained from Fluka and used as received. HPLC-grade tetrahydrofuran (THF),

HPLC-grade water, and diethyl ether were obtained from Fischer Scientific and used as received. Sodium acetate (NaOAc) (99.0%), sodium azide (99%), and ACS-grade glacial acetic acid (99.7%) were purchased from Alfa Aesar and used as received.

^{1}H and ^{13}C NMR spectra were recorded on a Varian Inova 400 MHz spectrometer. Chemical shifts are reported in ppm downfield from TMS using the residual protonated solvent as an internal standard (CD_3OD, ^{1}H 4.87 ppm and ^{13}C 77.0 ppm) (D_2O, ^{1}H 4.79 ppm). FAB-MS was obtained on a JOEL HX110 dual focusing mass spectrometer, and FTIR data were recorded on a Perkin Elmer Spectrum One FT-IR Spectrometer with a 1 mW He-Ne laser operating at a wavelength of 633 nm using a Spectrum v5.0.1 software package. *In situ* FTIR was performed with a Mettler Toledo ReactIR 4000 ATR apparatus equipped with a light conduit and a stainless steel insertion probe with a DiComp (diamond composite) probe tip. IR spectra were collected every minute with 256 scans per spectrum. Reaction analysis was performed with ReactIR 3.1 software provided by Mettler Toledo.

8.3.2 Synthesis of N,N,N',N'-tetramethyl-1,12-dodecanediamine

1,12-Dibromododecane (6.00 g, 18.3 mmol) was dissolved in THF (150 mL) in a two-necked, 500-mL round-bottomed flask and the solution was cooled to -78 ˚C. Dimethylamine (60% in water, 327 mL, 3.6 mol) was added to the flask, and the solution was magnetically stirred for 30 min. The solution was allowed to warm to room temperature and stir for an additional 24 h. The reaction solvent was removed under reduced pressure, and the subsequent white residue was dissolved in a 2.0 *M* NaOH aqueous solution (150 mL). Diethyl ether (150 mL) was added to the flask and the

mixture was magnetically stirred for 2 h. The organic layer was collected and concentrated, and a yellow oil was obtained. The crude product was purified via vacuum distillation (100˚C and 150 mTorr) from CaH_2 to provide a clear colorless product (yield 2.3 g, 47 %). ^{1}H NMR (400 MHz, CD_3OD): δ 2.26 (t, 4 H), 2.19 (s, 12 H), 1.45 (q, 4 H), 1.28 (s, 16 H). ^{13}C NMR (100 MHz, CD_3OD): δ=123.8, 59.7, 44.3, 29.6, 29.5, 27.5, 27.2. FAB-MS (m/z calculated = 256.48, found = 257.29); FTIR (oil) ν = 2925.1, 2853.2, 2812.8, 2761.1, 1459.2, 1041.9 cm^{-1}.

8.3.3 Preparation of Ammonium Ionene

In a typical synthesis, 1,12-dibromododecane (1.02 g, 3.1 mmol) was transferred into a two-necked, 50-mL round-bottomed flask, which was equipped with a reflux condenser and a mechanical stirrer. Methanol (2.25 g, 70.3 mmol) was added into the flask with a cannula under nitrogen, and the solution was refluxed. N,N,N',N'-tetramethyl-1,6-hexanediamine (0.53 g, 3.1 mmol) was quickly added into the flask, and additional purging with nitrogen was performed. The reaction was mechanically stirred for 24 h under reflux. Upon completion, the methanol was removed under reduced pressure at 25 ˚C to yield the polymer product. ^{1}H NMR (400 MHz, D_2O): δ 3.31 (m, 8 H), 3.05 (s, 12 H), 1.75 (m, 8 H), 1.31 (m, 20 H). M_n 14,000 – 41,500 g/mol, M_w 19,000 – 49,900 g/mol, PDI 1.31-1.36.

The 12,12-ionene was also prepared as described above. ^{1}H NMR (400 MHz, D_2O): δ 3.31 (m, 8 H), 3.05 (s, 12 H), 1.75 (m, 8 H), 1.31 (m, 32 H). M_n 8,000 – 30,700 g/mol, M_w 11,000 – 40,000 g/mol, PDI 1.26 to 1.42.

8.3.4 Aqueous SEC of Ammonium Ionenes

Aqueous-based SEC-MALLS was used to determine absolute molecular weights in acetate buffer solutions. The mobile phase consisted of 0.540 *M* sodium acetate in a ternary mixture of 54/23/23 water/methanol/glacial acetic acid v/v/v %. The pH of the resulting solution was 4.0, which was measured using a Thermo Orion 3 Star portable pH meter with a Thermo Orion Triode pH electrode. Sodium azide was added at 200 ppm to the solution as a precaution to prevent bacterial growth in the SEC system. Other compositions that employed different molarities of salt and varying mixtures of water, methanol and acetic acid, are noted in the discussion. The mobile phase solutions were vacuum filtered through NALGENE® MF75™ Series Media-Plus Filter Units with a minimum pore size of 0.200 μm. Samples were analyzed at 0.8 mL/min through 2x Waters Ultrahydrogel linear columns and 1x Waters Ultrahydrogel 250 column, with all columns measuring 7.8 x 300 mm and equilibrated to 30 ^{o}C. SEC instrumentation consisted of a Waters 1515 isocratic HPLC pump, Waters 717plus Autosampler, Wyatt miniDAWN multiangle laser light scattering (MALLS) detector operating a He-Ne laser at a wavelength of 690 nm, Viscotek 270 capillary viscosity detector, and a Waters 2414 differential refractive index detector operating at a wavelength of 880 nm and 35 ^{o}C. The only calibration constant, the Wyatt Astra V AUX1, was calculated using a series of aqueous sodium chloride solutions. The accuracy and reproducibility was confirmed with poly(ethylene oxide) and poly(methacrylic acid) sodium salt standards (Polymer Laboratories/Varian Inc.) ranging in molecular weight from 1,000 to 1,000,000 g/mol. Samples were processed using the Wyatt Astra V software package. Interdetector volume was determined through the superposition of a narrow polydispersity

poly(ethylene oxide) standard. Weight average molecular weights were determined from light scattering data using equation 1:

$$\frac{K^* c}{R(\theta)} = \frac{1}{M_w P(\theta)} + 2A_2 c \qquad (1)$$

where M_w is the weight average molecular weight, c is the concentration of the polymer, $R(\theta)$ is the measured excess Rayleigh ratio, $P(\theta)$ is the particle scattering function, A_2 is the second virial coefficient of the polymer-solvent system, and K^* is an optical scattering constant, determined using equation 2:

$$K^* = \frac{4\pi^2 n_o^2 (dn/dc)^2}{\lambda_o^4 N_A} \qquad (2)$$

where *dn/dc* is the specific refractive index increment, n_o is the refractive index of the solvent, λ_o is the wavelength of the incident laser in a vacuum, and N_A is Avogadro's number.

8.3.5 Determination of Specific Refractive Index Increments (dn/dc)

A Wyatt OptiRex differential/absolute refractive index detector operating at a wavelength of 690 nm and 30 ^oC was used for all specific refractive index increment measurements. Polymer samples (0.076 – 1.512 mg/mL) were allowed to dissolve in the appropriate solvent overnight. Samples were metered at 0.8 mL/min into the dRI detector at 30 ˚C using a syringe pump and a syringe affixed with a 0.45 μm PTFE syringe filter. The *dn/dc* values were determined using the Wyatt Astra V software package.

8.3.6 Dynamic Light Scattering

Dynamic light scattering measurements were performed on a Malvern Zeta Sizer Nano Series Nano-ZS instrument using Dispersion Technology Software (DTS) version 4.20 at a wavelength of 633 nm using a 4.0 mW, solid state He-Ne laser at a scattering angle of 173˚. The experiments were performed at a temperature of 25 ˚C. Polymer samples were prepared at 1 mg/mL and allowed to dissolve in the appropriate solvent overnight. Samples were syringed through 0.45 μm PTFE syringe filters directly into clean cuvettes. Data were observed for the presence or absence of aggregation peaks based on particle diameter size.

8.4 Results and Discussion

The syntheses of 6,12-ionenes were performed with commercially available monomers. N,N,N',N'-tetramethyl-1,12-dodecanediamine was synthesized according to a modified literature procedure from dimethyl amine and α,ω-dibromododecane.[21] The synthesis of aliphatic ammonium ionenes was performed via the Menshutkin reaction between the appropriate dihalide and di-tertiary amine in a methanolic solution under reflux for 24 h. Reaction progress was analyzed via *in situ* FTIR spectroscopy and growth of the C-$N^{\oplus}$ stretch at 920 cm^{-1} was observed as shown. The polymerization was complete after 20 h, based on the lack of further increase in the C-$N^{\oplus}$ stretch (Figure 2).[22] Our research group has shown *in situ* FTIR spectroscopy as a useful technique to monitor reaction progress and determine reaction kinetics.[23,24,] Upon removal of methanol, the resulting polymers formed colorless, transparent, and ductile films.

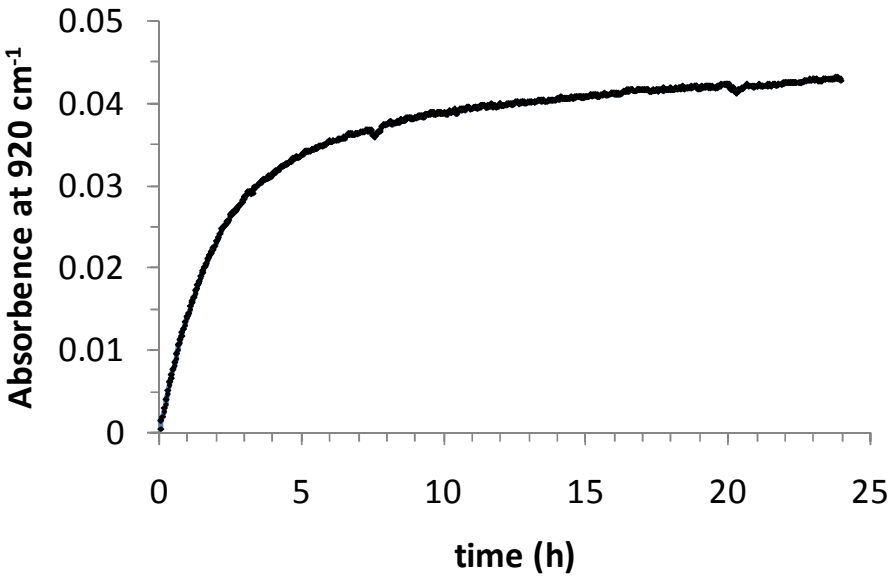

Figure 8.2. *In situ* FITR analysis of an ammonium 6,12-ionene polymerization. *In situ* absorbance at 920 cm^{-1} as function of reaction time.

The structures of ammonium 6,12- and 12,12-ionenes were confirmed via ^{1}H NMR spectroscopy. Both ionene structures exhibited similar chemical shifts, differing only in their relative peak integrations. A singlet at δ3.05 ppm corresponded to the methyl groups bonded to quaternized nitrogen atoms (CH_3-$N^{\oplus}$). A broad resonance centered at δ3.31 ppm corresponded to the methylene directly bonded to quaternized nitrogen atoms (-CH_2-$N^{\oplus}$). The methylene units beta to the quaternized nitrogen atoms had a broad resonance centered at δ1.75 ppm (-$CH_2CH_2N^{\oplus}$). A broad resonance centered at δ1.31 ppm corresponded to the methylene spacer units three or more units away from the quaternized nitrogen atoms (-CH_2-CH_2-).

Successful SEC of polyelectrolytes requires the elimination of polymer-polymer and polymer-stationary phase interactions. It is widely recognized that electrostatic

interactions between polymer chains or between the polymer and the stationary phase are effectively eliminated with an increase in ionic strength of the mobile phase.[25] Thus, sodium acetate was used in these studies; however, as the ionic strength of the solvent increased, it was presumed that hydrophobic interactions become more prevalent; thus, in order to overcome both polymer-polymer and polymer-stationary phase hydrophobic interactions, methanol was added to the mobile phase and glacial acetic acid was also determined to improve SEC separations. The acetic acid likely functioned as both an organic modifier to eliminate hydrophobic interactions, as well as, a proton donor to increase the ionic strength of the solvent. An increase in the ionic strength of the solvent is known to shield electrostatic interactions, due to the reduction in the Debye screening length.[25] As this occurs, the persistence length of the polymer decreases resulting in a more random coil-like conformation of the polymer chain, similar to neutral polymers.[26] Random coils are the preferred conformation for reliable SEC since chain-extended conformations fail to sample the available pore volume resulting in non-Gaussian distributions.[14] Decreasing the Debye screening length also helps to eliminate electrostatic interaction between the polyelectrolyte and the stationary phase, which can delay the elution of polyelectrolytes leading to tailing in chromatograms.[27] Charge screening also functions to eliminate ion-exclusion effects, which prevent polyelectrolyte chains from sampling smaller pore sizes leading to premature sample elution. The ionic strength that is necessary for reducing these effects depends on the chemo-physical properties of a given polymer/solvent/column system.

Ionic aggregation is generally considered detrimental to successful SEC since larger aggregates may impede instrumentation flow, elute prematurely, and/or skew

measurements of the molecular weight distribution.[27] In order to determine if the ionenes were aggregating in solution, DLS was first performed in a variety of potential mobile phase compositions. Ammonium 12,12-ionene samples that were dissolved in the mobile phase (54/23/23 v/v/v % water/methanol/glacial acetic acid, 0.54 *M* NaOAc, pH 4.0) showed insignificant aggregation behavior (Figure 8.3), and this observation suggested that the polymer-solvent composition fulfilled one of the requirements necessary for reliable SEC. Other solvent compositions consisting of lower amounts of organic co-solvent, lower sodium acetate concentrations, and/or higher pH exhibited notable aggregation; thus, these compositions were eliminated as mobile phases for the SEC of aliphatic ammonium ionenes. As shown in Figure 8.4, a decrease in the amount of methanol and glacial acetic, from 23 to 17 vol. %, resulted in bimodal DLS curves. Also, completely eliminating glacial acetic acid from the mobile phase composition promoted polymer aggregation (Figure 8.5). These mobile phase compositions were not pursued as possible mobile phases for the SEC of ammonium ionenes since they encouraged aggregation.

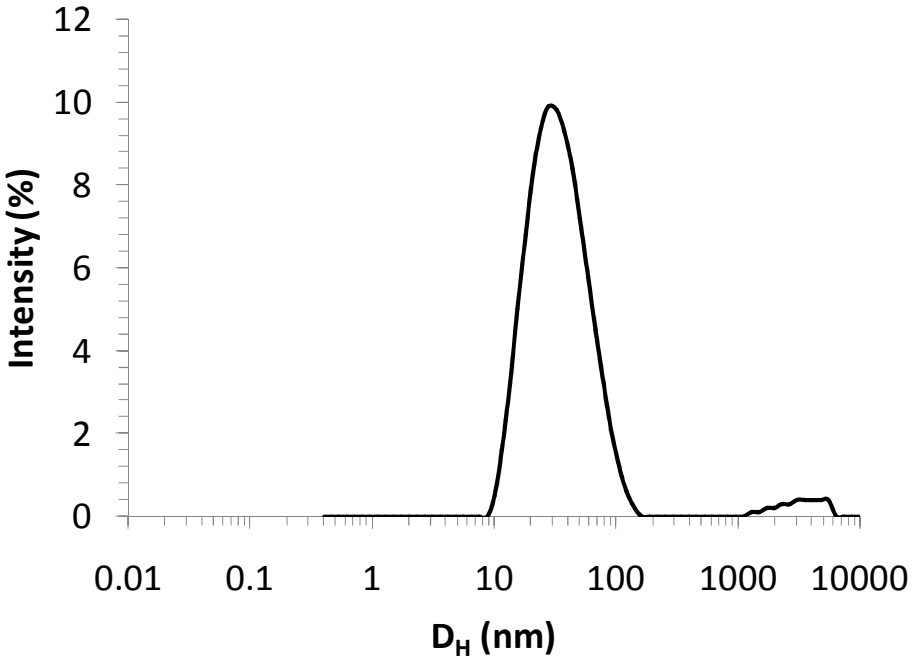

Figure 8.3**.** DLS analysis of ammonium 12,12-ionene (sample 6) in 54/23/23 (v/v/v%) water/methanol/glacial acetic acid, 0.54 M NaOAc, pH 4.0.

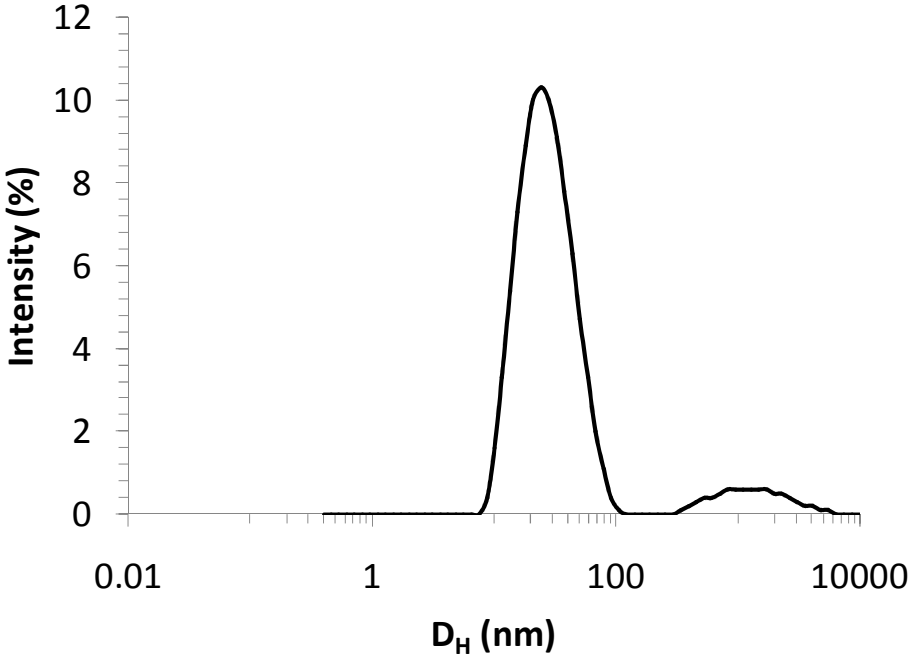

Figure 8.4. DLS analysis of ammonium 12,12-ionene (sample 6) in 66/17/17 water/methanol/acetic acid (v/v/v %), 0.42 M NaOAc, and pH 4.0.

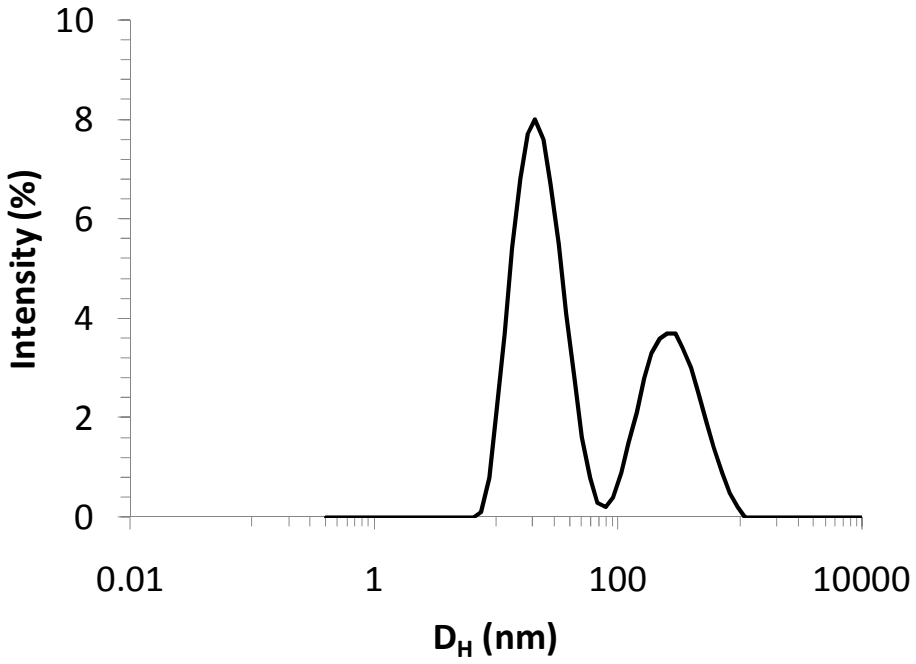

Figure 8.5. DLS analysis of ammonium 12,12-ionene (sample 6) in 80/20 water/methanol (v/v/v %), 0.50 M NaOAc, at pH 8.49.

The specific refractive index increment (*dn/dc*) corresponds to the dependence of the solution's refractive index on solute concentration.[14] The *dn/dc* of a polymer depends on the chemical composition of solute, solvent used to dissolve the solute, and wavelength of the incident laser.[28] The *dn/dc* of a polymer is usually considered as a constant in a given solvent; however, the contribution of end-groups becomes significant at lower molecular weights leading to dissimilar chemical compositions.[29] In the SEC-MALLS analysis of neutral polymers, *dn/dc* values are readily calculated online using 100% mass recovery methods. However, counter-ion dissociation and non-quantitative

sample recovery prevent online determination for SEC analysis of polyelectrolytes. Therefore, individual offline batch-mode measurements must be performed to determine accurate *dn/dc* values. In this study, an offline determination was performed on the ammonium ionenes to obtain accurate *dn/dc* values. Various polymer concentrations were prepared ranging from 0.076 mg/mL to 1.512 mg/mL. Differential refractive index data were obtained for each solution and plotted versus concentration using the Wyatt Astra V software package. The slope of the linear fit is the *dn/dc* of the polymer for this particular solvent. A typical *dn/dc* plot for an ammonium 12,12-ionene (sample 5) in the mobile phase, 54/23/23 (v/v/v%) water/methanol/glacial acetic acid, 0.54 *M* NaOAc, pH 4.0, is shown in Figure 8.6. In this study, all molecular weights of each ionene analyzed had similar *dn/dc* values within experimental error. The *dn/dc* values for ammonium 12,12- and 6,12-ionenes in this mobile phase are shown in Table 1.

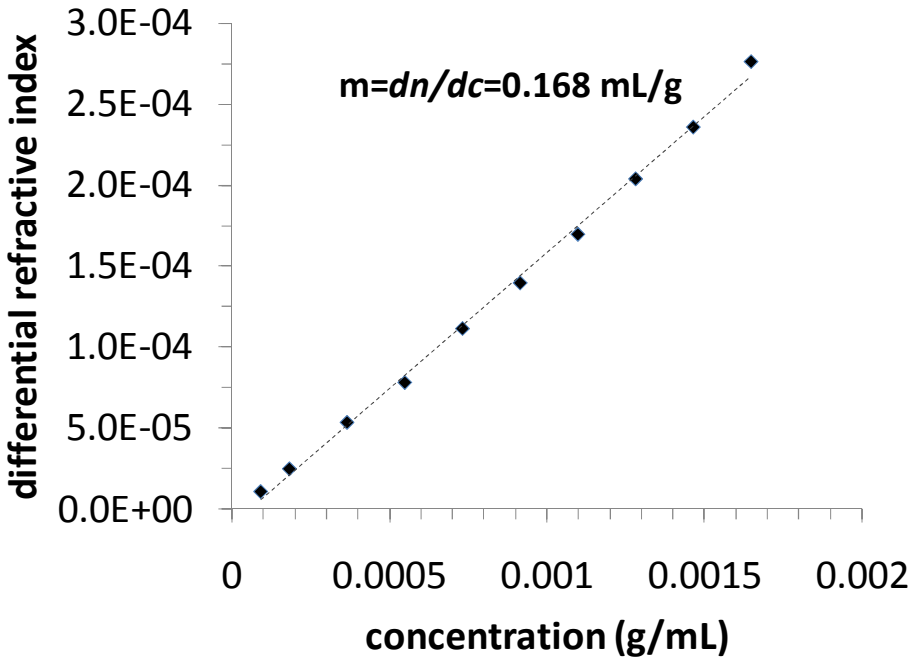

Figure 8.6. Typical dn/dc plot for an ammonium 12,12-ionene in 54/23/23 (v/v/v %) water/methanol/glacial acetic acid, 0.54 M NaOAc, pH 4.0. The dn/dc was determined to be 0.168 mL/g in this example.

Table 8.1 The *dn/dc* values for aliphatic ammonium ionenes.

	[a]*dn/dc* (mL/g)
Ammonium 12,12-ionene (sample 5)	0.168
Ammonium 6,12-ionene (sample 8)	0.154

[a] Each *dn/dc* was measured using 11 concentrations varying from 0.076 – 1.55 mg/mL in the mobile phase, 54/23/23 (v/v/v%) water/methanol/glacial acetic acid, 0.54 *M* NaOAc, pH 4.0.

Absolute moments of the molecular weight distribution were determined for ammonium 6,12- and 12,12-ionenes using 54/23/23 (v/v/v%) water/methanol/glacial acetic acid, 0.54 *M* NaOAc, pH 4.0 and are summarized in Table 2. Ammonium 12,12-ionene prepared from various dihalide:diamine monomer stoichiometries had number average molecular weights between 8,000 and 30,700 g/mol and weight average molecular weights between 11,000 and 40,000 g/mol. Ammonium 6,12-ionene prepared from various dihalide:diamine molar ratios had number average molecular weights between 14,000 and 41,500 g/mol and weight average molecular weights between 19,000 and 49,900 g/mol. As expected for a step-growth polymerization, molecular weights for ammonium ionenes increased as the molar ratios of the two difunctional monomers approached 1:1.

Table 8.2 Molecular weight characterization for aliphatic ammonium ionenes.

Sample	Ammonium x,y-Ionene	Monomer Stoichiometry (diamine:dihalide)	[a]M_n (g/mol)	[a]M_w (g/mol)	[a]M_w/M_n	[b]M_w/M_n
1	12,12	1:1.10[i]	3,500	4,300	1.26	2.11
2	12,12	1:1.07[i]	9,700	12,300	1.27	2.50
3	12,12	1:1.05[i]	11,600	14,600	1.26	2.45
4	12,12	1:1.03[i]	14,000	17,800	1.27	2.36
5	12,12	1:1[i]	18,700	24,900	1.33	2.15
6	12,12	1:1[ii]	20,600	26,000	1.26	2.03
7	12,12	1:1[iii]	30,700	39,600	1.29	2.28
8	6,12	1:1[ii]	10,700	14,300	1.34	2.15
9	6,12	1:1[iii]	30,500	43,300	1.42	1.74

[a]Molecular weights determined via SEC-MALLS in 54/23/23 (v/v/v%) water/methanol/glacial acetic acid, 0.54 *M* NaOAc, pH 4.0.
[b]Molecular weight distributions determined using poly(ethylene oxide) equivalent molecular weights.
[i]Ionene synthesis performed at 20 wt% solids, [ii]30 wt% solids, and [iii]50 wt% solids.

The SEC chromatogram for a typical ammonium 12,12-ionene in the mobile phase (54/23/23 (v/v/v %) water/methanol/glacial acetic acid, 0.54 *M* NaOAc, pH 4.0) including the dRI trace, MALLS trace, and molecular weight as a function of the molecular weight distribution is shown in Figure 8.7. The mono-modal, symmetrical peak in the MALLS and dRI chromatograms demonstrated reliable sample separation and provided additional support for the absence of polymer aggregation in solution. Thus, in addition to fulfilling the non-aggregating requirement, this mobile phase successfully reduced polymer-stationary phase interactions, which indicated that the ionic strength of the tested mobile phase was sufficient to discourage any electrostatic interactions that would otherwise lead to ion interaction or ion exclusion effects. When the organic content of the solvent was decreased, poor SEC separation was observed. In the case of the 12,12-ionene, decreasing the relative amount of methanol and glacial acetic acid, both from 23 to 17 vol %, resulted in bimodality and tailing in the SEC chromatograms (Figure 8.8). Similar to the 12,12-ionene, SEC-MALLS of the ammonium 6,12-ionene in

the same mobile phase also showed mono-modal peaks (Figure 8.9). However, unlike the 12,12-ionene, the asymmetric 6,12-ionene also showed mono-modal peaks in the mobile phase, 66/17/17 (v/v/v%) water/MeOH/AcOH, 0.42 *M* NaOAc, pH 4.0 solvent composition (Figure 8.10). Although this mobile phase works well for the ammonium 6,12-ionene, the mobile phase**,** 54/23/23 (v/v/v %) water/methanol/glacial acetic acid, 0.54 *M* NaOAc, pH 4.0, is more versatile since it provides reliable separations for both of the ionenes tested.

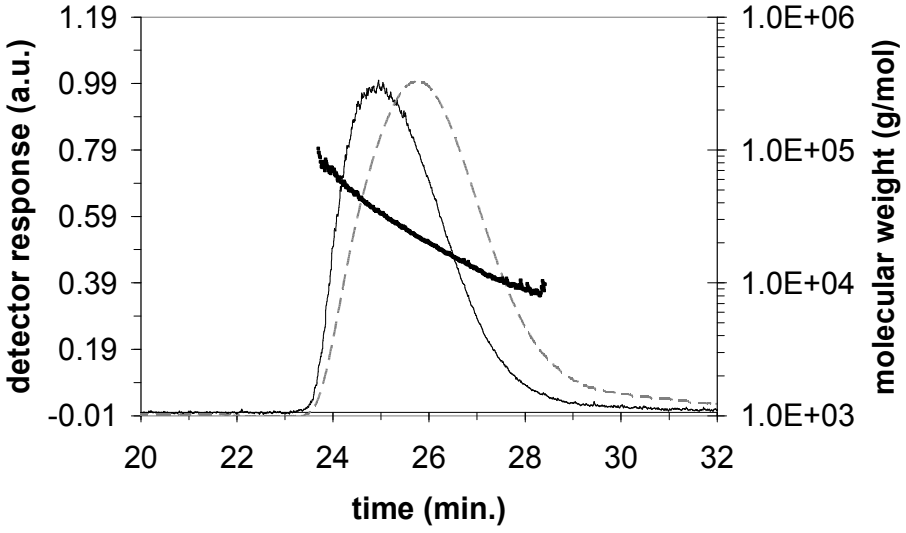

Figure 8.7. SEC chromatogram of ammonium 12,12-ionene (sample 5) showing the RI trace (dotted gray), MALLS trace (solid black), and molecular weight (bold black line) in 54/23/23 (v/v/v %) water/methanol/glacial acetic acid, 0.54 M NaOAc, pH 4.0.

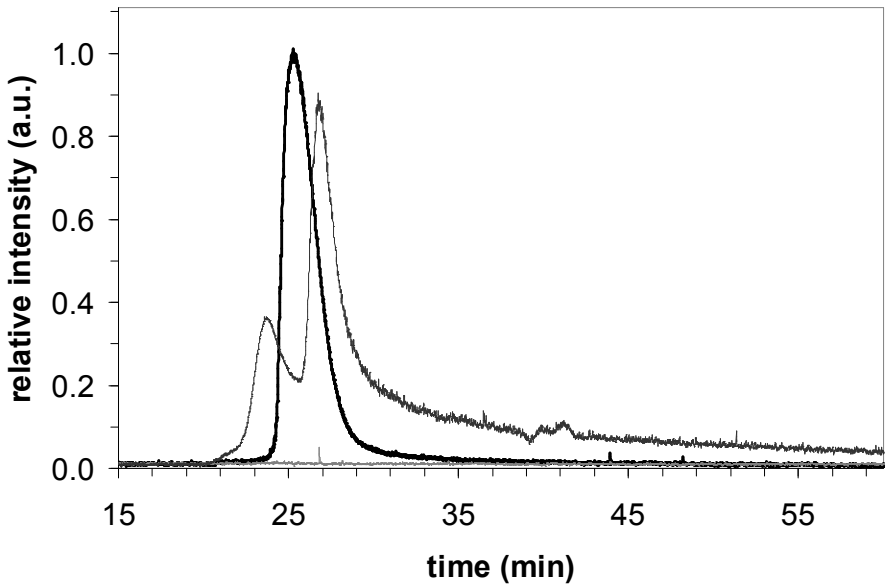

Figure 8.8. SEC chromatogram of ammonium 12,12-ionene (sample 6) showing the influence of the water/organic solvent ratio and NaOAc molarity on SEC separation. The three ratios were 74/8/18 water/methanol/acetic acid (v/v/v%), 0.57 *M* NaOAc, pH 4.0(light gray), 66/17/17 water/methanol/acetic acid (v/v/v%), 0.42 *M* NaOAc, pH 4.0 (dark gray), and 54/23/23 (v/v/v %) water/methanol/glacial acetic acid, 0.54 *M* NaOAc, pH 4.0 (bold black).

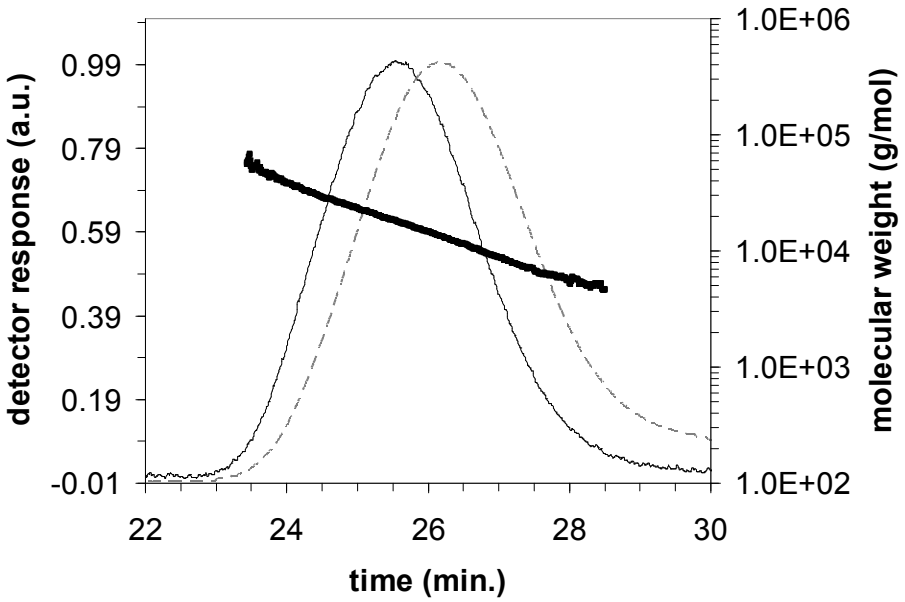

Figure 8.9. SEC chromatogram of ammonium 6,12-ionene (sample 8) showing the RI trace (dotted gray), MALLS trace (solid black), and molecular weight (bold black line) in the mobile phase (54/23/23 (v/v/v %) water/methanol/glacial acetic acid, 0.54 *M* NaOAc, pH 4.0).

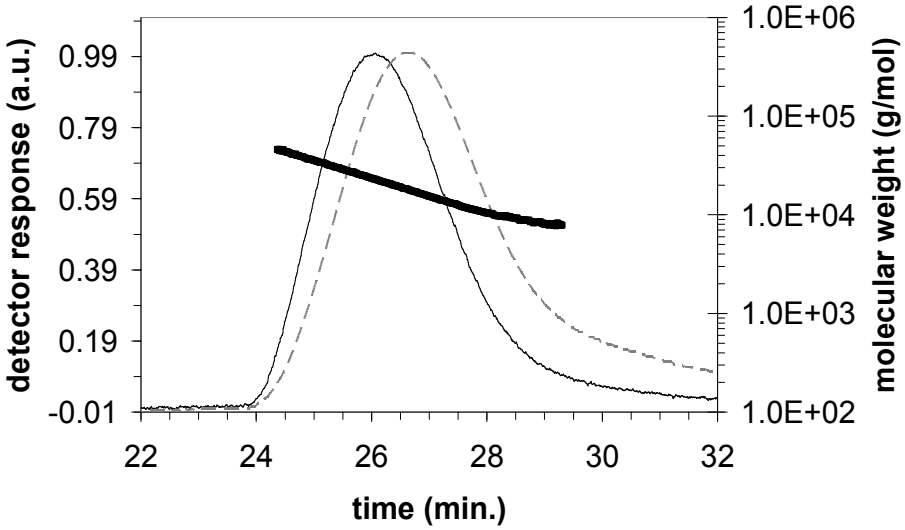

Figure 8.10. SEC chromatogram of ammonium 6,12-ionene (sample 8) showing the RI trace (dotted gray), MALLS trace (solid black), and molecular weight (bold black line) in 66/17/17 water/MeOH/AcOH (v/v/v %), 0.42 M NaOAc, pH 4.0.

Curiously, SEC-MALLS-obtained molecular weight distributions for all ammonium ionene polymers ranged from 1.26 to 1.42. The expected molecular weight distribution for conventional step-growth polymerization to form linear products is approximately 2.0 at high monomer conversion; however, the molecular weight distributions for ammonium ionenes were unexpectedly low. It is important to note that only the SEC-MALLS molecular weight distributions were low. We also calculated molecular weight distributions using poly(ethylene oxide)-equivalent molecular weights from dRI measurements and observed more reasonable values ranging from 1.74 to 2.50 (Table 2). Molecular weight distributions less than 2.0 in step-growth polymerizations can occur because of fractionation in the purification process or sample exclusion within the chromatography columns.[14] We excluded the possibility of fractionation since we solution-cast ionenes directly from the reaction mixture. Furthermore, samples were analyzed a second time using columns with a higher resolution (PL aquagel-OH 30 and PL aquagel-OH 40 measuring 7.5 x 300 mm), and we eliminated the possibility of excluding sample volume from the column pores.

Another explanation for step-growth polymerization leading to narrow molecular weight distributions is different reactivities of monomers relative to polymer chains.[30] Nanda demonstrated that distributions less than 2.0 were observed if reactivity decreased with increasing molecular weight.[31] It is plausible that the rate of addition of neutral

monomer to a charged species differs from reaction of two charged species. In addition, aggregation in solution of charged polymers may result in shielding of reactive chain ends. We measured the molecular weights of aliquots obtained during a 24 h polymerization of an ammonium 6,12-ionene and demonstrated that molecular weight increases throughout the polymerization process (Figure 8.11) and we are currently studying the reaction kinetics to determine if reactivity of monomers is greater than polymer chains. Wegner has studied the reaction kinetics of aliphatic ammonium ionenes with *in situ* NMR spectroscopy and demonstrated that monomer reactivity varied depending on the stage of polymerization.[32] For these reasons, reaction kinetics may be one explanation for narrow molecular weight distributions. On the other hand, although we have demonstrated that our mobile phase composition allows for reliable separations of aliphatic ammonium ionenes to achieve appropriate magnitudes of the weight-average molecular weight, this mobile phase may not perfectly separate these polyelectrolyte samples. If any adsorption is occurring between our polymer and the packing material of the SEC columns, imperfect separation will lead to an overestimate of the number-average molecular weight.[14,33] Thus, polydispersity of the sample will be underestimated. To investigate the possibly of sample adsorption, we injected an ammonium 12,12-ionene sample multiple times to evaluate the reproducibility of our SEC separations. As shown in Figure 8.12, the dRI chromatograms do not superimpose perfectly, likely due to slight sample adsorption resulting from hydrophobic interactions between the polymer and the column stationary phase. However, the deviations in retention time associated with adsorption are much smaller when compared to differences in retention times between

samples of different molecular weight. Also in Figure 8.12, the dRI chromatograms do not quite return to baseline, indicative of some sample adsorption.

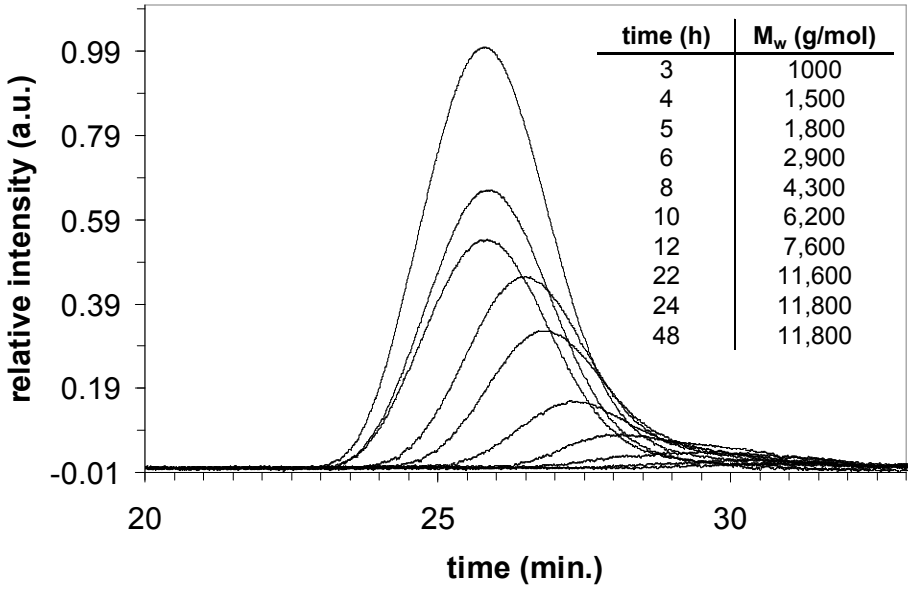

Figure 8.11. SEC chromatograms (MALLS traces) of aliquots sampled during a 24 h polymerization of ammonium 6,12-ionene showing molecular weight increased during the reaction. Inset table show weight-average molecular weight as a function of reaction time.

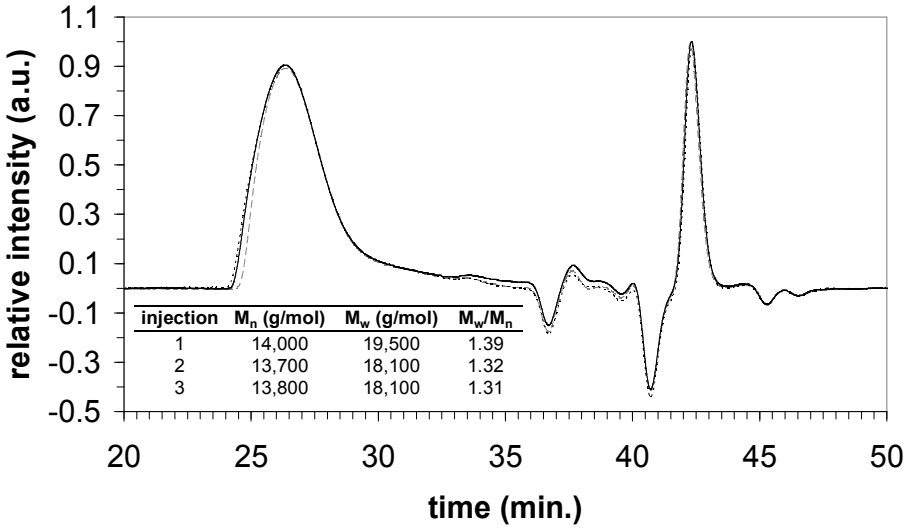

(a)

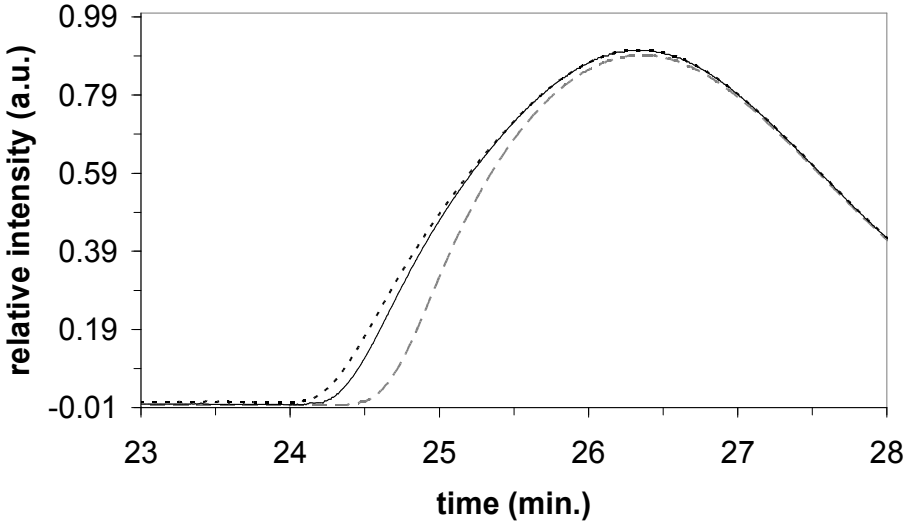

(b)

Figure 8.12. (a) Overlaid SEC chromatograms (dRI traces) of an ammonium 12,12-ionene injected three times in the mobile phase (54/23/23 (v/v/v %) water/methanol/glacial acetic acid, 0.54 *M* NaOAc, pH 4.0). Inset table shows SEC-MALLS caclulated molecular weights of each injection. (b) Zoomed-in portion of the chromatograms.

The solvent compositions that were employed in previous SEC-dRI investigations of ammonium ionenes were evaluated using our instrumentation.[19,20] In two prior studies, one mobile phase consisted of 0.020 *M* NaOAc in water with acetic acid added to adjust the pH to 5.2, and a second mobile phase comprised 20/80 acetonitrile/0.5 *M* sodium sulfate, 0.5 *M* acetic acid in water. However, peaks corresponding to polymer were not observed in either the RI or MALLS chromatograms in either of these solvents.

Utilizing an online viscosity detector, the intrinsic viscosity was determined across the molecular weight distribution. When plotted as the logarithm of intrinsic viscosity as a function of the logarithm of molecular weight, a linear fit yields constants for the well known Mark-Houwink-Sakurada (MHS) relationship, which is given as

$$\log[\eta] = \alpha \log M - \log k \qquad (3)$$

where $[\eta]$ is the intrinsic viscosity, and α and k are constants, which depend on the polymer and solvent used at a given temperature.[34] The MHS alpha parameter provides information about the solvent quality and/or chain stiffness for a polymer in solution. Typically, alpha values near 0.50 indicate theta solvent conditions whereas values near 0.80 indicate good solvent conditions.[30] Data obtained for both the 12,12- and 6,12-ionenes fit well to the linear MHS relationship. As shown in Figure 8.13, the MHS plot for the ammonium 12,12-ionene (sample **5**) in the mobile phase (54/23/23 (v/v/v %) water/methanol/glacial acetic acid, 0.54 *M* NaOAc, pH 4.0) at 30 ^{o}C yielded an alpha parameter of 0.63 and a k value of 5.3×10^{-4} dL/g. As shown in Figure 8.14, the MHS plots for the ammonium 6,12-ionene (sample **8**) in the same mobile phase at 30 ^{o}C yielded an alpha value of 0.75 and a k value of 1.6×10^{-4} dL/g. The higher alpha

parameter of 0.75 for the 6,12-ionene suggested that either the mobile phase was a better solvent for this sample compared to the 12,12-ionene and/or the 6,12-ionene has a stiffer chain conformation in the same solvent. The higher charge density of the 6,12-ionenes may lead to a greater polyelectrolyte effect which could be a possible explanation for any observed chain stiffness.

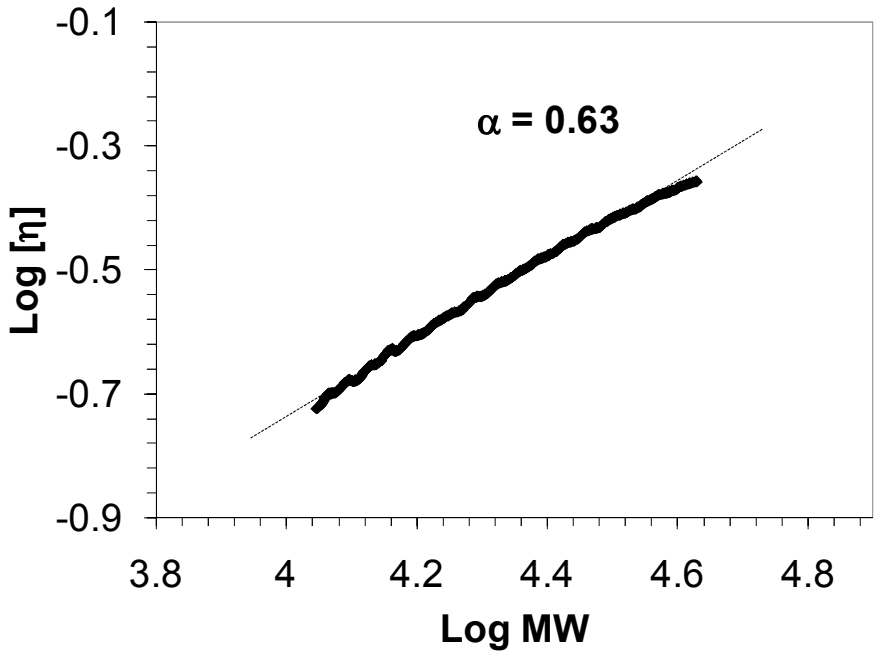

Figure 8.13. MHS plot for the ammonium 12,12-ionene (sample 5) in the mobile phase, 54/23/23 (v/v/v%) water/methanol/glacial acetic acid, 0.54 *M* NaOAc, pH 4.0. Measured intrinsic viscosities (black diamonds) were fitted with the logarithmic MHS relationship (dotted line).

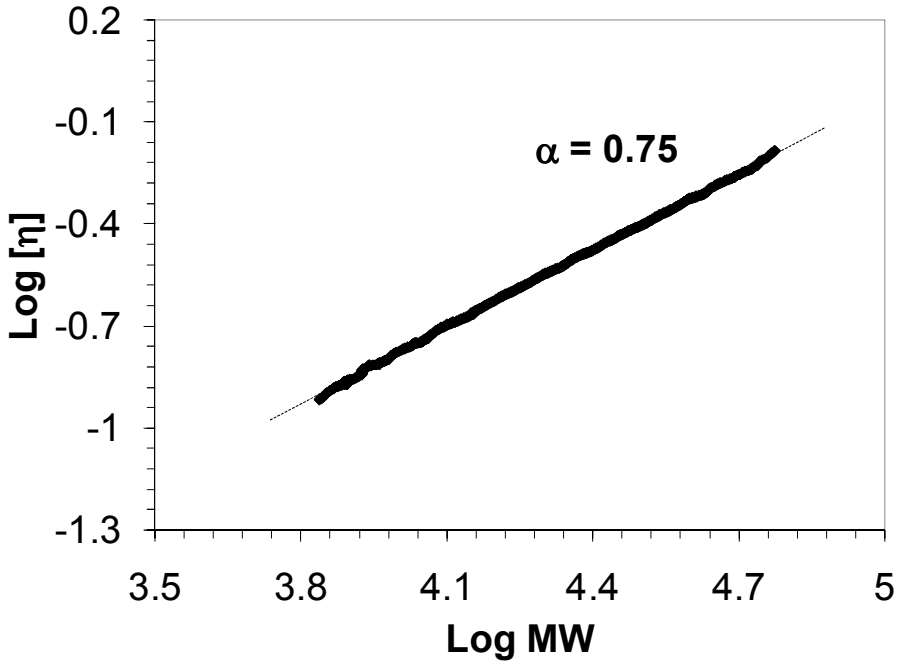

Figure 8.14. MHS plot for the ammonium 6,12-ionene (sample 8) in the mobile phase, 54/23/23 (v/v/v%) water/methanol/glacial acetic acid, 0.54 *M* NaOAc, pH 4.0. Measured intrinsic viscosities (black diamonds) were fitted with the logarithmic MHS relationship (dotted line).

8.5 Conclusions

Absolute molecular weight characterization of aliphatic ammonium ionenes was successfully accomplished using aqueous-based SEC-MALLS. A suitable mobile phase composition of 54/23/23 (v/v/v%) water/methanol/acetic acid and 0.54 *M* NaOAc at pH 4.0 was developed to reduce polymer-polymer and polymer-stationary phase interactions. Using this mobile phase composition, reasonable separations were obtained and accurate

measurements of the weight-average molecular weight were achieved. Ammonium 6,12-ionene had number-average molecular weights ranging from 14,000 – 41,500 g/mol and weight-average molecular weights ranging from 19,000 g/mol – 49,900 g/mol with molecular weight distributions ranging from 1.31 – 1.42. Ammonium 12,12-ionene had number-average molecular weights ranging from 8,000 – 30,700 g/mol and weight-average molecular weights ranging from 11,000 – 40,000 g/mol with molecular weight distributions ranging from 1.26 – 1.42. Additionally, intrinsic viscosity data was collected for ammonium 12,12- and 6,12-ionens as a function of molecular weight distribution to determine MHS parameters.

The apparently low molecular weight distributions are currently being studied in our laboratories. We have eliminated the possibilities of fractionation during purification and pore volume exclusion in the column, and thus, have concluded that either the reaction mechanism is producing molecular weight distributions lower than 2.0 or, more likely, imperfect SEC separation is leading to an underestimation of the molecular weight distribution. Ongoing work correlating MALDI-TOF measurements to SEC-MALLS data will be reported in the future.

8.6 Acknowledgments

Research was sponsored by the Army Research Laboratory and was accomplished under Cooperative Agreement Number W911NF-06-2-0014. The views and conclusions contained in this document are those of the authors and should not be interpreted as

representing the official policies, either expressed or implied, of the Army Research Laboratory or the U.S. Government. The U.S. Government is authorized to reproduce and distribute reprints for Government purposes notwithstanding any copyright notation heron. Additionally, the authors acknowledge the generous support of Kimberly-Clark Corporation for funding, and insightful discussions with Thomas Mourey at Kodak.

8.7 References

[1]Gibbs, C.F.; Littman, E.R.; Marvel, C.S. *J. Am. Chem. Soc.* **1933**, 55, 753-757.

[2]Lehman, M.R.; Thompson, C.D.; Marvel, C.S. *J. Am. Chem. Soc.* **1935**, 57, 1137-1139.

[3] Gibbs, C.F.; Marvel, C.S. *J. Am. Chem. Soc.* **1934**, 56, 725-727.

[4] Gibbs, C.F.; Marvel, C.S. *J. Am. Chem. Soc.* **1935**, 57, 1137-1139.

[5] Noguchi, H.; Rembaum, A. *Macromolecules* **1972**, 5 (3), 253-260.

[6] Noguchi, H.; Rembaum, A. *Macromolecules* **1972**, 5 (3), 261-269.

[7] Punyani, S., Singh, H. *J. Appl. Polym. Sci.* **2006**, 102, 1038-1044.

[8] Kourai, H.; Yabuhara, T.; Shirai, A.; Maeda, T.; Nagamune, H. *Eur. J. Medicinal Chem.* **2006**, 41, 437-444.

[9] Zelinkin, A. N.; Putnam, D.; Shastri, P.; Langer, R.; Izumrudov, V. A. *Bioconjugate Chem.* **2002***,* 13, 548-553.

[10] Rembaum, A. U.S. Patent 4,013,507, **1977**

[11] Narita, T.; Ohtakeyama, R.; Nishino, M.; Gong, J.P.; Osada, Y. *Colloid Polym. Sci.* **2000**, 278, 884-887.

[12]Lehman, M.R.; Thompson, C.D.; Marvel, C.S. *J. Am. Chem. Soc.* **1935**, 57, 1137-1139.

[13] Casson, D.; Rembaum, A. *Macromolecules* **1971**, 5 (1), 75-81.

[14] *Handbook of Size Exclusion Chromatography,* Wu, C.; Chromatographic Science Series; Marcel Dekker: New York, NY, **1995**, Vol. 69.

[15] Garcia, R.; Porcar, I.; Campos, A.; Soria, V.; Figueruelo, J. E. *J. Chromatogr. A* **1993***, 655* (2), 191-198.

[16] Barth, H. G.; Boyes, B. E.; Jackson, C. *Anal. Chem*., **1996***,* 68(12)*,* 445R-466R.

[17] Wittgren, B.; Welinder, A.; Porsch B. *J. Chromatogr. A* **2003**, 1002:101Y109.

[18] Jiang, X.; van der Horst, A.; van Steenbergen, M.J.; Akeroyd, N.; van Nostrum, C.F.; Schoenmakers, P.J.; Hennink, W.E. *Pharmaceutical Research* **2006**, 23(3), 595-603.

[19] Kopecká, K.; Tesařová, E.; Pirogov, A.; Gaš, B. *J. Sep. Sci*., **2002**, *25*, 1027-1034.

[20] Reisinger, T., Meyer, W.H., Wegner, G., Haase, T., Schultes, K., Wolf, B.A. *Acta Polym*., **1998**, *49*, 710-714.

[21]Spencer, T.A.; Onofrey, T.J.; Reginald, O.; Russel, S.J.; Lee, L.E.; Blanchard, D.E.; Castro, A.; Gu, P.; Jiang, G.; Shechter, I. *J. Org. Chem*. **1999**, 64 (3), 818.

[22] Colthup, N. B.; Daly, L. H.; Wiberley, S. E. *Introduction to Infrared and Raman Spectroscopy*, 3rd Ed.; Academic Press: New York, NY, **1975**, 344.

[23] Lizotte, J.; Long, T. E. *Macromol. Chem. Phys*. **2004**, 205, 692-698.

[24] Pasquale, A. J.; Allen, R. D.; Long, T. E. *Macromolecules* **2001**, 34, 8064-8071.

[25] Garcia, R.; Porcar, I.; Campos, A.; Soria, V.; Figueruelo, J. E. *J. Chromatogr. A* **1994**, 662, 61-69.

[26]Dobrynin, A.V. *Macromolecules* **2005,** 38*,* 9304-9314

[27]Barth, H. *Advances in Chemistry Series*, **1986**, 213, 31-55.

[28] Coto, B.; Escola, J. M.; Suarez, I.; Caballero, M. J. *Polymer Testing* **2007**, 26, 568-575.

[29] Grinshpun, V.; Rudin, A. *J. Appl. Polym. Sci*. **1986**, 32, 4303-4311.

[30] Gupta, S. K.; Kumar, A.; Bhargava, A. *Polymer* **1979***,* 20, 305-310.

[31] Nanda, V. S.; Jain, S. C. *Journal of Chemical Physics,* **1968***, 49*(3), 1318-1320.

[32] Wang, J.; Meyer, W. H.; Wegner, G. *Macromol. Chem. and Phys.* **1994***, 195*, 1777-1795.

[33] Balke, S.T.; Mourey, T.H. *J. Appl. Polym. Sci.* **2001**, 81, 370-383.

[34] Polymer Handbook, 4th Ed.; Brandrup, J.; Immergut, E. H.; Wiley-Interscience: New York, NY, **1989**.

Chapter 9. **Transfection Performance of Ammonium 12,12- and 12,6-Ionenes: Influence of Charge Density on DNA delivery *in vitro***

John M. Layman, Erika M. Borgerding, and Timothy E. Long

9.1 Abstract

Cationic polyelectrolytes are emerging as synthetic replacements to viral vectors in gene therapy. However, cytotoxicity and poor gene delivery efficiency have prevented wide-spread application. Additionally, the fundamental polymer structure-property-performance relationships are uncertain. In this work, the influence of charge density on transfection efficiency was evaluated using aliphatic ammonium ionenes. Step-growth polymerization methods were used to synthesize ammonium 12,6- and 12,12-ionenes, which produced polycations with two different charge densities. A luciferase expression assay was used to evaluate transfection efficiency in Cos-7 cells. The results revealed that the ammonium 12,6-ionen (higher charge density) was a slightly better gene delivery agent. However, both 12,6- and 12,12-ionenes were found to have decreasing transfection efficiencies as a function of increasing nitrogen to phosphorous (N/P) ratios. This observation was attributed to the toxicity of the ionenes.

Keywords: ammonium ionenes, gene therapy, plasmid DNA, charge density, Cos-7 cells

9.2 Introduction

Non-viral gene therapy has attracted attention as a therapeutic strategy to combat a variety of human disease and disorders. In gene therapy, nucleic acids are transferred through the cellular membrane and express a therapeutic level of a defective or deficient protein and/or down-regulate the expression of deleterious proteins.[1] Delivery agents, or vectors, are needed due to the polyanionic nature of nucleic acids which interacts unfavorably with the slightly negatively charged cellular membrane. Historically, a wide-variety of deactivated viruses have been used since these carriers provide the highest delivery efficiencies.[2, 3] However, despite being rendered replication deficient, viral vectors often provoke severe immune response in the host, tragically leading to fatalities in some pre-clinical gene therapy trials.[4] Non-viral agents, such as cationic polyelectrolytes, offer a synthetic alternative to viral vectors due to the reduction of immunogenic risk and the ability to tailor their macromolecular structure.[5-14] However, despite the advantages of non-viral agents, several investigators have shown that transfection efficiencies are considerably lower compared to viral vectors.[15, 16] Therefore, non-viral vectors will not find wide-spread clinical application until transfection efficiencies rival that of viral-based systems.

Cationic polymers spontaneously form nano-sized, electrostatic complexes with anionic nucleic acids, termed polyplexes.[17] Over the past decade, several investigators have employed various elements in the design of cationic polymers to steadily improve transfection efficiencies; this topic was recently comprehensively reviewed by Park et al.[7] and Putnam et al.[6] However, despite the improvements made to date, there are many unanswered questions associated with the fundamental mechanisms that govern non-viral

gene delivery. Our work aimed to elucidate clear structure-transfection relationships in polycation-mediated plasmid DNA delivery.

Ammonium ionenes are ion-containing macromolecules containing quaternary nitrogens in the main chain.[18-20] The ability to easily control charge density and counter anion through monomer selection makes ammonium ionenes an ideal model in the study of well-defined cationic polyelectrolytes. Previously Langer and Izumrudov et al. has reported on the cytotoxicity and transfection efficiency of ammonium 2,4-, 2,8- and 2,10-ionenes.[21] Their study demonstrated that transfection efficiency increased with increasing charge density.[21]

Here, we present our efforts to determine how seemingly small modifications in a polycation's structure influence its performance as DNA transfection agent *in vitro*. To evaluate the role of charge density on transfection, we synthesized a series of aliphatic ammonium 12,12- and 12,6-ionenes were the methylene spacer is varied to control charge placement along the backbone of the polymer, shown schematically in Figure 9.1. A luciferase expression assay was used to compare the relative transfection efficiencies of the two charge densities.

12,6

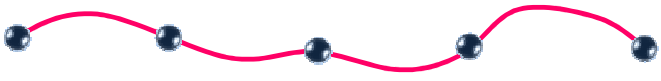

12,12

Figure 9.1. Schematic representation of aliphatic ammonium 12,6- and 12,12-ionenes showing the difference in charge densities. Black dots represent cationically charged quaterized ammonium groups and the red lines represent the aliphatic methylene spacer segments.

9.3 Experimental

9.3.1 General Methods and Materials

HPLC-grade methanol was obtained from Fischer Scientific and distilled from calcium hydride (reagent grade, 95%), which was obtained from Sigma-Aldrich and used as received. 1,12-dibromododecane (98%) was obtained from Sigma-Aldrich, recrystallized from ethanol (AAPER Alcohol and Chemical Co.) and dried under reduced pressure. N,N,N',N'-tetramethyl-1,6-hexanediamine (99%) was obtained from Sigma-Aldrich and distilled from calcium hydride.

^{1}H NMR were recorded on a Varian Inova 400 MHz spectrometer. Chemical shifts are reported in ppm downfield from TMS using the residual protonated solvent as an internal standard (CD_3OD, ^{1}H 4.87 ppm) (D_2O, ^{1}H 4.79 ppm).

Aqueous-based SEC-MALLS was used to determine absolute molecular weights in acetate buffer solutions. The mobile phase consisted of 0.540 *M* sodium acetate in a ternary mixture of 54/23/23 water/methanol/glacial acetic acid v/v/v %. Samples were analyzed at 0.8 mL/min through 2x Waters Ultrahydrogel linear columns and 1x Waters Ultrahydrogel 250 column, with all columns measuring 7.8 x 300 mm and equilibrated to 30 ^{o}C. SEC instrumentation consisted of a Waters 1515 isocratic HPLC pump, Waters 717plus Autosampler, Wyatt miniDAWN multiangle laser light scattering (MALLS)

detector operating a He-Ne laser at a wavelength of 690 nm, Viscotek 270 capillary viscosity detector, and a Waters 2414 differential refractive index detector operating at a wavelength of 880 nm and 35 ^{o}C.

9.3.2 Preparation of Ammonium Ionens.

In a typical synthesis, 1,12-dibromododecane (1.02 g, 3.1 mmol) was transferred into a two-necked, 50-mL round-bottomed flask, which was equipped with a reflux condenser and a mechanical stirrer. Methanol (2.25 g, 70.3 mmol) was added into the flask with a cannula under nitrogen, and the solution was refluxed. N,N,N',N'-tetramethyl-1,6-hexanediamine (0.53 g, 3.1 mmol) was quickly added into the flask, and additional purging with nitrogen was performed. The reaction was mechanically stirred for 24 h under reflux. Upon completion, the methanol was removed under reduced pressure at 25 ˚C to yield the polymer product. ^{1}H NMR (400 MHz, D_2O): δ 3.31 (m, 8 H), 3.05 (s, 12 H), 1.75 (m, 8 H), 1.31 (m, 20 H). M_n 14,000 – 41,500 g/mol, M_w 19,000 – 49,900 g/mol, PDI 1.31-1.36.

The synthesis of N,N,N',N'-tetramethyl-1,12-dodecanediamine was prepared as described previously.[22] The 12,12-ionene was also prepared as described above. ^{1}H NMR (400 MHz, D_2O): δ 3.31 (m, 8 H), 3.05 (s, 12 H), 1.75 (m, 8 H), 1.31 (m, 32 H). M_n 8,000 – 30,700 g/mol, M_w 11,000 – 40,000 g/mol, PDI 1.26 to 1.42.

9.3.3 Cell culture.

African green monkey kidney fibroblast (Cos-7, ATCC) were cultured in DMEM-based medium with 10% fetal bovine serum (Mediatech), 10% NuSerum (Becton Dickinson), 100 U/ml of penicillin, and 100 μg/ml of streptomycin (both reagents from Mediatech). Cultures were incubated at 37 °C in a humid atmosphere of 5% CO_2.

9.3.4 Luciferase Expression Assay

To prepare polyplexes for transfection experiments, pRL-SV40 plasmid (1 μg/μL in H_2O) was diluted in basal DMEM media to a concentration of 0.8 μg/mL and incubated at room temperature for 10 min. At the same time, the appropriate type and amount of ionene was diluted in basal DMEM to the final concentrations corresponding to the various nitrogen/phosphorus (N/P) ratios and allowed to incubate for 10 min at room temperature. Equal volumes of the plasmid and corresponding polymer solutions were combined (final pDNA concentration of 0.4 μg/mL) and incubated for 20-30 min at room temperature to complex the plasmid DNA with ionene polymers. Cos-7 cells were plated at a concentration of $2.0x10^5$ cells/well on 12-well plates 24 h prior to transfection. Each well was treated with 1 mL of transfection solution and then incubated for 12 h at 37 ^oC, 5% CO_2.. After 12 h, the transfection solution was replaced with complete DMEM growth media. The cells were then incubated for 24 h at 37^oC, 5% CO_2 to allow for protein expression. After incubation, the cells were rinsed with approximately 1 mL of PBS and 100 μL of lysis buffer was added. Immediately after adding lysis buffer, each well was scraped and incubated for 30 min at room temperature with gentle mixing. The lysate mixture was then subjected to two -80 ^oC/37 ^oC freeze/thaw cycles. *Renilla* luciferase activity was measured using a *Renilla* luciferase assay kit (Promega) and a Molecular Devices Corp. SPECTRAmax L luminometer according to the assay kit manufacturer's instructions.

9.4 Results and Discussion

Aliphatic ammonium ionenes were prepared via the Menshutkin reaction of the appropriate di-tertiary amine and dihaloalkane to achieve the desired methylene spacing between cationic ammonium groups, shown in Scheme 9.1. Previous work in our group reported the synthesis and aqueous size exclusion chromatography of aliphatic ammonium ionenes.[22] Proper characterization is critical to accurately determining fundamental structure-property correlations.

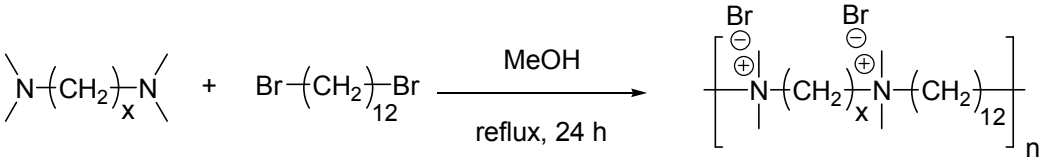

Scheme 9.1. Synthesis of aliphatic ammonium x,12-ionenes.

Figure 9.2 shows luciferase expression as a function of 12,6-ionene molecular weight and N/P ratio. All molecular weights were found to have transfection efficiencies significantly lower than Lipofectamine® (a commercially available transfection reagent). Even though ammonium ionenes display relative low transfection efficiencies, they still serve as a good model system since charge density can be easily controlled by selecting the appropriate monomers. As shown in the figure, a significant influence from molecular weight was not observed. However, it is important to note that the molecular weights only ranged from M_w=13,200 to 43,000 g/mol. Previous work in our laboratories (publication forthcoming) has shown that transfection efficiencies are only sensitive to large changes in molecular weight (M_w=40,000 to 915,000 g/mol in that work). The data also revealed that transfection decreased as a function of N/P ratio. Typically, the reverse

trend is observed with luciferase expression increasing as a function of N/P ratio. We attributed this decrease in transfection efficiency with the toxicity of ionenes. Rembaum et al. has shown that ionene-based polymers are significantly more toxic than other polycations.[23] However, cytotoxicity screening of the specific ionenes synthesized in this study is needed to determine to make this correlation with certainty.

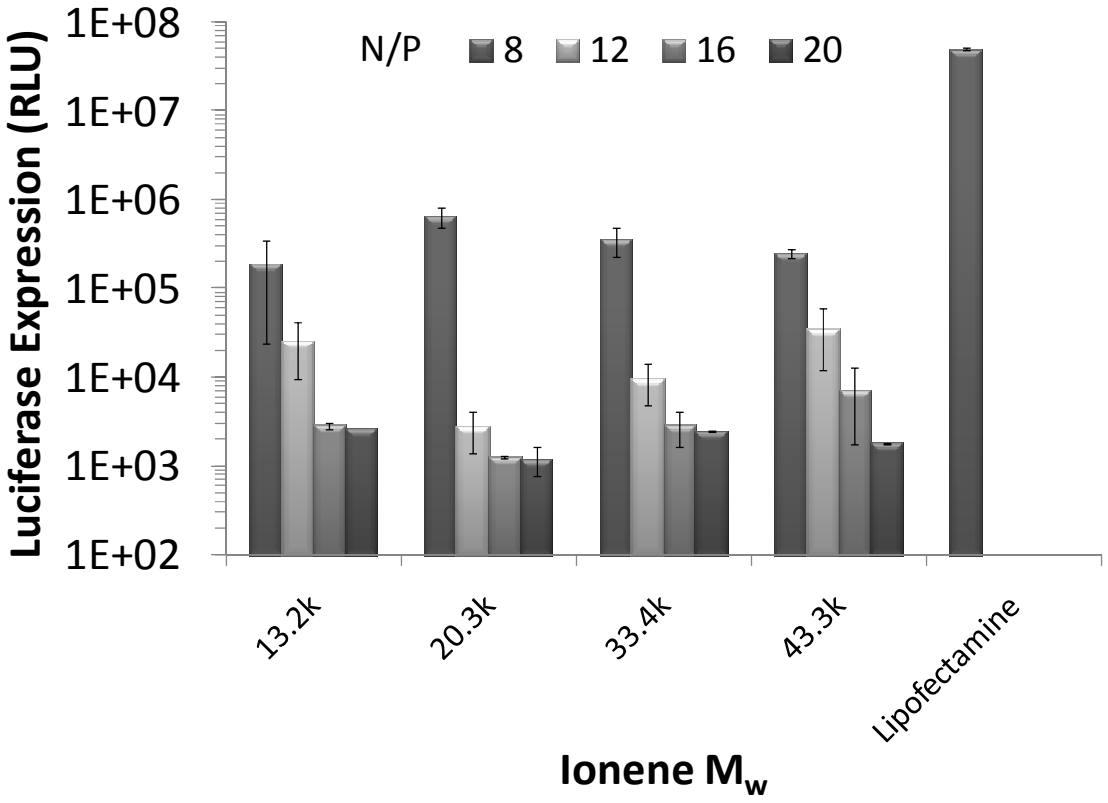

Figure 9.2. Luciferase expression as a function of ammonium 12,6-ionene molecular weight and N/P ratio. Values represent mean ± S.D. (n=4).

Figure 9.3 shows luciferase expression in Cos-7 cells as a function of N/P ratio for ammonium 12,6- and 12,12-ionenes. In this comparison, both ionenes had similar weight-average molecular weights (M_w=20,300 g/mol for the 12,6-ionene and

M_w=20,700 g/mol) in order to determine the influence of charge density alone. Again, we observed decreasing transfection efficiency as a function of increasing N/P ratio. However, ionene charge density had a significant influence on luciferase expression. At an N/P of 8, the ammonium 12,6-ionene (higher charge density) showed orders of magnitude greater luciferase expression than the 12,12-ionene. However, from these data alone, we cannot determine if charge density plays a role in the internalization of ionene-based polyplexes, or if 12,12-ionenes are more toxic, leading to reduced protein expression. Again, further experiments are needed to determine the influence of charge density on cell viability with the specific ionenes synthesized for this study.

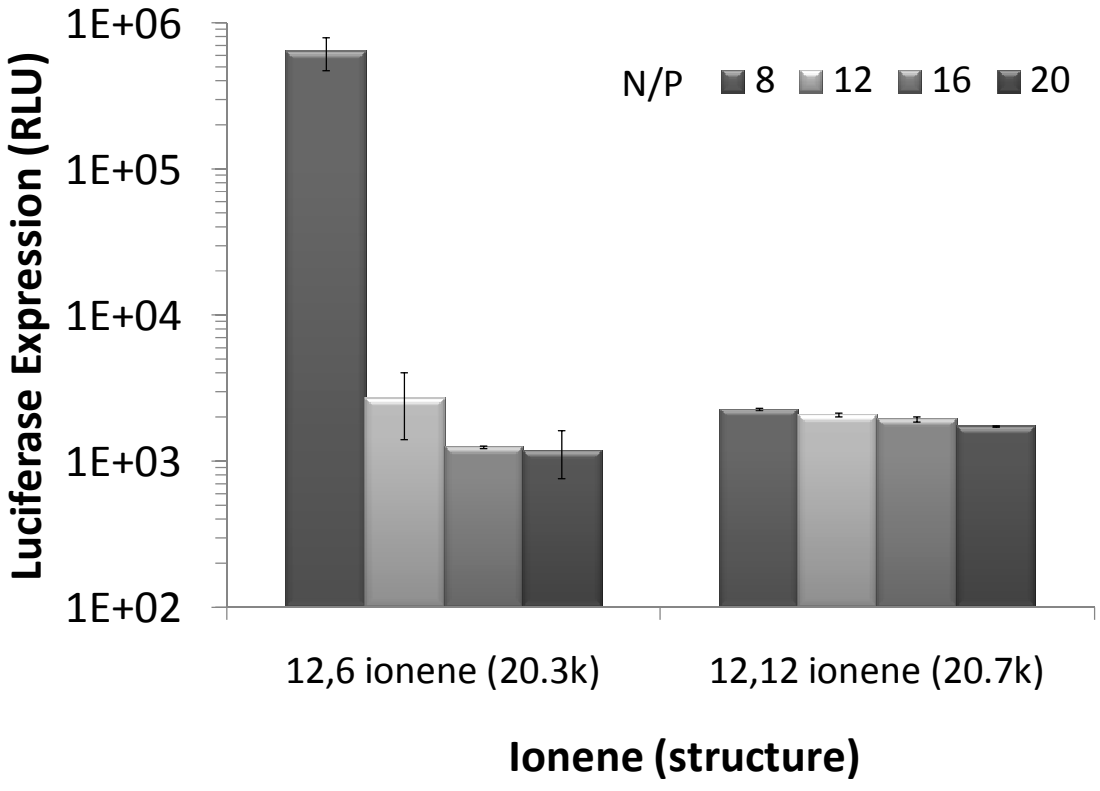

Figure 9.3. Luciferase expression as a function of ammonium ionene charge density (12,6 versus 12,12) and N/P ratio. Values represent mean ± S.D. (n=4).

9.5 Conclusions

A series of aliphatic ammonium ionenes were synthesized using step-growth polymerization. Specifically, ammonium 12,6- and 12,12-ionenes were synthesized in order to evaluate the influence of charge density on plasmid DNA transfection. We determined that transfection efficiency in Cos-7 was insensitive to 12,6-ionene molecular weight over the range tested. Additionally, all transfection experiments revealed that protein expression decreased as a function of increasing N/P ratio, likely due to reduced cell viability. The charge density of the aliphatic ammonium ionene was found to have a significant influence on transfection efficiency, with the higher charge density (12,6-ionene) showing orders of magnitude greater protein expression.

9.6 Acknowledgments

This material is based upon work supported in part by the Macromolecular Interfaces with Life Sciences (MILES) Integrative Graduate Education and Research Traineeship (IGERT) of the National Science Foundation under Agreement No. DGE-0333378.

9.7 References

[1]Emery, D. W., Gene therapy for genetic diseases: On the horizon. *Clinical and Applied Immunology Reviews* **2004,** 4, (6), 411-422.

[2]Kay, M. A.; Glorioso, J. C.; Naldini, L., Viral vectors for gene therapy: the art of turning infectious agents into vehicles of therapeutics. *Nat. Med.* **2001,** 7, (1), 33-40.

[3]Palmer, D. H.; Young, L. S.; Mautner, V., Cancer gene-therapy: clinical trials. *Trends in Biotechnology* **2006,** 24, (2), 76-82.

[4]Kaiser, J., CLINICAL RESEARCH: Death Prompts a Review of Gene Therapy Vector. *Science* **2007,** 317, (5838), 580-.

[5]Heath, W. H.; Senyurt, A. F.; Layman, J.; Long, T. E., Charged Polymers via Controlled Radical Polymerization and their Implications for Gene Delivery. *Macromolecular Chemistry and Physics* **2007,** 208, (12), 1243-1249.

[6]Wong, S. Y.; Pelet, J. M.; Putnam, D., Polymer systems for gene delivery--Past, present, and future. *Progress in Polymer Science* **2007,** 32, (8-9), 799-837.

[7]Jeong, J. H.; Kim, S. W.; Park, T. G., Molecular design of functional polymers for gene therapy. *Progress in Polymer Science* **2007,** 32, (11), 1239-1274.

[8]Morille, M.; Passirani, C.; Vonarbourg, A.; Clavreul, A.; Benoit, J.-P., Progress in developing cationic vectors for non-viral systemic gene therapy against cancer. *Biomaterials* **2008,** 29, (24-25), 3477-3496.

[9]Green, J. J.; Langer, R.; Anderson, D. G., A Combinatorial Polymer Library Approach Yields Insight into Nonviral Gene Delivery. *Acc. Chem. Res.* **2008,** 41, (6), 749-759.

[10]Tiera, M. J.; Winnik, F. M.; Fernandes, J. C., Synthetic and Natural Polycations for Gene Therapy: State of the Art and New Perspectives. *Current Gene Therapy* **2006,** 6, 59-71.

[11]Eliyahu, H.; Barenholz, Y.; Domb, A. J., Polymers for DNA delivery. *Molecules* **2005,** 10, (1), 34-64.

[12]Breitenkamp, R. B.; Emrick, T., Pentalysine-Grafted ROMP Polymers for DNA Complexation and Delivery. *Biomacromolecules* **2008,** 9, (9), 2495-2500.

[13]Liu, Y.; Reineke, T. M., Poly(glycoamidoamine)s for Gene Delivery. Structural Effects on Cellular Internalization, Buffering Capacity, and Gene Expression. *Bioconjugate Chem.* **2007,** 18, (1), 19-30.

[14]Liu, Y.; Reineke, T. M., Poly(glycoamidoamine)s for Gene Delivery: Stability of Polyplexes and Efficacy with Cardiomyoblast Cells. *Bioconjugate Chem.* **2006,** 17, (1), 101-108.

[15]Schaffert, D.; Wagner, E., Gene therapy progress and prospects: synthetic polymer-based systems. *Gene Ther.* **2008,** 15, (16), 1131-1138.

[16]Read, M. L.; Logan, A.; Seymour, L. W.; Leaf Huang, M.-C. H.; Ernst, W., Barriers to Gene Delivery Using Synthetic Vectors. In *Advances in Genetics*, Academic Press: 2005; Vol. Volume 53, pp 19-46.

[17]Prevette, L. E.; Kodger, T. E.; Reineke, T. M.; Lynch, M. L., Deciphering the Role of Hydrogen Bonding in Enhancing pDNA-Polycation Interactions. *Langmuir* **2007,** 23, (19), 9773-9784.

[18]Gibbs, C. F.; Littmann, E. R.; Marvel, C. S., Quaternary Ammonium Salts from Halogenated Alkyl Dimethylamines. II. The Polymerization of Gamma-Halogenopropyldimethylamines. *J. Am. Chem. Soc.* **1933,** 55, (2), 753-757.

[19]Noguchi, H.; Rembaum, A., Reactions of N,N,N',N'-Tetramethyl-α,ω-diaminoalkanes with α,ω-Dihaloalkanes. I. 1-y Reactions. *Macromolecules* **1972,** 5, (3), 253-260.

[20]Rembaum, A.; Noguchi, H., Reactions of N,N,N',N'-Tetramethyl-α,ω-diaminoalkanes with α,ω-Dihaloalkanes. II. x-y Reactions. *Macromolecules* **1972,** 5, (3), 261-269.

[21]Zelikin, A. N.; Putnam, D.; Shastri, P.; Langer, R.; Izumrudov, V. A., Aliphatic Ionenes as Gene Delivery Agents: Elucidation of Structure-Function Relationship through Modification of Charge Density and Polymer Length. *Bioconjugate Chem.* **2002,** 13, (3), 548-553.

[22]Layman, J. M.; Borgerding, E. M.; Williams, S. R.; Heath, W. H.; Long, T. E., Synthesis and Characterization of Aliphatic Ammonium Ionenes: Aqueous Size Exclusion Chromatography for Absolute Molecular Weight Characterization. *Macromolecules* **2008,** 41, (13), 4635-4641.

[23]Rembaum, A. Ionene polymers for selectively inhibiting the vitro growth of malignant cells. 75-547234, 4013507, 02-05-1975, 1977.

Chapter 10. **Imidazole-Substituted Poly(ethylene glycol): A Water-Soluble Polymer Synthesized from the Anionic Ring Opening Polymerization of Trityl-Protected Imidazole Epoxides**

John M. Layman, Sean M. Ramirez, Philippe Bissel, and Timothy E. Long

10.1 Abstract

Over the past three decades, poly(ethylene glycol) (PEG)-based macromolecules are being used in an increasing number of biomedical applications. Low toxicity, reduced immunogenicity, and resistance to protein adhesion have made PEG and PEGylated compounds attractive structures in the emerging field of polymer therapeutics. Here, we reported the synthesis and characterization of a new PEG-based polymer from the anionic ring opening polymerization of trityl-protected imidazole epoxides. The new polymer, poly(N-tritylimidazole-2-ethylene oxide) (PTIMEO) was synthesized in high yield (>75%) and ^{1}H NMR spectroscopy revealed relatively high molecular weights (M_n=32,000 g/mol). This result was remarkable since TIMEO monomer has an incredibly bulky triphenylmethyl substituent. In addition, CD spectroscopy demonstrated the PTIMEO likely adopted a helical conformation during polymerization. The PTIMEO was readily deprotected with trifluoroacetic acid to yield water-soluble poly(imidazole-2-ethylene oxide) (PIMEO). Potentiometric titration revealed that the PIMEO had an apparent pKa of approximately 4.

Keywords: ring opening polymerization, imidazole, epoxide, PEG, helical polymer

10.2 Introduction

Polymer therapeutics are emerging as a new platform in the treatment of human diseases and disorders.[1,2] The unique ability to control molecular size, architecture, and targetability has made polymers increasingly attractive for biomedical applications.[3] Polymers have shown utility as polydrugs, sequestering agents, and protein and gene delivery vehicles.[4,5] Despite the advantages of polymer-based therapeutics, many issues must be overcome before wide-spread clinical application can be realized. Specifically, the surface charge common to polymer-based therapeutics can lead to unwanted interactions with serum proteins and cause premature clearance by the reticuloendothelial system.[6,7] Several strategies have been developed to overcome these challenges including conjugation with neutral (macro)molecules such as glycopolymers[8] and water-soluble synthetic polymers.[7] To date, most strategies to modify polymer-based pharmaceuticals have employed the use of poly(ethylene glycol) (PEG). PEG's popularity is due in part to its low toxicity, reduced immunogenicity, and low protein binding affinity.[6] PEGylated macromolecules have been synthesized using a variety of strategies including ring opening polymerization (ROP) from functional groups (commonly hydroxyl) on the parent molecule and conjugation with PEG containing reactive end-groups.[9] To the best of our knowledge, there have been no reports of PEG-based polycations from the direct synthesis of substituted epoxides.

In this work, we report a new synthetic strategy towards PEG-based polymers for therapeutic applications. We synthesized a new oxarine monomer based on a trityl-protected imidazole. The monomer was then readily polymerized under anionic ring opening polymerization conditions to give a trityl-protected, imidazole-substituted PEG. The resulting polymer was then deprotected to yield a water-soluble imidazole-substituted PEG. These polymers are intriguing candidates for drug and gene delivery due to the imidazole substituent, which mimics the functionality of the amino acid histidine.

10.3 Experimental

10.3.1 General Methods and Materials.

^{1}H and ^{13}C NMR spectra were recorded on a Varian Inova 400 MHz spectrometer. Chemical shifts are reported in ppm downfield from TMS using the residual protonated solvent as an internal standard ($CDCl_3$, ^{1}H 7.26 ppm) (D_2O, ^{1}H 4.79 ppm). FAB-MS was obtained on a JOEL HX110 dual focusing mass spectrometer. Circular dichroism (CD) spectra were obtained using a JASCO Corp. J-815 spectrometer at 25^{o}C.

10.3.2 Synthesis of N-tritylimidazole

Triethylamine (2.5 ml) was added to a solution of imidazole (0.68 g) in DMF (10 ml), and Ph_3CCl (3.6 g) was added. The reaction was stirred at room temperature for 16 h. The resulting suspension was quenched with water. The white precipitate was collected

by filtration, washed with cold water, and dried over Na_2SO_4 and concentrated. The crude product was purified by column chromatography (15% ethyl acetate/hexanes) to yield *N*-tritylimidazole as a white solid (2.8 g, 91%).

10.3.3 Synthesis of N-tritylimidazole-2-carboxaldehyde

1.5 mL of 1.6 M n-BuLi in hexane was added to a solution of 620 mg of *N*-tritylimidazole in 25 mL of THF at 0 ^{o}C. After 2 h at RT, the red solution was cooled to 0 ^{o}C, and 0.508 mL of DMF was added dropwise. After 1 h at 0 ^{o}C, the reaction mixture was poured into 25 mL of water. After concentration of the solution by rotary evaporation, ethyl acetate extraction, and silica gel chromatography (20% ethyl acetate/hexanes), 1-Trityl-1H-imidazole-2-carbaldehyde was obtained (0.61 g, 90% yield).

10.3.4 Synthesis of N-triylimidazole-2-ethylene oxide

To 0.09 g of NaH (60% in paraffin oil) was added 1 ml of DMSO. The mixture was stirred at 70 ^{o}C for 1 h and, after cooling down to RT, 2 ml of THF was added. The solution was cooled down to -5 ^{o}C and a solution of trimethylsulfonium iodide (0.4 g) in 2 ml of DMSO was added dropwise. The mixture was stirred for 10 min, and 0.34 g of the aldehyde was added in portions. After 20 min the cooling bath was removed and stirring for 1 h at rt. The slurry was poured into a mixture of 10 ml of cold H_2O and 10 ml of hexanes. The solid oxirane was filtered, washed with water and hexanes and silica gel chromatography purification (30% ethyl acetate/hexanes). The epoxide was obtained as a white solid (0.3 g 85%).

10.3.5 Polymerization of N-triylimidazole-2-ethylene oxide

1.0 g of *N*-triylimidazole-2-ethylene oxide was dried under high vacuum for at least 2 h in a 20mL reactor bomb equipped with a magnetic stir bar. After drying, 2 mL of anhydrous toluene or THF was added to the reaction vessel under N_2. Then, 0.1, 0.2, or 0.3 mL of potassium *tert*-butoxide solution (1M in THF) was added the monomer slurry solutions under N_2. The sealed reactor bomb was then submerged into an oil bath preheated to 80 ^oC. After 30 – 60 min, the reaction solutions became homogenous and dark yellow. The solutions were then stirred for 15 to 24 h. Polymerizations from toluene were precipitated in hexanes, filtered, and dried under vacuum. The filtered product was then dissolved in chloroform, extracted with DI-H_2O, and dried over $MgSO_4$. The polymer was then precipitated in hexanes and recovered upon filtration through a 100nm filter membrane. Polymerizations from THF were precipitated in methanol and recovered upon filtration through a 100nm filter membrane.

10.3.6 Deprotection of poly(N-tritylimidazole-2-ethylene oxide)

200 mg of poly(N-tritylimidazole-2-ethylene oxide) was added to 1 mL of trifluoroacetic acid (TFA). The reaction was magnetically stirred for 2 h at 25 ^oC. The TFA was removed under reduced pressure at 35 ^oC. The resulting product was dissolved in 1 mL of DI-H_2O and extracted twice with 1 mL of diethyl ether. Poly(imidazole-2-ethylene oxide) was recovered upon liophillization.

10.3.7 Potentiometric of poly(imidazole-2-ethylene oxide).

pH measurements were performed using a Thermo Orion 3 Star portable pH meter equipped with a Thermo Orion Triode pH electrode. PTIMEO was dissolved at 1 mg/mL in ultrapure water having a resistivity of 18 MΩ·cm. Using 10 mL of polymer solution, the pH was then adjusted to ~3 using 0.1 M HCl. The solutions were then titrated with 5 μL aliquots of 1 M NaOH. The pH of the solution was measured after the addition of each aliquot.

10.4 Results and Discussion

N-tritylimidazole-2-ethylene oxide (TIMEO) was prepared using a 3-step synthetic approach, shown in Scheme 10.1. First, imidazole was reacted with trityl chloride to produce *N*-protected imidazole. Second, the N-tritylimidazole was reacted with n-BuLi/DMF to produce N-triytylimidazole-2-carboxaldehyde. The aldehyde adds to the 2-position due to favored carbanion formation between the two nitrogen atoms in the imidazole ring. The aldehyde was then converted to an oxarine using the Corey-Chaykovsky epoxidation[10] strategy. Figure 10.1 shows the ^{1}H NMR spectrum of the TIMEO monomer.

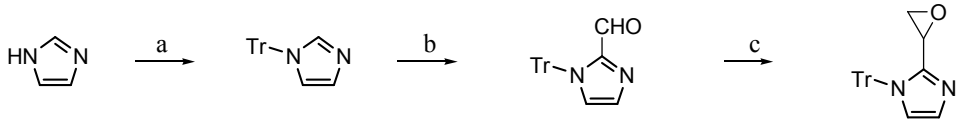

a) TritylCl; b) BuLi, DMF; c) Me_3SI, NaH

Scheme 10.1. Synthesis of *N*-triylimidazole-2-ethylene oxide.

TIMEO monomer was readily polymerized in the presence of potassium tert-butoxide, shown in Scheme 10.2. ^{1}H NMR spectroscopy of PTIMEO, shown in Figure 10.1, confirmed the chemical structure of the polymer. Compared to the monomer, broad peaks were observed in the PTIMEO spectrum. The fact that polymerization occurred was remarkable since the triphenylmethyl substituent associated with the trityl protection is incredibly bulky. It is widely known that hindered epoxides, such as styrene oxide, are difficult to polymerize due to the difficulties associated with sterics. However, we were encouraged by the work of Yang et al. who were able to form oligomers via the ring opening polymerization of triphenylmethyl-substituted epoxides.[11] However, the investigators were only able to achieve weight-average molecular weights up to 10,000 g/mol (DPs up to 12).[11]

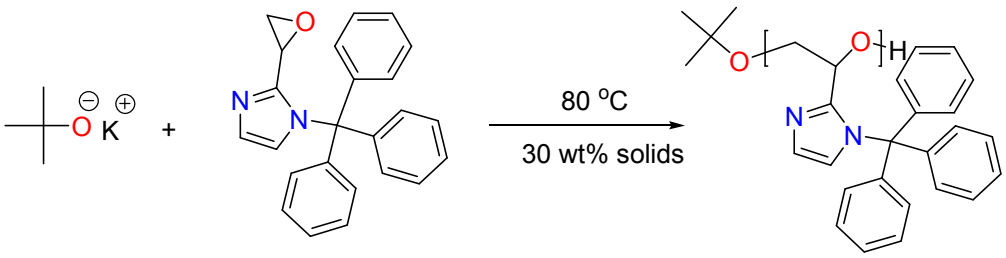

Scheme 10.2. Anionic ring opening polymerization of *N*-triylimidazole-2-ethylene oxide.

In our work, we were able to achieve number-average molecular weights up to 30,000 g/mol (DPs up to 90). As expected, the DP of the PTIMEO polymer was sensitive to initiator concentration and reaction solvent. Polymerizations were performed in THF and toluene/THF mixtures to determine the influence of solvent on the anionic ring opening polymerization of the epoxide. In both solvents, PTIMEO polymer was

isolated with yields greater than 50%. Table 10.1 summarizes the synthetic conditions and DPs of the resulting PTIMEO polymers. Polymerizations in THF (samples **1** – **3**) produced the high molecular weight PTIMEO with M_ns up to ~30,000 g/mol. Additionally, the anionic ring opening polymerization occurred in a controlled manner as demonstrated by a plot of experimental DP versus theoretical DP. Figure 10.2 shows the plot of DPs of PTIMEO determined with ^{1}H NMR spectroscopy versus calculated DPs. As shown in the figure, a linear trend was observed in the data (trendline R^2=0.996). The slope of the trendline indicated that the polymerizations occurred with an average initiator efficiency of 23%. Polymerizations were also performed in toluene/THF mixtures (samples **4** – **6**). The solvent mixtures resulted from charging toluene reactions with increasing volumes of 1M potassium tert-butoxide initiator solutions. As the amount of initiator was systematically increased, the amount of THF relative to toluene also increased. After a few hours of polymerization, white, solid PTIMEO polymer began crashing out of solution. This occurred with all three ratios of toluene to THF. As shown in Table 10.1, these polymerizations resulted in significantly lower molecular weights (M_n's only up to ~4,500 g/mol). We attributed the lower molecular weights to the heterogeneity of the toluene-based polymerization solvent. Also, we observed an undetected trend in experimental versus predicted DPs, with higher initiator concentrations producing higher molecular weights. However, it is important to note that the amount of THF in the reaction solvent was inherently higher in samples with higher amounts of initiator. The higher molecular weights were likely due to the better solvent quality (more THF) in reactions charged with a greater volume of initiator solution.

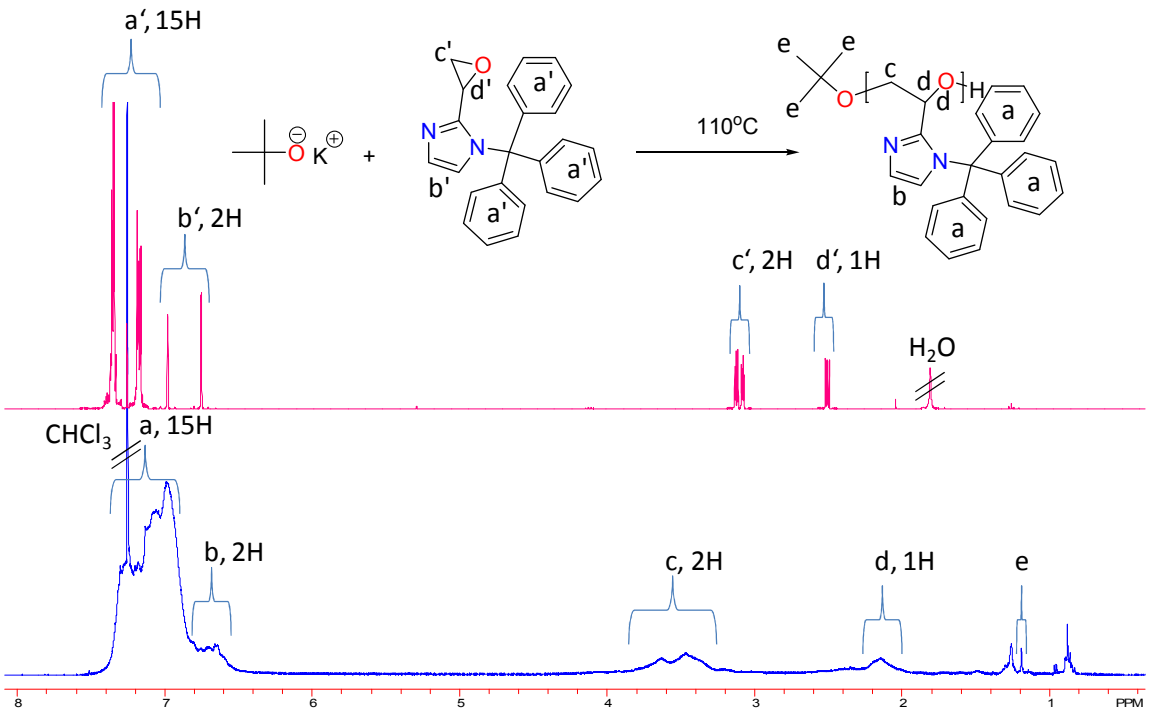

Figure 10.1. ^{1}H NMR spectra of N-tritylimidazole-2-ethylene oxide and poly(N-tritylimidazole-2-ethyleneoxide). Both monomer and polymer were dissolved in $CDCl_3$ for NMR spectroscopy.

Table 10.1. Synthetic conditions and resulting degrees of polymerization for the ring opening polymerization of *N*-tritylimidazole-2-ethylene oxide.

sample	solvent	$[M_o]/[I_o]$	[b]% conv.	$DP_{predicted}$	[a]DP_{actual}	[a]M_n (g/mol)
1	THF	28	75	21	90	31,700
2	THF	14	82	12	45	15,900
3	THF	9	78	7	30	10,600
4	toluene/THF [c](95/5)	28	50	14	8	2,800
5	toluene/THF [c](90/10)	14	49	7	11	4,000
6	toluene/THF [c](85/15)	9	59	6	13	4,500

[a]Determined using ^{1}H NMR spectroscopy.
[b]Calculated from isolated polymer yield.
[c]Volume/volume ratio of respective solvents.

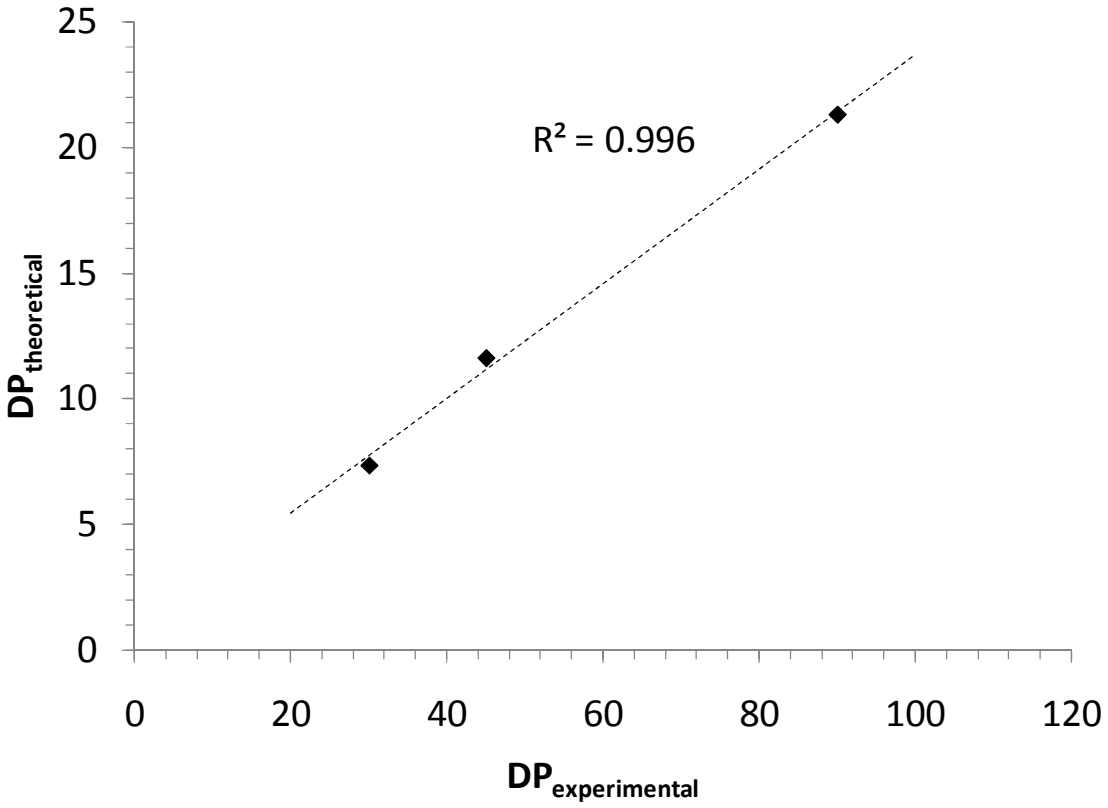

Figure 10.2. Experimental DP versus calculated DP for PTIMEO samples (**1** – **3**) polymerized in THF.

Due to the bulky nature of the trityl-protected monomer, we anticipated that, in order to have sequential monomer addition, the polymer must adopt an irregular conformation during polymerization. Therefore, CD spectroscopy was used to determine if the resulting PTIMEO was helical or otherwise showed any optical activity. Figure 10.3 shows the CD spectrum of PTIMEO (sample **1**) in THF (0.1 mg/mL). As shown in the figure, positive CD absorption was observed at wavelengths of 205 to 240 nm. The strong CD absorbance is likely indicative of a helical structure in solution; however, further experiments are needed to address this issue with any certainty.

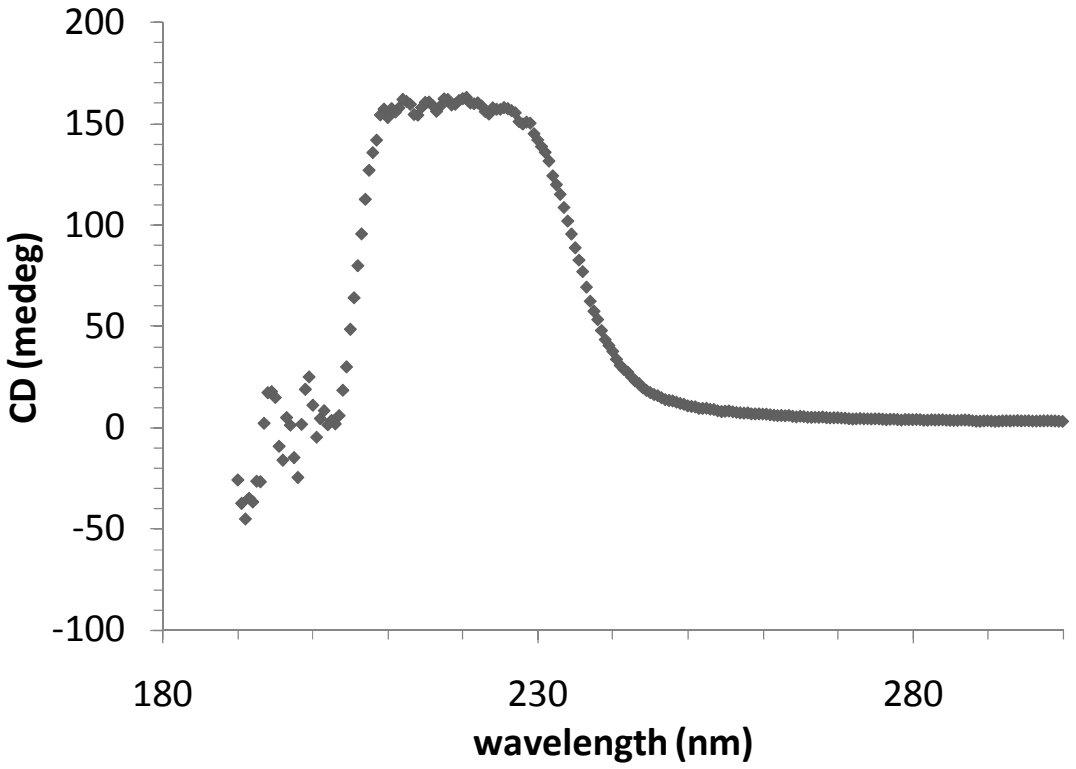

Figure 10.3. CD spectrum of poly(N-tritylimidazole-2-ethylene oxide) (sample **1**) in THF (~0.1 mg/mL). CD spectroscopy was performed at 25 ^{o}C.

PTIMEO was deprotected using trifluoracetic acid to yield poly(imidazole-2-ethylene oxide) (PIMEO), as shown in Scheme 10.3. The resulting polymer was isolated in quantitative yield and was water soluble. ^{1}H NMR spectroscopy verified the structure of PIMEO, as shown in Figure 10.4. In addition, we were able to isolate and confirm the structure of triphenylmethanol (the by-product of the trityl deprotection). Furthermore, the TFA deprotection reaction solution had a brilliant yellow appearance, which is commonly observed for triphenylmethanol in acidic solvents.

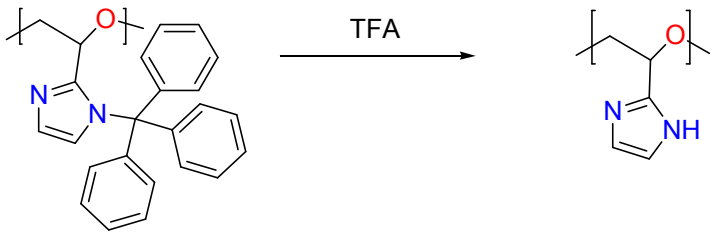

Scheme 10.3. Deprotection of to yield poly(imidazole-2-ethylene oxide).

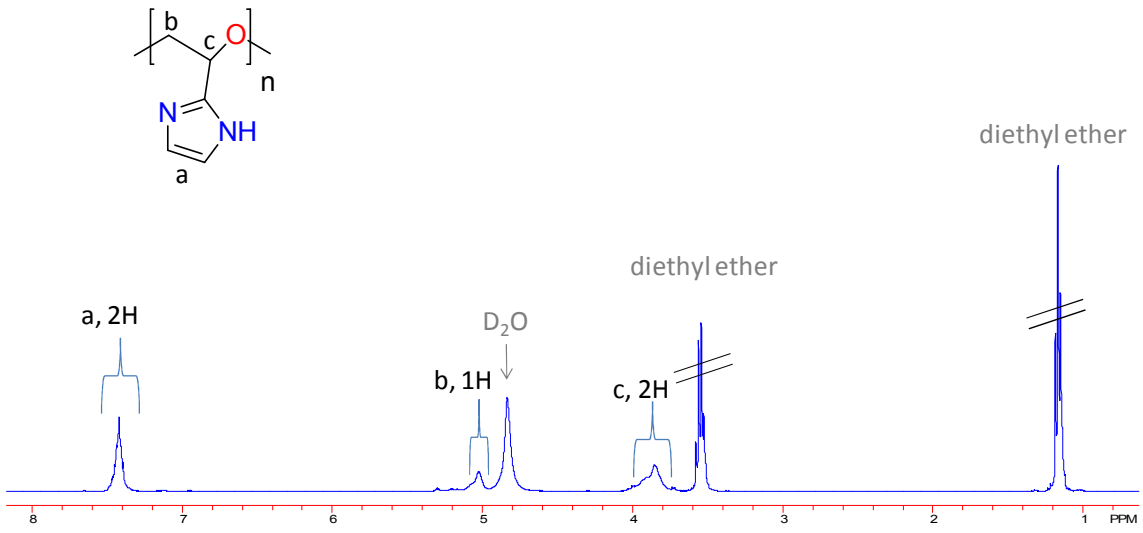

Figure 10.4. ^{1}H NMR of poly(imidazole-2-ethylene oxide) (PIMEO) in D_2O.

The sensitivity of a protonatable polymer to the pH of its aqueous environment is an important parameter when these systems are used as drug or gene delivery vehicles. Therefore, we explored the buffering capacity of PIMEO. Figure 10.5 shows the titration curve for PIMEO. The pH of the PIMEO aqueous solution was first adjusted to ~3 using HCl. The resulting solution was then titrated with μL aliquots of 1M NaOH. As shown in the titration curve, PIMEO buffered over the pH range of ~3 to 6.5. At a pH of approximately 7.5, the PIMEO solution became turbid (note the discontinuity in the

titration curve in this pH range), and at pH's greater than 7.5, the PIMEO crashed out of solution and became insoluble. However, the polymer became soluble once acid was added to the titration solution (not shown in the titration curve).

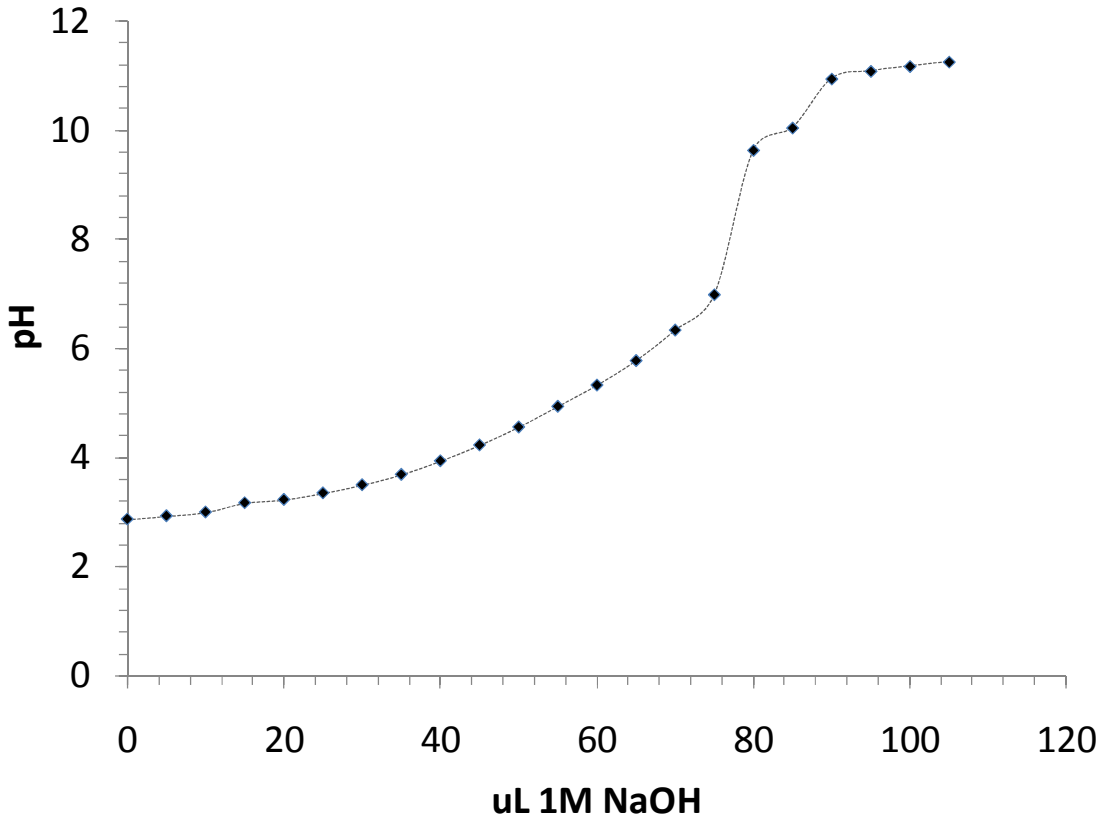

Figure 10.5. Potentiometric titration of PIMEO.

10.5 Conclusions

Imidazole-substituted epoxide monomers (specifically *N*-tritylimidazole-2-ethylene oxide) were successfully synthesized and polymerized via anionic ring opening polymerization. The resulting polymers were synthesized with high yields and ^{1}H NMR analysis revealed that the PEG-based polymers had relatively high degrees of polymerization (DPs up to 90, M_n's up to ~30,000 g/mol). CD spectroscopy of the trityl-

protected PEG-imidazoles indicated that the polymer likely adopted helical conformations during polymerization. However, this topic requires further investigation. Poly(*N*-tirtylimidazole-2-ethylene oxide) was readily deprotected to yield poly(imidazole-2-ethylene oxide), a water-soluble polymer. We are currently exploring regioisomers of imidazole epoxides and evaluating these new PEG-based polymers for their ability to complex and deliver plasmid DNA.

10.6 Acknowledgments

This material is based upon work supported by the U.S. Army Research Laboratory and the U.S Army Research Office under grant number W911NF-07-1-0452 Ionic Liquids in Electroactive Devices (ILEAD) MURI. This material is based upon work supported in part by the Macromolecular Interfaces with Life Sciences (MILES) Integrative Graduate Education and Research Traineeship (IGERT) of the National Science Foundation under Agreement No. DGE-0333378.

10.7 References

[1]Duncan, R.; Ringsdorf, H.; Satchi-Fainaro, R. In *Polymer Therapeutics I* 2006, p 1-8.

[2]Anderson, D. G.; Burdick, J. A.; Langer, R. *Science* **2004**, *305*, 1923-1924.

[3]Kiick, K. L. *Science* **2007**, *317*, 1182-1183.

[4]Dhal, P.; Holmes-Farley, S.; Huval, C.; Jozefiak, T. In *Polymer Therapeutics I* 2006, p 9-58.

[5]Wong, S. Y.; Pelet, J. M.; Putnam, D. *Progress in Polymer Science* **2007**, *32*, 799-837.

[6]Alexis, F.; Pridgen, E.; Molnar, L. K.; Farokhzad, O. C. *Mol. Pharmaceutics* **2008**, *5*, 505-515.

[7]Davis, M. E.; Chen, Z.; Shin, D. M. *Nat Rev Drug Discov* **2008**, *7*, 771-782.

[8]Davis, M. E.; Brewster, M. E. In *Nature Reviews Drug Discovery*; Nature Publishing Group: 2004; Vol. 3, p 1023-1035.

[9]Pasut, G.; Veronese, F. M. *Progress in Polymer Science* **2007**, *32*, 933-961.

[10]Corey, E. J.; Chaykovsky, M. *J. Am. Chem. Soc.* **1965**, *87*, 1353-1364.

[11]Cao, J.; Yang, N.-F.; Li, J.-C.; Yang, L.-W. *Polymer Bulletin* **2007**, *59*, 481-490.

Chapter 11. **Therapeutic Delivery of Superoxide Dismutase Plasmids Using Gene Therapy**

11.8 Introduction to Reactive Oxygen Species and Oxidative Stress

It is an extreme irony that oxygen, a molecule critical to sustaining life in aerobic organisms, is also involved in deleterious mechanisms that damage and disturb vital cellular functions. Reactive oxygen species (ROS) have been implicated in the pathanogenic pathways of an increasing number of age-related diseases and disorders.[1,2,3,4,5,6] First reported by Harman in 1956[7], it is a widely accepted hypothesis that the fundamental mechanisms of cellular aging, in and of itself, are related to the over-production of oxygen-centered free radicals.

Free radicals, in general, damage cells by altering protein structure (and therefore function), mutating DNA, and oxidizing cell-membrane lipids. The high reactivity of free radicals allows them to attack almost any molecule they encounter; thus, they are non-specific, non-discriminating toxins. However, certain lipids are particularly sensitive to oxidation due to the occurrence of unsaturated carbon-carbon double bonds in their chemical structure. The allylic, or β-hydrogen, has a relatively weak bond dissociation energy (BDE), allowing for easy hydrogen abstraction. Peroxidized lipids, apart from no longer being able to function in the cellular membrane, can do further stochastic damage to proteins and DNA.[8] Often, the degree of oxidative-stress an organism is experiencing is measured by determining the amount of peroxidized lipid products.[9,10]

Cells produce ROS at a steady state concentration and actually depend on such compounds for the destruction of invading organisms, cell signaling pathways[11], and several enzyme oxidation processes.[12] Under normal physiological conditions, approximately 1-2% of the oxygen consumed is converted into ROS.[13] The superoxide anion is one such ROS that is a naturally produced in the mitochondria of cells. In fact, the mitochondrion is responsible for producing over 90% of all ROS found in cells.[14] Superoxide is produced during oxidative phosphorylation in the one electron oxidation of a semiquinone to quinone, which results in the one electron reduction of molecular oxygen, shown in Scheme 11.1 below.

$$O_2 + e \rightarrow O_2^-$$

Scheme 11.1. One electron reduction of molecular oxygen.

The lifetime of superoxide is relatively short, with a rate constant of decay around 10^7 mol^{-1} s^{-1} in aqueous solutions.[15] The harmful effects of superoxide are more indirect than direct. In other words, superoxide is utilized as a critical intermediate in reactions to produce other toxic ROS that more readily attack vital cellular compounds, rather than oxidizing these compounds directly. Haber and Weiss proposed the following reaction in which superoxide is used as a reducing agent in the reaction of superoxide and hydrogen peroxide[16], shown in Scheme 11.2.

$$O_2^- + H_2O_2 \rightarrow OH^- + {}^{\cdot}OH + O_2$$

Scheme 11.2. The Haber-Weiss reaction.

The Haber-Weiss reaction produces the extremely reactive hydroxyl radical[17], which is involved in a number of aromatic hydroxylation reactions.[15] Superoxide is also a reducing agent in its reaction with ferroctyochrome c, shown in Scheme 11.3. The standard reduction potential for this reaction was measured as *Eo*=+0.27 V by Rao and Hayon[18]

$$\text{cty c } (Fe^{3+}) + O_2^- \rightarrow \text{cty c } (Fe^{2+}) + O_2$$

Scheme 11.3. Reduction of cty c by superoxide.

Perhaps the most common fate of the superoxide anion is its dismutation into hydrogen peroxide and molecular oxygen, shown in Scheme 11.4.

$$2O_2^- + 2H^+ \rightarrow H_2O_2 + O_2$$

Scheme 11.4. Dismutation of superoxide into hydrogen peroxide and molecular oxygen.

This reaction is catalyzed by a number of specific metalloenzymes called superoxide dismutases (SOD).[19] As written in the reaction scheme, the dismuation reaction in acidic aqueous solutions occurs with a rate constant of 10^7 mol^{-1} s^{-1}.[20] However, when catalyzed by superoxide dismutases, this reaction proceeds with a rate constant of 10^9 mol^{-1} s^{-1}.[12] The discovery of superoxide dismutase by McCord and Fridovich was actually the first evidence, although admittedly indirect, that proved the existence of the superoxide anion.[21] There are several types of superoxide dismutase, differing by the metal ion they contain and the cellular environment they occupy. Extracellular superoxide dismutase (EC-SOD) is a glycoprotein that contains both copper and zinc metal ions. Cu/Zn-SOD is sometimes referred to as SOD1. EC-SOD is found in

the interstitial spaces of tissues and in plasma, lymph, and synovial fluids.[22] The structure of EC-SOD will depend on its source. Bovine EC-SOD is a dimmer with a molecular weight of 2x16,300 Da.[23] Human EC-SOD is a tetramer with a molecular weight of 2x23,300 Da.[23] A non-extracellular Cu/Zn-SOD is found in the cytosol of cells. Another main type of SOD exists with a Manganese (Mn) ion, also referred to as mitochondrial SOD or SOD2. Mn-SOD is usually found in the matrix of the mitochondria. Mn-SOD is sometimes found with a Fe metal atom. Last reported in 1999, the structures of eight different types of Cu/ZN-SODs and nine Mn or Fe-SOD have been determined.[24] The active site on Cu/Zn-SOD is a histidine-complexed Cu^{2+} atom. The catalytic mechanism involves alternating reactions of the Cu/Zn-SOD with superoxide[25], shown in Scheme 11.5 below.

$$\text{Enzyme-Cu}^{2+} + O_2^- \rightarrow \text{Enzyme-Cu}^{+} + O_2$$

$$\text{Enzyme-Cu}^{+} + O_2^- + 2H^+ \rightarrow \text{Enzyme-Cu}^{2+} + H_2O_2$$

Scheme 11.5. Catalytic mechanism of CuZn-SOD.

The accessible surface of a dimeric iron containing SOD showing an active site is shown in Figure 11.1.

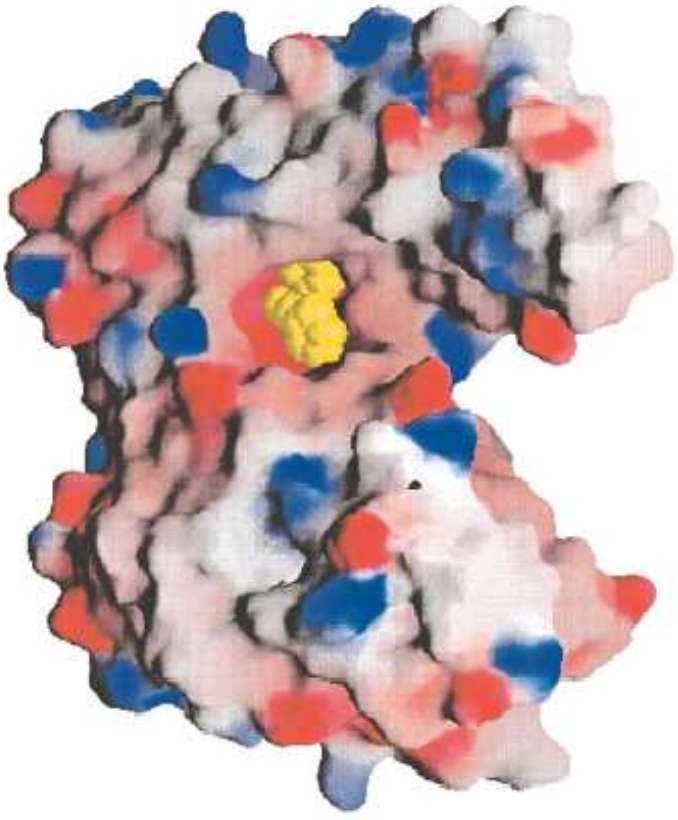

Figure 11.1. Surface active site for FE-SOD.[24] Reprinted from Journal of Molecular Biology, Vol /286, Thomas Ursby, Bianca Stella Adinolfi, Salam Al-Karadaghi, Emmanuele De Vendittis and Vincenzo Bocchini, "Iron superoxide dismutase from the archaeon Sulfolobus solfataricus: analysis of structure and thermostability", Copyright 1999, with permission from Elsevier.

SOD is one of many enzymes that make up the cells natural antioxidant defense system. By definition, an antioxidant is a molecule or compound that will react with a toxic ROS to form a stable product, usually still a radical, which will no longer attack vital molecules in the cell. Once superoxide is converted into hydrogen peroxide by SOD, catalase (CAT) converts hydrogen peroxide into water and molecular oxygen. The

dismutation of hydrogen peroxide by CAT is augmented by peroxiredoxin (PRX) and glutathione peroxidase (GPX). The flow of electrons through the cytochrome chain and the sites of superoxide generation, as wells as the antioxidant enzymatic pathway are shown in Figure 11.2.

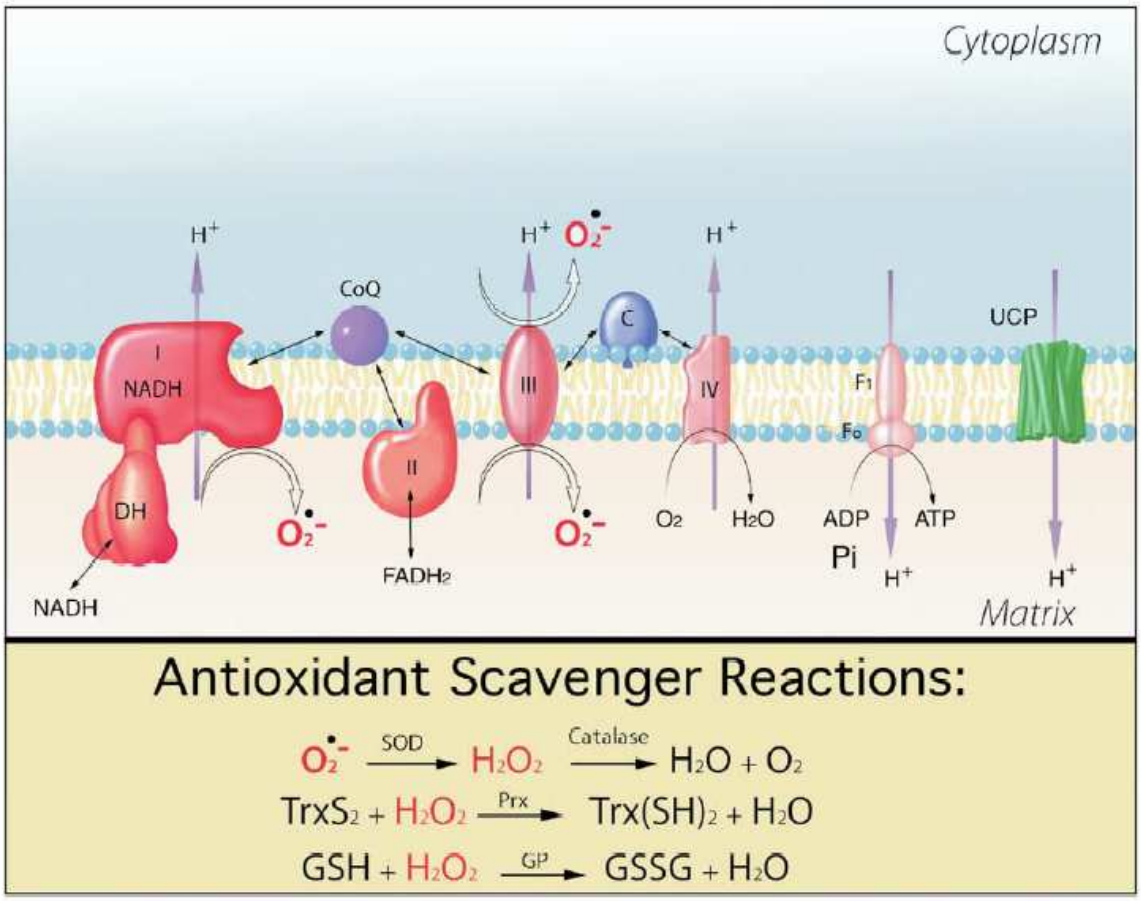

Figure 11.2. The major production sites of the superoxide anion as well as the ROS scavenging pathways associated with its dismutation. [14] Reprinted from Cell, Vol 120, Robert S. Balaban, Shino Nemoto and Toren Finkel, "Mitochondria, Oxidants, and Aging", Copyright 2005, with permission from Elsevier.

When cells are placed under oxidative stress, they compensate by increasing the expression of key antioxidant enzymes.[26,27,28] However, as organisms age, the integrity

of the antioxidant defense system is comprised and the amount of antioxidant enzymes decrease.[29,30] The system, that could once handle the detoxification of ROS, suffers an imbalance which allows ROS to increases in concentration and damage cellular proteins and DNA. The inactivation of extracellular superoxide dismutase SOD1 or mitochondrial superoxide dismutases SOD2 has been shown to increase cell sensitivity to oxidative stress and reduce the life span of certain organisms.[31,32] Damaged cellular components leads to malfunctioning cells. In higher life-forms, the accumulation of damaged cells leads first to diseased tissues, which further leads to organ failure, and ultimately death of the organism. A logical solution to this problem is to restore balance to the oxidant/antioxidant-defense system. Since the lack of antioxidant enzymes leads to excess ROS, which leads to diseased cells, then introducing the deficient antioxidant enzyme should return the cells ROS to normal levels. Thus, returning the level of antioxidant enzymes to normal values has the potential to treat diseases caused by oxidative stress.[33]

Gene therapy, discussed previously, has the ability to treat oxidative stress by incorporating antioxidant enzymes into diseased cells. The gene for human SOD1 is localized on Chromosome 21, and the gene for human SOD2 is localized on Chromosome 6.[41,34] Plasmids containing SOD genes (both SOD1 and SOD2) have been constructed and successfully transfected and expressed in a variety of cell lines. Specific examples on the therapeutic effects from SOD gene transfer will be discussed in the following section.

Before discussing the benefits of overexpressing SOD in the treatment of oxidative stress-related diseases, it is important to note that the imbalance of antioxidant

enzymes has been found to have a negative effect on the proliferation of certain cells.[35,36] This antiproliferative effect is even being considered as a way to suppress the growth of malignant tumors in certain cancers.[37,38] Investigators have also found that while cell growth may be inhibited by the overexpression of SOD, protection against induced oxidative stress is still observed.[39,40] Since SOD catalyzes the decomposition of superoxide into hydrogen peroxide, adequate amounts of catalase and glutathione peroxidase are required to scavenge the accumulated H_2O_2 before it decomposes through the Haber-Weiss reaction to produce hydroxyl radicals, shown earlier in Scheme 11.2. However, the catalytic activity of SOD is regulated by the concentration of hydrogen peroxide.[19] Further, it has been shown that if SOD is expressed in excess, the other main antioxidants (CAT and GPX) will up-regulate to meet the demands of produced hydrogen peroxide.[11] Investigators have also found that patients with Down Syndrome (DS), a common postnatal chromosomal abnormality which is caused by the trisomy of Chromosome 21, have elevated levels of SOD1 which cannot be matched by normal production of GPX and CAT.[41,42] If the ratio of SOD1 or SOD2 to CAT or GPX is 1.5:1 or greater, oxidative stress is observed as the additional H_2O_2 produced cannot be neutralized by GPX and CAT.[43]

11.9 Gene Therapy with SOD to Treat ROS Related Diseases

Several investigators have shown that ROS, particularly the superoxide anion, contribute significantly to myocardial ischemia/reperfusion injury.[44] Intravenous administration of antioxidant enzymes has been shown to alleviate postischemic dysfunction (myocardial stunning) .[44] Li et al. utilized gene therapy (in *vivo*) to infect rabbits with extracellular SOD (EC-SOD).[45] In this study, rabbits were intravenously

given cDNA for human EC-SOD behind the cytomegalovirus (CMV) promoter incorporated into a replication-deficient adenovirus. Three days after administration of the EC-SOD gene, the rabbits were subjected to a sequence of six coronary occlusions for three days. The severity of the myocardial stunning was quantified by measuring the left ventricular systolic wall thickness. It was found that the cells infected with the EC-SOD were protected from myocardial stunning. A separate work by Li et al. provided evidence that gene therapy with EC-SOD also protects conscious rabbits from myocardial infarction.[46] In another study, Abou El Hassan et al. found that the gene transfer of Cu/Zn-SOD did not protect cardiac cells against doxorubicin-induced oxidative stress.[47] Additionally, Jeroudi et al. found that the cytosolic form of Cu/Zn-SOD alone, delivered via gene therapy, does not protect cells from myocardial stunning.[48] Cytosolic Cu/Zn-SOD gene transfer must be accompanied by the simultaneous transfer of catalase or glutathione peroxidase.[48] Li et al. hypothesized that the extracellular isoform of SOD expressed alone provides a cardioprotective effect against oxidative stress due to the fact that the enzyme is anchored to the glycocalyx of cardiomyocytes, allowing it to detoxify intracellular superoxide.[45] The cardioprotective effect of SOD gene therapy is also sensitive to high viral dosages, as shown by Omar et al.[49]

Oxidative stress has been implicated in vascular dysfunction, which is the principle phenotype associated with atherosclerosis and hypertension.[50] Lipopolysaccharide has been shown to impair vascular function by the generation of ROS, especially superoxide.[51,52] Lund et al. found that adenovirus-mediated gene transfer of EC-SOD reduces the level of superoxide in blood vessels and improves the relaxation of the aorta after treatment with endotoxin.[53] Supporting the findings of Lund

et al., Fennell et al. found that *in vivo* adenovirus-mediated gene transfer of EC-SOD improved endothelial function in a rat model of hypertension.[54] Interestingly, in this study it was also found that gene transfer of Mn-SOD (mitochondrial SOD) did not provide a protective effect.

Hearing loss in mammals is caused by the reduction of cochlear hair cells. Hair cell loss leads to permanent sensory-neural impairment. Cochlear hair loss is often a side effect of using aminoglycoside antibiotics.[55] Aminoglycoside antibiotics are highly effective against severe bacterial infections, such as tuberculosis. However, the clinical use of these antibiotics is limited due to ototoxic side effects.[56] The side effect damage by aminoglycoside antibiotics is initiated by ROS.[57] Using gene therapy with SOD2, Kohei et al. found that the hearing threshold can be significantly protected in a guinea pig model challenged with an aminoglycoside antibiotic.[58] Figure 11.3 below shows the dramatic protective effect of an SOD2 (Figure 11.3e) treated cochlea compared to an untreated cochlea (Figure 11.3f) when challenged with aminoglycoside-induced oxidative stress.

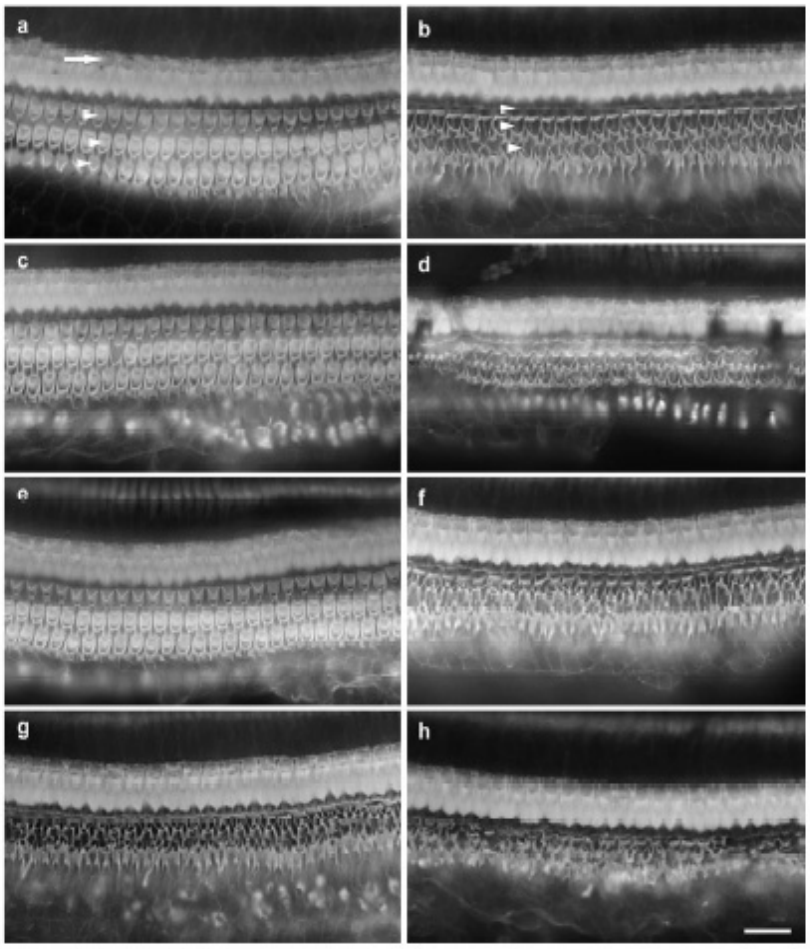

FIG. 1. Phalloidin-stained whole mounts of basal cochlear turns. (a) Ad.cat-inoculated cochlea with well-preserved inner (arrow) and outer hair cells (arrowheads). (b) Contralateral ear of (a) with outer hair cells entirely absent, replaced by scars (arrowheads). Inner hair cells are intact. (c) Ad.SOD1-inoculated cochlea with nearly normal outer hair cell population and a full complement of inner hair cells. (d) The contralateral cochlea of (c) in Ad.SOD1-treated guinea pig showing a complete destruction of outer hair cells. (e) Ad.SOD2-treated left cochlea with a normal organ of Corti. (f) The contralateral cochlea of the Ad.SOD2 animals with a complete loss of outer hair cells. (g) Ad.null-inoculated ear showing extensive damage to the organ of Corti with a complete loss of outer hair cells. (h) The contralateral ear in a guinea pig receiving Ad.null showing a severe cochlear lesion in the outer hair cell area. Bar, 25 μm.

Figure 11.3. Phalloidin-stained whole mounts of basal cochlear turns. (a) Ad.cat-inoculated cochlea with well-preserved inner (arrow) and outer hair cells (arrowheads). (b) Contralateral ear of (a) with outer hair cells entirely absent, replaced by scars (arrowheads). Inner hair cells are intact. (c) Ad.SOD1-inoculated cochlea with nearly normal outer hair cell population and a full complement of inner hair cells. (d) The contralateral cochlea of (c) in Ad.SOD1-treated guinea pig showing a complete destruction of outer hair cells. (e) Ad.SOD2-treated left cochlea with a normal organ of Corti. (f) The contralateral cochlea of the Ad.SOD2 animals with a complete loss of outer

hair cells. (g) Ad.null-inoculated ear showing extensive damage to the organ of Corti with a complete loss of outer hair cells. (h) The contralateral ear in a guinea pig receiving Ad.null showing a severe cochlear lesion in the outer hair cell area. Bar, 25 Am.[58] Reprinted by permission from Macmillan Publishers Ltd: Molecular Therapy **2004**, 9, 173-181, copyright 2004

ROS are generated in various liver injuries such as drug toxicity, ischemia, and alcohol metabolism.[59] Gene delivery of EC-SOD has been shown to protect transgenic mice from acute liver injury.[59] In a study by Wu et al., polycationic liposome-mediated EC-SOD gene delivery was found to protect HepG2 cells from oxidative stress induced by D-galactosamine and lipopolysaccharide intoxication.

Reperfusion injury in the liver is common after liver transplantation. Reperfusion leads to hepatocellular injury by the generation of ROS, which results in inflammation, necrosis, and apoptosis.[60] Lehmann et al. found that delivery of SOD1 via gene therapy decreases hepatic injury and increases the survival of liver cells against oxidative stress associated with liver transplantation.[61] In this study, all rats survived after liver transplantation with treatment of adenovirus-mediated gene transfer SOD1. Only 20-25% of rats survived without treatment of gene-delivered SOD1. Under conditions of non-survival, hypoxia was detected.[62] Hypoxia has been shown to produce the superoxide anion through xanthine oxidase.[60] Additionally, approximately 20% of hepatocytes were necrotic after transplantation, whereas necrosis was nearly undetectable in grafts from SOD1-treated rats.[61] In a separate study by Lehmann et al., only 10% rats

receiving a fatty liver transplant survive, whereas 100% of rats survive with a fatty liver transplant accompanied with a simultaneous treatment of SOD1 using gene therapy.

Similar to liver hepatocytes, grafts of pancreatic cells are susceptible to damage by ROS after transplantation.[63] Macrophage cytotoxicity, together with a relatively low level of antioxidants enzymes, makes pancreatic islets particularly sensitive to oxidative stress. Karsten et al. found that adenovirus-mediated gene transfer of catalase and SOD increases the survival of pancreatic cells after hydrogen peroxide induced oxidative stress.[64] Figure 11.4 shows the percentage of cell viability with and without gene therapy of CAT and SOD.

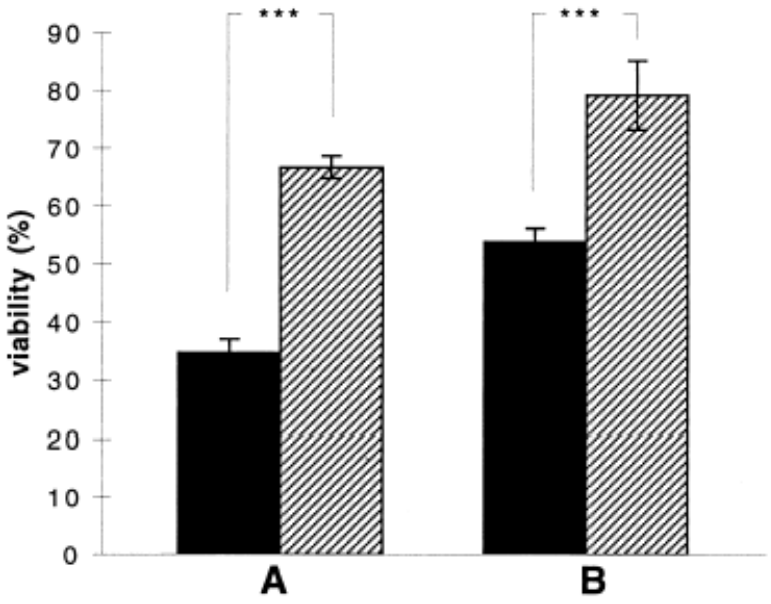

Figure 11.4. Pancreatic Cell viability without (filled box) and with gene delivered antioxidant enzymes CAT(A) and SOD(B) .[64] Reprinted with permission by Taylor & Francis.

Reperfusion injury also leads to ROS generation in transplanted kidney cells.[6,65] Ming et al. has shown that adenovirus-mediated gene transfer of SOD, given intravenously, attenuates ischemia-reperfusion injury in rat kidney cells.[66] Urinary lactate dehydrogenase (LDH) concentrations, which signifies the level of oxidative stress[66], were elevated after reperfusion injury in control groups, however, LDH levels in SOD treated rats were 50% lower.

In all cases where transplanted cells (liver, pancreatic, kidney) are prone to ROS injury, gene therapy with SOD has been shown, in the aforementioned studies, to alleviate oxidative stress and may prove beneficial in the long-term clinical success of organ allografts.

Reperfusion injury and ionizing radiation have been shown to induce oxidative stress in human lung cells.[6,67] Epperly et al. and Zwacka et al. have shown that adenovirus-mediated gene therapy with Mn-SOD protects lung epithelial cells against ionizing irradication.[67,68,69] However, in a separate study, Epperly et al. found that Mn-SOD gene transfer does not provide intrinsic protection to alveolar type II cells against ionizing irradiation-induced oxidative stress.[70] Danel et al. found that adenovirus-mediated gene transfer of human Cu/Zn-SOD protects lung L2 cells from hyperoxia but not ischemia-reperfusion lung injury.[71] In fact, in this study, gene transfer of Cu/Zn-SOD alone worsened ischemia-reperfusion injury. Also, to support the hypothesis that SOD needs to be expressed along with CAT or GPX, the authors found that if SOD was expressed simultaneously with CAT, the worsening of reperfusion injury was prevented, however, there was still no significant protection. Komada et al. found that lipofectin-mediated gene transfer of human Cu/Zn-SOD protected L2 lung cells against paraquat-

induced oxidative stress.[72] In this study, approximately 90% of lung cells treated with SOD gene transfer survived the challenge of oxidative stress, compared to only 60% of control cells. The investigators also measured lipid peroxidation and observed an inverse relationship between cell survivability and lipid peroxidation.[72]

Oxidative stress has been shown to be an important contributor in several neurodegenerative diseases, including Alzheimer disease, Parkinson disease, Huntington's disease, amyotrophic lateral sclerosis, Friedreich' ataxia and dementia.[13,73,74] Barkats et al. has shown that adenovirus-mediated gene transfer of human SOD1 increased the survival of primary culture dopaminergic cells by 50% when challenged with oxidative stress.[75] Neurotoxin 6-hydroxdopamine was used to induce oxidative stress.

Interestingly, Barkats et al. also observed that cells infected with an adenovirus expressing glutathione peroxidase did not show increased survival when challenged by 6-hydroxydopamin.[75] Fluid percussion-induced brain injury has been found to be associated with the generation of superoxide on the cerebral cortex by NAD(P)H oxidase.[76] Kim et al. found that adenovirus-mediated gene transfer of Cu/Zn-SOD to cerebral vessels prevents fluid percussion-induced cerebral blood flow autoregulatory dysfunction.[77] Shin et al. has also shown that gene transfer of Cu/Zn-SOD1 to cerebral vessels prevents impairment of cerebral blood flow autoregulation.[78] In this study, the oxidative stress was induced via subarachnoid hemorrhage. Infected cultures showed a decrease in the accumulation of superoxide anion.

Optic neuropathy has been linked to the toxic effects of ROS.[79] The most common mechanism is ROS triggered cell death through an apoptotic pathway.[80] Qi et al. has found the adenovirus-mediated gene transfer of SOD2 protects cells from optic neuropathy induced by deficiency of complex I.[81] The deficiency of complex I was accomplished by ribozyme-mediated suppression of the NDUFA1 gene.

Investigators have determined that ROS, particularly superoxide, are involved in the pathogenesis of rheumatoid arthritis.[82] Work by Iyama et al. has shown that gene transfer of EC-SOD has a therapeutic effect against rheumatoid arthritis induced by collagen.[83] Histological studies conducted on terminated models showed that typical abnormalities associated with arthritis, including destruction of cartilage and bone, infiltration of mononuclear cells, and proliferation of synovial cells, were greatly improved in EC-SOD infected mice compared to controls. Further work by Dai et al. found that gene transfer of EC-SOD in a rat model reduces knee joint swelling, decreases infiltration of inflammatory cells within the synovil membrane, and reduces gelatinase activity in knee joints.[84]

Vascular dysfunction caused by oxidative stress has been shown to cause male erectile dysfunction.[85] Bivalacqua et al. found that adenovirus-mediated gene transfer of EC-SOD improves erectile function in aged rats.[86] It was also found that superoxide formation was decreased in treated rats with improved erectile function.

11.10 Conclusions

Considerable evidence supports the use of superoxide dismutase gene transfer to treat several diseases and ailments related to oxidative stress. The findings reviewed not only suggest the therapeutic potential and benefit of SOD gene therapy, but also further implicate ROS, particularly the superoxide anion, in the pathogenesis of the explored diseases. The ability to treat several diseases with the delivery of one antioxidant protein is an attractive starting-point for therapeutic gene therapy.

11.11 References

[1] Halliwell, B. and Gutteridge, J.M.C. *Free Radicals in Biology and Medicine*; 3rd edition; Oxford Press: Oxford, 1999.

[2] *Oxy-radicals in Molecular Biology and Pathology*; Cerutti, P.; Fridovich, I.; and McCord, J.; Alan R. Liss: New York, NY,1988.

[3] Dufour, E. and Larsson, N. "Understanding aging: revealing order out of chaos" *Biochimica et Biophysica Acta*. **2004**, 1658, 122-132.

[4] Hensley, K. and Floyd, R. A. "Reactive Oxygen Species and Protein Oxidation in Aging: A Look Back, A Look Ahead" *Archives of Biochemistry and Biophysics*. **2002**, 397(2), 377-383.

[5] Stadman, E. R. "Role of oxidant species in aging" *Current Medicinal Chemistry*. **2004**, 11(9), 1105-1112.

[6] McCord, J.M. "Oxygen-derived free radicals in postischemic tissue injury" *New England Journal of Medicine*. **1985**, 312, 159-163.

[7] Harman, D. "Aging: A theory based on free radical and readiation chemistry" *J. Gerontol*. **1956**, 11, 298-300.

[8] Hall, E.D.; et al. "Relationship of oxygen radical induced lipid peroxidative damage onset and progression in a transgenic model: Familial ALS" *J. of Neuroscience Research*. **1998**, 53, 66-77.

[9] Sohal, R.S. and Brunk, U.T. "Lipofuscin as an indicator of oxidative stress and aging" *Adv. Exp. Med. Biol.* **1989**, 266, 17-29.

[10] Borchman, D. and Sinha, S. "Determination of products of lipid oxidation by Infrared Spectroscopy" *Methods in Molecular Biology*. **2002**, 186, 21-28.

[11] Kahl, R.; Kampkotter, A; Watjen, W.; and Chovolou, Y. "Antioxidant Enzymes and Apoptosis" *Drug Metabolism Reviews*. **2004**, 36, 747-762.

[12] Fridovich, I. "Superoxide Dismutase" *Adv. Enzymol.* **1974**, 41, 35-97.

[13] Emerit, J.; Edeas, M.; and Bricaire, F. "Neurodegenerative diseases and oxidative stress" *Biomedicine and Pharmacotherapy.* **2004**, 58, 39-46.

[14] Balaban, R.S.; Nemoto, S.; and Finkel, T. "Mitochondria, Oxidants, and Aging" *Cell*. **2005**, 120, 483-495.

[15] Lee-Ruff E. "The Organic Chemistry of Superoxide" Chem. Soc. Rev. **1977**, 6, 195-214.

[16] Haber, F. and Weiss, J. "The catalytic decomposition of hydrogen peroxide by ion salts" *Proc. Roy. Soc.* **1934**, A147, 332-351.

[17] Yim. M.B; et al. "Copper, zinc superoxide dismutase catalyzes hydroxyl radical production from hydrogen peroxide" *Proc. Nat. Aca. Sci*. **1990**, 87, 5006-5010.

[18] Rao, P.S. and Hayon, E. "Redox Potentials of Free Radicals" *Journal of Physical Chemistry*. **1975**, 79, 397-402.

[19] Fridovich, I. "Superoxide radicals and superoxide dismutases" *Annual Review of Biochemistry*. **1995**, 64, 97-112.

[20] Czapski, G. and Bielski, B.H.J. "THE FORMATION AND DECAY OF H_2O_3 AND HO_2 IN ELECTRON-IRRADIATED AQUEOUS SOLUTIONS" *J. Phys. Chem*. 1963, 67, 2180-2184.

[21] McCord, J.M. and Fridovich, I. "Superoxide dismutase. An enzymic function for erythrocuprein (hemocuprein)" *J. Biol. Chem*. **1969**, 244, 6049-6055.

[22] Michal, S. and Hanna, C. "Extracellular superoxide dismutase (EC-SOD)—structure, properties and functions" *Postepy Hig Med Dosw*. **2004**, 58, 301-311.

[23] Keele, B.B.; McCord, J.M.; and Fridovich, I. "Further characterization of bovine superoxide dismutase and its isolation from bovine heart" *J. Biol. Chem.* **1971**, 246, 2875-2880.

[24] Ursby, T.; Adinolfi, B.S.; Al-Karadaghi, S.; De Vendittis, E.; and Bocchini, V. "Iron Superoxide Dismutase from Archaeon *Sulfolobus solfataricus*: Analysis of Structure and Thermostability" *J. Mol. Biol*. **1999**, 286, 189-205.

[25] Klug-Roth, D.; Fridovich, I.; and Rabani, J. "Pulse radiolytic investigations of superoxide catalyzed disproportionation. Mechanism for bovine superoxide dismutase" *Journal of the American Chemical Society*. **1973**, 95, 2786-2790.

[26] Azbill, R.D.; et al. "Imparied mitochondrial function, oxidative stress and altered antioxidant enzyme activities following traumatic spinal cord injury" *Brain Res.* **1997**, 765, 283-290.

[27] Concenc, S.; et al. "Effects of footshock stress on superoxide dismutase and glutathione peroxidase enzyme activities and thibarbituric acid reactive substances levels in the rat prefrontal cortex and striatum" *Neurosicence Letters*. **2000**, 289, 107-110.

[28] Goss, J.R. et al. "The antioxidant enzymes glutathione peroxidase and catalase increase following tramumaic brain injury in the rat" *Exp. Neurol*. **1997**, 146, 291-294.

[29] Shigenaga, M.K.; et al. "Oxidative dmage and mitochondrial decay in againg" Proc. Natl. Acad. Sci. 1994, 91, 10771-10778.

[30] Beyer, W.; Imlay, J.; and Fridovich, I. "Superoxide dismutases" *Progress in Nucleic Acid Research and Molecular Biology*. **1991**, 40, 221-253.

[31] Mackay, W.J. and Bewley, G.C. "The genetics of catalase in *Drosophila melanogaster*: isolation and characterization of acatalasemic mutans" *Genetics*. **1989**, 122, 643-652.

[32] Phillips, R.J.; et al. "Nul mutation of copper/zinc superoxide dismutase in transfenic *Drosophila melanogaster*" *Arch. Biochem. Biophys*. **1999**, 371, 260-269.

[33] Fukai, T.; et al. "Extracellular superoxide dismutase and cardiovascular disease" *Cardiovasc. Res*. **2002**, 55, 239-249.

[34] Creagan, R.; et al. "Chromosome assignmens of gene in man using mouse-human somatic cell hybrids" mitochondrial superoxide dismutase (indophenol oxidase-B, tetrameric) to chromosome 6" *Human Genetik*. **1973**, 20, 203-209.

[35] Li, N.; et al. "Overexpression of maganes superoxide dismutase in DU145 human prostate carcinoma cells has multiple effects on cell phenotype" *Prostate*. **1998**, 35, 221-233.

[36] Kahols, K.; et al. "Proliferation, apoptosis, and manganese superoxide dismutase in malignant mesothelioma" *Int. J. Cancer*. **2000**, 88, 37-43.

[37] Safford, S.E.; et al. "Supression of ibrosacrcoma etastasis by elevated expression of manganese superoxide dismutase" *Cancer Research*. **1994,** 54, 4261-4265.

[38] Chen, J.; et al. "Effects of manganes superoxide dismutase transfection on the proliferation of SGC7901 gastric cancer cell" *Fudan Xuebao, Yixueba*. **2004**, 31, 19-23.

[39] Bernard, D.; et al. "Antiproliferative and antiapoptotic effects of cRel may occur within the same cells via the up-regulation of manganese superoxide dismutase." *Cancer Res*. **2001**, 61, 2656-2664.

[40] Bernard, D.; et al. "The c-Rel transcription factor can both induce and inhibit apoptosis in the same cells via the upregulation of MnSOD" *Oncogene*. **2002**, 21, 4392-4402.

[41] Sinha, S. "Anti-oxidant gene expression imbalance, aging and Down syndrome" *Life Sciences*. **2005**, 76, 1407-1426.

[42] Cristiano, F.; et al. "Changes in the levels of enzymes, which modulate the antioxidant balance occur during again and correlate with cellular damge" *Mecchanism of Againg and Development*. **1995**, 80, 93-105.

[43] Percy, M.E.; "Red cell superoxide dismutase, glutathione peroxidase and catalase in Down syndrome patients with and without manifestation of Alzheimer disease" American Journal of Medicine and Genetics. **1990**, 35, 459-467.

[44] Bolli, R. "Oxygen-derived free radicals and myocardial reperfusion injury: an overview" *Cardiovasc Drugs Ther*. **1991**, 5, 249-268.

[45] Li, Q.; et al. "Gene Therapy with Extracellular Superoxide Dismutase Attenuates Myocardial Stunning in Conscious Rabbits" *Circulation*. **1998**, 98, 1438-1448.

[46] Li, Q.; et al. "Gene Therapy with Extracellular Superoxide Dismutase Protects conscious Rabbits Against Myocardial Infarction" *Circulation*. **2001**, 103, 1893-1898.

[47] Abou El Hassan, M.A.I.; et al. "The protective effect of cardiac gene transfer of CuZn-SOD in comparison with the cardioprotector monohydroxyethylrutoside against doxorubicin-induced cardiotoxixity in cultured cells" *Cancer Gene Therapy*. **2003**, 10, 270-277.

[48] Jeroudi, M.O.; et al. "Effect of superoxide dismutase and catalase, given separately, on myocardial stunning" *Am. J. Physiol*. **1990**, 259, 889-901.

[49] Omar, B.A.; et al. "Cardioprotection by Cu, Zn-superoxide dismutase is loast at high doeses in the reoxygenated heart" *Free Radic. Biol. Med*. **1990**, 9, 465-471.

[50] Biguad, M.; et al. "Endotoxin-induced impairment of vascular smooth muscle contraction elicited by different mechanism" *Eur. J. Pharmacol*. **1990**, 190, 185-192.

[51] Gunnett, C.A.; et al. "IL-10 deficiency increases superoxide and endothelial dysfunction during inflammation" *Am. J. Physiol Heart Circ. Physiol.* **2000**, 279, 1555-1562.

[52] Jialal, I.; et al. "Oxidative stress, inflammation and diabetic vasculopathies: the role of alpha tocopherol therapy" *Free Radic. Res.* **2002**, 36, 1331-1336.

[53] Lund, D.D.; et al. "Gene transfer of extracellular superoxide dismutase improves relaxation of aorta after treatment with endotoxin" " *Am. J. Physiol. Heart Circ. Physiol*. **2004**, 287, 805-811.

[54] Fennell, J.P.; "Adenovirus-mediated overexpression of extracullular superoxide dismutase improves endothelial dysfunction in a rat model of hypertension" *Gene Therapy*. **2002**, 9, 110-117.

[55] Forge, A. and Schacht, J. "Aminoglycoside antibiotics" *Audiol. Neurootol*. **2000**, 5, 3-22.

[56] Swan, S.K. "Aminoglycoside nephrotoxicity" *Semin. Nephrol*. **1997**, 17, 27-33.

[57] Priuska, E. M. and Schacht, J. "Formation of free radicals by gentamicin and iron and evidence for an iron/gentamicin complex" *Biochem. Pharmacol*. **1995**, 50, 1749-1752.

[58] Kohei, K.; et al. "Antioxidant Gene Therpay Can Protect Hearing and Hair Cells from Ototoxicity" *Molecular Therapy*. **2004**, 9, 173-181.

[59] Wu, J.; et al. "Liposome-Mediated Extracellular Superoxide Dismutase Gene Delivery Protects Against Acute Liver Injury in Mice" *Hepatology*. **2004**, 40, 195-204.

[60] Arthur, M.J.P.; et al. "Oxygen-derived free radicals promote hepatic injury in the rat" *Gastroenterology*. **1985**, 89, 1114-1122.

[61] Lehmann, T.; et al. "Delivery of Cu/Zn-superoxide dismutase genes with a viral vector minimizes liver injury and improves survival after liver transplantation in the rat" *Transplantation*. **2000**, 69, 1051-1057.

[62] Lehmann, T.; et al. "Role of Kpffer cells in graft failure after liver transplantation: Oxidative stress and gene therapy" *Cells of the Hepatic Sinusoid*. **2001**, 8, 302-307.

[63] White, S.A.; et al. "Human islet cell transplantation future prospects" *Diabetic Medicine*. **2001**, 18, 78-103.

[64] Karsten, V.; et al. "How can Adenovirus-Mediated Catalase and Superoxide Dismutase Gene Transfer Improve the Outcome of Pancreatic Cells for Transplantation" *Transplantation Proceedings*. **2001**, 33, 575-576.

[65] Paller, M.S. "Free radicals-mediated post ischemic injury in renal transplantation" *Ren. Fail*. **1992**, 14, 257-260.

[66] Ming, Y.; et al. "Cu/Zn-Superoxide Dismutase Gene Attenuates Ischemica-Reperfusion Injury in the Rat Kidney" *J. Am. Soc. Nephrol*. **2001**, 12, 2691-2700.

[67] Epperly, M.W.; et al. "Prevention of late effects of irradiation lung damge by manganese superoxide dismutase gene therapy" *Gene Therapy*. **1998**, 5, 196-208.

[68] Zwacka, R.M.; et al. "Redox gene therapy protects human IB-3 lung epithelial cells against ionizing radiation-induced apoptosis" *Human Gene Therapy*. **1998**, 9, 1381-1386.

[69] Epperly, M.W.; et al. "Intratracheal injection of adenovirus containing the human MnSOD transgene protects athymic nude mice from irradiation-induced organizing alveolitis" *Int. J. Radiat. Oncol. Biol. Phys*. **1999**, 43, 169-181.

[70] Epperly, M.W.; et al. "Overexpression of Manganese Superoxide Dismutase (MnSOD) in Whole Lung or Alveolar Type II Cells of MnSOD Transgenic Mice Does Not Provide Intrinsic Lung Irradiation Protection" *Int. J. Cancer.* **2001**, 96, 11-21.

[71] Danel, C.; et al. "Gene therapy for oxidant injury-related diseases: adenovirus-mediated transfer of superoxide dismutase and catalase cDNAs protects against hperoxia but not agaisn't ischemia-reperfusion lung injury" *Human Gene Therapy*. **1998**, 9, 1487-1496.

[72] Komada, F.; et al. "Effect of transfection with superoxide dismutase expression plasmid on superoxide anion induced cytotoxity in cultured rat lung cells" *Biologicl and Pharmaceultical Bulletin*. **1996**, 19, 274-279.

[73] Beal, M.F. "Aging, energy, and oxidative stress in neurodegenerative diseases" *Ann. Neurol*. **1995**, 38, 357-366.

[74] Radunovic, A.; et al. "Incrased mitochondrial superoxide dismutase activity in Parkinson's disease but not amyotrophic lateral sclerosis motor cortex" *Neuroscience Letters*. **1997**, 239, 105-108.

[75] Barkats, M.; et al. "Neuronal transfer of the human Cu/Zn superoxide dismutase gene increases the resistance of dopaminergic neurons to 6-hydroxydopamin" *J. of Neurochemistry*. **2002**, 82, 101-109.

[76] Armstead, W. M. "Superoxide generation links protein kinase C activation to impaired ATP-sensitive K^+ channel function after brain injury" *Stroke*. **1999**, 30, 153-159.

[77] Kim, C. D.; et al. "Gene transfer of Cu/Zn-SOD to cerebral vessels prevents FPI-induced CBF autoregulatory dysfunction" *Am. J. Physiol. Heart Circ. Physiol*. **2002**, 282, 1836-1842.

[78] Shin, H.K.; et al. "Prevention of Impairment of Cerebral Blood Flwo Autoregulation During Acute Stage of Subarachnoid Hemorrhage by Gene Transfer of Cu/Zn SOD-1 to Cerebral Vessels" *J. Cerebral Blood Flow and Metabolism*. **2003**, 23, 111-120.

[79] Sandbach, J.M.; et al. "Ocular pathology in mitochondrial superoxide dismutase (SOD2)-deficient mice" *Invest. Ophthalmol. Vis. Sci*. **2001**, 42, 2173-2178.

[80] Wallace, D.C. "Mouse models for mitochondrial disease" *Am. J. Med. Genet*. **2001**, 106, 71-93.

[81] Qi, X.; et al. "SOD2 Gene Transfer Protects against Optic Neuropathy Induced by Deficiency of Complex I" *Ann. Neurol*. **2004**, 56, 182-191.

[82] Tiku, M.L.; Shah, R.; and Allsion, G.T. "Evidence linking chondrocyte lipid peroxidation to cartilage matrix protein degradation" *J. Biol. Chem*. **2000,** 275, 20069-20076.

[83] Iyama, S.; et al. "Treatment of Murine Collagen-Induced Arthritis by Ex Vivo Extraceullular Superoxide Dismutase Gene Transfer" *Arthritis and Rheumatism*. **2001**, 44, 2160-2167.

[84] Dai, L.; et al. "Amelioration of antigen-induced arthritis in rats by transfer of extracullular superoxide simutase and catalase genes" *Gene Therapy*. **2003**, 10, 550-558.

[85] Bicalacqua, T. J.; et al. "Adenoviral gene transfer of endothelial nitric oxide synthase (eNOS) to the penis improves age-related erectile dysfunction in the rat" Int. J. Impot. Res. 2000, 3, S8-S17.

[86] Bivalacqua, T. J.; et al. "Gene transfer of extracellular SOD to the penis reduces $O_2^{-\cdot}$ And improve erectile function in aged rats" Am. J. Physiol. Heart Circ. Physiol. 2003, 284, 1408-1421.

Chapter 12. **Summary and Conclusions**

Non-viral gene delivery agents, such as cationic polyelectrolytes, are attractive replacements to viruses due to the absence of potential immunogenic risk and the ability to tune their macromolecular structure. Although non-viral vectors possess numerous design advantages, several investigators have shown that transfer efficiencies are considerably lower when compared to viral vectors. The work reported in this dissertation aimed to fundamentally understand the underlying structure-transfection relationships involved in polycation-mediated gene delivery. Efforts focused on the influence of molecular weight, macromolecular topology, carbohydrate modifications, and charge density on the overall transfection activity in vitro. Several families of polycations were synthesized in order to correlate chemo-physical characterization with transfection results. Results revealed that seemingly small changes in the structure of cationic polyelectrolytes can have profound consequences on their transfection activity. The major findings from this work are listed below.

1. Conventional free radical polymerization was used to synthesize linear and randomly branched cationic polyelectrolytes based on PDMAEMA. Rheological methods were used to determine the level of branching, calculated as the g' contraction factor. Four samples, grouped according to similar weight-average molecular weights (M_w=110,000 and 215,000 g/mol), were comparatively analyzed for their ability to form complexes with and transfect plasmid DNA *in*

vitro. Gel electrophoresis and CD spectroscopy demonstrated that the topology of PDMAEMA did not influence its binding with plasmid DNA. For both HBMEC and Cos-7 cells *in vitro*, the topology of the PDMAEMA did not have a significant influence on gene transfection efficiency.

2. Conventional free-radical polymerization was used to synthesize various molecular weights of PDMAEMA. Aqueous SEC-MALLS determined that the synthesized polymers had weight-average molecular weights between 43,000 and 915,000 g/mol. An MTT assay revealed that lower molecular weight PDMAEMA (M_w=43,000 g/mol) was slightly less toxic to HBMEC cells, however, cell viabilities were found to be more sensitive to polymer concentration. An LDH release assay determined that the primary mode of PDMAEMA toxicity to HBMEC cells was membrane destabilization. Furthermore, LDH release results showed the same molecular weight/toxicity trend as the MTT assay. An electrophoretic gel shift assay showed that all PDMAEMA molecular weights completely bound with plasmid DNA. However, heparin competitive binding assays revealed that higher molecular weight PDMAEMA (M_w=915,000 g/mol) had a greater binding affinity towards plasmid DNA compared to lower molecular weight (M_w=43,000 g/mol). The molecular weight of PDMAEMA was found to have a dramatic influence on transfection efficiency, with gene expression increasing as a function of increasing molecular weight. However, the molecular weight of PDMAEMA did not have any influence on the cellular uptake of polyplexes. DLS experiments indicated the absence of a direct correlation of polyplex size to transfection efficiency.

Collectively, our data suggested that the intracellular fate of the polyplexes was more important to overall transfection efficiency than barriers to entry (such as polyplex size). Moreover, polymer binding affinity was likely a significant parameter associated with the polyplex's intracellular journey.

3. The influence of glucose and maltose modifications (degrees of substitution >90%) on the cytotoxicity and gene transfection performance of hyperbranched PEI in HBMEC cells was evaluated. Aqueous SEC and zeta-potential characterization of the synthesized polymers determined that the carbohydrate substitutions eliminated the cationic charge of hyperbranched PEI. Titration experiments showed that the internal amines of peripherally substituted hyperbranched PEI were not accessible to protonation. Gel electrophoresis revealed that glucose and maltose substitutions prevented electrostatic binding with plasmid DNA. We determined that peripherally decorating PEI with either glucose or maltose significantly reduced toxicity, but these modifications also reduced transfection efficiency.
4. Absolute molecular weight characterization of aliphatic ammonium ionenes was successfully accomplished using aqueous-based SEC-MALLS. A suitable mobile phase composition of 54/23/23 (v/v/v%) water/methanol/acetic acid and 0.54 *M* NaOAc at pH 4.0 was developed to reduce polymer-polymer and polymer-stationary phase interactions. Using this mobile phase composition, reasonable separations were obtained and accurate measurements of the weight-average molecular weight were achieved. Ammonium 6,12-ionenes had number-average molecular weights ranging from 14,000 – 41,500 g/mol and weight-average

molecular weights ranging from 19,000 g/mol – 49,900 g/mol with molecular weight distributions ranging from 1.31 – 1.42. Ammonium 12,12-ionenes had number-average molecular weights ranging from 8,000 – 30,700 g/mol and weight-average molecular weights ranging from 11,000 – 40,000 g/mol with molecular weight distributions ranging from 1.26 – 1.42. Additionally, intrinsic viscosity data was collected for ammonium 12,12- and 6,12-ionens as a function of molecular weight distribution to determine MHS parameters.

5. A series of aliphatic ammonium ionenes were synthesized using step-growth polymerization. Specifically, ammonium 12,6- and 12,12-ionenes synthesized in order to evaluate the influence of charge density on plasmid DNA transfection. We determined that transfection efficiency in Cos-7 was insensitive to 12,6-ionene molecular weight over the range tested. Additionally, all transfection experiments revealed that protein expression decreased as a function of increasing N/P ratio, likely due to reduced cell viability. The charge density of the aliphatic ammonium ionene was found to have a significant influence on transfection efficiency, with the higher charge density (12,6-ionene) showing orders of magnitude greater protein expression.
6. Imidazole-substituted epoxide monomers (specifically *N*-tritylimidazole-2-ethylene oxide) were successfully synthesized and polymerized via anionic ring opening polymerization. The resulting polymers were synthesized with high yields and ^{1}H NMR analysis revealed that the PEG-based polymers had relatively high degrees of polymerization (DPs up to 90, M_n's up to ~30,000 g/mol). CD spectroscopy of the trityl-protected PEG-imidazoles indicated that the polymer

likely adopted helical conformations during polymerization. However, this topic requires further investigation. Poly(*N*-tirtylimidazole-2-ethylene oxide) was readily deprotected to yield poly(imidazole-2-ethylene oxide), a water-soluble polymer. We are currently exploring regioisomers of imidazole epoxides and evaluating these new PEG-based polymers for their ability to complex and deliver plasmid DNA.

Chapter 13. **Suggested Future Work**

13.1 Determine the influence of molecular weight on gene transfection using other cationic polymers.

Although PDMAEMA serves as a good model system for the determination of structure-transfection relationships, its transfection efficiency is lower when compared to other polycationic delivery systems. Therefore, the influence of molecular weight using more clinically relevant polymers should be investigated. Poly(ethylene imine) would be the next logical polymer to study since it shows high transfection efficiency and varying molecular weights can be easily synthesized.

13.2 Determine the influence of molecular weight in polycation-mediated gene delivery *in vivo*.

The work reported in this dissertation determined that the molecular weight of the polycation had a significant influence on PDMAEMA-mediated transfection *in vitro*. For successful clinical implementation, gene therapy system will have to demonstrate their efficacy *in vivo*. There are many additional barriers to gene transfection *in vivo*, such as polyplex stability in serum, circulation lifetime, and the targeting of polyplexes to specific tissues. Therefore, the influence of PDMAEMA molecular weight should be investigated in animal models. The distribution of polyplexes in organ systems should be evaluated.

13.3 Determine the influence of hydrogen bonding in polycation-mediated gene delivery.

The inter- and intra-molecular interactions between positively charged polymers and negatively charged DNA has a profound impact on transfection efficiency. The ability of the polycation to protect DNA from nuclease degradation as well the ability to release DNA inside the cell all depend on polyplex binding affinity. Therefore, the influence of secondary interaction on DNA binding and transfection, such as hydrogen bonding, should be evaluated. This can be accomplished via the synthesis of copolymers using monomers with hydrogen bonding functionality.

13.4 Fractionate cationic polymers with preparative size exclusion chromatography and determine the influence of polydispersity on gene delivery.

In addition to polymer molecular weight, the influence of polydispersity should be evaluated. Polyplex morphology and polydispersity should be directly influence by the heterogeneity of the polycation. Narrow dispersity polymers can either be synthesized via controlled radical polymerization techniques, or prepared from the fractionation of a polydisperse sample. The latter offers the ability to produce narrow dispersity polymers with high molecular weights since living polymerization techniques can only control molecular weight up to approximately 100,000 g/mol. Preparative aqueous size exclusion chromatography (SEC) can be used for fractionation directly in physiological buffers. Alternatively, solvent/non-solvent precipitation methods can also be utilized to achieve the same objective. In addition to transfection studies with narrow dispersity

polycations, the fractions should then be mixed to evaluate the transfection efficiency of polycations with high polydispersities.

13.5 Gene delivery using imidazole-based polymers.

The imidazole ring is found naturally in the amino acid histidine. Nitrogens in the imidazole ring can be protonated around physiological pH to yield a cationic structure. Polyimidazoles have the potential to serve as good transfection agents due to their histidine-mimicking properties. Future experiments should evaluate the structure-property relationships in polyimdiazole-mediated transfection. Additionally, the PEG-based imidazole polymers described in this dissertation should be evaluated for their ability to bind and transfect plasmid DNA. These polymers should demonstrate reduced cytotoxicity due to their PEG-based nature.

13.6 Synthesize and polymerize regioisomers of PEG-based imidazole epoxides.

PEG-based imidazoles were synthesized from N-tritylimidazole-2-ethylene oxide in the work reported in this dissertation. However, other regioisomers should be synthesized, such N-tritylimidazoles substituted at positions 1, 4, or 5. Polymer synthesis and characterization should be comparatively analyzed for the various regioisomers. Additionally, the transfection behavior as a function of the epoxide ring position should also be investigated.